The impact of host stress on virulence phenotypes in the malaria parasite *Plasmodium falciparum*

Linda Onyeka Anagu

Submitted in partial fulfilment of the requirements of the Degree of Doctor of Philosophy

June 2020

Centre for Applied Entomology and Parasitology

Keele University

ABSTRACT

Plasmodium falciparum encodes a family of key virulence genes called *var* genes. These encode adhesive proteins that are expressed on infected erythrocytes in a mutually exclusive manner. The parasite's sirtuins have been implicated in epigenetic selection of the expressed *var* gene(s). In field isolates, associations have been made between upregulation of sirtuins and two host stress factors that define severe malaria, and increased *var* gene expression. The parasite may specifically respond to these host factors, fever and hyperlactatemia, through sirtuins, leading to phenotypic variation.

In this thesis, both laboratory and field strains of *P. falciparum* were used to investigate these relationships in culture. Heat shock at 40°C can modestly increase the expression of *PfSir2B* in the trophozoite or *PfSir2A* in the ring stages. *PfSir2B* was also decreased in the rings. Severe disease associated *var* gene subsets, groups A, B and E, were predominantly upregulated upon stress or after the parasites were allowed to recover within one asexual cycle. There was a general upregulation of *var* transcript levels majorly after recovery. Thus, both upregulation of specific *var* gene subset and total *var* gene expression may manifest as strategies to cope with heat stress. High lactate exposure, meanwhile, had no clear association with sirtuin or *var* gene expression, suggesting that the *in-vivo*-observed association of high lactate concentration with the sirtuins and *var* genes appeared to be coincidental. Interestingly, however, lactate positively impacted parasite growth in culture at low parasitaemia. Finally, these stressors may reduce gametocytogenesis, which was investigated in one of the three field strains as it was able to produce gametocytes. The present study will inform the development of interventions against chronic or fatal severe *falciparum* malaria.

Table of Contents

Acknowledgements

My career progress has been hinged on getting a PhD qualification, a journey which was equally exciting and difficult. But, I have been helped along the way by my faith in God and all the good people I have the opportunity of meeting either during the honeymoon first year, the challenging second year or the highly effective third year of my PhD.

Firstly, my gratitude goes to my first supervisor, Dr. Catherine Merrick, for her ever constant superb accommodation and learning support throughout my PhD. Her scientific input and positive feedback helped me rise above any challenges. She designed most aspect of this study and assisted in the cloning of the PfSir2A-luc line. She ensured I was up-to-date with my research using her inspiration, encouragement and attention. She believed I could do this research and that support produced wonderful research outputs. I did tell her she will make a good mother one day.

Secondly, my gratitude goes to my second supervisor, Dr. Srabasti Chakravorty, my former advisor, who became a supervisor when Dr. Catherine Merrick moved to Cambridge. She helped me overcome my shortfalls and strengthened my pro-activeness. She helped me ease from mostly laboratory-related research to writing the thesis, and managed the academic/administrative aspect involved in preparing a PhD student for the Viva examination. She also supported my soapbox public engagement training and my aspirations in preparing for career development post-PhD.

Thirdly, I am grateful to Prof. Paul Horrocks, who has supported me in putting my head above the water during my financial difficulties. He assisted in a supervisory/advisory role which helped me improve some protocols in this thesis. His greatest impact has been in convincing the faculty that my financial debt should be cleared. His PhD student, Mufuliat

Famodimu, provided a much needed assistance in learning the protocols for the luciferase and MSF assay.

I will not forget Dr. Imran Ullah for his preliminary work on the effect of 41°C temperature on parasite growth, thus enabling us to make the decision of using a lower temperature for the heat shock treatment.

Other staff and post-doctoral fellows within the school including members of CEAP have helped me in communicating my findings, expanding my knowledge and fine-tuning some laboratory skills. They include; Dr. Helen Price, Dr. Sarah Berry, Dr. James Small-bone, Dr. Lynne Harris, Dr. Florian Nuolin, Dr. Holly Mathews, Dr. Craig Duffy and Dr. Lisa Rump. Dr. David Hulse learnt his expertise advice and support in the use of statistical analysis, and I am grateful for this. The laboratory technicians in the teaching laboratory, school administrative team and manager, Jane Bromley, have equally been helpful.

Most notably, I will forever appreciate my parents (both direct and in-laws), husband, siblings, children and colleagues who have seen me at my best and worst, and have not judged. There physical support and kind words have helped boosted my mental health amidst all challenges. My husband took care of our children while I was at school and even when I had to be in the laboratory during odd hours of the day. My friends and colleagues especially; Emma Whittle, all the other Emma, Anya Osborne, Nwamaka Akpodiete, Nana Efua Andoh, Emmanuel Ottih, Atieme Ogbolosingha, James Hyatt, Joe Roberts, Lekia Kumbe, Henry Dick; will all always be remembered.

Finally, I am grateful to the Tertiary Education Trust fund (TETfund) in Nigeria for fundamentally sponsoring my PhD. However, this award would not be given if the faculty had not paid-off my deficit in tuition funding and given me a peace of mind to be able to complete my studies and I remain forever grateful for this.

List of Figures

Chapter 1

Chapter 2

Chapter 3

Chapter 5

Chapter 6

Chapter 7

Chapter 8

List of Tables

Chapter 2

Chapter 3

Chapter 4

Chapter 5

Abbreviations

ARD – Acute respiratory distress

ATS - acidic terminal segment

CD36 - cluster determinant 36

cDNA – complementary DNA

CIDR - cysteine-rich interdomain regions

CM – Cerebral malaria

CSA - chondroitin sulphate A

DBL - Duffy binding-like domains

DC - domain cassette

DNA – Deoxyribonucleic acid

DTT - Dithiothreitol

EPCR - endothelial protein C receptor

gDNA – genomic DNA

HDAC – Histone deacetylase

hpi – hour post invasion

ICAM 1 - intercellular adhesion molecule-1

IDC – intraerythrocytic development cycle

IL - interleukin

iRBC – infected Red Blood Cells

LAS - Luciferase assay substrate

mRNA – messenger RNA

ncRNA – non coding RNA

PAM – Pregnancy associated malaria

PCR – Polymerase chain reaction

PfEMP1 - *P. falciparum* erythrocyte membrane protein 1

PMSF - phenylmethylsulfonyl fluoride

PTM – Post-translational modification

RCN – Relative copy number

RIFINs - repetitive interspersed families of polypeptides

RNA – ribonucleic acid

SAHA - Suberoylanilide hydroxamic acid

SG – SYBR Green

TNF – tumor necrosis factor

WHO – World Health Organization

Chapter 1: Introduction

1.1 Malaria overview

Death following malaria infection is principally caused by *Plasmodium falciparum* infection, and occurred in about 0.2% of malaria infected people in 2017 (435,000 people), of which 61% of these people were children (World Health Organization 2018). This is a sharp decline from the approximately 1 million deaths that occurred about 10 years ago (World Health Organization 2008). Whilst malaria infections dropped from 247 million 10 years ago to 219 million reported cases in 2017, analysis revealed that in the past few years there has been a steady incidence rate with no significant decline. Of the 219 million cases, 92% occurred in WHO African region with Nigeria accounting for 25% of the cases and 19% of the fatal cases. There has thus been no significant reduction in death from severe cases in this region compared to 3 years ago. Globally, in at risk populations, 59 out of 1000 people will be infected per year, but this rises to 219 persons in WHO African region. However, not all *P. falciparum* infections result in a clinical manifestation of malaria. There are several outcomes of this infection ranging from asymptomatic to uncomplicated to severe forms of malaria (World Health Organization 2018).

Global concerted efforts to eradicate this disease have very much improved through research and implementation of research-informed disease control strategies which include vector control, chemotherapeutic drugs and vaccine development. However, it is possible that the resulting reduction of 'herd immunity' due to reduced transmission in an endemic area may lead to an increased incidence of severe malaria, if any of the control measures fails dramatically. Virulence phenotypes in *P. falciparum* present a challenge to the development of control strategies.

1.1.1 Biology of *Plasmodium falciparum*

P. falciparum is a unicellular, primarily intracellular parasite, with two transition forms, sporozoites and merozoites, residing briefly outside the host's cell before they invade the cell. Its lifecycle (Fig. 1.1) involves two hosts, with the mosquito host, the female Anopheles, being a vector that transmits the parasite to the human host.

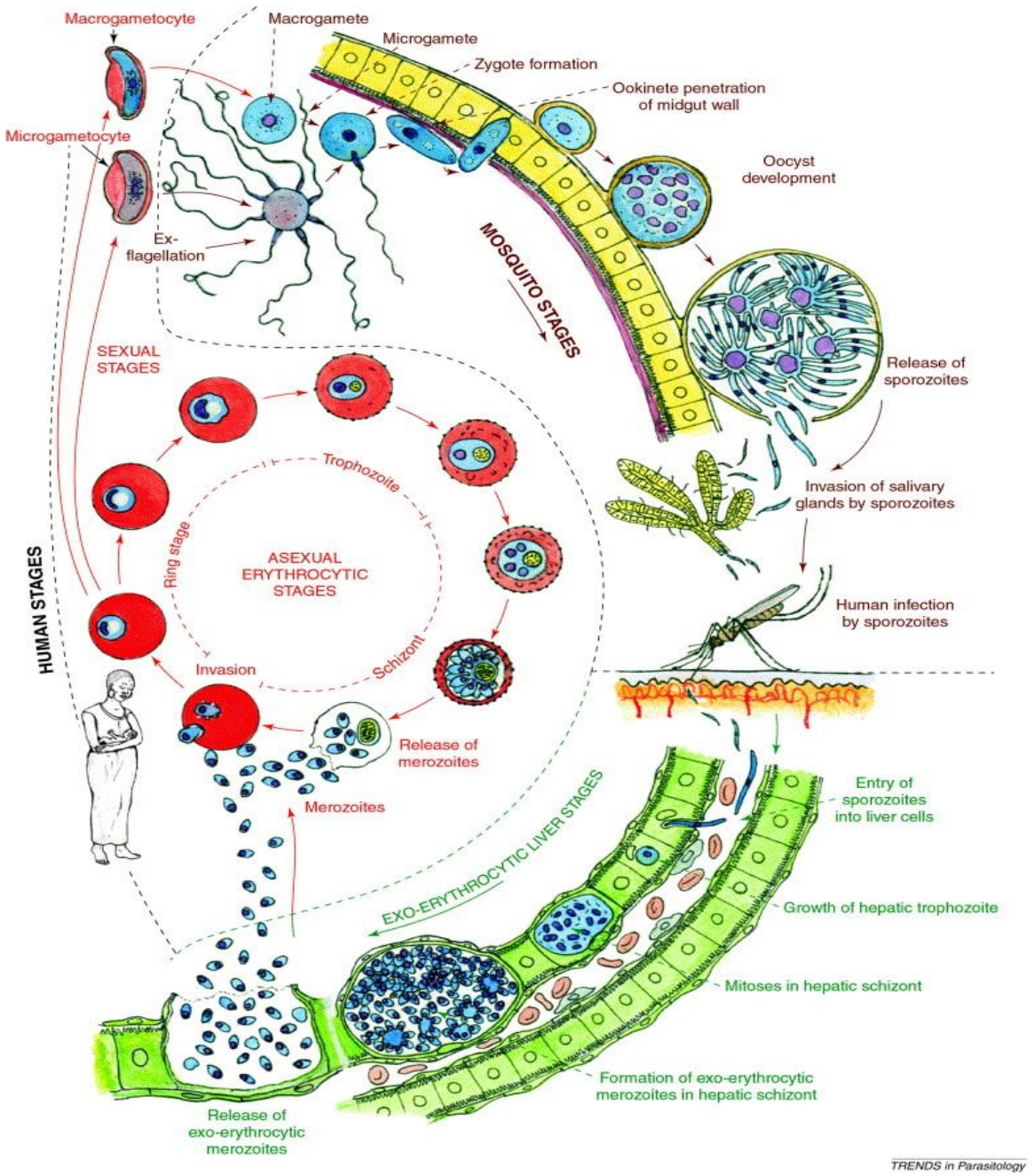

Figure 1.1: Life Cycle of the Malaria Parasite (Bannister, Mitchell 2003)

An infected mosquito transmits the sporozoites, to the human host during a blood meal. The sporozoites then disrupt the skin blood vessels, move through the blood circulation and invade the hepatocytes. In the hepatocytes they differentiate into trophozoites and then mature to schizonts, a process called schizogony. At the end of schizogony, fully mature schizonts undergo mitosis (asexual reproduction) into a number of daughter cells contained in host-cell-derived vesicles called merosomes. These merosomes then bud off the hepatocytes covered by the host cell membrane and become released as merozoites in the lung's capillaries (reviewed in (Vaughan, Aly et al. 2008; Silvie, Mota et al. 2008; Ménard, Heussler et al. 2008)).

Released merozoites invade erythrocytes and develop into various asexual blood stages of the parasite, a part of the lifecycle called the intraerythrocytic development cycle (IDC). It is during this cycling that the infection manifests clinically. There are two distinct forms of the parasite during the IDC: the merozoite and infected red blood cells (iRBCs), which contains several developmental stages: three asexual stages and one sexual stage.

The invading merozoites develop into the biconcave-shaped ring asexual forms surrounded by a parasitophorous vacuole membrane (PVM) and consume haemoglobin. They grow rapidly and then remodel the surface of the iRBCs, this enabling their adherence to cell linings of blood vessels. Older rings then mature into rounded trophozoites forms, which contain a malaria pigment that is made up of polymerized haem, the by-product of haemoglobin digestion. This form feeds more actively and remodels the iRBC surface much more resulting in consequent increased adhesion to the endothelium of blood vessels, a phenomenon called cytoadherence. This sequesters the trophozoites in blood vessels of specific tissues/organs and away from the blood circulation, thus protecting them from splenic clearance/destruction. Trophozoite-iRBCs may also undergo agglutination (adhere with other iRBCs) or rosetting (adhere with uninfected RBCs). The trophozoite enlarges and matures

into the schizont stage or form where in undergoes nuclear division (mitosis) into an average of 16 nuclei and synthesizes/assembles molecules needed for reinvasion. The nuclei are packaged into merozoite buds which are released upon lysis of the iRBC membrane and the PVM (Bannister, Mitchell 2003).

The released merozoites then continue in the asexual cycling by invading new RBCs. However, a small fraction of the merozoites become sexually committed and differentiate into the gametocyte sexual form or stage of the parasite through a process called gametocytogenesis. The decision to develop sexually is triggered in a fraction of maturing schizonts and thus all merozoites arising from the sexually committed schizont develop as gametocytes of the same sex (Smith, Lourenco et al. 2000). The duration of development of gametocytes of *P. falciparum* takes 10 - 12 days and occurs in five morphologically distinct stages (Josling, Williamson et al. 2018). The gametocytes sequester and develop in the bone marrow and spleen where they mature and are released as stage V gametocytes into the blood circulation (Tibúrcio, Dixon et al. 2015) and reviewed in (Dantzler, Ravel et al. 2015). Mature gametocytes are taken up by the mosquito during a blood meal; they develop into male and female gametes (through gametogenesis) and undergo fertilization to give rise to sporozoites in the mosquito's salivary glands.

P. falciparum is unique compared to other human-malaria-causing *Plasmodium species* as it has a shorter hepatic development period (5 - 7 days) and incubation period (interval between infection and onset of symptoms). It also produces a higher number of merozoites per schizont. Potentially lethal threshold levels of parasitaemia which could vary with transmission intensity are reached after 6-8 cycles post the first round of erythrocyte invasion, with much fewer cycles required to reach this level in younger children due to their smaller blood volume. This contributes to its virulence and ability to cause fatal malaria (reviewed in (Newton, Krishna 1998) among other factors during the pathogenesis of malaria.

1.1.2 Pathogenesis of falciparum malaria

Infection by *P. falciparum* usually results in uncomplicated malaria, which is a mild febrile illness categorized by intermittent occurrence of fever and peaks of parasitaemia, usually controlled by the body's immune system, and/or antimalarial chemotherapy. However, sometimes the disease can be severe especially in immune-naive individuals, including children in malaria endemic areas, and may be fatal. About 1 % of symptomatic uncomplicated cases will develop fatal severe malaria, either due to delayed treatment or inadequate therapy. In areas where artemisinin-combination therapies (ACTs) are used as first line therapy this has reduced to 0.1% (World Health Organization 2014). The infection can also be asymptomatic. Asymptomatic infections are reservoirs for continual transmission of the disease by the mosquito vector. The pathogenesis of malaria usually follows through from uncomplicated malaria to severe malaria to fatal malaria. Asymptomatic infections can also become clinical malaria following dramatic increase in the parasite population. Non-hyperparasitemic uncomplicated malaria has been proposed to represents an earlier stage in the natural history or pathogenesis pathway of a malaria infection. A stage where the host–parasite process has progressed beyond asymptomatic infection and produced symptoms, but it may yet diverge along several possible pathways ranging from spontaneous resolution to hyperparasitemia, cerebral malaria or other severe syndromes, and death (Kyriacou, Stone et al. 2006) reviewed in (Cowman, Healer et al. 2016).

A number of factors contribute to the pathogenesis of the disease, with a potential for clinical manifestation once the parasite has invaded the erythrocyte. *P. falciparum* invades erythrocytes of all ages (Anstey, Russell et al. 2009). Upon maturity, the parasites sequester and reduce the deformability of the iRBC as well as place antigenically variant protein family groups on the surface of the RBC they inhabit. One of such protein family is *P. falciparum* erythrocyte membrane protein 1 (PfEMP1).

1.1.2.1 The role of iRBC surface-expressed proteins in malaria pathogenesis

Within 16 hours of merozoite invasion, the parasite exports antigenically variant strain-specific PfEMP1 on to the surface of the iRBCs, (Gardner, Pinches et al. 1996) which enables it to bind to different protein and carbohydrate ligands on the surfaces of endothelial cells (Fig. 1.2). Attached iRBCs do not detach until the rupture of schizonts and cytoadherence becomes more effective in subsequent asexual cycling. This may be due to an increased expression of PfEMP1 or a switch to a different PfEMP1 (Abdi, Warimwe et al. 2016). The majority of the parasites cytoadhere to endothelial ligands and sequester in microvessels of organs away from splenic clearance. These contribute to the total parasite biomass in the human host in addition to the merozoite form and the ring stage of the parasite circulating in the plasma. Up to 40 times more parasite than the burden in circulation has been found to sequester in the cerebrovascular endothelium and recirculation of parasites may be unlikely (Silamut, Phu et al. 1999) until they mature to produce new progeny. Therefore, the circulating parasitaemia, evaluated through microscopy, underestimates the parasite biomass. Parasite biomass is quantified by measuring the plasma *P. falciparum* histidine rich protein-2 (HRP2) levels. Parasite biomass is related to the pathogenesis and severity of the disease (Cunnington, Bretscher et al. 2013), and independently correlates to/predicts disease outcome (Fox, Taylor et al. 2013) compared to peripheral parasitaemia (Rubach, Mukemba et al. 2012). Although another study did demonstrate that peripheral parasitaemia (referred to as circulating biomass in the study) was significantly higher in severe malaria but not the sequestered biomass alone (Cunnington, Bretscher et al. 2013). However, sequestration of iRBCs in the microvessels of organs causes varying degrees of obstruction of the microcirculation which contributes to the disease pathogenesis

.

Agglutination and rosetting (Fig. 1.2) may also contribute to the pathogenesis of this disease. PfEMP1 and to a lesser extent RIFINs, another antigenic variant protein family, mediate rosetting as RIFINs show a preference for blood group A (Goel, Palmkvist et al. 2015), and blood group O was shown to be protective against severe malaria caused by the parasite rosetting phenotypes with concomitant reduced rosettes formation (Rowe, Handel et al. 2007). The same parasites that form rosettes may also cytoadhere to host brain cells via heparin sulphate proteoglycans ligands as shown *in vitro* (Adams, Kuhnrae et al. 2014). Self-agglutination (Fig. 1.2) is mediated by a variety of receptors on the platelet including; CD36 (Pain, Ferguson et al. 2001), P-selectin (Wassmer, Taylor et al. 2008) and globular C1q receptor (gC1qR), which it equally uses to bind the endothelial cells (Biswas, Hafiz et al. 2007), although it is not yet clear if it is mediated by the parasite's PfEMP1. However, to date agglutination and rosetting have only been observed outside the human host suggesting that such parasite phenotypes may be sequestered away from the circulation (reviewed in (Wassmer, Grau 2017)). So both self-agglutinated iRBCs and rosettes (Fig. 1.2) may sequester and may also interfere with the metabolism and function of the vascular endothelium (World Health Organization 2014).

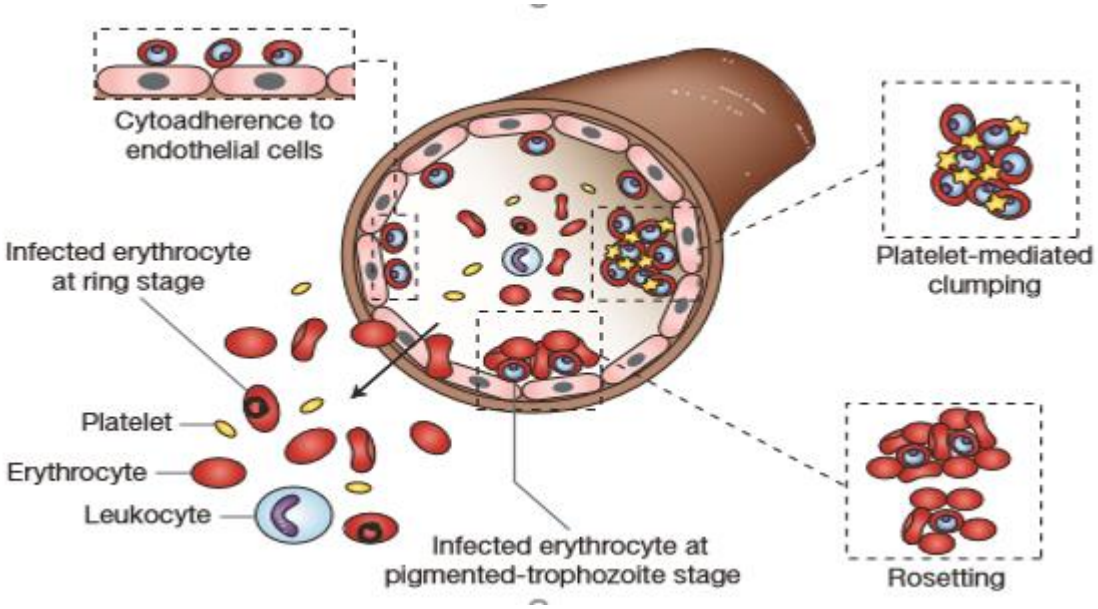

Figure 1.2: Binding of iRBCs to human cells through cytoadhesion, resetting and self-agglutination. Merozoites (not shown) and rings do not bind to human cells and circulate freely. When rings mature to the pigmented-trophozoite stage they bind to human cells through three different processes; cytoadhesion, resetting and agglutination; using any of the PfEMP1 protein family member placed on the surface of the iRBCs (adapted from Rowe, Claessens et al. 2009).

Adherent iRBCs trigger coagulation by inducing tissue factor and activating thrombin on the apical surface of endothelial cells. Thrombin catalyzes fibrin deposition in the blood vessels, amplification of inflammation and disruption of endothelial barrier integrity through protease-activator receptor signalling. This leads to further obstruction of microvessels and injury of endothelial cells. This in turn will cause tissue hypoxia which contributes to metabolic acidosis, a severe malaria syndrome. These mechanisms contribute to severe malaria organ-specific syndromes such as cerebral malaria, placental malaria, respiratory distress etc. (Miller, Ackerman et al. 2013) but other factors are at play.

1.1.2.2 Other contributing factors in this pathogenesis

Haemolysis of infected RBCs occurring due to release of merozoites and uninfected by-stander RBC lysis causes anaemia that may be exacerbated by impaired erythropoiesis. Haemolysis also contributes to endothelial injury and dysfunction due to free haemoglobin (Elphinstone, Riley et al. 2015). Reduced deformability of iRBCs is extended to uninfected RBCs in severe malaria, further worsening the compromised flow and increasing the fragility of the RBC. However, splenic immunologic and filtration clearance functions are then augmented and this accelerates the removal of both parasitized and uninfected RBCs (World Health Organization 2014).

Not all iRBCs are cleared, as the remaining mature sequestered trophozoites/schizonts will mature and rupture to release merozoites and red cell material, which will lead to fevers and rigors. The fever that accompanies each burst of mature schizonts synchronises the asexual cycling in the untreated host as this temperature is damaging to mature parasites. This parasite age-related synchrony leads to regular fever spikes, chills and rigors; such regularity is used to classify the malaria fever pattern as quotidian, tertian or quartan (World Health Organization 2014). The occurrence of fever, rigors and chills is mediated by the activation of monocyte-macrophages and excess production of TNF-α&β, with a burst of TNF-β being closely associated with faster parasite growth and suppression of pro-inflammatory cytokines (Walther, Tongren et al. 2005). Host innate immune response and inflammatory related cytokines and chemokines play a major role in disease severity (reviewed in Stevenson, Riley 2004) and it has been shown that there is a heritable strain dependent induction of specific cytokines and chemokines which may control parasitaemia in murine models (Pattaradilokrat, Li et al. 2014). There is also elevated levels of circulating cytokines, including; interleukin (IL) -1β, IL-6, IL-8, IL-10, and HMGB-1 (Francischetti, Seydel et al. 2008) during the elevated body temperature. Adaptive immunity in the form of antibodies produced against

antigenically variant protein family groups exposed on the surface of iRBCs including PfEMP1, SURFINs and RIFINs also reduces the host's parasite burden. Other surface antigen family groups include STEVORs, PfMC-2TMs and SURFINs, but PfEMP1 family is the most important (reviewed in Chan, Fowkes et al. 2014). Immune mediators have varying effects on the parasite biology and may influence the disease manifestation (LeRoux, Lakshmanan et al. 2009; Quintana, Ch'ng et al. 2018).

In addition to the microcirculatory obstruction, endothelial cell dysregulation and immune activation, the parasite exhausts the host's nutrients especially glucose, with a potential for a development of hypoglycaemia in the host which may be further complicated by a reduced appetite or the presence of starvation. Sequestered parasites may compete for host nutrients directly with an adjacent endothelial cell, and this deprivation can contribute to the pathogenesis of *P. falciparum* (reviewed in Newton, Krishna 1998).

It is important to note that a combination of mechanical microcirculatory stress due to sequestration and an excess of inflammatory response encompasses the mechanisms that lead to the various severe malaria disease phenotypes. An in-depth discussion on one of the parasite virulence factors that specifically mediates immune evasion, the PfEMP1, will be presented in subsequent chapters. Also, the various syndromes arising from the development of a severe disease will be discussed in the next section.

1.1.3 Severe disease phenotypes

Severe malaria is characterized by high parasitaemia (World Health Organization 2014), with corresponding increase in microcirculatory and metabolic pathological effects following endothelial activation and pro-inflammatory/pro-coagulatory events. This leads to syndromes of severe malaria including acute respiratory distress (ARD) due to metabolic acidosis, cerebral malaria (CM) and severe anaemia mainly in children. In addition to these,

adults may also have organ specific syndromes like placental malaria, renal failure and liver dysfunction. One or more of these syndromes may manifest in the severe disease and other symptoms like pulmonary oedema, hypoglycaemia and disseminated intravascular coagulation may be pronounced (World Health Organization 2014). When multiple organ dysfunctions become evident, death may be inevitable (Gomes, Vitorino et al. 2011).

The case fatality rate of severe malaria, especially CM, has not changed significantly for two decades (Manning, Laman et al. 2014). It manifests as unarousable coma often with convulsions, and not due to other causes. A Glasgow coma score of < 11 for adults or a Blantyre coma score of < 3 for children (World Health Organization 2014; Miller, Ackerman et al. 2013) is indicative of this syndrome. Visual examination of the retina enhances the coma diagnosis and the occurrence of papilledema and retinal haemorrhage indicates increased fatality (Miller, Ackerman et al. 2013). The blood brain barrier (BBB) is functionally intact in adult CM despite a mild generalized increase in vascular permeability. However, in children with CM, there is disruption of the endothelial tight junctions of the cerebral capillaries such that the BBB losses some of its integrity. Therefore, a raised intracranial pressure occurs more commonly in children than in adults. Among those that survive CM, < 3% of adults will suffer some neurological sequelae, whereas 3-15% of children, especially those with other severe malaria syndrome(s), will have some neurological disorder such as; hemiplegia, cortical blindness, cerebral palsy, impaired cognitive and learning ability (World Health Organization 2014). The pathology of CM may be driven by thrombin, a factor that is involved in endothelial activation and platelet induced agglutination, which also mediates pro-and anti-inflammatory pathways in CM (Wassmer, Grau 2017).

Severe anaemia is a frequent, rapidly occurring clinical feature of malaria with a 1% fatality (Miller, Ackerman et al. 2013), and is most common in young children in areas of moderate and high transmission (World Health Organization 2014). It is a haemoglobin

concentration of ≤ 5 g/dL or haematocrit of ≤ 15% (Newton, Krishna 1998) in children or < 7 g/dl or < 20% in adults (World Health Organization 2014). Pregnant women and children are particularly susceptible. Anaemia results from splenic clearance of iRBCs and uninfected RBCs, and this is especially increased in severe malaria as the erythrocytes become less deformable. Lysis of iRBCs upon release of merozoites contributes to it. Immune-mediated lysis and phagocytosis plays a major role in the pathogenesis of malaria anaemia (reviewed in Autino, Corbett et al. 2012). It was detected in 79% of children infected with the malaria parasite in areas of high transmission between 2015 and 2017 (World Health Organization 2018).

Metabolic acidosis, manifesting physically as ARD, occurs in 40-60% of severe malaria cases and has a 15% mortality rate. It occurs due to a shift from aerobic metabolism to anaerobic metabolism in inadequately perfused tissues. Lactate accumulates due to production via anaerobic respiration, which is not matched by increased excretion in severe malaria (Newton, Krishna 1998). The parasite also produces lactate. Other organic acids also accumulate and this is why some authors refer to metabolic acidosis as just acidosis in severe malaria and not lactic acidosis (World Health Organization 2014). Indeed, recent studies demonstrated a delay in the clearance of some unmeasured acids also strongly associated with severe malaria (Leopold, Ghose et al. 2018; Herdman, Sriboonvorakul et al. 2015). Ten of these acids had originated from the gut microbiota and may have entered into the blood circulation following a compromised gut barrier (Leopold, Ghose et al. 2018). The accumulated lactate is, however, not adequately cleared due to reduced blood flow to the liver and kidney, as a result of sequestered iRBCs. One of the unmeasured acids, p-hydroxyphenyllactic acid (pHPLA), in the blood and plasma is closely associated with acute kidney injury in severe malaria (Sriboonvorakul, Ghose et al. 2018). Increased muscle activity during seizures, increased nutritional requirement and inhibition of mitochondrial glucose

oxidation will lead to increased anaerobic metabolism following poor tissue perfusion (Gomes, Vitorino et al. 2011). Acidosis in severe malaria is characterized by plasma bicarbonate of < 15mM or venous plasma lactate of ≥ 5mM. The protons from the dissociated acids, including lactic acid, and protons not used up in the Tricarboxylic acid cycle reduce the blood pH. Blood levels of lactate or bicarbonate, indirectly, predicts the severity of the disease (World Health Organization 2014). In fatal malaria, this may be accompanied by circulatory failure, refractory to intravenous bolus or inotropic drug administration, and respiratory arrest may result. Metabolic acidosis may be compounded by ketoacidosis in children or acute renal failure in adults (World Health Organization 2014) or anaemia (Gomes, Vitorino et al. 2011).

Complications from malaria infection can also be due to immune mediated inflammatory activity and endothelial damage resulting in pulmonary oedema (referred to as acute lung injury (ALI) or ARDS) (Autino, Corbett et al. 2012). Increased haemolysis and tissue consumption of glucose contributing to jaundice and/or haemoglobinuria and hypoglycaemia, respectively, have been reported (World Health Organization 2014).

Other complications of severe malaria following sequestration of the malaria parasite through its PfEMP1, in the microvasculature supplying a specific organ can occur and may include placenta malaria or pregnancy associated malaria (PAM), acute renal injury or liver dysfunction and other associated diseases or symptoms like jaundice and hypoglycaemia. PAM often leads to premature delivery, mortality of the foetus and severe anaemia in the mother (Pasternak, Dzikowski 2009) and a specific PfEMP1 variant, VAR2CSA, is known to be involved.

1.1.4 PfEMP1 in malaria pathogenesis

Binding of an iRBC to endothelial cells lining blood vessels is mediated by members of the PfEMP1 protein family. The expressed PfEMP1 protein varies and is selected for by a number of host factors, as has been demonstrated by PfEMP1-specific antibodies (Bull, Lowe et al. 1998). They are encoded by a diverse family of 60 *P. falciparum* genes called *var*, expressed as a full length transcript at the ring stage, with expression diminishing in the early trophozoites stage (Su, Heatwole et al. 1995; Kyes, Pinches et al. 2000). The *var* genes repertoire are grouped into three major subgroups; A, B and C and two intermediate groups; B/A and B/C; with the unique *var* gene *var2csa* standing alone as group E (Lavstsen, Salanti et al. 2003). The specific PfEMP1 variant adhesive property of the iRBCs plays a role in the pathology of malaria. PfEMP1s are associated with the presence of penetrating knobs on the RBC surface (Horrocks, Pinches et al. 2005), with their cytoplasmic tail anchored on Knob Associated Histidine Rich Protein (KAHRP) (Pasternak, Dzikowski 2009).

PfEMP1s are large proteins that are made up of an N terminal segment (NTS), variable numbers of Duffy binding-like domains (DBL; α-ε), one or two cysteine-rich interdomain regions (CIDR; α-γ) except for VAR2CSA, a trans-membrane (TM) domain and a conserved intra-cellular acidic terminal segment (ATS) (Mayer, Slater et al. 2012). However, their amino acid sequence differs considerably among the different parasite isolates, mainly in the DBL extracellular adhesion domains. Diversity is created by genetic recombination that generates new combinations of PfEMP1 structural domains. Thus, unlimited PfEMP1 variants can be generated, each with distinctive antigenic features within a parasite population (reviewed in Pasternak, Dzikowski 2009). PfEMP1 is important for building natural acquired clinical immunity, albeit a slowly developing incomplete one, synonymous with the recombination and slow switching of *var* expression that has been observed.

PfEMP1 is an antigen that elicits antibody-dependent immunologic responses which initially may enable the host to clear most of the infected cells from the circulation. However, the remaining parasites can switch their PfEMP1 to a different variant and avoid antibody-mediated clearance, thus increasing their biomass and maintaining a chronic infection (reviewed in Pasternak, Dzikowski 2009).

PfEMP1s are inserted into knobs on the iRBC where they bind to protein and carbohydrate ligands on the surfaces of endothelial cells, including cluster determinant 36 (CD36) (Robinson, Welch et al. 2003), intercellular adhesion molecule-1 (ICAM-1), platelet/endothelial cell adhesion molecule (PECAM) (Berger, Turner et al. 2013), complement receptor-1 (CR1) (Rowe, Moulds et al. 1997), heparin sulphate, endothelial protein C receptor (EPCR) (Turner, Lavstsen et al. 2013) and chondroitin sulphate A (Fried, Duffy 1996), etc. Different binding phenotypes cause sequestration in different organs leading to varying clinical presentations of severe malaria. PfEMP1 variants containing the DBLβ, principally the DBL2β member, encoded by upsA *var* group, binds ICAM-1 (Oleinikov, Amos et al. 2009). However, there is no clear association between ICAM-1 binding and severe malaria. Most PfEMP1s bind CD36 but such binding has only been shown to be associated with severe disease in two small studies done in Asia (as reviewed in Rowe, Claessens et al. 2009) but, a recent study showed that freshly grown iRBCs from uncomplicated malaria cases were significantly highly bound to CD36 compared to those from severe malaria cases (Ochola, Siddondo et al. 2011). Complement receptor-1 (CRI)-mediated rosetting may contribute to the pathogenesis of malaria as it binds PfEMP1. Rosetting frequency has been shown to be associated with disease severity and correlates well with DBLα1 PfEMP1 variant, encoded by *var* gene group upsA that are predominantly expressed in cerebral malaria patient parasite isolates (Kyriacou, Stone et al. 2006).

Expression of some of these receptors is partly mediated by tumour necrosis factor (TNF) and other inflammatory cytokines (Francischetti, Seydel et al. 2008, Wassmer, Grau 2017).

Recently, EPCR interaction with PfEMP1 subtypes has been proposed as a key player in the pathogenesis of severe malaria (Jespersen, Wang et al. 2016), following *in vitro* demonstration of interaction of recombinant(r) or native PfEMP1 subtypes with rEPCR/native EPCR. This settled the controversial involvement of coagulation cascade in the pathogenesis of malaria. Specific PfEMP1 subtypes containing domain cassette (DC) 8, 13 and 15, associated with severe malaria, were demonstrated to bind EPCR, inhibiting the binding of the cytoprotective activated protein C. DC8 was also demonstrated to bind to EPCR on endothelial cells of tissues of diverse origin (Turner, Lavstsen et al. 2013). PfEMP1s with DC8 are encoded by the upsB/A hybrid *var*, while those with DC13 & 15 are encoded by the upsA *var* (Lavstsen, Turner et al. 2012).

Parasites causing severe malaria most likely bind EPCR more than ICAM-1 (Turner, Lavstsen et al. 2013), but some PfEMP1 DC13 EPCR binding phenotypes use ICAM1 as a co-receptor (Avril, Bernabeu et al. 2016). Previous studies have shown that more than one receptor acts in concert to enhance cytoadherence (Baruch, Gormely et al. 1996; Scherf, Hernandez-Rivas et al. 1998), and recently, this has been demonstrated for iRBCs from cerebral malaria patients which bound to EPCR and ICAM 1, and additional binding to CD36 seemed to be important (Tuikue Ndam, Moussiliou et al. 2017). However, a recent study queried the effectiveness of EPCR binding using laboratory strain iRBCs expressing PfEMP1 variant containing DC8 and 13, with no binding for DC13 expressing phenotypes to EPCR on brain endothelial cells and a binding by DC8 expressing phenotypes, which was inhibited by normal human serum. Both variants bound significantly to other endothelial cell surface ligands that have not been shown to be associated with severe disease (Azasi, Lindergard et al. 2018). Contrarily, low level of EPCR binding was demonstrated to be required for the

interference of its function by PfEMP1 with DC8 (Bernabeu, Danziger et al. 2016) and additional binding to ICAM-1 may enhance EPCR binding in the severe disease (Avril, Bernabeu et al. 2016).

In addition to the existence of PfEMP1 variants binding to more than one endothelial receptor, a single iRBC in one study has been shown to express two distinct binding PfEMP1 variants on its surface and bind doubly effectively than single-PfEMP1-expressing iRBC (Joergensen, Bengtsson et al. 2010). This suggests that the prevailing dogma that each iRBC can express only one of the *var* gene repertoire at a time may be over simplified. Similarly, multi-specificity in PfEMP1 binding phenotypes can have important implications. For example, platelet-mediated clumping is important in the pathogenesis of cerebral malaria and CD36 is poorly expressed by the vascular endothelial cells of the brain but is present on the surface of platelets that accumulate in the brain microvasculature of cerebral malaria patients. A subset of PfEMP1s that are ICAM1 binders also bind CD36, although ICAM1 is the predominant vascular adhesin in the brain (Pasternak, Dzikowski 2009, Almelli, Ndam et al. 2014, Avril, Bernabeu et al. 2016). Co-receptor may thus function to enhance adherence.

A single distinct form of PfEMP1 encoded by *var2csa* is highly expressed by placental isolates, binds chondroitin sulphate A (CSA) and ultimately leads to clinical malaria in pregnancy which could be severe (Salanti, Staalsoe et al. 2003, Salanti, Dahlbäck et al. 2004, Tuikue Ndam, Salanti et al. 2005). CSA is present in the intervillous blood spaces of the placenta (McGregor, Wilson et al. 1983; Pasternak, Dzikowski 2009). *Var2csa* is relatively conserved and encodes a unique DBL domain different from that of other *var* genes (reviewed in (Rowe, Kyes 2004)). Other *var* genes types have been shown to be associated severe malaria in various studies as discussed below.

1.2 Association of severe malaria and *var* gene types

1.2.1 The structure of *var* genes and their chromosomal location

Most *var* genes are located near the telomeres of their respective chromosomes. The *var* gene coding region has two exons, with their DNA sequence encoding the various subunits of PfEMP1 protein as earlier explained in section 1.1.4 and shown in Fig. 1.3B; the first exon is polymorphic and encodes an external binding region of the PfEMP1, the second exon is conserved and encodes a tail region (ATS) in contact with the cytoplasm (Gardner, Hall et al. 2002). A *var* intron separates these two exons. *Var* genes have two promoters, one in the 5'UTR and another within the intron (Gardner, Hall et al. 2002; Deitsch, Calderwood et al. 2001), which encodes ncRNA (Frank, Dzikowski et al. 2006).

Var genes are grouped based on the sequence similarities of their coding region and their upstream region (ups), chromosomal location and transcription direction (Fig. 1.3A). Group A *var* are subtelomeric located, transcribed towards the telomere, share an ups region and most occur head to head with a *rif* gene. For group B *var*, the largest group, the upsB flanks their coding region, they are transcribed towards the centre and most members are telomerically located. Group C *var* are centrally located and share the upsC flanking region. The intermediate groups B/A have an upsB-like region but their coding sequence is similar to upsA, while B/C have characteristics similar to the major groups B and C. *Var2csa*, the unique *var* gene with the upsE region is located at a subtelomere (Lavstsen, Salanti et al. 2003).

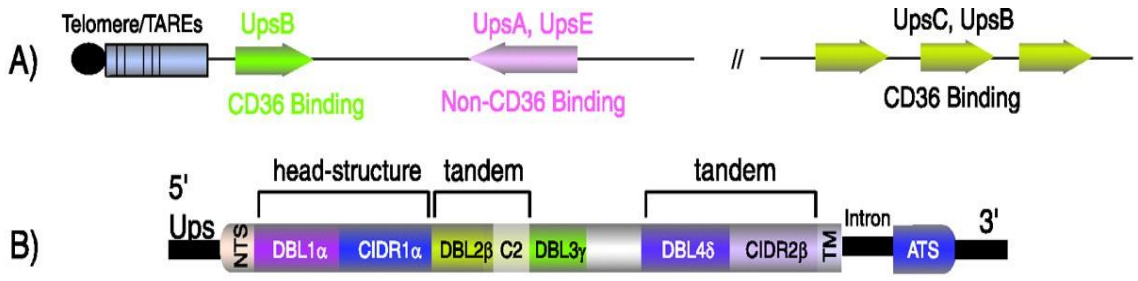

Figure 1.3: Chromosomal organization of *var* genes (Kyes, Kraemer et al. 2007). **A**: *var* genes are classified according to upstream promoter type and are found at the ends of most of the 14 *P. falciparum* chromosomes and clustered in internal regions on chromosomes 4, 7, 8, and 12. Arrows indicate the direction of transcription. TAREs, telomere associated repeat elements. **B**: The extracellular binding region of the PfEMP1 proteins now consists of three domain types: DBL, CIDR and the TM domains, explained in section 1,1,4. C2 is now part of the DBLβ domain (Howell, Levin et al. 2008; Rask, Hansen et al. 2010). DBL and CIDR domains are classified according to sequence similarity. VAR2CSA has no CIDR domain (reviewed in Kyes, Kraemer et al. 2007). NTS and ATS are segments.

The encoded PfEMP1 variants are functionally classified into domain cassette (DC) types based on the conserved arrangement of tandem cysteine-rich adhesion domains DBL and CIDR (Rask, Hansen et al. 2010). Despite the tendency of PfEMP1s to bind the major receptor on endothelial cells, CD36, some of the 10 members of the upsA *var* genes encode non-CD36 binders, PfEMP1s with DC13 head structure. Those with DC8 encoded by the B/A hybrid are also non-CD36 binders. UpsB and C are CD36 binders, while *var2csa* binds to only CSA (Francischetti, Seydel et al. 2008; Robinson, Welch et al. 2003; Avril, Bernabeu et al. 2016).

1.2.2 *Var* gene types and severe malaria

In the field, associations have been made between the following: *var* upsA and B/A and severe malaria (Kyriacou, Stone et al. 2006; Lavstsen, Turner et al. 2012; Jensen, Magistrado et al. 2004; Claessens, Adams et al. 2012; Storm, Jespersen et al. 2019; Rottmann, Lavstsen et al. 2006; Abdi, Fegan et al. 2014) ; upsB and either mild clinical or severe malaria compared to asymptomatic infections (Kaestli, Cockburn et al. 2006; Rottmann, Lavstsen et al. 2006); upsB and severe malaria (Merrick, Huttenhower et al. 2012) and *var2csa* and severe malaria in pregnancy (Salanti, Dahlbäck et al. 2004).

Distinct *var* subsets thus play a role in the parasite's virulence and disease presentation. To this end, a narrow range of *var* group subsets may be implicated in the severe disease presentations (Rottmann, Lavstsen et al. 2006; Almelli, Ndam et al. 2014). Broader *var* group subsets are expressed in the uncomplicated disease and it has been suggested that some uncomplicated disease may become severe with time following selection for parasites expressing a more limited *var* group subset (Kyriacou, Stone et al. 2006). In this study children with no symptom or sign of severe malaria had an equally high level of parasitaemia to children with cerebral malaria. The difference between the two groups was *P. falciparum* isolates from the children with cerebral malaria predominantly transcribed upsA or B/A *var* gene groups. The abundance of upsA and B var gene groups have been demonstrated to follow a pattern based on disease severity: it is more abundantly expressed in severe infections compared to uncomplicated malaria, and is more abundant in clinical malaria compared to asymptomatic infections. This highlights a 'bet-hedging' strategy and a tendency for parasites to cause a severe infection if they predominantly express upsA or B *var* or a hybrid of both groups (Kyriacou, Stone et al. 2006; Rottmann, Lavstsen et al. 2006,). In addition, upsA transcript tends to decrease with age in uncomplicated malaria (Rottmann, Lavstsen et al. 2006). UpsC *var* genes may be more abundant in asymptomatic infections

(Kaestli, Cockburn et al. 2006) or may not be different in the three outcomes of *Plasmodium* infection (Rottmann, Lavstsen et al. 2006).

The prognosis of malaria will thus vary as a result of differential expression of *var* gene subsets dependent on immune competency of the host at the time of infection. Two different serological profiles of antigenic response in malaria separated children that succumbed to severe malaria from those that had a mild malaria. Antigenic response has been shown to be narrower and short-lived in the severe disease compared to the mild disease (Tuju, Mackinnon et al. 2019). How these serological profiles relate to the upsA or B/A *var* gene groups and severe malaria remains to be explored. However, the level of *var* expression also plays a role in establishing disease (Abdi, Warimwe et al. 2016). Some specific host and parasite factors observed during severe malaria may be associated with *var* gene types that have been demonstrated to correlate with the severity of malaria.

1.2.3 Association between host or parasite factors in severe malaria and *var* gene type

Following repeated malaria infections, immunity develops slowly within a few years, capping at a partial immunity leading to majorly asymptomatic chronic infection (World Health Organization 2014). Resistance to severe malaria in children is not dependent on their ability to control the prevailing parasite burden (Gonçalves, Huang et al. 2014; Kyriacou, Stone et al. 2006) but their ability to persistently close gaps in their pre-existing more stable antibody repertoire (Bull, Lowe et al. 1998; Tuju, Mackinnon et al. 2019), staying ahead of the parasite's ability to switch to predominantly *var* genes of the upsA and B/A types (Abdi, Hodgson et al. 2017) or *var2csa* in pregnancy. These *var* types have previously been shown to be negatively associated with anti-PfEMP1 antibodies at the time of the disease (Warimwe, Keane et al. 2009) in addition to a possible selection against high *var* expression (Abdi, Warimwe et al. 2016). Futhermore, asymptomatic infections have higher homogenous *var*

expression than clinical infections and a broader host antibody response (Warimwe, Recker et al. 2013; Duffy, Noviyanti et al. 2016). Thus, although the parasite switches to PfEMP1 variants that enable it to effectively adapt, causing a severe disease, the host's immunity eventually catches up in most cases. But in some cases the disease becomes severe.

In patient isolates, expression of different PfEMP1 groups has been shown to vary independently with an additional likelihood of a reduced global level of *var* expression contributing to the ability of the parasites to evade the host's immunity (Abdi, Warimwe et al. 2016). Surface expression of PfEMP1 can also be modulated due to altered transport, and was reduced on iRBCs causing a severe disease (Tonkin-Hill, Trianty et al. 2018). This can be likened to an early *in vitro* study where reduced adhesion of knobless clone A4 iRBCs was due to about 50% reduced protein level of PfEMP1 expression and similarly reduced exposure of PfEMP1 on its surface compared to knobby clones; however, the *var* transcript levels of both clones were similar (Horrocks, Pinches et al. 2005). Thus, PfEMP1 expression can be varied at multiple levels, including transcription, translation and protein export.

Specific host factors in severe malaria (febrile temperature and blood lactate level) have been shown to be positively associated with the parasite sirtuins. Febrile temperature has been shown to be associated with high expression of parasite sirtuins; PfSir2A and B-which silence inactive *var* genes, considerably (Merrick, Huttenhower et al. 2012,) or marginally (Abdi, Warimwe et al. 2016). Equally hyperlactatemia has been shown to be positively associated with these sirtuins. However, only increased *PfSir2A* was in turn associated with increased expression levels of a subset of severe disease-associated *var* genes; upsB *var* in Gambian children with severe malaria *vs* mild malaria. This was in line with a transgenic 3D7 laboratory strain that over expresses *PfSir2A* (Merrick, Huttenhower et al. 2012). In addition, a more recent study has extended this positive association to upsA, upsB/A and upsC, with antibodies to the iRBC being negatively associated with *PfSir2A* (Abdi, Warimwe et al.

2016). The research within this thesis was devoted to following up on this association, as detailed in section 1.6. But first, a review of the regulation of the *Plasmodium* genome and *var* genes specifically is needed to foster an understanding of how the parasite responds to changes in host factors.

1.3 Transcriptional regulation of *Plasmodium* gene expression

1.3.1 Transcriptional regulation of the *Plasmodium* genome

10 years ago, the basis for multi-layered regulatory framework acting in concert to regulate the *Plasmodium* genome was extensively reviewed (Horrocks, Wong et al. 2009). The authors emphasized that although there could be a layer of hard-wired control of gene expression, temporal control is majorly manifested throughout the parasite's multi-staged lifecycle. Hard-wired control was proposed to break down when the parasite encounters stress as it would in the human host. This was supported by the poor correlation between mRNA abundance and protein accumulation at some points in time in the parasite's lifecycle, which may imply that gene expression is predominantly controlled post-transcriptionally (Horrocks, Wong et al. 2009). In addition, the paucity of trans-acting transcriptional regulatory factors of *Plasmodium* gene expression indicated that there may be a major posttranscriptional mechanism at play or alternatively, a hardwired transcriptional programme requiring usually few specific transcription factors. Proteins that may modulate mRNA decay or translation rates were suspected to be abundant (Coulson, Hall et al. 2004). However, recent studies have identified a number of transcriptional regulatory proteins (still a small number compared to > 1600 in humans (Lambert, Jolma et al. 2018) and other layers of transcriptional regulation. Such regulatory proteins include 27 putative AP2 (Apetala2)-integrase DNA binding domain transcription factors in apicomplexans (Jeninga, Quinn et al. 2019; Balaji, Babu et al. 2005) also called the ApiAP2 family of DNA-binding proteins.

Timely transcriptional regulation during the IDC of *P. falciparum* is important as it is required to maintain its distinct morphological stages in its varying niches/host environment and for the generation of antigenically diverse phenotypes needed to ensure establishment of a chronic infection. One way to achieve this would be the 'just in time' transcriptional cascade proposed by Bozdech (Bozdech, Llinás et al. 2003), with the master-regulator AP2 transcription factors probably controlling the cascade. However, this model is simple and is probably nuanced by other factors like post-transcriptional and translational regulation, and possibly by elements of responsiveness to environmental conditions.

The "just in time" hypothesis has been supported by the finding that peak mRNA transcription occurs before peak mRNA abundance for the majority of genes. There are majorly four bursts in mRNA regulatory activity which coincide with stage transitions (Painter, Chung et al. 2018), thus mirroring temporally discrete clusters of function- or process-related mRNA transcript accumulation (Horrocks, Wong et al. 2009). The first burst involves maximum transcription/stabilization of antigenic variation-related genes at the mid-ring stage. Phase-specific genes are transcribed maximally at the various developmental phases of the trophozoite stage. Thus, the second burst involves transcription of genes unique and functionally important for the early trophozoite stage. Thirdly, maximum transcription/stabilization of genes encoding amino acids, tRNA and ncRNA, and metabolic process-related genes occurs at the mid-trophozoite stage of peak parasite metabolism. And, finally, transcription/stabilization of genes involved in the regulation of DNA metabolism and replication enriches the last burst of mRNA peaking at the late trophozoite stage (Painter, Chung et al. 2018). However, it was earlier shown that a continuous cascade of accumulation of mRNA does occur for a majority of genes, transcribed simultaneously during the trophozoite stage of the IDC with only a small subset of genes being subject to differential transcriptional timing. RNA polymerase II was shown to engage with promoter regions prior

to this transcriptional burst and this implicates RNA pol II as a dominant gene regulator in this parasite stage (Lu, Batugedara et al. 2017). But this discrepancy was linked to the application of chemical perturbation that likely biased the measurement of mRNA turnover (Painter, Chung et al. 2018).

In addition, Painter *et al.*, showed that a few genes are maximally transcribed/stabilized at time points in the life-cycle, other than described above, reflecting schizogony/schizont burst or merozoite invasion. At 48hpi more transcript stabilization occurred than transcription (Painter, Chung et al. 2018) reflecting an increased mRNA half-life as demonstrated earlier (Shock, Fischer et al. 2007; Ponts, Harris et al. 2010). And, maximum mRNA transcription of genes encoding invasion process-related and niche-establishment-related proteins occurs at this time point. The highest peak transcription occurs at 1hpi and involves genes that encode RNA metabolic process-related proteins (Painter, Chung et al. 2018).

One layer of temporal control of *P. falciparum* gene expression is the binding of trans-acting factors to specific sequences upstream of the transcription start site (TSS) of a coding region. Bioinformatics analysis has revealed that *P. falciparum* has key components of the pre-initiation complex including 12 subunits of RNA polymerase II. However, the GTF TFIID complex appears to be different from that of eukaryotes. The PfTATA binding protein (PfTBP) component of TFIID binds to the TATA core promoter sequence upstream of the TSS, a region that has not yet been well defined/conserved in *P. falciparum*. PfTBP potentially recognises and promotes transcription from cryptic TATA box sequences (reviewed in Horrocks, Wong et al. 2009). Cis and trans-acting factor(s) will typically control the activity of RNA pol II on the gene promoter, but this has been strongly proposed as a major regulatory mechanism during the ring-stage development compared to other stages of the parasites asexual development (Russell, Emes et al. 2015).

Thus, morphological transitions during blood stage asexual cycling of *P. falciparum* indicates stage-specific regulation of mRNA turnover and a dynamic control of gene expression facilitated by layers of regulatory mechanisms including cis/trans factor modulation of promoter transcription initiation. These include posttranscriptional regulation and epigenetic control mechanisms (Volz, Carvalho et al. 2010), which could be pre/post-transcriptional, translational or post-translational (Vembar, Scherf et al. 2014).

1.3.2 Genetic and epigenetic regulation of the *Plasmodium falciparum* genome

Epigenetics is the chemical alteration of the genetic machinery in order to regulate gene expression without changing the genetic code, and the resulting chemical markings can be passed from one generation to the next. It has been suggested that due to parasite diversity in the field and the array of host factors which is obtainable *in vivo*, the epigenetic control mechanism as we currently know it through *in vitro* studies may be different from the *in vivo* situation (Merrick, Duraisingh 2010).

The expression of *P. falciparum* genome is easily modulated in order for it to adapt to different environmental changes and develop distinct morphological stages during its lifecycle. This involves chromatin remodelling. The parasite genome has been shown to be in a transcription-permissive state during most of its lifecycle, specifically in the early trophozoite and schizont stage. This is brought about by a change of chromatin to a euchromatic state after the parasite invades the red blood cell and a reversal back to a heterochromatic state before the end of its lifecycle. The nucleosomes have a high density at 0-12 hour post invasion (hpi) of the ring stage, and are massively depleted at about 18 hpi. This is followed by a gradual repositioning from about 24 hpi, with maximum repositioning at 36 hpi. The promoter regions seemingly follow this change in nucleosome occupancy except for promoter regions of *var* genes and genes expressed at the early stage of the parasite's

lifecycle. At the ring stage there may be a classical chromatin loosening/tightening in phase with genetic expression, as the chromatin is generally denser (Ponts, Harris et al. 2010). This observation is supported by the work of Painter *et al*. (Painter, Chung et al. 2018). However, it also reveals that the process driving gene expression in *P. falciparum* does not occur mostly at the transcription initiation level (Ponts, Harris et al. 2010).

Exons are mostly bound to histones and show higher nucleosome occupancy compared to introns. Chemical residues are placed on these histones, with resultant modulation of the accessibility of the transcription machinery. This leads to a remodelling of the chromatin which has been shown to occur in more than half of the genes with the exception of ring stage-specific genes (Ponts, Harris et al. 2010; Bunnik, Polishko et al. 2014).

It has been suggested that *P. falciparum* uses 'Bet-hedging' to adapt to changes in the host environment. This describes the alteration to transcriptional responses that directs a subset of the parasite population to diversify their gene expression. This is supported by the finding that a genetically homogenous clonal parasite population in the asexual blood stage shows a heterogeneous expression pattern of specific genes and gene families, many of which are subtelomeric and encode proteins exported to the surface of the iRBCs. This heterogeneity was demonstrated to be regulated epigenetically and the genes impacted are majorly genes involved in host-parasite interactions, with a minority being genes for erythrocyte remodelling, protein folding, transcriptional regulation, etc. This indicates that epigenetics results in both antigenic and functional variation (Brancucci, Bertschi et al. 2014). This heterogeneity was demonstrated to favour a survival of the fittest under environmental pressure with an adaptation being maintained after removal of the stressor, thus suggesting an involvement of epigenetics (Rovira-Graells, Gupta et al. 2012).

Epigenetics in the *Plasmodium* genome occurs through the following processes: replacement of histones by histone variants, post-translational modifications (PTM) of histones, chromosome remodelling, DNA methylation, sub-nuclear localization of expression competent sites (reviewed in Cui, Miao 2010), and the emerging regulation of DNA by noncoding RNA (reviewed in Vembar, Scherf et al. 2014). A specific combination of these epigenetic modifications that determines the functional and structural features of each genomic region is what is referred to as the epigenetic histone code (Trelle, Salcedo-Amaya et al. 2009; Rovira-Graells, Gupta et al. 2012).

1.3.3 The histone code in *P. falciparum*

P. falciparum has 8 histones; H4, 3 H3s (H3, H3.3 & H3 centromeric(CenH3) and 4 H2s (H2Bv, H2A, H2A.Z and H2B). Each has a basic N-terminal tail, a globular domain (the histone fold) and a C-terminal tail. cenH3, H3.3, H2Bv and H2A.Z are variant histones different from the core histones encoded by eukaryotes. The N-terminal tail plays a role in regulating higher order chromatin structure. Histones undergo numerous post-translational modifications (PTMs) (Fig. 1.4), individually and with each other, most of which are associated with a euchromatic state (Trelle, Salcedo-Amaya et al. 2009; Karmodiya, Pradhan et al. 2015; Coetzee, Sidoli et al. 2017). PTMs can be reversed. The major modification is acetylation, a mark associated with activation for example H3 is acetylated at the lysine (K) residue at position 9,14,18,23,27and 56; H3.3 in all these positions except position 56; while H4 is acetylated at K5, K8, K12 and K16 (Trelle, Salcedo-Amaya et al. 2009). H2Bv, H2A and H2A.Z are mostly acetylated. Other residues could be marked with methyl, phosphoryl, SUMOyl and ubiquityl markers. Most possible modifications are depicted in Figure 1.4 below and multiple modifications occur. Histone modifications that generate a permissive or poised

gene state are commonest throughout the genome (Trelle, Salcedo-Amaya et al. 2009).

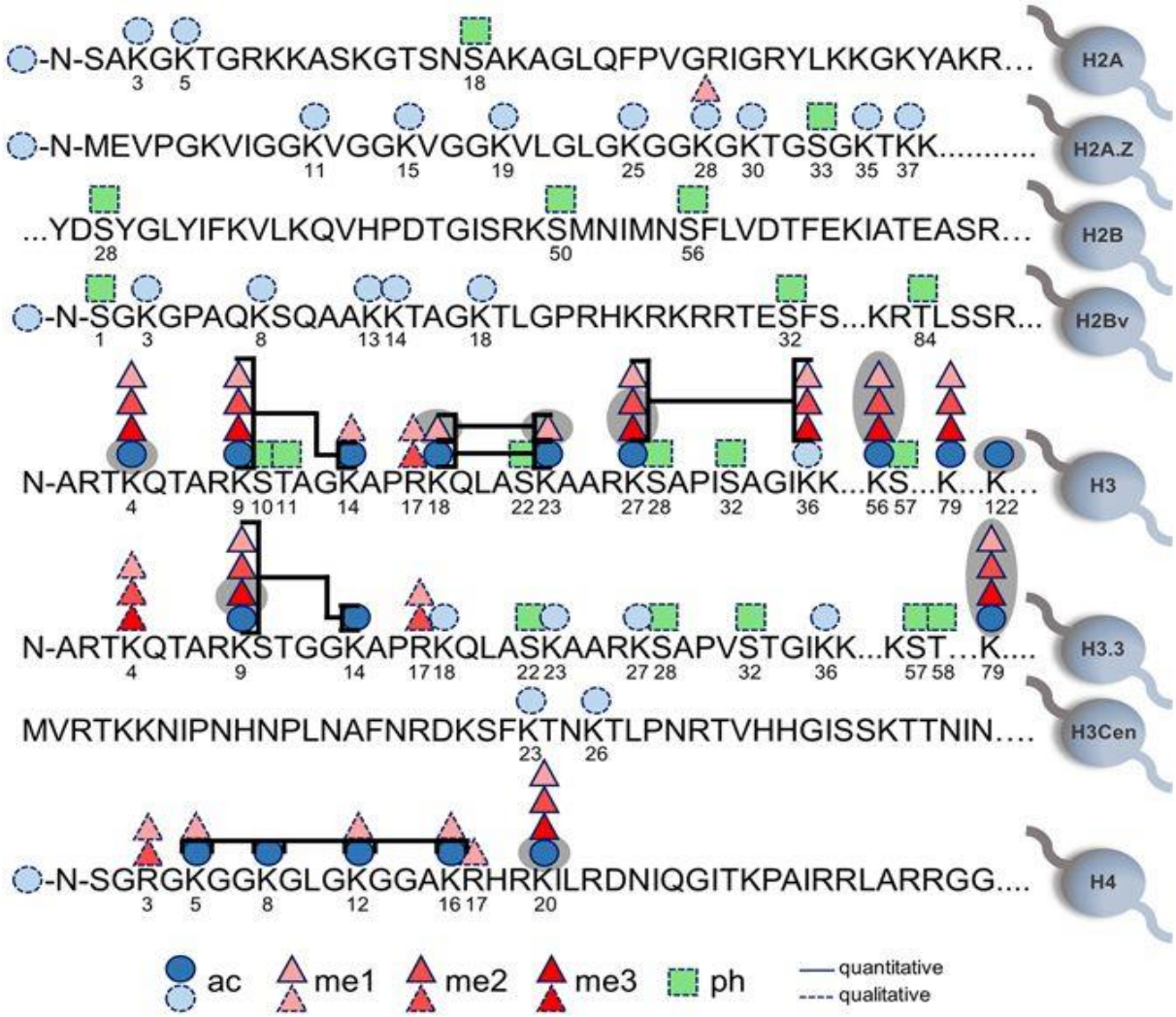

Figure 1.4: Histone Modifications of core and variant histones (Coetzee, Sidoli et al. 2017)

A wide array of histone PTMs is shown including 15 novel PTMs that were identified for the first time (Grey shaded PTMs) in the above study. 106 PTMs were identified (qualitative, dashed line), but only 46 of these were quantifiable in all stages over life cycle development (quantitative, solid line). Co-existing histone PTMs on individual peptides were also identified (brackets). The histone markings represented are ac for acetylation, me1 for monomethylation, me2 for dimethylation, me3 for trimethylation and ph for phosphorylation.

The degree of PTM of histones is possibly regulated by the readers, trans-acting factors that may recruit writer proteins that deposit these epigenetic markings, and erasers that remove such epigenetic markings. Writer proteins include families of histone methyltransferases (HMTs), demethylases, histone acetyltransferases (HATs) and deacetylases (HDACs).

HATs acetylate histones and examples include the *P. falciparum* GCN5 homologue (PfGCN5) (Fan, An et al. 2004) and *P. falciparum* MYST (PfMYST) HAT (Miao, Fan et al. 2010). PfGCN5 preferentially acetylates H3, adding acetyl residues at position K9 and K14. PfGCN5may also interact with *P. falciparum* alteration/deficiency in activation protein 2 (PfADA2) *in vivo* as it does *in vitro* (Fan, An et al. 2004). PfMYST preferentially acetylates H4 at K5, K8, K12 and K16, *in vitro* (Miao, Fan et al. 2010). In mammalian systems some TATA binding associated proteins have been shown to have HAT activity. *PfGCN5* has a bromodomain region (Fan, An et al. 2004) and acetylated histone tails may directly recruit trans-factors through the binding of bromodomain proteins (Volz, Carvalho et al. 2010). Therefore, HATs may be involved in transcription initiation.

Acetyl residues are removed by epigenetic erasers like *P. falciparum* histone deacetylases (PfHDACs) belonging to class I, II and III. These include PfHDAC1, PfHDA1 & 2 and the *P. falciparum* sirtuins (PfSIR2A and B) (Joshi, Lin et al. 1999; Coleman, Skillman et al. 2014, Freitas-Junior, Hernandez-Rivas et al. 2005, Tonkin, Carret et al. 2009) discussed in section 1.5. The importance of PfHDACs in the regulation of *Plasmodium* genome has been demonstrated by a study that showed the inhibition of HDAC class 1 and 2 deacetylase activity by apicidin led to deregulation of the parasite genome with a 90% reduction in parasite growth. This was characterized by rapid activation and repression of a large portion of the genome as a result of the disruption of histone modification manifesting as hyperacetylation. This resulted in the induction of genes normally repressed or vice versa,

at a particular stage, during the IDC, and exoerythrocytic genes. This may have resulted from an up-regulation of genes that encode stage-specific transcriptional factors generally (Chaal, Gupta et al. 2010).

PfSET2, a HMT, has been found to enrich telomeres with H3K36me3. In gene bodies H3k36me3 has been found to moderately positively correlate with transcription (Karmodiya, Pradhan et al. 2015). By contrast, a global repression of gene transcription by the H3K36me2 mark, when virulence genes were excluded, was revealed by a genome wide mapping of multiple histone modifications in the ring, trophozoite and schizont blood stages. On a particular histone residue more than one marking may occur (Fig 1.4) at different degrees. This highlights the complexity of the histone code, and the possibility of genes being activated dependent on the ratio of activation marks to repressive marks (Karmodiya, Pradhan et al. 2015). Indeed, acetylation occurs in a coordinated fashion with methylations at the N-terminal of histones H3 and H3.3 (Coetzee, Sidoli et al. 2017). H3K27me3 is also another silencing mark (Trelle, Salcedo-Amaya et al. 2009). Peak histone marking occur at the 5' end of highly expressed single transcript genes, while genes associated with stimulus dependent function, and having bidirectional promoters, have peak markings in their gene body (Karmodiya, Pradhan et al. 2015). (A diagram here would be nice as suggested by prof.)

H3K4me2, H3K9ac, H3K14ac and H3K4me3 are active marks that occur in multiples at the promoter regions and positively correlate with transcription. When this occurs in an H2A.z histone, the chromatin will be active or 'poised' (i.e. high histone activation with no transcription) (Karmodiya, Pradhan et al. 2015; Rovira-Graells, Gupta et al. 2012). The intergenic regions of transcribed genes are enriched in H3K9ac and H4K8ac (Trelle, Salcedo-Amaya et al. 2009). Intergenic regions of genes whether transcribed or not are enriched in H3K4me3 (Gupta, Chin et al. 2013) but the level is reduced in repressed genes (Karmodiya, Pradhan et al. 2015). In addition, there appears to be a stage specificity of histone markings.

In rings, H3K4me3 and H3K9ac are homogenous across the genes, marking active and inactive genes equally, whereas in schizonts, they are enriched at the 5′ end of active genes (Salcedo-Amaya, van Driel et al. 2009).

Nucleosomes are generally transcriptionally repressed at the ring stage and replacement of the core histones with variant ones during active replication can alter their stability and chromatin pattern. Expression of core histones increases 2-3 folds during the transition from ring to early trophozoite, peaking at the late trophozoite and schizont stage with a 4-fold increase. H2Bv slightly decreases in early and mid trophozoite. H2A.Z increases 5 fold in schizonts and H3.3 has a 2.4-fold increase in schizonts (Miao, Fan et al. 2006). However, the regulation of clonally variant multi-copy (CMV) genes, for example the *var* gene family is different from the rest of the *Plasmodium* gene.

1.4 Regulation of *var* gene expression

Allelic exclusion of *var* genes is not absolute for all the parasite strains. However, a single dominant *var* within one life-cycle is exclusively transcribed for most parasite strains (Painter, Chung et al. 2018). NF54 strain has been shown to undergo mutually exclusive expression of *var* genes (Merrick, Jiang et al. 2015); the A4 strain shows this to an extent; however, this does not occur in 3D7 with more than one *var* being transcribed to similar levels in a clonal population (Joergensen, Bengtsson et al. 2010). Furthermore, levels of *var* expression in 3D7 may be 10 times higher than in NF54 (Merrick, Jiang et al. 2015).

Antigenic variation of the expressed PfEMP1 protein is achieved by the switching off of the active *var* gene and the switching on of a different *var* gene by the parasite, bringing about encoding of a different PfEMP1 variant on the surface of the iRBCs. The rate at which *var* genes are activated (switched-on) or silenced (switched-off) varies dramatically for different *var* and the rate of switching is dependent on the *var* local chromatin environment

and there is an in-between repressive (poised) state of the active *var* (Horrocks, Pinches et al. 2004). A clonal population of parasites expressing central *var* genes rarely undergoes transcriptional switching in the absence of a selective pressure but a population expressing subtelomeric *var* genes has a higher off rate and switches to an alternative *var* readily. Switching is determined by the chromosomal location of the *var* gene (Frank, Dzikowski et al. 2007). For example, a centrally located upsB *var* gene, PFD0625c, was continually transcribed in clones of 3D7 with negligible off rate over 145 generations (Merrick, Dzikowski et al. 2010). In addition, there are differential inter strain and inter clone switching rates (Frank, Dzikowski et al. 2007; Recker, Buckee et al. 2011).

There appears to be no predetermined order of *var* switching *in vitro*, with switching history having no effect on switch direction *in vitro* (Frank, Dzikowski et al. 2007) and *ex vivo* (Ye, Zhang et al. 2015). However, there could be an element of a structured switching during the early phase of an infection as the parasite attempts to balance out intrinsic parasite switching and immune selection. A more structured switching is needed to maintain a chronic infection in an immune naive individual and re-establish infection in a semi-immune individual (Recker, Buckee et al. 2011). It has been established that *var* genes do not always switch to predominantly *var2csa* following prolonged *in vitro* culture without selection (Merrick, Dzikowski et al. 2010) as previously suggested (Mok, Ribacke et al. 2008), possibly because *var2csa* has a high off rate (Frank, Dzikowski et al. 2007). But it has been proposed that activation of a singular *var2csa* could be an intermediary switching route used by parasite as it attempts to maintain antigenic variation (Ukaegbu, Zhang et al. 2015), as *var2csa* is not subject to the same control as other *var* genes (Mok, Ribacke et al. 2008; Amulic, Salanti et al. 2009; Bryant, Regnault et al. 2017). In addition, PfSET2 recruitment by RNA pol II is probably required for the activation of other *var* genes except *var2csa*, as its transcription is not consistent with the recruitment of PfSET2 by RNA pol II (Ukaegbu, Kishore et al. 2014).

This possibly signals that *var* gene switching is triggered at the level of transcription initiation and directed by the alteration of the chromatin marking at various gene regulatory regions. Despite a discrepancy in the order of *var* gene switching or route, what can be agreed is that a regulated switching rate is needed for establishing a chronic infection, where all the *var* genes are not expressed within a few generations (Chookajorn, Dzikowski et al. 2007). This requires an epigenetic memory.

Fastman *et al.*, used promoter titration to silence all *var* genes to minute levels in order to study *var* gene expression pattern and switch rate of an antigenically naïve merozoite during asexual cycling. The authors demonstrated that at the onset of *var* switching, multiple *var* genes are expressed to similar low levels, with the level of expression increasing with generations and a switch to particular *var* subset away from the Ups A group after 3 months of culturing and a tendency for internal/central *var* genes to be expressed. Low proportions of *var* genes are highly activated under normal *in vitro* culture conditions. Ups A *var* genes are highly conserved and have a low probability of being activated (Fastman, Noble et al. 2012).

DNA methylation was previously thought not to regulate *var* expression (Choi, Keyes et al. 2006); however, non-CpG island hypermethylation in the TSS and end of genes has now been described, with hypomethylation occurring at the 5' flanking region of highly expressed genes. These methylations constantly occur around the H3K9me3 and H4K20me3 epigenetic silencing marks, implicating them in gene silencing (Ponts, Fu et al. 2013).

Var gene expression follows a temporal pattern, occurring within the first half of the parasite's lifecycle at the ring stage, and reaching a maximum at 11 hpi (Painter, Chung et al. 2018). The control of *var* genes has been suggested to be different for the different *P. falciparum* strains (Merrick, Jiang et al. 2015) but involves different layered mechanisms that co-exist. *Var* gene expression is regulated at the level of individual *var* genes and is 5'

promoter driven, but these promoters are regulated at the level of initiation of transcription, post-transcriptionally, and epigenetically along with nuclear repositioning of chromatin.

Var gene promoter initiation of transcription is regulated. Bidirectional promoters within the *var* intron specifically produce both sense and antisense long non coding RNA (lncRNA) which regulates exon 2 and 1, respectively (Epp, Li et al. 2009). The role played by noncoding RNAs in the mediation of the epigenetic regulation is explained here (Vembar, Scherf et al. 2014). *Var* introns are able to encode ncRNA which interacts with the *var* promoter to mediate silencing (Frank, Dzikowski et al. 2006). Upon spontaneous deletion of this cis-acting element in the intron, the *var* can be activated. Disruption of intronic cis-acting DNA elements has been shown to suppress the expression of upsA, B and C *var* genes but not *var2csa*. Cis-acting elements specific to each *var* gene subgroup; introns and 3'UTRs have been shown to regulate *var* group A *var* expression. Their introns decreased the promoter activity of a lowly expressed, inactive upsA *var* gene, in a process involving blunting of maximal expression at 10-16 hpi, while their highly conserved 3'UTR, called DownsA further decreased expression. This study was done using a transgenic line and did not demonstrate if the UpsA gene was translated at biologically active levels into PfEMP1s. But both elements were shown to delay time to maximal *var* expression. In addition, DownsA non-specifically reduced mRNA stability. DownsA may contain an insulator that restricts the spread of an epigenetic mark of silencing (H3K9me3) for *var* genes (Muhle, Adjalley et al. 2009).

In the same vein, antisense lncRNA originating from the conserved *var* introns has been demonstrated to be associated with a single active *var* where it is incorporated into chromatin (Epp, Li et al. 2009) in order to maintain epigenetic memory. Interruption of this antisense lncRNA resulted in a downregulation of the active *var* and activation of a silenced *var* when in trans (Amit-Avraham, Pozner et al. 2015). Similarly, an exogenous artificial antisense lncRNA was demonstrated to be responsible for the expression of an additional *var*

together with the dominant active *var* (Jing, Cao et al. 2018). Transcription of lncRNAs from the *var* introns by RNA polymerase II leads to the recruitment of PfSET2 (Epp, Li et al. 2009; Kyes, Kraemer et al. 2007) to both silent and active *var* genes (Ukaegbu, Kishore et al. 2014).

A particular *var* gene may be expressed but it may not be translated to functional PfEMP1, as this protein does not feedback on the *var* gene (Dzikowski, Frank et al. 2006). Indeed, parasites have been demonstrated to switch to *var* genes that are highly transcribed, sparsely translated to PfEMP1 and not exposed on the iRBC (Mok, Ribacke et al. 2008; Bryant, Regnault et al. 2017). This indicates that translational or post-translational mechanisms may regulate PfEMP1 expression.

Var genes were previously shown to be regulated exclusively at the level of transcription using transgenic lines (Dzikowski, Frank et al. 2006) but this has been disproved as post-transcriptional control has been demonstrated both for upsC *var*, by elements in the 5'UTR (Brancucci, Witmer et al. 2014) and for *var2csa* (Mok, Ribacke et al. 2008) which is reversible (Amulic, Salanti et al. 2009; Bancells, Deitsch 2013; Bryant, Regnault et al. 2017). Recently, deletions of *var* intron using CRISPR technology in the native chromatin resulted in the upregulation in *var2csa* transcript at the ring stage and the corresponding PfEMP1, suggesting that it may be subject to intronic suppressing elements. However, normal temporal regulation and subsequent transcriptional silencing and reactivation were not affected and all the elements of the epigenetic layer of regulation were intact in this system (Bryant, Regnault et al. 2017). The nonessential role of the intronic regulation of *var2csa* may be gene specific but may also be an observation made because the gene was left in its natural environment and hence similar observation may apply to other *var* genes.

A second layer involves histone modifications that alter the chromatin state making the gene coding regions accessible for transcription by RNA pol II or vice versa for the heterochromatic state. Numerous studies have shown that the pattern of *var* gene expression is

modified by chromatin-modifying proteins for example PfHP1 (Flueck, Bartfai et al. 2009), histone methyl transferases and histone deacetylases, and markings by these epigenetic writers and erasers are distinct in clonally variant multi-copy (CMV) genes (Merrick, Jiang et al. 2015, Karmodiya, Pradhan et al. 2015, Chookajorn, Dzikowski et al. 2007).

A third layer involves nuclear repositioning which involves movement of the active *var* genes to a position different from silent clusters at the nuclear periphery. These last 2 layers will be reviewed in the next sections.

1.4.1 Post-translational modification of Histones

Epigenetic marking of CMV genes is different from the rest of the parasite genes and so a histone marking that may be activating may not be so for these genes. Such markings do still alter chromatin structure. CMVs appear to be poised, with the occupancy of most histone PTM and H2A.Z being lower compared to ring-expressed genes except for H3K9me3 and H4ac in gene centres. For example, H3K9ac and H3K4me3 active marks, and the global repressive H3K36me2, are comparatively lower (Karmodiya, Pradhan et al. 2015).

Active promoters occupy specific zones at the nuclear periphery enriched with H3K9ac marks (Lopez-Rubio, Gontijo et al. 2007). Embelin, a specific inhibitor of *PfGCN5* family of HAT, selectively decreases total H3K9ac acetylation levels (but not H3K14ac levels) around the *var* gene promoters (this was demonstrated using *var2csa*), leading to the downregulation of *var* gene expression (Srivastava, Bhowmick et al. 2014). H3K27Ac is enriched at the active *var* promoter in the ring stage and even later in the parasite's asexual cycling when this active *var* is poised, thus implicating this marking in epigenetic memory (Duffy, Tang et al. 2017). PfMYST HAT is also recruited to the active *var* promoter (Miao, Fan et al. 2010). H3K4me3 or me2 at the 5'UTR of *var* genes marks the active *var* and remains present during transient repression of the same *var* in the mature stages (Lopez-

Rubio, Gontijo et al. 2007) and this marking is deposited by PfSET10 (Volz, Bártfai et al. 2012).

Silent promoters have H3K9me3 which extends into the coding region throughout the parasite's lifecycle, antagonizing H3K4me3 or me2 (Lopez-Rubio, Gontijo et al. 2007), and is bound by PfHP1 (Pérez-Toledo, Rojas-Meza et al. 2009). But this marking is reduced at the intron and 3'UTR, probably because of the needed transcription of ncRNA. This marking has been shown to maintain epigenetic memory of *var* genes that are not to be expressed for >35 lifecycles (Chookajorn, Dzikowski et al. 2007). H3K9me3 also competes with H3K9ac to establish the silent *var* (Lopez-Rubio, Gontijo et al. 2007). Silent *var* promoters are also enriched with H3K36me3 in their TSS and gene body compared to the active *var* and this marking is broadly involved in mutually exclusive expression of the predominant *var*(s). The responsible SET protein for this PTM was therefore named *P. falciparum* variant silencing SET protein (PfSETvs) (Jiang, Mu et al. 2013). Spreading of silencing markings may be achieved by the promoter (Lopez-Rubio, Gontijo et al. 2007; Muhle, Adjalley et al. 2009). Generally, methylations could be activating or silencing depending on the position of the altered histone residue and the gene or gene state. They are present along the whole genes of silent *var*, i.e. when these regions are heterochromatic (Lopez-Rubio, Gontijo et al. 2007). Depletion of PfHP1 leads to a loss of a singular *var* choice with the expression of almost all *var* genes at very high levels, but the previously predominant *var* is expressed at the same level or slightly induced. PfHP1 regulates H3K9me3 by probably recruiting H3K9-specific HMTs that spread the heterochromatic mark in newly replicated chromatin (Brancucci, Bertschi et al. 2014).

PTM may also moderate *var* gene switching. It has been demonstrated that the disruption of the binding of PfSET2 to the unphosphorylated form of the C-terminal domain (CTD) of RNA pol II induces rapid switching (high switching rate) in *var* gene expression to

predominantly *var2csa* (Ukaegbu, Kishore et al. 2014). However, its recruitment by RNA pol II is not consistent with mRNA transcription. Equally, the epigenetic mark H3K36me3, deposited by PfSET2, is enriched at both the active and silent *var* gene loci, suggesting that recruitment of PfSET2 may be involved in or is needed for the transcription of noncoding-RNA from *var* intron for another layer of the regulation of *var* expression (Ukaegbu, Kishore et al. 2014). It has also been suggested that epigenetic memory altering the deposition of epigenetic marks at *var* genes, even temporarily, can disrupt the long-term switching pattern of the *var* gene family (Ukaegbu, Zhang et al. 2015).

Variant histones play a role in regulation of *var* genes as silent heterochromatic *var* genes are deficient in H2A.Z and 2Bv, even at their telomeric start site (TSS), while the active *var* gene(s) is/are enriched with these variants in the ring stage parasites. As the parasite matures, the occupancy of PfH2A.Z at the TSS of active *var* genes is antagonized by PfSir2A (Petter, Lee et al. 2011).

1.4.2 Nucleosome Occupancy/Chromatic Remodelling and *var* expression

Various epigenetic histone markings are linked and at a particular chromatin site they specify if genes in that region are to be transcribed or not. For example, H3K36me3 enrichment at the telomere and sub-telomere of especially CVM is linked to higher nucleosome occupancy at the early trophozoite stage, when gene silencing of the multiple gene families is needed. For the euchromatic chromatin, depletion of histones at intergenic regions occurs and the same regions are enriched with activating acetylation markings. While nucleosome density of the rest of the genome is low at 18 hpi, that of the telomeric and subtelomeric regions, mostly occupied by the *var* genes, is high (Ponts, Harris et al. 2010), indicating a heterochromatic state. These regions of chromatin mostly occupy the perinuclear site as clusters, with the active *var* gene(s) occupying a specific perinuclear *var* expression

site (Duraisingh, Voss et al. 2005) that is formed *in situ* (Duffy, Tang et al. 2017), different from potential repressive sites (Lopez-Rubio, Mancio-Silva et al. 2009). All epigenetic writers also localise to these distinct compartments (Volz, Carvalho et al. 2010). To buttress the role of nucleosome occupancy, the nucleosome is repositioned during the regulation of the *var2csa* gene. This gene associates with the telomeric clusters (rep20) when it is not the predominantly transcribed *var* and dissociating from the telomeric clusters and heterochromatin in more than 80% of the parasites upon activation (Mok, Ribacke et al. 2008).

The epigenetic regulation of *var* genes is illustrated in Figure 1.5.

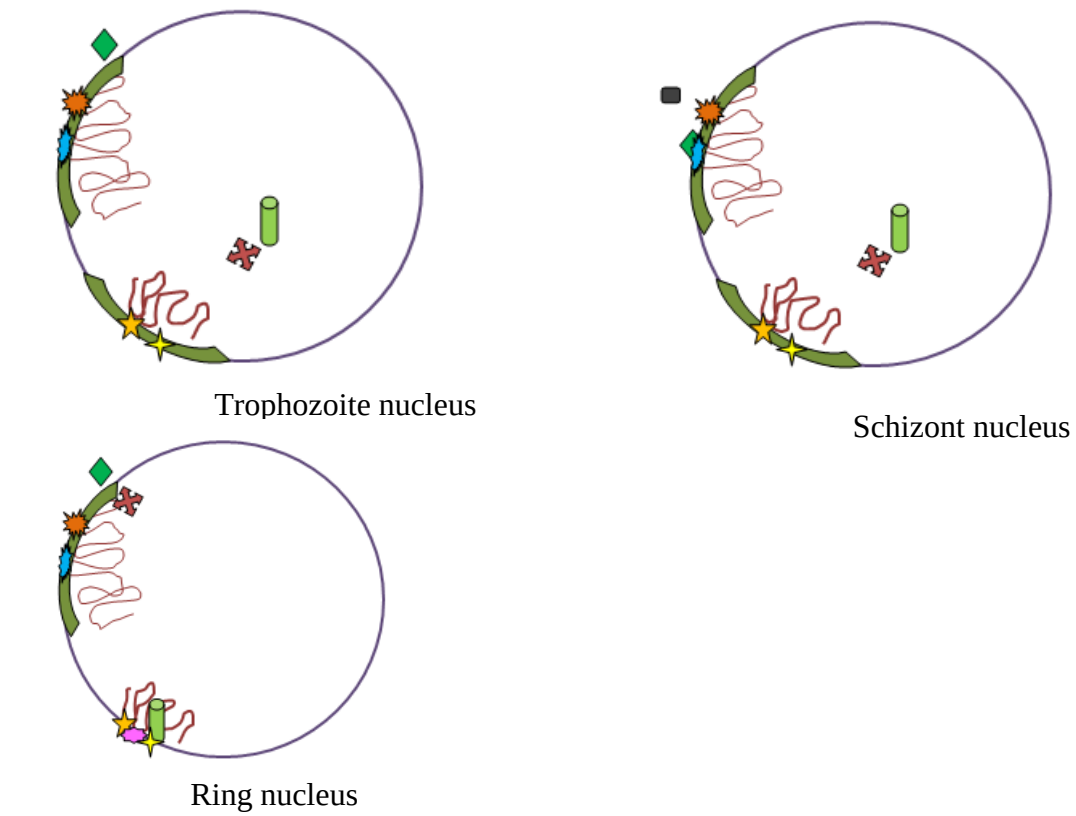

Figure 1.5: Schematic of epigenetic regulation of *var* gene expression

The thick green lining of the nucleus indicates a denser nucleosome positioning within the chromatin. *Var* genes are located in heterochromatic regions where all the *var* genes are majorly silent except one or more, which escapes silencing and is/are exclusively transcribed in a single parasite or a homogenous clonal parasite population during a single asexual cycle. The expressed *var* occupies the euchromatic region and its TSS is enriched with the activating marks H3K9ac and H3K4me3. As the parasite matures to the trophozoites stage, the previously active *var* gene becomes poised and epigenetically marked with a repressing histone code: H3K4me2 or me3 and H3K27Ac, an epigenetic memory for reactivation of this same *var* gene(s) in daughter cells. The other *var* genes in the heterochromatic region are deacetylated by PfSir2A and 2B histone deacetylase enzymes and are thus deficient in the H3K9ac mark. In the Schizont nucleus, PfHP1 binds H3K9me3 heterochromatic regions at the subtelomeric non-coding repeat regions of the ring stage parasite and recruits H3K9-specific HMTs that spreads the heterochromatic mark in newly replicated chromatin.

Writers and erasers of PTM of histones play a major role in epigenetic transcriptional regulation of the genome of *P. falciparum* during its complex life cycle, especially the histone deacetylases, PfSir2 homologues and other HDACs. In the presence of a PfHDAC class I and II inhibitor, apicidin, deregulation of multiple stage-specific genes occurs and alteration in various epigenetic histone markings occurs in addition to hyperacetylation (Chaal, Gupta et al. 2010).

1.5 Regulation of *var* expression by *Plasmodium falciparum* sirtuins

1.5.1 Sirtuins and the *var* genes

HDACs are epigenetic erasers that belong to either the histone deacetylase family or the Sir2 regulatory family (Seto, Yoshida 2014). In *P. falciparum*, the 5 identified HDACs (Kanyal, Rawat et al. 2018) are grouped into three classes based on their sequence homology to yeast HDACs. Classes I and II are zinc dependent deacetylases (reviewed in Yang, Seto 2008); of which a homologue to class I (PfHDAC1) (Joshi, Lin et al. 1999) and two to class II (PfHda1 & 2) have been identified in *P. falciparum* (Coleman, Skillman et al. 2014). Class III are nicotinamide adenine dinucleotide (NAD^+)-dependent histone deacetylase enzymes, also called sirtuins, of which two homologues have been identified in *P. falciparum*. The homologues are PfSir2 A (*P. falciparum* silence information regulator 2A), previously called PfSir2, (Freitas-Junior, Hernandez-Rivas et al. 2005) and PfSir2B (Tonkin, Carret et al. 2009), which both reversibly deacetylate histones leading to a hypoacetylated chromatin. They are both NAD^+-dependent HDAC enzymes that remove acetyl residues from histones. However, PfSir2A has been shown to have a weak histone deacetylase activity, but a strong deacylase activity, and it has been suggested that it and other sirtuins with weak or no deacetylase activity should be referred to as NAD^+-dependent deacylases (Zhu, Zhou et al. 2012).

PfSir2A is a 30kDa (Merrick, Duraisingh 2007) 'type III' sirtuin encoded by the PF3D7_1328800 gene on chromosome 13. While, PfSir2B is a 150kDa 'type IV-like' sirtuin encoded by the PF3D7_1451400 gene on chromosome 14. PfSir2 paralogues; PfSir2A and PfSir2B cooperate in the epigenetic silencing of *var* genes by directly regulating *var* gene promoters and ensuring cis spreading of silent chromatin, with silencing reaching adjacent neighbouring genes in both central and sub-telomeric regions of the chromosome, but spreading appears to be less reliant on PfSir2B (Tonkin, Carret et al. 2009).

PfSir2A binds telomeric electron-dense heterochromatin in the nuclear periphery, a binding which spreads repression to the subtelomeric regions including to Rep20 that is adjacent to the 5'UTR of the subtelomeric *var* genes. The promoter of the inactive gene forms a complex with PfSir2A, which is lost upon gene activation. This was demonstrated with *var2csa* and was shown to occur for this subtelomeric *var* but not chromosome central upsC *var* (Freitas-Junior, Hernandez-Rivas et al. 2005). Disruption of *PfSir2A* leads to activation of some subtelomeric *var* genes like group A and *var2csa*, suggesting that upsB may be subject to an additional deacetylation layer of epigenetic silencing (Duraisingh, Voss et al. 2005). This was soon discovered to be deacetylation by PfSir2B. However, a more recent study demonstrated chromosome central *var* genes and hybrid *var* with a upsA or C promoter (BC *var* and BA *var*) to be highly transcribed in addition to the above *var* groups on disruption of *PfSir2A*, indicating that its silencing is not telomere-restricted, but may simply involve co-localization to the nuclear periphery. PfSir2B was shown to mainly silence upsB *var* and 2 hybrid *var* BC and BA following disruption of the encoding gene (Tonkin, Carret et al. 2009).

In an experiment using 3D7 unselected parasite populations, the total *var* transcript level was doubled in the absence of *PfSir2A* (3D7ΔSir2A) compared to the wild-type parasite. In addition, the wild-type expressed more varied *var* subsets while the subset of *var* expressed by 3D7ΔSir2A was more homogenous across all clones, with the greatest upregulation of the

singular upsE *var*, *var2csa*, followed by the hybrid ups BA and then A. upsB was generally downregulated while the loss of repression of upsA *var* occurred in all 3D7ΔSir2A clones. Furthermore, it was shown that *var2csa*, which was derepressed in 3D7ΔSir2A, was translated to the antigenic VAR2CSA PfEMP1 (Merrick, Dzikowski et al. 2010). Disruption of either sirtuin leads to loss of mono-allelic mutual exclusive expression of *var* genes with multiple PfEMP1 variants on the iRBC surface. However, this loss also results in an increased expression of *var* gene groups it does not majorly regulate, in addition to the derepression of the *var* gene group it majorly silences, thus indicating a cooperative function between the two sirtuins (Tonkin, Carret et al. 2009).

Different *Plasmodium* strains: NF54, 3D7 and FCR-3 has been shown to express varying *var* subsets in their unselected clonal population. 3D7 clones predominantly expressed several groups A and B *var* genes, while NF54 clones did not highly express upsA *var* genes and tended to express a single dominant *var* of mainly the group B and C types. The transcript level of *PfSir2B* may contribute to this as it has been shown to differ amongst these strains with 3D7 encoding a lower transcript level than NF54 and FCR-3 strains (Merrick, Jiang et al. 2015). This probably indicates that the level of *PfSir2B* expression may alter the degree of regulation of mutually exclusive *var* gene expression. Strain specific differences has been observed on disruption of *PfSir2A*: 3D7 displayed a more dramatic alteration of *var* gene regulation manifesting as an elevated transcript level and extensive relaxation of the silencing programme (Merrick, Dzikowski et al. 2010), while the FCR-3 strain showed a switch to the expression of upsC *var* genes with no significant change in transcript abundance. In contrast, loss of *PfSir2B* led to an increased expression of almost exclusively upsB *var* genes in 3D7 (Tonkin, Carret et al. 2009), but for the other strains subtle changes with a switch to predominantly upsC *var* genes: NF54 lost its stricter mutually exclusive *var* gene expression and slightly increased total *var* transcript level, while FCR-3

slightly decreased transcript levels of *var* genes (Merrick, Jiang et al. 2015). These suggest strain specific variations in the control of *var* gene expression by the sirtuins. In addition, loss of *PfSir2A* has been shown to hinder the switch rate to a different *var* in 3D7 for a while (Merrick, Dzikowski et al. 2010). The mechanism of the parasite's sirtuins although not completely understood gives an insight into its epigenetic regulation of *var* genes expression.

1.5.2 Mechanism of Action of PfSir2 on *Plasmodium* histones

PfSir2B has two predicted catalytic domains that are separated by 180 amino acids. To date PfSir2B has not been well characterized but recombinant PfSir2A has been shown to have a large Rossmann-fold domain and a small domain containing a Zn^+ binding module. Its catalytic domain is located in a cleft between the Rossmann-fold and the zinc-binding domain. Its substrate and NAD^+ binds to the cleft (Zhu, Zhou et al. 2012).

The amino acid residues in the cleft are conserved in the sirtuin family and this is where their substrates interact with NAD^+ (Seto, Yoshida 2014), and simultaneous binding of the substrate through hydrogen bonds is required for NAD^+ to adopt a productive conformation (Avalos, Boeke et al. 2004). The peptide substrate binds before NAD^+ binding (Chakrabarty, Saikumari et al. 2008). However, different from the well-characterized *S. cerevisiae* sirtuin, Hst2, a non-conservative change was observed for one of its amino acid residues in contact with its substrate. This was subsequently suggested to possibly alter the specificity and efficacy of its HDAC activity by influencing binding of the acetyl-lysine substrate. PfSir2A may exist as a monomer or multimer and this may alter the efficiency and specificity of its substrate binding (Merrick, Duraisingh 2007). It has been shown to exist as a trimer in solution when no ligand is bound but dissociates into monomers on binding of NAD^+ (Chakrabarty, Saikumari et al. 2008).

The mechanism of action of sirtuins on histones, Fig. 1.6, involves removal of acetyl residues, a hydrolysis activity dependent on NAD^+, during which 2 intermediate reaction products are formed, as reviewed in (Seto, Yoshida 2014).

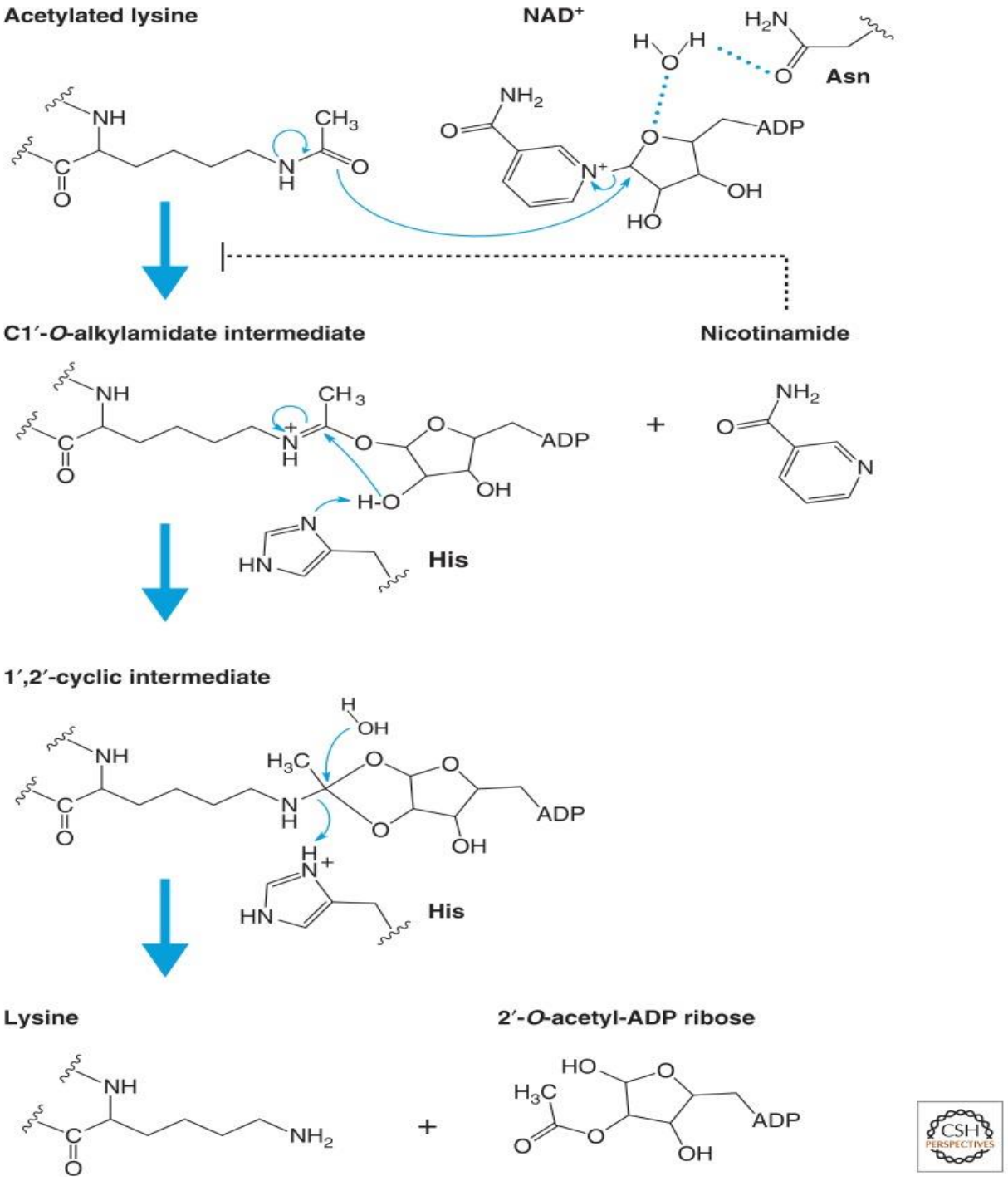

Figure 1.6: Mechanism of action of sirtuins (Seto, Yoshida 2014).

Sirtuins bind to their substrate through a reversible interaction, and using the oxidized form of NAD^+ as a cofactor, it removes the acetyl residues in the lysine tail of histones (Avalos, Boeke et al. 2004). NAD^+ is reduced to nicotinamide (NAM) to produce 2'-O-acetyl-ADPribose with the acetyl residue here coming from the acetylated histone which becomes deacetylated with NAM as by-product.

PfSir2A is able to deacetylate H3K9ac and K14, markings of activation, and H4K5ac or K16 and to an extent K12 (Merrick, Duraisingh 2007; French, Cen et al. 2008). It was more active *in vitro* in deacetylating H3 acetylated lysine residues than H4 residues. However, the NAD^+-dependent deacetylase activity of recombinant PfSir2A is 7x lower than that of recombinant Hst2 (Merrick, Duraisingh 2007). Its nicotinamide by-product can promote a backward reaction non-competitively, dose-dependently with complete inhibition at 10mM. The ribose by-product gives it an additional ADP-ribosyltransferase activity of native histone; the four major histones plus a variant, H2Bv; and itself. This activity can also be inhibited by NAM. This bifunctional activity suggests three slightly different mechanisms of action for PfSir2A (Fig. 1.7), different from that of Hst2. This highlights that its activity goes beyond deacetylation with some residues in the deacetylated histone potentially being ribosylated, including ribosylation of histones that it does not natively deacetylate (Merrick, Duraisingh 2007) (reviewed in Seto, Yoshida 2014).

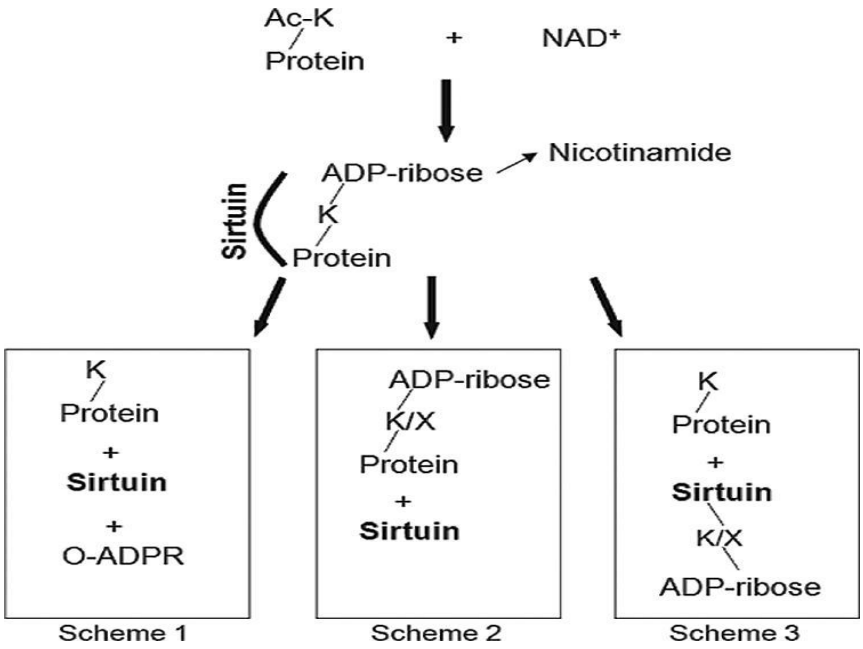

Figure 1.7: Schemes showing alternative routes of ribosyl transfer by PfSir2A apart, from the classical route (Scheme 1) (Merrick, Duraisingh 2007). The mono-ADP-ribosyltransferase activity of PfSir2A indicates that the deacetylated protein (Scheme 2) or PfSir2A (Scheme 3) itself may receive an ADP-ribose residue following its default deacetylation reaction.

By deacetylating the histones in the majority of the *var* genes, the chromatin is then expected to become heterochromatic and these genes will not be transcribed. Conversely, upon activation of the *var* gene, PfSir2A is removed from the promoter region. PfSir2A creates a heterochromatin gradient that may spread down an average distance of 30 kb of the chromosome length (Freitas-Junior, Hernandez-Rivas et al. 2005), an effect called telomere position effect (TPE), which has been suggested as the possible mechanism through which this sirtuin mediated silencing spreads from telomeres, among subtelomeric *var* genes. 3D7 parasites overexpressing PfSir2A have a shortened telomere length and thus an altered position of the *var* genes relative to the telomere. This shortening may also lead to weaker TPE and a greater possibility of the most subtelomeric *var* upsB to be expressed. This *in vitro* observation could reflect the situation *in vivo* when *PfSir2A* is increasingly expressed in the

severe disease. This increase correlates with increased expression of *var* gene upsB (Merrick, Huttenhower et al. 2012), an effect synonymous with the disruption of *PfSir2B* as discussed above.

In mammalian systems sirtuin activity has been shown to be regulated by PTMs, or the absence or presence of other proteins needed to enhance or repress their activity, or levels of the cofactor, NAD^+ (reviewed in Seto, Yoshida 2014). Other roles played by the parasite sirtuins during development does contribute to it primary role of regulating antigenic variation.

1.5.3 Other possible roles of sirtuins in *Plasmodium falciparum*

PfSir2s are needed for maintenance of telomere ends, with specifically PfSir2A protecting telomere ends. This may subsequently affect the spreading of silencing as loss of *PfSir2A* in 3D7 causes considerable elongation of telomeres and in FCR-3 causes a slight elongation. In contrast, loss of *PfSir2B* has the opposite effect, generally, for 3D7, NF54 and FCR-3 strains (Merrick, Jiang et al. 2015; Tonkin, Carret et al. 2009).

PfSir2A has been shown to alter temporal transcription of another CMV gene family, the *rif* genes, while PfSir2B leads to loss of transcription of *rif* genes at the schizont stage (Tonkin, Carret et al. 2009). Sirtuins, especially PfSir2A, have been implicated in the regulation of the expression of certain genes located subtelomerically, such as the *pfmc-2tm* gene family, *stevor*, *etramp* and some other genes transcribed in the ring stage parasites (Tonkin, Carret et al. 2009). PfSir2A may also have roles in maintaining genome stability because chromosomal changes, with gene amplification and deletion mutations, have been observed on half of the *P. falciparum* chromosomes following the loss of *PfSir2A* gene. Most of such changes involved *var* gene regions (Merrick, Jiang et al. 2015).

1.6 Aims and objectives

1.6.1 Background to this study

In a study termed an epigenetic dysregulation of virulence gene expression in severe falciparum malaria, a field study demonstrated that body temperatures of more than 37.5°C and high blood lactate in severe malaria were two host factors positively associated with expression of the parasite's sirtuins and severe-disease-associated *var* genes. This suggests that stress can modify the parasite's gene expression, resulting in an acute severe malaria in lieu of a chronic infection. The dynamics of malaria infection model showed a switch to acute infection when the stressors impacted an increased expression of *var* genes and PfEMP1. The authors queried if the distinct patterns of infection dynamics represented either a failed attempted adaptive response or a loss of control of *var* gene switching when the parasite population exceeds a certain threshold. One assumption of this model is that *var* gene expression is perturbed above this threshold with concomitant broadening of *var* gene switching, potentially to generate antigenic variants with high growth rates. There was evidence to support that overexpression of *PfSir2A* led to an upregulation of *var* transcription with a bias towards upsB *var*. As severe malaria is characterized by increased parasitaemia, the assumption of a fast growing antigenic variant(s) was valid (Merrick, Huttenhower et al. 2012).

Among the sirtuins only upregulation of *PfSir2A* was associated with increased expression of a sub-set of severe-disease-associated-*var* genes, upsB, in Gambian patients (Merrick, Huttenhower et al. 2012). In a second study, *PfSir2A* expression was also associated with upsA, upsB/A and non-severe-disease-associated-*var*, upsC, specifically the primed upsC2 region, in Kenyan patients (Abdi, Warimwe et al. 2016). This implied that host factors

may be potential stimuli for sirtuin upregulation and consequent alteration of *var* expression, leading to the development of a severe disease.

Plasmodium sirtuins regulate mutually exclusive *var* gene expression by silencing most of the 60 membered *var* genes, thus preventing an exhaustion of the variety of PfEMP1 that can be used to mask the parasite from antibody attack. This presents the parasite with an opportunity to evade clearance and establish a chronic infection. The antibody repertoire of a host is built on a learned response (humoral) following previous asexual cycling, where a number of *var* gene subsets are expressed by the parasite. Subsequent cycling may lead to a switch to different *var* gene subsets. An expression of broader *var* gene subsets has been linked to non-severe form of malaria, while the expression of a limited subset(s) leads to a severe form of the disease. Cytoadherence becomes more effective in subsequent asexual cycling. This may be due to a variation in the expression of PfEMP1 or a switch to a different PfEMP1. Indeed, antibodies to the iRBCs at the time of the disease have been shown to be negatively associated with *PfSir2A* expression (Abdi, Warimwe et al. 2016) implying that its increased expression in the severe disease antagonises the expression of virulence phenotypes that the host's antibodies can recognize.

A number of studies have indicated that commitment to sexual development in the parasite is associated with the variant expression of *var* genes, with both processes potentially being controlled by the same epigenetic mechanism (Coleman, Skillman et al. 2014; Brancucci, Bertschi et al. 2014; Tibúrcio, Dixon et al. 2015). This implies that any sirtuin-mediated epigenetic response should alter *var* gene expression and gametocytogenesis as *PfSir2A* was shown to be positively associated with the markers of gametocyte commitment. However, the selection of PfEMP1 virulent phenotypes by the host's antibodies may occur independently of the gametocyte phenotype (Abdi, Warimwe et al. 2016).

PfSir2A may be involved in metabolic sensing, as indicated for the yeast model system (Lu, Lin 2010) in which sirtuins sense and respond to cellular levels of NAD^+. NAD^+ levels have been shown to be elevated in iRBCs compared to the metabolically distinct non-infected RBCs (Zerez, Roth et al. 1990), this occurs primarily in trophozoite and schizonts (Beri, Ramdani et al. 2019). There is increased lactate production in these late stages, consequently generating more NAD^+ from its reduced form (Olszewski, Morrisey et al. 2009). The level of *PfSir2A* transcription is increased in these stages compared to the ring stage (Otto, Wilinski et al. 2010) and the resultant sirtuin enzyme will act dependent upon levels of this regenerated NAD^+. Maybe the increased sirtuin production is needed at these late stages to maintain silencing of inactive *var* genes in the daughter cells. These findings imply that the parasites can respond to host stress through their sirtuins which then modify their *var* expression and possibly other virulence phenotypes.

1.6.2 Rationale of this research

This study was based on established concepts:

i. Increased sirtuin expression was associated with severe malaria, specifically two host factors that define severe malaria, in a Gambian patient cohort. These are high body temperatures and high blood lactate. In severe malaria, the parasite usually encounters temperature fluctuations up to 41°C during fever, and a characteristic high lactate level of ≥ 5 mM. Under normal conditions, *P. falciparum* is cultured at 37°C, a temperature which they would encounter *in vivo* in the asymptomatic host. In this host, the parasite will also usually encounter a lactate level lower than 5mM, and consistent with this, *in vitro* culturing does not include lactate as a culture ingredient. An inclusion of high temperature and lactate in *in vitro* culture conditions may lead to the differential expression of genes and manifestation of virulence phenotypes.

ii. Severe-disease-associated *var* genes are particularly upregulated in the severe disease. Maximum expression of the active *var* in an unselected parasite population occurs at about 10 hpi and again at about 22 hpi (Dahlbäck, Lavstsen et al. 2007). The specific PfEMP1 encoded is then exported to the surface of the iRBC at about 18 hpi, which the parasite uses to sequester away from circulation. Genetic studies have indicated that there is a delay between mRNA abundance and protein abundance, a delay of about 11 h (Kriek, Tilley et al. 2003; Foth, Zhang et al. 2011), matching the first burst of *var* expression to the export of the encoded PfEMP1. However, what could happen following the second burst of *var* expression remains unknown, but can reasonably be assumed to be the export of more of the PfEMP1 protein some 11h later, enabling greater binding between the antigenic proteins and the host's endothelial cell receptor ligands. We therefore looked at *var* expression around these two bursts, specifically at 8 ± 2 hpi and 18 ± 2 hpi.

iii. The expression of sirtuins is naturally low. So we decided to use two methods to establish this relationship: firstly, quantitative PCR of the sirtuin transcripts and secondly a genetically engineered reporter system designed to measure the activity of sirtuin gene promoters independent of their mRNA expression, by using the firefly luciferase reporter under a sirtuin promoter. This will also isolate any promoter activity-associated-stress response from any in-parasite cellular feedback attempting to restore homeostasis resulting from an altered sirtuin mRNA level. Thirdly, a determination of the enzymatic activity of the sirtuins was also attempted to see if any changes in mRNA expression translated into changes in activity at the protein level.

iv. Since alteration of *var* gene expression and commitment to gametocytogenesis may both be influenced by an increased *PfSir2A* expression, alteration of gametocytogenesis in stress-exposed parasites was measured, moving beyond both

mRNA and protein level to the cellular level. The induction of the transmission stages, gametocytes, as a result of the two host stress factors was assessed.

v. Then, the potential of an effect of lactate on parasite viability and protection from heat shock was also investigated.

The aim of this study was to establish a cause and effect relationship between the putative stress factors and the parasite sirtuins and *var* genes. Such a relationship will mean that the parasite uses its sirtuin to sense changes in the host condition and vary its var gene expression in other to ensure its survival. This involved looking at the direct effect of febrile temperature of 40°C and high lactate on the parasite's alteration of its sirtuin expression and *var* gene(s) expression in *in vitro* cultured parasites. The *in vitro* culture system is independent of immunomodulation or other physiologic or genetic host factors.

Ultimately, we propose that the parasite can sense an increased host stress, manifesting as high temperature following a proinflammatory responses and high lactate following hypoxia. Sirtuin expression is increased in response and this in turn regulates *var* expression, causing a switch to *var* subsets that would provide the parasite with the best chance of survival under stressed conditions. Our null hypothesis is that high temperature and lactate, when applied to *in vitro* cultured parasites, do not lead to an increased expression of sirtuins and *var* subsets associated with severe malaria.

In summary, two naturally occurring host conditions during severe malaria that had been shown to correlate with increased expression of sirtuins and associated *var* genes in infected patients were incorporated into *in vitro* growth conditions in order to get some insights into the potential alteration of important parasite virulence determinants in the course of a malaria infection.

Chapter 2: General experimental methods

2.1 Culturing of parasites

The culturing of *Plasmodium falciparum* was performed in a containment level 3 (CL3) facility which is approved by the Health and Safety Executive (HSE) for the use of *Plasmodium falciparum* according to the rules in the CL3 suite code of practice. The reference strain of *P. falciparum* 3D7 (obtained from MR4) was cultured in Leukocyte-depleted human blood O^+ erythrocytes obtained from the National Blood Transfusion Service (NBTS) (Edgbaston, UK) at 4% haematocrit in RPMI 1640 based complete media (Sigma-Aldrich, USA) containing 25 µg/ml gentamicin sulphate, 0.2% sodium bicarbonate (Sigma, USA), 0.2% Albumax II (Life technologies, NewZealand), and 4.3% pooled human serum. The human blood and serum were stored in 50ml aliquots at 4^{o}C. Storage and disposal of blood were done in accordance with the Human Tissue Authority (HTA) license held by Keele University.

Standard continuous culturing was carried out as described (Ménard 2013). Culturing was done in sterile Petri dishes by splitting down to a lower parasitaemia (0.5%) every 48 h to prevent the culture from dying due to increased metabolic waste products from the growing parasite population. Staging and parasitaemia were assessed from a Hemacolor® Rapid (vwr, UK)-stained thin blood smear, made with 1-2 µl of the settled infected erythrocytes (IE) from each Petri dish. Smears were used to calculate the dilution required to maintain a healthy culture and for subsequent viability and replicate comparison studies. Dilutions were done by first changing the media, and then diluting with 4% erythrocytes in complete media. The smears were visualized using the eye piece graticule at 10× eye magnification of a light microscope (VWR, UK) with a 100× oil immersion objective lens. The Petri dishes were placed in a modular incubator chamber (Billups-Rothenberg Inc., USA), gassed with 1% O_2, 3% CO_2, balance N_2 and incubated at 37°C in an incubator.

2.2 Synchronization of parasites

Synchronization of *P. falciparum* parasites involves methods of purifying *P. falciparum* so as to obtain distinct stages of the parasite population as is obtainable during its *in vivo* development in the host. *Plasmodium* gene expression is stage specific and synchrony in transcriptional studies is required to ensure that transcript levels reflect the temporal pattern of gene expression. Two methods of synchronization were adopted based on the experiment that the parasites were to be used for. Percoll synchronization gives a highly synchronous culture but the yield is low while sorbitol synchronization gives a less synchronous but higher parasitaemia culture. A combination of both methods can produce a highly synchronous culture but the yield will still be low, unless the process is repeated (Childs, Miao et al. 2013). A Percoll (Ménard 2013), and sorbitol based method was done to prepare parasites that were to be used for characterization of the temporal gene expression throughout the intraerythrocytic development cycle (IDC) of the parasite. Low but highly synchronous parasite culture was required as the parasites were assayed throughout its 48-h IDC.

Percoll synchronization was done on late trophozoites and schizonts of *P. falciparum*. 90% Percoll in phosphate-buffered saline (PBS, VWR, UK) was prepared by mixing 1 ml of filter sterile 10X PBS and 9 ml of 100% Percoll. 65% Percoll was freshly prepared by mixing 6.5 ml of 90% Percoll and 2.5 ml of filter sterile 1X PBS. 2.5 ml aliquots of this was placed in 15 ml falcon tubes (Fisher Scientific, UK) and warmed to 37°C, during the time of which 10 ml of the parasite cultures were centrifuged at 830 x g in 15 ml falcon tubes for 4 min, using a centrifuge (5702 RH, Eppendorf, UK). 8.5 ml of the supernatant media was aspirated leaving about 1 ml of media on top of the parasite pellet. The pellet was re-suspended and slowly overlaid on the 65% warmed Percoll without mixing. This was then centrifuged at 1,870 x g for 10 min. The brown interface (as shown in Fig. 2.1) enriched with the late stages of the parasites was transferred into a fresh 15 ml falcon tube, after gently pipetting off the medium

above the interface. Fresh RBCs were added to give 200 µl pellet size, and the resulting mixture was gently washed with complete media, centrifuged at 830 x g and the supernatant gently aspirated leaving behind 1 ml of media on top of the fragile pellet. 200 µl of blood was added to bring the haematocrit to 4% in a 10 ml culture dish. The parasites were then cultured for 7 h, after which it was synchronized with sorbitol to kill off any remaining late stages, leaving only very young rings of about 0-7 hpi. Experiments were performed 55 h after the Percoll synchronization.

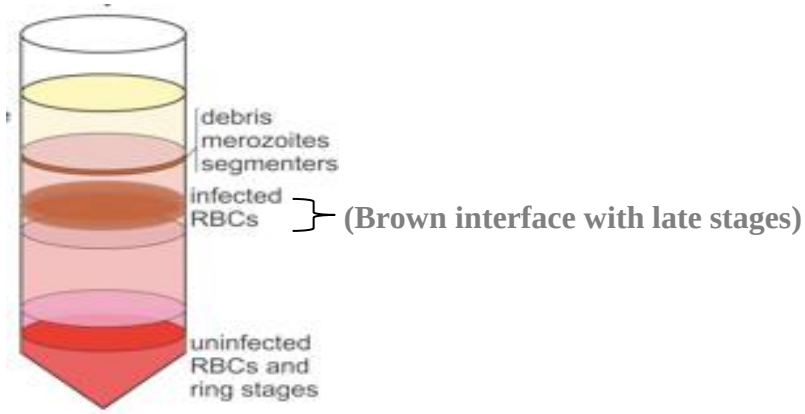

Figure 2.1: Percoll synchronization

A sorbitol-only method (Lambros, Vanderberg 1979) was used to synchronize parasites used for the stress experiment. A highly synchronous culture was required but it was equally important to have enough parasites for subsequent RNA extraction. Here, standard cultures of *P. falciparum* 3D7 comprised of mostly rings were tightly synchronized with 5ml of sterile 5% sorbitol solution in distilled deionized water added to ~ 0.4 ml culture pellet, for 10 min at 37ºC, so as to kill off all the mature blood stages, thus allowing a fairly uniform culture of ring forms to proliferate. Sorbitol synchronization was done 16 h apart for experiments involving trophozoite or schizont parasite stages and 20 h apart for experiments with the ring stage to ensure a tight synchrony.

2.3 Stress treatment of parasites

Plasmodium parasites were subjected to high temperature and high lactate levels, mimicking the febrile episodes and hyperlactatemia in severe malaria, respectively. A high body temperature of 40ºC was chosen for the treatment as severe malaria is defined by body temperature of above 39ºC from various studies in endemic regions (Krishna, Waller et al. 1994; Mockenhaupt, Ehrhardt et al. 2004). However, lower temperatures have been recorded in some cerebral malaria cases and the WHO has excluded the temperature criteria from the list of clinical features defining the severe disease (World Health Organization 2014). A temperature of above 40ºC has been shown to almost kill off mature forms of the blood stage (Oakley, Kumar et al. 2007) and as seen in a preliminary study done by Dr. Imran Ullah in our laboratory. 5mM of lactate was chosen as the defining level for hyperlactatemia as specified in a number of studies and in the World Malaria Report (Agbenyega, Angus et al. 2000; Casals-Pascual, Kai et al. 2006; Krishna, Waller et al. 1994; World Health Organization 2018) and so the parasites were exposed to this level.

Stress experiments were performed using tightly synchronized blood stages of *P. falciparum* strains. Synchrony was confirmed by counting the number of stages in a thin blood smear of the parasite culture before the stress experiment. Synchronized seed cultures of ring or trophozoite or schizont-staged *P. falciparum* were divided into 8, put in 50 ml falcon tubes and exposed to a 40°C temperature and/or 5mM lactate (Alfa Aesar®, Thermofisher Scientific, UK) stress treatment, alone and in combination, for 2 and/or 6 h as shown in the schema in Fig. 2.2. The falcon tubes were gassed and incubated at a 45° angle in a water bath. Two of the falcon tubes were incubated without lactate and temperature stress for 2 and 6 h as controls. The 2 and 6 h time points were chosen because the febrile malaria

paroxysms can last as long as these times (Bartoloni, Zammarchi 2012), although high blood lactate can last for days even after recovery from severe malaria. Malaria paroxysms result from immune responses which trigger a high body temperature (Gazzinelli, Kalantari et al. 2014), and high blood lactate (LAC) results due to decreased lactate excretion following blockage of microcirculation by sequestered parasites and coagulation (Gomes, Vitorino et al. 2011).

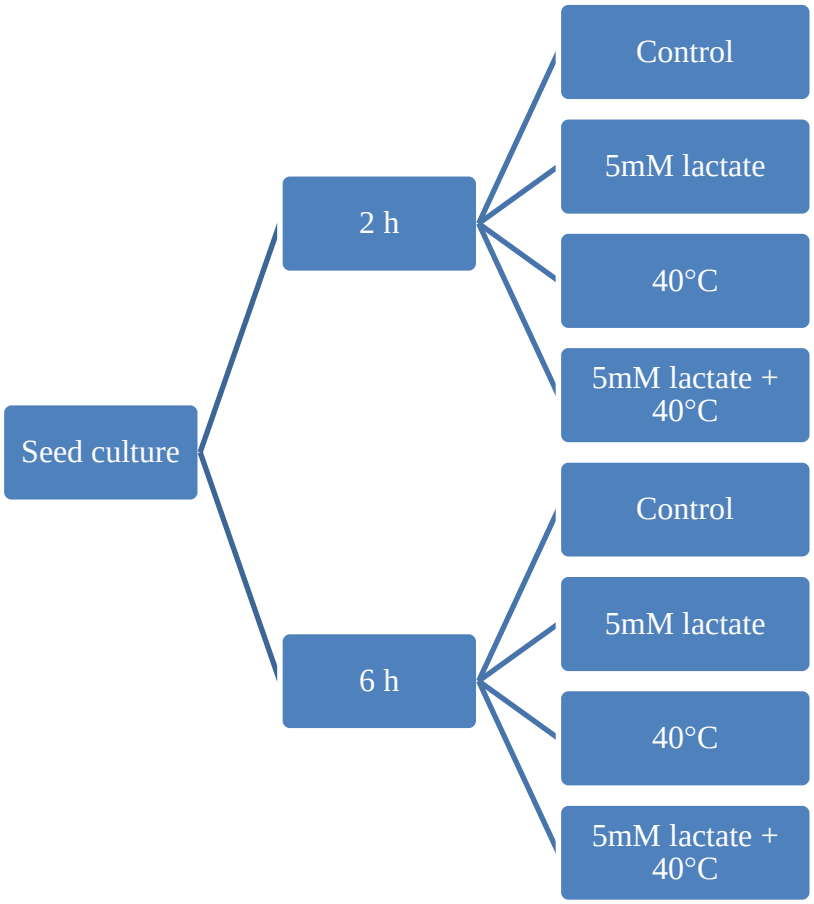

Figure 2.2: **Schema of design for the stress experiment**

After each stress treatment, the cultures were centrifuged; a thin blood smear made from the pellet, and the media was changed. An aliquot of the sample culture was appropriately diluted with 4% blood in complete media and cultured for 48 h for the

trophozoites and schizonts or 72 h for the rings, to determine survival of the parasites after stress. The rings were stressed for only 6 h after which they were left to recover for 10 h before the 72 h sub-culturing. Survival was determined from parasitaemia following microscopy and/or fluorescence reads following SYBR Green (SG) 1-based fluorescence growth assessment (see section 2.4) of the 48/72 h cultures. Survival rate of the parasite was subsequently determined using the equation below. Survival was a measure of the number of parasites that were unaffected by the treatment compared to the control, and were able to grow and multiply giving rise to new daughter cells. The rest of each of the sample cultures were harvested and lysed using saponin at a concentration of 0.1%, (using equal volume of a 0.2% solution of saponin to the pelleted blood) so as to release the parasites. The free parasites were washed with equal volume of 1X sterile PBS and then re-suspended in 20 µl of this buffer by vortexing. 20 or 10 pellet volumes of pre-warmed Trizol (Thermofisher Scientific, USA) at 37ºC were added to trophozoites/schizont or rings sample pellet, respectively, vortexed and incubated for 5 min at 37ºC. It was then stored at -80ºC until the total RNA was extracted, which was within 1 day to 3 weeks.

$$Survival\ rate = \frac{Parasitemia\ of\ Stress\ sample}{Parasitemia\ of\ Control\ sample} \text{ x } 100$$

2.4 SYBR Green 1-based fluorescence growth assessment

Growth of the parasites after exposure to stress was also assessed using the DNA intercalating dye SYBR Green-1. Here, treated parasites were cultured (post stress) at about 0.5% starting parasitaemia in a multi-well plate for 48/72 h. After this time, 100 µl of the culture was mixed with 100 µl of Malaria SYBR Green 1-based fluorescence (MSF) lysis buffer containing SYBR green at a 1:5000 dilution (Lysis Buffer = 20mM Tris pH 7.5, 5mM EDTA, 0.008% v/v saponin and 0.08% v/v Triton X-100) in the wells of a 96 well black plate (CellStar, Greiner-bio-one, Germany), in the dark. The plates were then incubated for 1 h in

the dark at room temperature and the fluorescence intensity measured using a 490 nm excitation and 510-570 nm emission filter in a Glomax-Multi Detection System (Promega, UK). The mean fluorescence intensity from technical replicate was determined and used to calculate the survival rate of each stressed sample culture as follow:

$$Survival\ rate = \frac{SYBR\ read\ of\ Stress\ sample}{SYBR\ read\ of\ Control\ sample} \text{ x } 100$$

Histograms of mean or pooled mean survival from independent biological replicates for each treatment sample were plotted on a graph. However, the survival rate gotten from the above calculation was exaggerated as there was a failure to account for background fluorescence resulting from the intercalation of SYBR Green-1 with the nucleic acid from dead parasites which can still be intact for several days after the death of the parasite. This background fluorescence has to be subtracted from the stress sample and the control, by using a chloroquine control containing a supra-lethal dose of chloroquine. We failed to use this in the growth assessment. For example, if the following fluorescence measurement were obtained after an experiment; Control sample = 4, stress sample = 3 and background = 1, then the survival rate would be overstated as 75% instead of 66.7%. The higher the growth rate, the lower the discrepancy in the two survival rates, as if the control and stress sample fluorescence measurements were changed to a 6 and 5 respectively, then the overstated survival rate would be 83.3%, while the actual rate would be 80%. Therefore, the survival rate is actually less than reported in subsequent chapters except for the growth rate in chapter 7, in which the correct formula and control were used.

2.5 RNA harvest, purification and cDNA synthesis

Total RNA was extracted from the parasites as described (Kyes, Pinches et al. 2000) using Trizol LS Reagent (Invitrogen, UK). 0.2 Trizol volume (volume of the Trizol previously added to the released parasite pellet) of chloroform was added to the defrosted

RNA samples stored in Trizol, and shaken for 15 s. After shaking the samples were left for 3 min at room temperature. This mixture was then centrifuged at 9800 rpm for 30 min at 4ºC in a centrifuge (U-32 R, BOECO, Germany), and 0.6 Trizol volume of the upper aqueous layer was collected carefully without disturbing the DNA interface between this aqueous layer and the non-aqueous layer. 0.5 Trizol volume of isopropanol was then added to the aqueous layer and the RNA in the mixture was left to precipitate at 4ºC, for at least 2 h, and up to 24 h.

After precipitation, the mixture was spun at 13000 rpm and at 4ºC for 30 min. The resulting supernatant was discarded and 500 µl of cold 75% ethanol in DEPC water (Thermoscientific, USA) added to wash the precipitate. The precipitate was allowed to air dry for 5 min after which it was dissolved in DPEC water. The quantity of extracted RNA was determined by optical densitometry using Nanospec 1000 (Thermoscientific, USA). Up to 2 µg of RNA was DNase treated with DNase 1 (Thermoscientific, USA) at 37ºC for 30 min (to 1 h), after which the DNase was inactivated by adding 2 µl of 25 mM EDTA for 10 min at 65ºC. The quantity of RNA in each sample treated with DNase varied by ~50% of the mean quantity of the all samples in a biological replicate experiment. The quality of the DNase treated RNA was determined by running the samples on a 1.2% agarose gel. DNA complementary (cDNA) to the prepared RNA from each sample was synthesized using iScript™ cDNA synthesis kit (Bio-Rad, UK) and the random primer provided in the kit, according to the manufacturer's instructions.

2.6 Reverse transcription quantitative polymerase chain reaction (RT-qPCR) for changes in gene expression

Changes in transcript levels of the genes under study, compared to a control, were determined using RT-qPCR or simply qPCR. But first, the integrity of the cDNA previously synthesized was determined using PCR and primers that spans around introns of the gene EBA165 (PF3D7_0424300, formerly PFD1155w, (PlasmoDB) as previously described

(Merrick, Dzikowski et al. 2010). Primers used were: GCA GG AAA GGT TTT TCA AG (PFD1155w Fwd) and AAA GCT GAA TCT TGG CCC GG (PFD1155w Rev) or ACC ATT TAA CTC ATT GTC TTC A (PFD1155w Rev2); to detect the presence of genomic DNA. Genomic DNA of 3D7 Wild Type was used as a template for the positive control experiment. The PCR reaction formula and conditions are outlined in Tables 2.1 and 2.2.

Table 2.1: PCR formula for detecting the presence of genomic DNA in the cDNA samples

Component	**Quantity (µl)**
2X MyTaq™Red Mix	10
Primers (10 µM)	0.4 each
Template	1
ddH_2O	8.2

Table 2.2: PCR Conditions for detecting the presence of genomic DNA in the cDNA samples

Condition (ºC)	**Time**	
95	2 min	
95	15 s	x 35
52	20 s	
72	15 s	
72	2 min	

cDNA free of genomic DNA contamination was diluted at a ratio of 1:20 with DEPC water, and used for SYBR green-based Singleplex RT-qPCR by Comparative C_T method in

an Applied Biosystems StepOne and StepOne Plus™ Real-time PCR machine. This assay was performed using the DNA dye SensiFAST™ SYBR (Bioline, UK) and a final primer concentration of 0.125 µM in a 20 µl reaction mixture also containing the template cDNA. At this concentration the primers were determined to give minimal or no dimers and still gave a single PCR product of the target, visualized on an agarose gel. Primers were also determined to be gDNA-free. The following primers, Table 2.3, were used to measure the relative quantity of expressed *PfSir2A* and *2b* (Merrick et al., 2012), in addition to the control heat shock gene, *Hsp70*. *Hsp70* primers were designed in Snapgene software, and included in the reactions to establish that a heat shock response had occurred for the parasites incubated at the higher temperature. A no template control (NTC) was also included in the study. The formula for the qPCR reaction and cycling conditions are summarized in tables 2.4 and 2.5, respectively. The relative copy number (RCN) of each target gene was calculated by comparison to the average level of expression of 3 reference genes; serine--tRNA ligase (previously called seryltRNA synthetase), FBP aldolase and actin as used in Merrick et al., (2012) (Merrick, Huttenhower et al. 2012), and the primers are also in Table 2.3.

Table 2.3: Primers used for the qPCR (including the reference genes)

Gene (PlasmoDB)	Fwd Primer	Rev Primer	Product size(bp)
PfSir2A (PF3D7_1328800)	GGGAATGTATTTGAAGCAGT	CGATGTGCCAATTACTAAAA	231
Hsp70 (PF3D7_0818900)	CAATCAAATGCTGTCCAAGA	GTTAAGGCTCTTTCACCTTC	200
PfSir2B (PF3D7_1451400)	GTCCCGGCTAGCTCTTATCC	AATTGGGCACCTA	213
seryltRNA--ligase (PF3D7_0717700)	AAGTAGCAGGTCATCGTGGTT	TTCGGCACATTCTTCCATAA	158
FBP aldolase (PF3D7_1444800)	TGTACCACCAGCCTTACCAG	TTCCTTGCCATGTGTTCAAT	167
actin (PF3D7_1246200)	AGCAGCAGGAATCCACACA	TGATGGTGCAAGGGTTGTAA	160

Table 2.4: Formula for the RT-qPCR reaction mixture

Component	Quantity (µl) (NTC)	Quantity (µl) (Test)
SensiFAST™ SYBR	10	10
Primer pair (0.625 µM)	4	4
cDNA	-	2
ddH_2O	6	4

Table 2.5: Conditions for the qPCR

Condition (ºC)	**Time**
50	2 min
95	3 min
95	15 s
54	40 s x 40
60	1 min
Optional Dissociation Step	

All reactions were set up in a PCR cabinet. Independent biological replicates of each experiment were performed. Specificity of primers to their target genes was determined by looking at the melting temperatures (Tm) after a melt curve runs in the dissociation step, and by an agarose gel run.

2.7 Analysis of RT-qPCR data

This was done using the $2^{-\Delta\Delta Ct}$ method adopted from the Livak method (Livak, Schmittgen 2001) but with multiple endogenous reference genes, which enables accurate measurement of small changes in expression. Ct is now called Cq and will be used throughout the thesis. This is an easy method of analysing changes in gene expression data from a RT-qPCR experiment relative to a control sample. It is more convenient than the Pfaffl method as it assumes that the primer efficiency is between 90-110% in doubling the PCR product. So there is no need to determine PCR efficiency. Expression of *PfSir2A*, *PfSir2B* and *Hsp70* were normalized to the pooled mean Cq from 3 reference as mention earlier. Relative copy numbers ($2^{-\Delta Cq}$) were determined in technical triplicate for each biological replicate using the ΔCq calculated as the Cq of the target gene minus the pooled mean Cq of the reference genes

from. Relative copy numbers for each gene were then compared to gene expression in unstressed control parasites using the ΔΔCq method, to obtain the mean relative quantity ($RQ=2^{-\Delta\Delta Cq}$). These calculations can also be done by the StepOne™ Software v.2.3 installed in the Applied Biosystems StepOne and StepOne Plus™ Real-time PCR machine using the comparative Cq (ΔΔCq) method. Other software for analysis of Cq data exist but this package is unique as you can generate your data in Real-time PCR Data Markup Language (RDML) formats which can be used in many platforms. Error bars were plotted showing the 95% confidence interval, calculated using the software, for single experiments, or standard error mean (SEM) for biological replicate experiments. Kruskal-Wallis/Mann-Whitney test was performed for non-normally distributed data (after assessment using Anderson-Darling test for normality) at $\alpha = 0.05$. For normally distributed data the parametric alternative, ANOVA/2-sample t-test, was used.

Chapter 3: Use of luciferase to assess changes in *PfSir2* promoter activity

3.1 The use of luciferase reporters to investigate absolute/temporal changes in gene expression

Regulation of the expression of elements like *P. falciparum* sirtuins which may themselves regulate expression of other genes can be analysed by an investigation of the promoter activity of genes that encode these proteins. This has the advantage of separating promoter activity from any homeostatic feedback exerted from the encoded protein itself. Various reporter genes have been used to dissect gene regulation, including chloramphenicol acetyl transferase (CAT), β-galactosidase, luciferase, alkaline phosphatase and green fluorescent protein (GFP) (Sambrook 2001). Such studies usually involve cloning of the promoter regions of the gene under study, upstream of the reporter gene. When stimulated, the reporter gene then codes for a protein whose activity can be easily detected using various methods. Luciferase reporter genes are highly sensitive due to their low background, and are thus very suitable for weak promoters (Sambrook 2001). A number of luciferase reporters exist including firefly, modified firefly, click beetle, sea pansy luciferases. These transgenes can be expressed internally or secreted from the cell (Thorne, Inglese et al. 2010), thus emitting light qualitatively/quantitatively as a result of changes in biological systems. The light emission is thus called bioluminescence. For the firefly luciferase (Fluc), light emission is due to this luciferase protein catalysing the oxidation of a specific luciferin (luciferase substrate) in the presence of ATP and Mg^{2+} with the consequent emission of light as shown in the reaction below (Ignowski, Schaffer 2004):

$$\text{ATP + LUCIFERIN + } O_2 \longrightarrow \text{AMP + oxyluciferin + PPi + hv +} CO_2$$

Despite early development of Fluc as a reporter for expression in biological assays involving mammalian cells (reviewed in Thorne, Inglese et al. 2010), it was first expressed in

an avian species, *Plasmodium gallinaceum,* in 1993 through transient transfection. *Fluc* was inserted in frame into the coding region of *pgs28* of *P. gallinaceum*. This opened up the possibility of the use of this reporter in *Plasmodium* gene regulatory studies (Goonewardene, Daily et al. 1993).

Fluc was used in our cell based study as it was readily available and was the most extensively used in the analysis of the role of cis/trans-regulatory elements in gene expression.

3.1.1 Examples of the use of luciferase reporter construct

Luciferase reporter constructs have been successfully used to analyse the contribution of cis-trans regulatory factors in the absolute level of gene expression. However, their use in dissecting the temporal control of gene expression by such elements has not been very successful (Komaki-Yasuda, Okuwaki et al. 2008; Frank, Dzikowski et al. 2006). This failure has been reported despite the development of systems for stable transfection of reporter transgenes in lieu of transient transfection. This was suspected to be due to the use of 3'UTR sequences from another gene to drive the expression of the luciferase gene in such methods, therefore the use of matched 5' and 3'UTRs both from the endogenous gene was proposed (Wong, Hasenkamp et al. 2011).

However, the contribution of the 3'UTR to the temporal control of gene expression in a reporter construct could not be demonstrated in the above study by Wong et al. The 5'UTR (1418 bp) and 3'UTR (647 bp) regions of *Pfpcna* (*Plasmodium falciparum* proliferating cell nuclear antigen) were included in the reporter construct, an integrated luciferase cassette, using the bxbI integrase-mediated transfection system (Nkrumah, Muhle et al. 2006). A sequential deletion of the 5'UTR reduced the transcript level of luciferase, while deletion of the polyadenylation sites in the 3'UTR regions resulted in complete loss of bioluminescence.

Cis-elements within the 3'UTR region of *Pfpcna* are thus needed to maintain transcript stability and shares consensus sequences with other eukaryotic elements. The authors concluded that an element of temporal control of gene expression occurs post-transcriptionally (Wong, Hasenkamp et al. 2011).

Luciferase transgenic constructs have been used in *Plasmodium* in a number of gene regulatory studies with translatable outcomes including;

1. *In vivo* confirmation of the stage specificity of liver-specific protein 2 (lisp2) and quantification of its promoter activity using a dual luciferase construct system with robustness for extensive mutation and deletion studies needed to further understand the regulation/function of the parasite's liver-stage-specific genes. This also potentially provides a model for the assay of liver-stage drugs, and characterization of genetically attenuated parasites and liver-stage vaccines (De Niz, Helm et al. 2015). It has successfully been used in vaccine research (Othman, Marin-Mogollon et al. 2017).

2. Stably transformed *var-luc* reporter lines have been used to establish that *var* gene silencing is regulated at the gene level. *Var* intron included in the construct silenced a single *var* promoter activity, without any effect on neighbouring *var* genes (Frank, Dzikowski et al. 2006).

These precedents encouraged us to use a luciferase reporter gene system to measure sirtuin promoter activity after parasites were exposed to the putative stress conditions. The sirtuins have a low expression compared to other genes and since it takes a long time to clone *Plasmodium* genes, we began our study by creating a luciferase reporter parasite line, which expresses luciferase under the control of *PfSir2A* promoter. This would give an independent readout of the sirtuin expression isolated from any negative feedback regulation mechanism by the endogenous *PfSir2A* gene, thus highlighting its promoter activity.

3.2 Methodology

3.2.1 Cloning of reporter luciferase gene under *PfSir2A* and *PfSir2B* promoter

Cloning involves construction of a cloning vector and introduction of this DNA construct into a competent organism. Cells can even take up foreign genes from their environment naturally but at a much lower efficiency than when heat shock or electroporation is applied. The clone (organism carrying the foreign gene) then multiplies and produces progeny that carry replicates of this transgene. Subsequent steps involve ensuring that supposed clones are equally carrying the correct transgene. But first, the cloning vector must be constructed by joining the gene of interest with a vector, which then carries this gene of interest into the competent organism or cell and ensures that the gene is replicated. A cloning vector must ideally be less than 10 kb for easy manipulation and stability in *E. coli* (Brown & Brown, 2016) or any other microbe.

Traditionally, cloning vectors for transfecting *Plasmodium* parasites are episomal plasmids and must first be mass-produced in *E. coli* before introduction into the parasites. These constructs are usually circular. *Plasmodium* genes are very AT-rich with about 19.4% GC content (Gardner, Hall et al. 2002). This makes it very difficult to clone in *E. coli* due to unstable replication of introduced episomal construct. In addition, to ensure that the construct is stably replicated in *E. coli* and maintained in *P. falciparum* two selectable markers amenable to both systems must be included in the episomal construct. These markers select for clones that have the transgene thus ensuring stable maintenance and expression of the transgene (Epp, Raskolnikov et al. 2008). These selectable markers can be a drug resistance gene, like the ampicillin resistance (AmpR) gene, or a gene that compensates for an essential gene that is defective in the cell line to be transfected.

A luciferase reporter gene can be included as the gene of interest, thus making a reporter construct. A reporter episomal construct containing a selectable marker can be maintained in *P. falciparum* under drug pressure during regular culture maintenance.

3.2.1.1 Extraction and Digestion of the Vector Backbone

The vector pLNSir2aGFP (or pLNSir2AGFP) with the *GFP* gene under *PfSir2A* promoter (reffered to as pLNSG vector here) and containing the AmpR gene (Merrick, Huttenhower et al. 2012), was amplified by cloning this vector into competent *E. coli* (PMC103 strain, ATTC) via electroporation. The plasmid map of this vector is shown in appendix I. 25 µl of gently thawed competent cells and 1 µl of this plasmid were mixed, left on ice for 15 min and put into an ice cooled 1mm gap-width cuvette (Bio-Rad, UK). The cuvette content was electroporated at 1.8 kV and recovered in 300 µl of warm SOC broth (formula in appendix II) for 1 h in a shaking incubator at 37°C. The recovered culture was centrifuged at 6000 rpm for 1 min to form a pellet. 200 µl of the supernatant was discarded and the remaining supernatant was mixed with the pelleted culture. This mixture was added to 5 ml of LB (Luria-Bertani) broth (Fisher Scientific, UK) containing 5 µl of ampicillin, 100 mg/ml, and subsequently incubated at 37°C overnight in a shaking incubator. pLNSG was subsequently extracted from *E. coli* by using the Qiaprep®Spin Miniprep Kit (QIAGEN GmbH, Germany).

The amount of extracted plasmid vector was determined using NanoDrop spectrophotometer 1000 (Thermo Scientific, USA) so as to determine the quantity of enzymes needed to linearize the vector by restriction digest. AflII (also called BSPT1, (10 U/µL)) and AvrII (also called XmaJ1, (10 U/µL)) (Thermo Scientific, USA) enzymes were used to restrict the *PfSir2A* and GFP gene in pLNSG, making it linear. The most compatible buffer, yellow buffer (Thermo Scientific, USA), for both enzymes was selected. 1 unit of enzyme will digest 1 µg of DNA in 1 h at 37°C, so ¼ unit of enzyme was used based on the conditions

and quantity of DNA being digested. A large quantity of the extracted plasmid was digested in a 100 µl reaction, composed of the ingredients outlined in Table 3.1, at 37°C for 2 h.

Table 3.1: Formula for restriction digest of pLNSG

Component	**Quantity (µl)**
10X Conc. Yellow Buffer	20
pLNSG (46.3 ng/µl)	43.2
Enzymes	0.5 of each enzyme
ddH_2O	Up to 100

Digested pLNSG was purified using agarose gel electrophoresis (0.8 percent agarose in 1X TBE, which was made from 5X TBE, the formula is in appendix II) and the level of purity/intactness assessed visually.

The backbone (pLNSir2apro) was extracted from the gel after by using the QIAquick®Gel Extraction kit (QIAGEN GmbH, Germany). The resulting plasmid vector was digested a second time using half of the original concentrations of enzyme and 0.5 µl of alkaline phosphatase (1 U/µL, Thermo scientific, USA) was added 30 min before the end of the digestion to reduce the chance of self-ligation. The double digested plasmid was then purified by phenol chloroform clean up and ethanol precipitation. This involved adding equal volume of phenol/chloroform/isoamylalcohol (Thermo Scientific, USA) solvent mixture and vortexing to extract all the enzymes and other contaminating protein/additives. This mixture was separated into an aqueous and non-aqueous layer by centrifugation at 8000 rpm for 1 min. The aqueous layer was collected using a pipette and put into fresh 1.5 ml eppendorf tube. 0.1 volume of 3 M sodium acetate was then added to the aqueous layer and mixed. Thereafter, 2 volumes (2X volume of the above mixture) of absolute ethanol was added to the above,

mixed and left at -20°C, overnight or at -80°C, for 2 h so as to de-salt and precipitate the DNA out from the solution. Afterwards, the mixture was centrifuged at 4°C, 14000 rpm, for 30 min. The supernatant was almost completely removed and the pellet formed was washed with cold 70% ethanol by spinning at 4°C, 14000 rpm, for 10 min.

3.2.1.2 Purification and amplification of the Fluc insert using Polymerase Chain Reaction

The *Fluc* or simply *luc* (abbreviation for luciferase gene) coding sequence was amplified from the template pmPLP1, appendix III, a generous gift from P. Horrocks laboratory (Wong, Hasenkamp et al. 2011) using polymerase chain reaction (PCR) and the following *luc* primers; GATCCCTAGGATGCATGAAGACGCCAAAAA (LUCAvrII Forward) and GATCCTTAAGTTACAATTTGGACTTTCCGCC (LUCAflII Reverse). The primers were designed using the Snapgene software (GSL Biotech LLC) and the oligonucleotide sequences were ordered from Eurofins mwg®. The primers had the AvrII and AflII enzyme site attached at the ends. The ingredients for the PCR reaction are outlined in Table 3.2 and the PCR conditions are shown in Table 3.3 below.

Table 3.2: Formula for PCR of *luc*

Component	**Quantity (µl)**
5X MyFi Buffer (Bioline, USA)	10
Template (1 ng/µl)	2.5
Primers (10 µM)	1 (0.5 each) (0.1 µM final concentration of each primer)
MyFi DNA Polymerase (Bioline, UK)	2
ddH2O	Up to 50

Table 3.3: PCR conditions for multiplication of *luc*

Temperature (°C)	Time
95	1 min
95	15 s
55	15 s × 35 cycles
72	30 s
72	2 min

The PCR product insert was purified by agarose gel electrophoresis, extracted from the gel using the QIAquick®Gel Extraction kit (QIAGEN GmbH, Germany) and restriction digested with AflII and AvrII. The digest was then purified by phenol chloroform clean up and ethanol precipitation. 1 µl of the cleaned up PCR product and plasmid vector backbone were analysed by using agarose gel electrophoresis and the NanoDrop spectrophotometer.

3.2.1.3 Ligation of the backbone and the insert, and detection of positive clones

The *luc* insert and linearized plasmid vector were ligated using a T4 ligase (Thermoscientific, USA) in a thermocycler at 16°C, overnight. The formula used for this reaction is shown in Table 3.4 below. The molar ratio of insert to vector was 86:1. A control reaction was included to determine the extent of self-ligation or re-cloning of uncut vectors. The resulting pLNSir2aproluc (*PfSir2A-luc* reporter) construct, appendix IV, was purified by phenol chloroform clean up and precipitated using the ethanol precipitation method. 1 µl of yeast tRNA (Thermoscientific, USA) was added to a final concentration of 0.2 µg/µl, before the sodium acetate was added during the clean-up of the construct. The construct was dissolved in 10 µl of ddH_20 and 5 µl of the construct solution was then used to transform 50 µl of electrocompetent *E. coli* by electroporation as described in section 3.2.1.1. 200 µl of the

resulting clear supernatant were discarded and the bacterial pellets were gently mixed with the remaining supernatant and cultured by spreading on an oven-dried sterile LB agar plate (formula in appendix II), containing 100 µg/µl of ampicillin.

Table 3.4: Formula for the ligation reaction

Component	**Test (µl)**	**Control (µl)**
10X ligase buffer (Thermo Scientific, USA)	2	2
Plasmid pLNSir2apro backbone (21.6 µg/ml)	0.8 (17.28 ng)	0.8 (17.28 ng)
T4 ligase (5 U/µl)	0.5 (2.5 units)	0.5 (2.5 units)
luc PCR product insert (43.4 µg/ml)	8 (347.2 ng)	-
ddH_2O	Up to 20	Up to 20

The ratio of colonies on the test plate (*luc* :: pLNSir2apro ligation) to the control plate (pLNSir2apro alone) was checked, then a number of colonies from the test plate was subcultured in 2 ml LB broth, containing 100 µg/µl of ampicillin at 37°C, overnight, in a shaking incubator. The plasmid was extracted from the resulting culture of each colony using the Qiaprep®Spin Miniprep Kit (QIAGEN GmbH, Germany) and digested using AvrII and AflII. The digest was run on the gel to identify positive clones.

Various modifications to the cloning protocol were done after failure to transform *E. coli* with the construct. Such modifications included

- Double digestion of the luciferase (*luc*) insert and increasing the insert to vector molar ratio to 95:1 for ligation. Colony PCR was conducted followed by miniprep on a potential transformant, picked up by the colony PCR, but this failed to identify any positive transformant despite an aggressive or liberal restriction digest with increased quantity of enzymes or buffer. A no template negative control and 2 positive controls (templated on the

construct and on the construct plus a bacterial colony from the cloning control agar plate) were included in the colony PCR. The formula for the colony PCR is detailed in Table 3.5 below. The conditions for this PCR are similar to that for the PCR of the *luc* insert.

Table 3.5: Colony PCR formula

Component	**Test (µl)**
2X MyTaqRed (Bioline, USA)	7.5
luc primers (detailed above) Mix (10 µM)	0.3
ddH_2O	7.2

• Repeat ligation with an insert to vector molar ratio of 43:1. The amount of insert (89.46 ng) was ~10X the amount of the vector (9 ng) in a 20 µl ligation reaction volume (a final DNA concentration of about 5 µg/ml). This was an optimal weight ratio for difficult to clone insert and the total concentration of both the insert and vector is well within the range for optimal ligation (1-10 µg/ml).

• A switch to infusion cloning with a modified insert and the same vector backbone. The modified *luc* insert was amplified by PCR with the following modified *luc* primers containing 15 bp overlap complementary to the ends of the linearized vector: ATTATATATTCCTAGGATGCATGAAGACGCCAAAAA (*luc*Infusion AvrII Forward) and ATAACTCGACCTTAAGTTACAATTTGGACTTTCCGCC (*luc*Infusion AflII Reverse). The primers were designed using the In-fusion cloning online tool (www.takarabio.com , Clontech, Takara Bio, USA). The formula and PCR conditions were exactly the same as that used for the *luc* primers but the elongation time was increased to 45 s. The actual infusion ligation and transformation reaction involved a protocol described in the

In-fusion® HD Cloning Kit user manual, which is discussed in section 3.2.1.5 under the cloning of *PfSir2B* promoter.

These modifications were all unsuccessful, but a successful *PfSir2A-luc* reporter construct shown in appendix IV, was subsequently cloned by my supervisor, Dr. Catherine Merrick, using an insert to vector molar ratio of 43:1. The amount of insert (150 ng) was ~10X the amount of the vector (15 ng) in a 20 µl ligation reaction volume (a final DNA concentration of ~8 µg/ml). The same digestion, PCR and ligation protocols as described above were used. Plasmids from two positive clones were sent for sequencing by Eurofins mwg® using 4 sequencing primers; GATCCCTAGGATGCATGAAGACGCCAAAAA (LUCAvrII Forward), GATCCTTAAGTTACAATTTGGACTTTCCGCC (LUCAflII Reverse), GGGGTGATGATAAAATGAAAG (hsp86term_Seq) and GCAATTGTTCCAGGAACCAG (LUC_Seq) generated in Snapgene software (GSL Biotech LLC). The sequence trace was then aligned with the original sequence in Snapgene software (GSL Biotech LLC) and any mutation was verified.

3.2.1.4 Preparation of maxi preps for large scale extraction of PfSir2A-luc reporter construct

This protocol is similar to plasmid mini prep but involves the use of supersize kits and equipment needed for preparation of large amounts of plasmids used in transfecting large populations of protozoa or mammalian cells, and for low copy number plasmids. Maxi prep of a 500 ml culture of transformed *E. coli* with this construct was used to prepare the *PfSir2A-luc* reporter construct. This DNA was used for transfecting *P. falciparum* 3D7, and for cloning the *PfSir2B* promoter in place of the *PfSir2A* promoter (section 3.2.1.5). *E. coli* carrying the *PfSir2A-luc* reporter construct was grown in 500 ml LB broth, overnight in a shaking incubator at 37°C. The plasmid was then extracted from the resulting culture using the large scale QIAGEN Plasmid Maxi Kit (QIAGEN GmbH, Germany) with a yield of 578

µg. Digestion of a small aliquot of the extracted plasmid construct was used to validate the plasmid. The plasmid was precipitated by ethanol precipitation and 50 µg was dissolved in 30 µl of ddH_20. This was then used for the subsequent transfection of *P. falciparum*.

3.2.1.5 Converting PfSir2A-luc reporter construct to a vector backbone for cloning of a PfSir2B-luc reporter construct

81.4µg of the *PfSir2A-luc* reporter construct was digested at 37°C for 2 h using the outlined enzymes in the following formula below, Table 3.6, so as to remove the *PfSir2A* promoter region. The resulting linearized vector, pLNluc was to be used in cloning the *PfSir2B* promoter region before the luciferase gene.

Table 3.6: Formula for Digestion of *PfSir2A-luc* reporter construct

Component	**Quantity (µl)**
10X Tango Buffer (Thermo Scientific, USA)	10
PfSir2A-luc (10 µg/µl)	8.14
ApaI	1
AvrII	0.5
ddH_2O	Up to 100

Agarose gel electrophoresis was used to purify the digest and the corresponding backbone band was extracted, eluted in a 30 µl elution buffer and digested a second time at 37°C for 2 h using the formula below, Table 3.7.

Table 3.7: Formula for Second Digest of *PfSir2A-luc* reporter construct

Component	**Quantity (µl)**
10X Tango Buffer (Thermo Scientific, USA)	5
PfSir2A-luc (10 µg/µl) (3.2.1.4)	30
ApaI	1
AvrII	0.5
ddH_2O	Up to 50

Alkaline phosphatase was added during the last 30 min of digestion. This digest was purified using phenol/chloroform and precipitated with ethanol at -20°C, overnight.

3.2.1.6 Multiplication and cloning of the PfSir2B promoter Insert

A putative 5'UTR sequence 1677bp upstream of the *PfSir2B* gene on chromosome 14 of the *P. falciparum* genome was amplified using PCR and the following primers; GACCGGGCCCCATATTCTTTGTTATTATAAATTC (*PfSir2B* ApaI Fwd) and GGCCCCTAGGTGTTTTTAAATATGTAAATAATATG (*PfSir2B* AvrII Rev), designed using the Snapgene software (GSL Biotech LLC) and the oligonucleotides ordered from Eurofins mwg®. The primers had the AvrII and ApaI enzyme sites attached at the ends. *P. falciparum* 3D7 genome was extracted using the Qiagen DNA extraction kit (QIAGEN GmbH, Germany) and used as template for the PCR. The formula for the PCR reaction mixture is shown in Table 3.8 and the PCR conditions are shown in Table 3.9. A shortening of annealing or elongation time resulted in no PCR product.

Table 3.8: Formula for PCR of *PfSir2B* promoter

Component	**Quantity (µl)**
5X MyFi Buffer (Bioline, USA)	10
Template (24 ng/µl)	2
Primers (10 µM)	1 (0.5 each) (0.1 µM final concentration of each primer)
MyFi DNA Polymerase (Bioline, UK)	2
ddH_2O	Up to 50

Table 3.9: PCR conditions for *PfSir2B* promoter

Temperature (°C)	**Time**
95	1 min
95	15 s
50	30 s × 35 cycles
65 (specific for *Plasmodium* genome)	2 min
72	2 min

The PCR yielded the correct DNA product (1687 bp size) and an extra slightly smaller DNA product (~1550 bp), after gel filtration. Subsequent extraction of the correct band from the gel and phenol/ethanol purification resulted in low insert yield, but this was still used for downstream reactions. However, ligation and transformation, as described above for the luciferase insert, were unsuccessful. A few things were done to resolve PCR/yield issues and included;

- The use of gradient PCR to determine the optimal annealing temperature using a range from 42 to 56°C. Based on the result, subsequent PCR was done at Ta of 54.9°C, a temperature that gave the least amount of contaminating PCR product, and with half the amount of DNA template. Purification of the PCR product by gel filtration was avoided so as to increase the insert yield. Digestion, phenol chloroform extraction and gel filtration were done, giving a yield of 50 ng/µl. However, transformation following ligation was still unsuccessful.

- Designing and using an alternative Fwd primer GACCGGGCCCGTTTGGTTTTAAAATATATATTT (*PfSir2B* ApaI Fwd2) (appendix V). The resulting product was 1212 bp upstream the *PfSir2B* gene. The PCR was performed as outlined above in tables 3.8 and 3.9 with Ta of 54.9°C not 50°C and 1 µl of template DNA. Although, the ratio of the required product to the contaminating product was higher, the yield was 22.1 ng/µl, and transformation was unsuccessful.

- Design and use of infusion primers 1292 bp upstream of the *PfSir2B* gene; TTAGCTAAGCATGCGGGCCCGATAACTAAACCCTCATT (Fragment.FOR) and CTTCATGCATCCTAGGTGTTTTTAAATATGTAAATAATATG (Fragment.REV), thus creating a fragment *in silico* as shown in appendix V. Afterwards, PCR was done using CloneAmp™HiFi PCR Premix protocol outlined below in tables 3.10 and 3.11, (www.clontech.com) but with Ta of 54.9°C. The resulting *PfSir2B* promoter insert was cloned into the pLNluc vector using in-fusion cloning.

Table 3.10: Formula for PCR of *PfSir2B* promoter using CloneAmp™HiFi PCR premix

Component	**Quantity (µl)**
2X CloneAmp™HiFi PCR Premix	25
Template (24 ng/µl)	1
Primers (10 µM)	1 (0.5 each) (0.1 µM final concentration of each primer)
ddH_2O	Up to 50

Table 3.11: PCR conditions for *PfSir2B* promoter using CloneAmp™HiFi PCR premix

Temperature (°C)	**Time**
98	10 s
54.9	15 s × 35 cycles
65	2 min

3.2.1.5 In-fusion cloning of PfSir2B promoter into pLNluc vector and detection of positive clones

Ligation of the insert and pLNluc backbone was done using infusion cloning protocol described in the In-fusion® HD Cloning Kit user manual. The cloning reaction mixture is presented in Table 3.12.

Table 3.12: In-fusion HD Cloning of *PfSir2B* promoter before the luciferase gene in pLNluc

Component	**Test Cloning (µl)**	**Negative Control (µl)**	**Positive Control (µl)**
PCR Fragment	0.5 (62.75 ng)		2
pLNluc vector	0.5 (94.4 ng)	1 (188.8 ng)	1 (188.8 ng)
5X In-fusion HD enzyme Premix	2	2	2
ddH_2O	to 10	to 10	To 10

A negative control reaction was included to determine the extent of self-ligation or re-cloning of uncut vectors. A positive control reaction with a pUC19 vector was included to determine cloning efficiency. The insert used for the positive control reaction was a 2 kb control insert provided with the In-fusion kit.

All reaction components were mixed and incubated at 50°C in a heat block for 15 minutes, and were placed immediately on ice. Transformation was done using 2.5 µl of each reaction mixture and 50 µl of thawed competent *E. coli* and Stellar cells provided with the In-fusion cloning kit. The reaction mixture and competent cells were mixed in a microtube and placed on ice for 30 minutes. *E. coli* was transformed by electroporation as previously described while the Stellar cells mixture was heat shocked at 42°C, for 60 seconds and then placed on ice for 2 minutes. The transformed cells were recovered with 447.5/300 µl of warmed SOC broth (at 37°C) for the Stellar cells/*E. coli* at 37°C for 1 h in a shaking incubator. 2 and 10 fold dilutions of the transformants were plated in LB agar containing ampicillin, 100µg/ml, while the rest were spun at 5000 rpm for 5 min and suspended in 100 µl

of SOC broth. These were then plated using the same agar medium. All the plates were incubated at 37°C overnight. The positive PUC 19 control had colonies which indicated that the cloning had worked. Positive clones were identified using colony PCR first even though there was a 13:1 ratio of suspected test colonies to negative control colonies. The plasmid of 6 colonies suspected to carry the correct insert after a colony PCR was extracted and digested using the ApaI and AvrII enzymes. Of these, only 4 had the correct backbone and insert. The plasmids of 2 of these were sent off for sequencing, using the following oligonucleotides; CTTCATGCATCCTAGGTGTTTTTAAATATGTAAATAATATG (Fragment.REV), TGTTTTTAAATATGTAAATAATATG (Sir2bPrRev), GACCGGGCCCGTTTGGTTTTAAAATATATATTT (Sir2ProFwd2) and TTAGCTAAGCATGCGGGCCCGATAACTAAACCCTCATT (Fragment FOR.).

3.2.1.6 Complete restriction analysis of the plasmid constructs

PfSir2A-luc and *PfSir2B-luc* construct were restricted using 5 restriction enzymes that cleave at various restriction sites in the plasmid which resulted in different sized segments containing the different components of the plasmid. The following FastDigest enzymes (ThermoFisher, UK) were used for the *PfSir2A-luc* construct: EcoRV, AvrII, ApaI, SacI and SalI. The reaction components and conditions are presented in Table 3.13. The following FastDigest enzymes (ThermoFisher, UK) were used for the *PfSir2B-luc* construct: EcoRV, ApaI, SacI and SalI. A conventional enzyme BglII (Thermo Scientific, USA), was included in this array. The reaction components and conditions are presented in Table 3.14. The reaction was set up and the components put in the order described by the manufacturer.

Table 3.13: Formula and reaction condition for the restriction digest of *PfSir2A-luc* construct

Components	**Reaction quantity/condition in each digest**					
	Tube 1	**Tube 2**	**Tube 3**	**Tube 4**	**Tube 5**	**Tube 6**
10X FastDigest Green Buffer (µl) (ThermoFisher, UK)	1	2	2	3	4	5
PfSir2A-luc construct (µl)	1	2	2	2	2	2
Number of enzymes	-	1	2	3	4	5
ddH_20 (µl) up to	10	20	20	30	40	50
Incubation time (min)	20	5	10	13	20	20
Incubation temperature (°C)	37	37	37	37	37	37

Tube 1 is the control reaction. For other tubes, 1µl of each enzyme was added with the previous enzyme(s) being compulsorily part of the reaction of the reaction component. For example, in tube 3 a second enzyme was added in addition to the enzyme that was added to tube 2.

Table 3.14: Formula and reaction condition for the restriction digest of *PfSir2B-luc* construct

Components	**Reaction quantity/condition in each digest**					
	Tube 1	**Tube 2**	**Tube 3**	**Tube 4**	**Tube 5**	**Tube 6***
10X FastDigest Green Buffer (µl) (ThermoFisher, UK)	1	2	2	3	4	5
PfSir2A-luc construct (µl)	0.5	1	1	1	1	1
Number of enzymes	-	1	2	3	4	5
ddH_20 (µl) up to	10	20	20	30	40	50
Incubation time (min)	10	5	5	8	10	130
Incubation temperature (°C)	37	37	37	37	37	36 & 37*

*****Reaction was set up as per tube 5 and incubated for 10 min, after which 8 µl of 10X Tango Buffer (Thermo Scientific, USA) and 1 µl of BglII was added to 31 µl of this reaction mixture. The resulting mixture was incubated for 2 h.

3.2.2 Culturing of Parasites

Culturing was done according to section 2.1. 2 µg/ml of Blasticidin S deaminase (BSD, 10 mg/ml, Fisher, UK) was added to the complete media used to culture the transfected parasites.

3.2.3 Transfection of *P. falciparum* 3D7 with *PfSir2A-luc* reporter construct and detection of the transgenic parasites

P. falciparum 3D7 was transfected with *PfSir2A-luc* reporter construct. This was performed as previously described (Deitsch, Driskill et al. 2001), with some modifications. Briefly, 50 µg of the plasmid was first introduced into uninfected red blood cells (RBCs) that had been washed in incomplete CytoMix, (Menard, 2013). This introduction was carried out

by electroporation of a mixture of 30 µl of a solution of the plasmid construct (1.67 µg/µl) in sterile ddH_2O, 170 µl of CytoMix and 200 µl of the washed RBCs, in a 0.2 cm cuvette with a GenePulser II electroporator (Bio-Rad) at 0.31 kV and 960 or 950 µF (microfarads), aiming for a time constant of between 10 to 14 ms. The DNA loaded RBCs were then recovered with 5 ml of complete media and washed twice with the complete media in a Falcon tube.

0.5 ml of the parasites in untransformed RBCs at about 5% parasitaemia was then cultured in 4.5 ml of the transformed RBCs in complete media at ~2.5% haematocrit. They were allowed to multiply, reinvade the transformed RBCs, and spontaneously take up the introduced plasmid. 2 µg/ml (of the final culture volume) of BSD, a drug that selects for the transfected parasites, was then added 48 h later. The parasite culture media was regularly changed in order to remove dead parasites and refresh the parasite nutrients. The drug was added with each media change until drug resistant parasites emerged and thereafter. 50 µl of 100% RBCs was added every week until the transfected parasites came up. Parasite detection was done by microscopy and bioluminescence signal was measured using a luciferase assay system (Promega, UK) and a luminometer, Glomax-Multi Detection System (Promega, UK). The luciferase assay system contained 5X Passive lysis buffer (PLB) and Luciferase assay substrate (LAS).

The protocol used to detect this luciferase activity of parasite culture was the improved Single-Step Lysis Protocol (Hasenkamp, Wong et al. 2012). Here, 10 µl of 5X PLB, warmed to 37°C, was homogenized with 40 µl of parasite culture in the wells of a 96-multiwell white plate (Grenier-bio-one, Germany), by rocking/swirling. This was then mixed with 50 µl of LAS, at room temperature. This was done in triplicate for each *Plasmodium* sample and the bioluminescence was measured in light unit using the Glomax-Multi detection immediately.

3.2.5 Synchronization of parasites

This was done according to section 2.2, on the transfected 3D7 and a *Pfpcna-luc* strain of *P. falciparum* (a generous gift from the Horrock's laboratory, School of Life Sciences, Keele University, UK), as control.

3.2.6 Characterization of 3D7 *PfSir2A-luc* reporter and *Pfpcna-luc* lines

Asynchronous parasite population of 3D7 *PfSir2A-luc* reporter line was used to determine the effect of parasitaemia on bioluminescence by serial dilution from 2.5% parasitaemia down to 0.5% parasitaemia. Parasites tightly synchronized by Percoll and sorbitol were used to determine the bioluminescence of the 3D7 *PfSir2A luciferase* reporter line, alongside the well characterized Dd2 *luciferase, Pfpcna-luc,* reporter line (Wong, Hasenkamp et al. 2011), throughout their IDC. The experiment was begun 55 h and 48 h after the Percoll and sorbitol synchronizations respectively (i.e. 7 h post invasion (hpi),) and the parasites were assessed to conform to the required stage by Giemsa stained thin blood smear which indicated at least 82% purity of the required stage. The parasite samples were harvested when they were at most 7, 10, 21, 24, 27, 30, 45, 48, 51, and 54 hpi and their bioluminescence determined using the improved Single-Step Lysis Protocol, earlier described. The signal was normalized to 1% parasitaemia. A thin blood smear was also made for the different time points, stained and photographed using Leica® camera attached to a light microscope.

3.2.7 Stress treatment of parasites and luciferase assay

This was done according to section 2.3 on tightly synchronized blood stages of 3D7 *PfSir2A-luc* reporter line, so as to investigate the dynamic changes in activity of the *PfSir2A* promoter, independent of the *PfSir2A* gene, in response to host stress factors. The 2 and 6 h time points also allowed for turnover of the luciferase protein before the second time point as Fluc has a half-life of ~1.5 h in *P. falciparum* (Hasenkamp, Sidaway et al. 2013). After each stress treatment, the bioluminescence signal of each of the culture samples was measured

immediately as previously described, and the relative luciferase activity calculated as described in section 3.2.10 below. The parasites survival rate at 48 h was also determined for the trophozoites alone according to section 2.4.

3.2.8 RNA harvest, purification and cDNA synthesis

This was done according to section 2.5.

3.2.9 RT-PCR for changes in gene expression

This was done according to section 2.6, with the addition of the primers in Table 3.15 for *Fluc* which were designed in Snapgene software, and included in the reactions to determine changes in transcript levels of the *Fluc* gene. A second *Fluc* primer was designed to reassess the upregulation of *luc* by the lactate only stress.

Table 3.15: Primers used for the qPCR

Gene	**Fwd primer**	**Rev primer**	**Product size(bp)**
Fluc	TTACAATTTGGACTTTCCGC	ACGATGACGGAAAAAGAG	180
Fluc (alternative region)	GACCTTTCGGTACTTCGTC	CGTGGCAGGTCTTCCC	173

3.2.10 Analysis of data

RT-qPCR data was analysed according to section 2.7. After the stress experiments, bioluminescence signals were converted to relative luciferase activities following a comparison of bioluminescence of the stressed samples relative to the untreated group using the equation:

$$Relative\ luciferase\ activity = \frac{bioluminiscence\ of\ Stress\ sample}{bioluminiscence\ of\ Control\ sample}$$

Mean luciferase activity was the mean of at least two biological or three technical replicates for preliminary supportive findings. Statistical significance was determined by comparing to the control using Kruskal-Wallis test for non-normally distributed data (Anderson-Darling test for normality), since the group sample size was less than 15 for a sample group. Where normality of data was indicated, the parametric alternative, ANOVA, was used. Levels of significance were assessed at $\alpha = 0.05$. The error bars were represented as either the propagated standard deviation (SD) for technical replicate or standard error of mean (SEM) for biological replicate. Propagated error was calculated as the square root of the sum of squares of %SEM for the recovery rate data derived from the luciferase activity and survival rate data.

3.3 Results

3.3.1 Creation of *P. falciparum* 3D7 *PfSir2A* and *PfSir2B* promoter luciferase reporter lines

Two reporter constructs were made using the firefly luciferase reporter gene, *Fluc*, coding sequence from *Photinus pyralis*. The amplified sequence was 1.676 Kb (Fig. 3.1A), the coding sequences for AflII and AvrII enzyme sites were also included, with some 10 extra base pairs (5 at each end) to ensure restriction enzyme binding. Firstly, a plasmid containing *Fluc* was constructed from the existing plasmid vector pLNSir2aGFP under Sir2 pro (pLNSG) vector. This vector was constructed by Dr. Merrick as a cloning vector in a previous study (Merrick et al., 2012). *Fluc* or simply *luc* was ligated to the linearized pLNSG, 7.053 Kb, Figure 3.1B, between the AvrII and AflII enzyme sites, under the Sir2A promoter, with *luc* coding sequence replacing the *PfSir2A* and GFP coding sequences. The size of the resulting reporter construct, pLNSir2aproluc, was 8.720 Kb, Figure 3.1C. A schema of the

cloning process is shown in the Snapgene plasmid map construction flow chart, Figure 3.3. The luciferase gene should be transcribed to a similar level as endogenous *PfSir2A* because the promoter region of *PfSir2A* contained in pLNSG vector was previously shown to be transcribed to a similar level as the endogenous gene (Merrick et al. 2012).

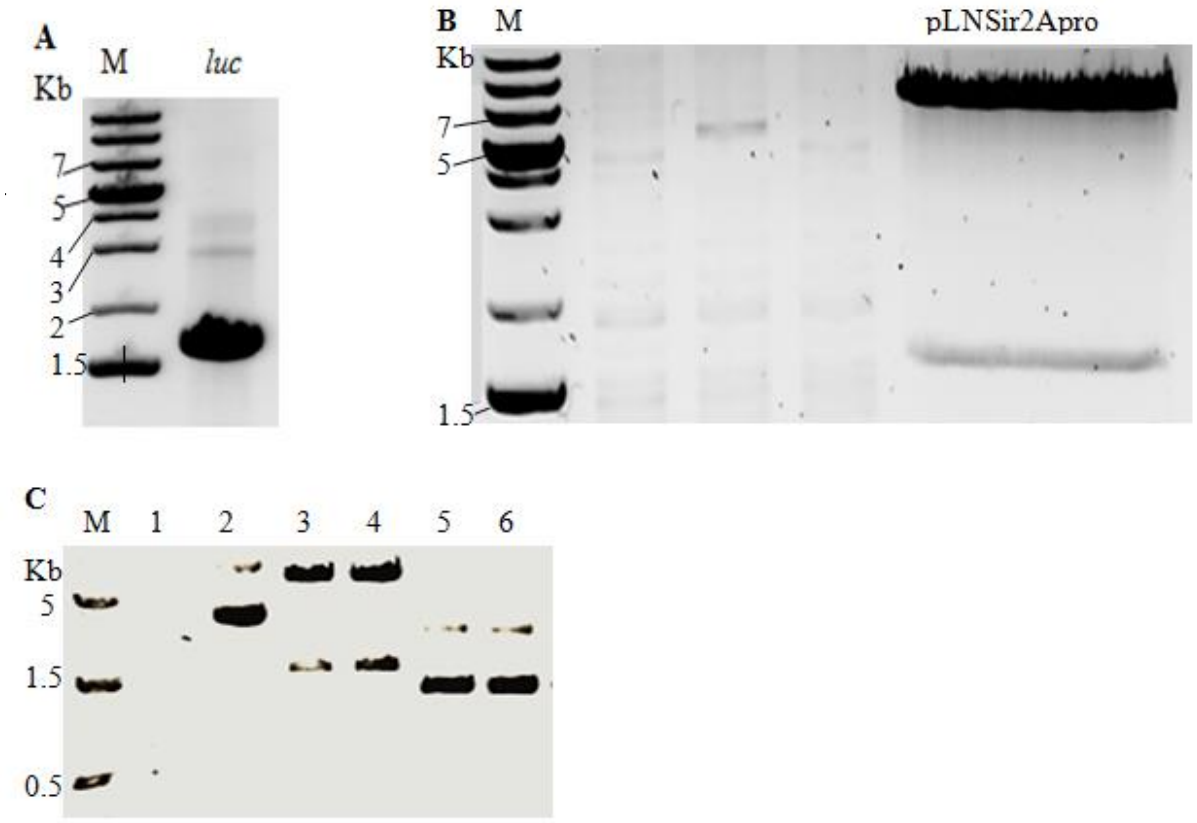

Figure 3.1: **Restriction analyses of the *luc* insert and vector backbone used in cloning of the *PfSir2A-luc* construct, and DNA of clones carrying this construct A.** *luc* insert band generated by PCR. **B.** Digested pLNSG vector = pLNSir2Apro backbone, as the *Sir2A* and *GFP* genes were removed**.** After digestion with AvrII and AflII, the bigger band is the vector backbone, while the smaller faint band is the excised *PfSir2A* and GFP gene. **C.** Digested plasmids from selected transformed *E. coli* colonies of the restriction cloning by Dr. Catherine Merrick in 2016. Lanes 1–6 are plasmid from 'potentially' positive colonies from the test agar plate, which have been digested with (continues on the next page)

3 and 4 digested correctly to give bands of 1.676 Kb for the *luc* insert and 7.053 Kb for the pLNSir2Apro backbone. M is the DNA marker (Thermo Fisher Scientific, UK) band in all the Figure panels.

Secondly, the *PfSir2B* promoter region was cloned into the *PfSir2A-luc* construct, Figure 3.2, before the luciferase gene. The position of *luc* in this construct was verified by restriction digest (Fig. 3.2A). 1.292 Kb upstream of the *PfSir2B* was amplified by PCR from *P. falciparum* 3D7 genome as a fragment containing AvrII and ApaI enzyme sites (Fig. 3.2B). Infusion cloning was highly successful (Fig. 3.2C) with the fragment joined to linearized vector construct of a band size of 6.972 Kb, after excision of the *PfSir2A* promoter sequence. The size of the resulting reporter construct, pLNSir2bproluc (*PfSir2B-luc* reporter construct), was 8.264 Kb. This construct and the *PfSir2A-luc* construct as well, digested correctly to give the correct band size of the promoter regions under investigation (Fig. 3.2D). A schema of the cloning process is shown in the Snapgene plasmid map construction flow chart, Figure 3.4 below.

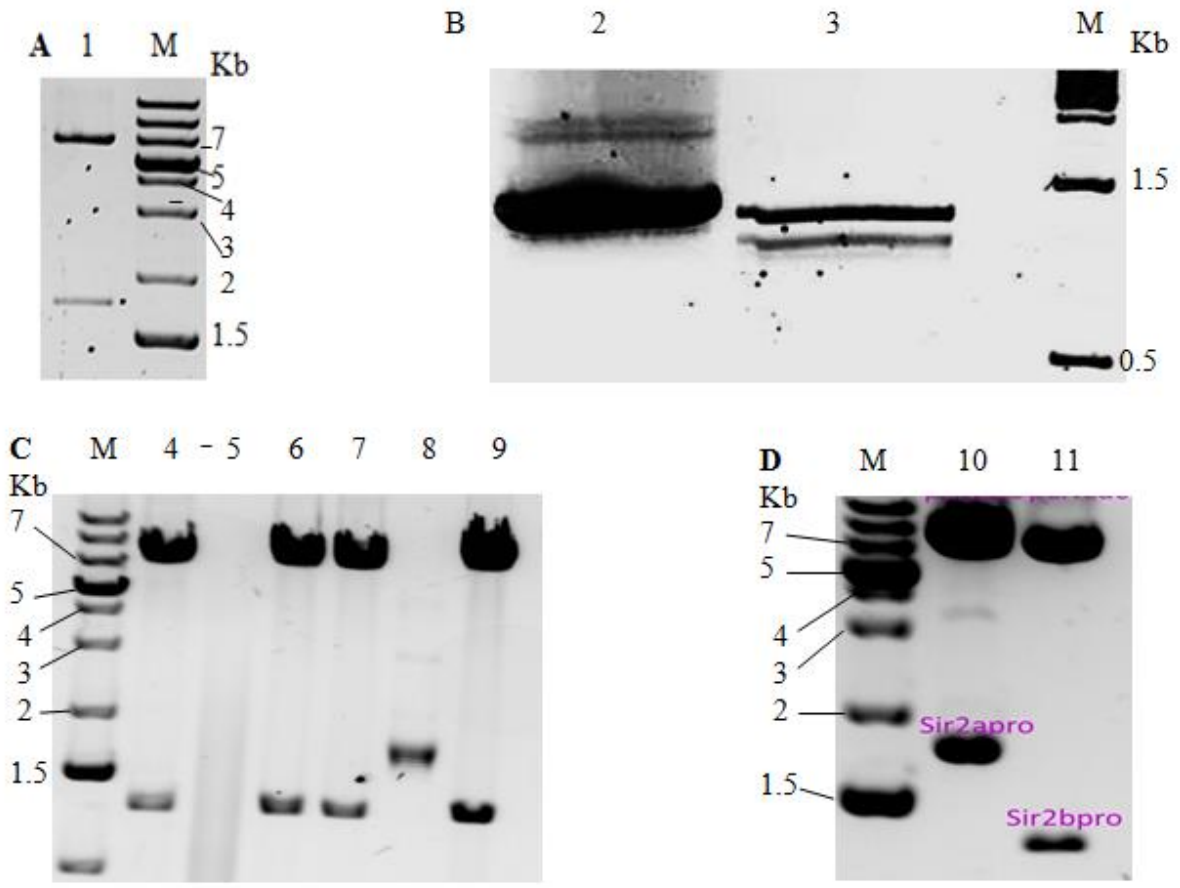

Figure 3.2: **Restriction analyses of the *PfSir2A-luc* plasmid and *PfSir2B* promoter used in cloning of the *PfSir2B-luc* construct, and DNA of clones carrying this construct A.** 1= *PfSir2A-luc* plasmid which was digested with ApaI and AvrII, the bigger band is the pLNluc vector backbone, while *PfSir2A* promoter (smaller band) is excised. **B.** *PfSir2B* promoter insert was generated by CloneAmpPCR premix (lane 2) and MyFi DNA polymerase (lane 3). 125.5 ng/µl *of PfSir2B* promoter PCR product was gotten after gel purification. More of the *PfSir2B* promoter PCR product was generated by MyFi DNA polymerase than the contaminating product, after optimizing the PCR conditions. **C.** Plasmids from selected colonies after the Infusion cloning were digested. Lanes 4, 6, 7 & 9 are plasmids from potentially positive colonies from the test agar plate, which have been digested with AvrII and ApaI. 4 of the 6 colonies digested correctly to give bands of 1.329 Kb for the *PfSir2B* promoter insert and 6.972 Kb for the luciferase backbone. (continues on the next page)

D. The two luciferase constructs, pLNluc under *PfSir2A* pro (*PfSir2A-luc* construct) and pLNluc under *PfSir2B* pro (*PfSir2B-luc* construct), digested properly into pLNluc bigger band and smaller bands of the respective promoters (lanes 10 and 11). M is the DNA marker band in all Figure panels.

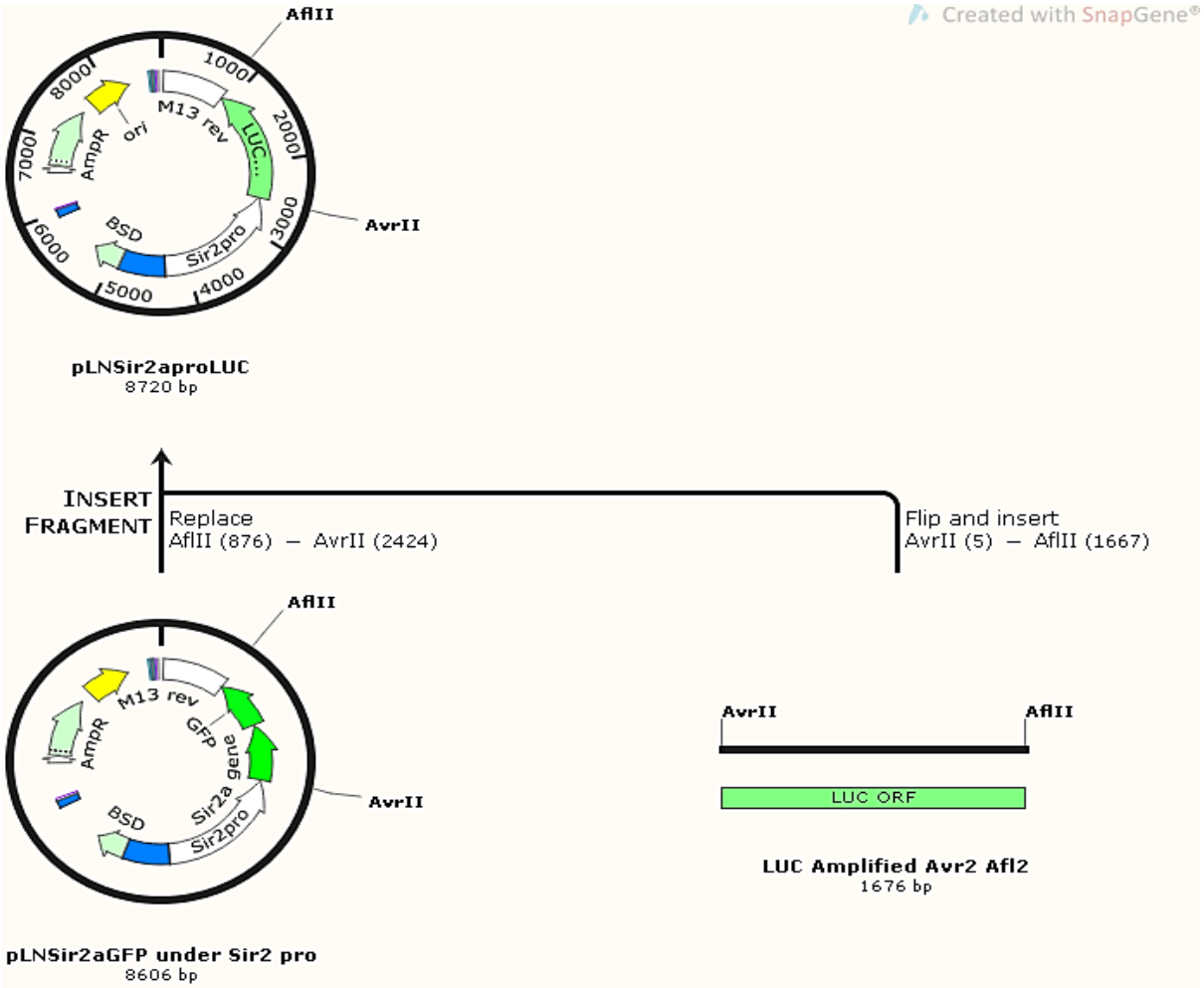

Figure 3.3: Snapgene plasmid map construction flow chart of pLNSir2aproluc. *Fluc* was amplified from pmPLP1 and ligated with pLNSir2apro to give the pLNSir2aproluc

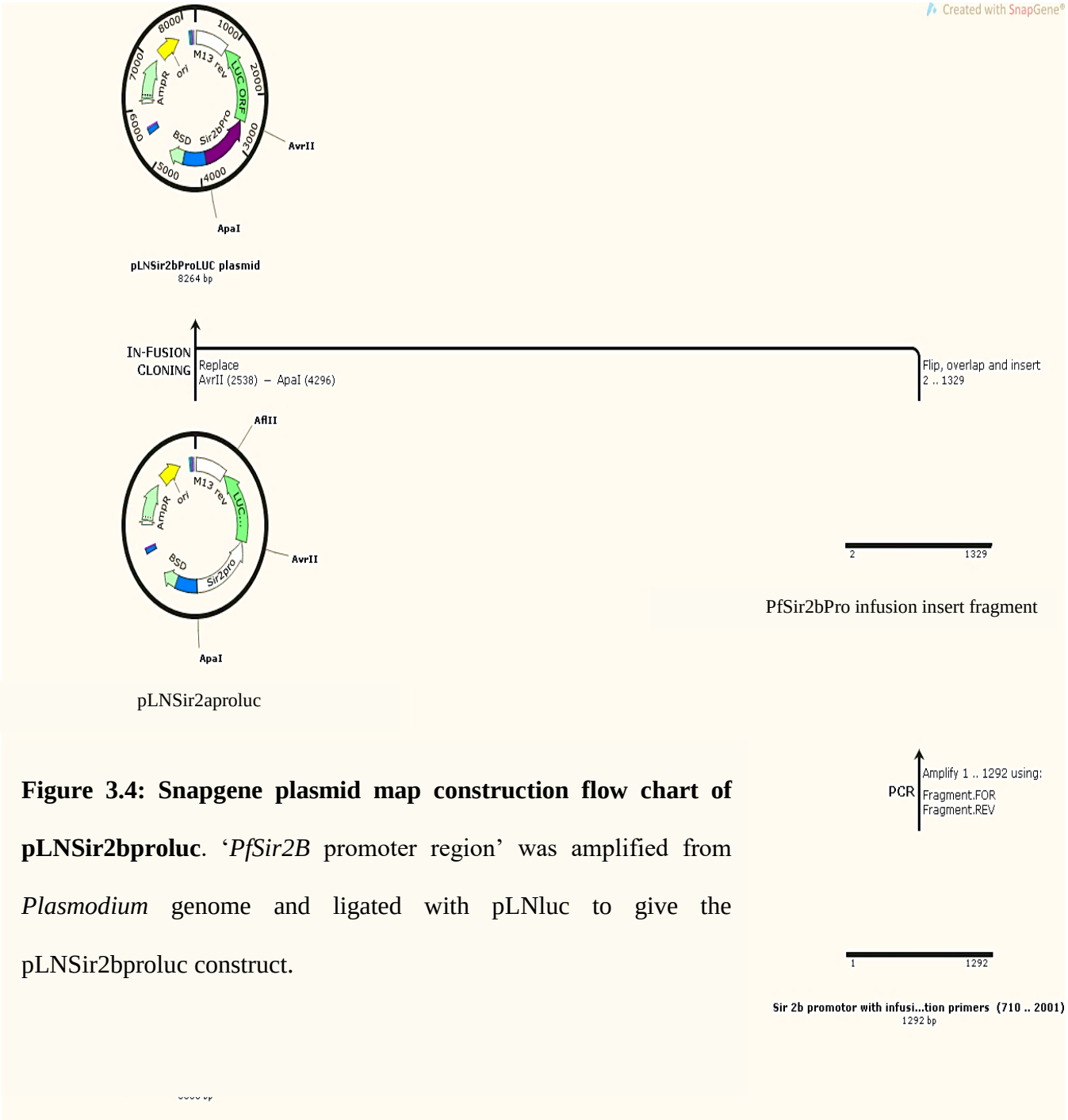

Figure 3.4: Snapgene plasmid map construction flow chart of pLNSir2bproluc. '*PfSir2B* promoter region' was amplified from *Plasmodium* genome and ligated with pLNluc to give the pLNSir2bproluc construct.

A complete restriction analysis of the two plasmid constructs is presented in Figure 3.5. This restriction map proves that the plasmids were correctly made.

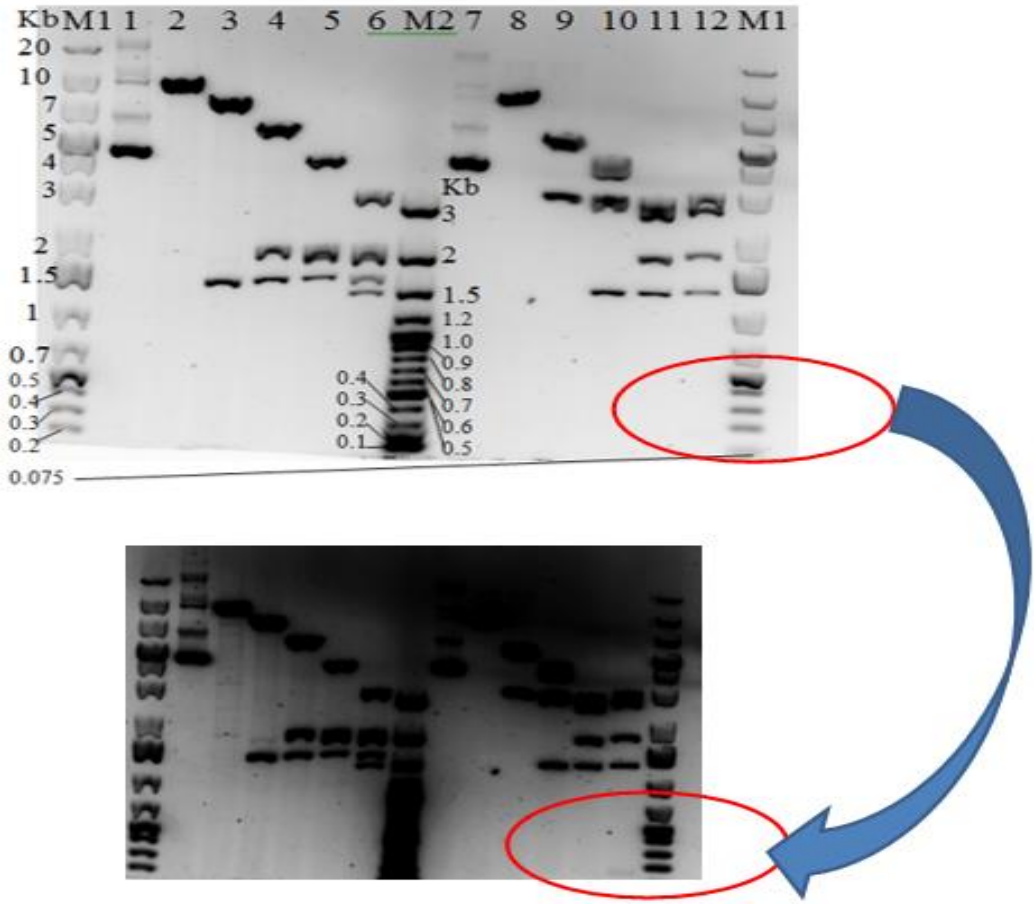

Figure 3.5: Complete restriction analysis of *PfSir2A-luc* construct and *PfSir2B-luc* construct. Lanes are: M1 = 1Kb plus DNA ladder, 1= uncut *PfSir2A-luc construct*, lanes 2 - 6 are restriction digest from tube 2 – 6 and are 2 = EcoRV alone, 3 = EcoRV AvrII band (1.34 Kb) + backbone, 4 = EcoRV AvrII band (1.34 Kb) + AvrII ApaI band (1.76 Kb) + backbone, 5 = EcoRV AvrII band (1.34 Kb) + AvrII ApaI band (1.76 Kb) + the barely distinct ApaI SacI band (1.62 Kb) + backbone and 6 = every band bit in lane 5 with the additional SalI EcoRV band (1.17 Kb), with the backbone being a SacI SalI band (2.83 Kb). M2 = 100 bp plus DNA ladder. Band 7 = uncut *PfSir2B-luc construct*, lanes 8 – 12 are restriction digest from tube 2 – 6 and are 8 = SalI alone, 9 = SalI SacI band (2.83 Kb) + the rest of the plasmid, 10 = SalI SacI band (2.83 Kb) + SalI Eco RV band (1.17 Kb) + the rest of the plasmid, 11= SalI SacI band (2.83 Kb) + SalI Eco RV band (1.17 Kb) + (continues on the next page)

ApaI SacI (1.62 Kb) + the rest of the plasmid and 12 = every band in 11, with an Eco RV BglII band (2.49 Kb) and the additional BglII Apa I band (0.152 Kb) which becomes visible when you increase the exposure of the agarose gel.

The 3D7 *PfSir2A* luciferase reporter lines were visible in culture 19 days after the parasite took up the pLNSir2aproluc construct loaded into fresh red blood cells. This construct was episomally located but is likely to be maintained as large, stable concatamers due to the persistent BSD drug pressure it was under (O'Donnell, Preiser et al. 2001). The reporter line was confirmed to express luciferase due to its facilitation of the reaction of luciferin with oxygen and subsequent release of light as detected by the luminometer (Fig. 3.6A). 3D7luc@960, the one with the higher TC, was subsequently used in further experimentation as it appeared to have grown better giving a higher bioluminescence reading even though exactly the same population of parasite were transfected at the different capacitances, 960 and 950 µF. A restriction digest of its plasmid DNA, extracted and digested with AvrII and AflII enzymes, gave the *Fluc* band and the pLNSir2apro band (Fig. 3.6B).

Transfection of the second luciferase construct, pLNSir2bproluc, into 3D7 was halted as problems were encountered in using the *PfSir2A* promoter in the 3D7 *PfSir2A* luciferase reporter line as shown in subsequent experiments (see later sections of this chapter).

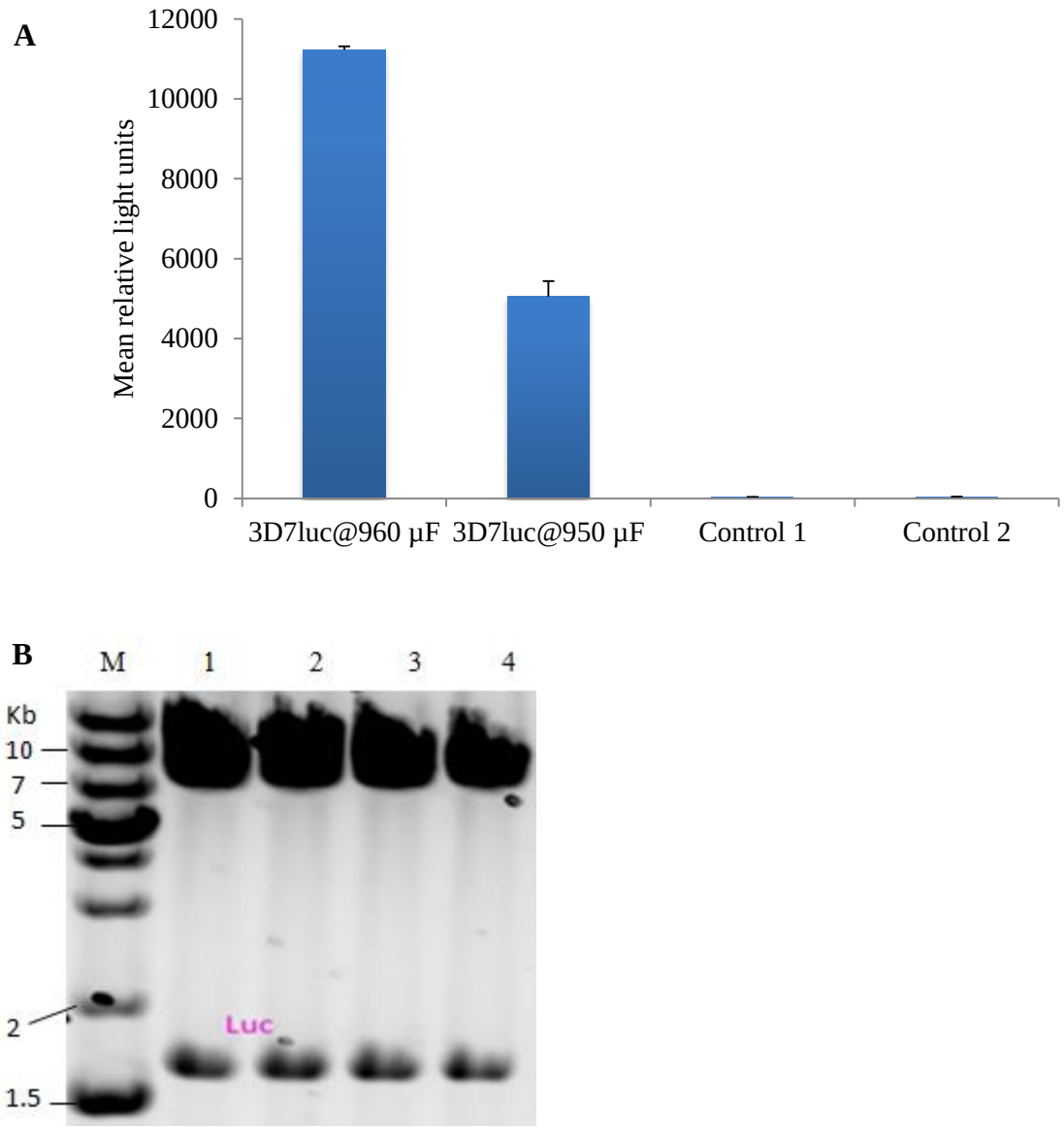

Figure 3.6: Detection of bioluminescence in the cloned 3D7 *PfSir2A-luc* lines. A. Bioluminescence signal was detected in a 96 well plate after the transformants: 3D7luc@960/@950 µF (3D7 *PfSir2A* luciferase reporter lines transformed at 960 and 950 µF) were left to come up ~19 days post transformation. Values are in mean of three technical replicates in light units. Error bars are standard deviation of the technical replicates from the mean. Media and 4% RBC in complete RPMI controls were included as control 1 and 2 respectively. **B.** AvrII and AflII digest of plasmid DNA extracted from two 3D7 *PfSir2A* luciferase reporter lines. Two transfections were done at 960 µF and 950 and they gave two

different time constants (TC), 16.4 and 15 ms respectively, which were reasonable values but not within the ideal range of 10 to 14 ms. However, both these transfections came up and plasmids rescued from the resultant parasites. The restricted plasmids were loaded in duplicate lanes, lanes 1 & 2 are for 3D7luc@960, while lanes 3 & 4 are for 3D7luc@950, all giving pLNSir2apro backbone and *luc* insert bands.

The bioluminescence signal of 3D7 *PfSir2A* luciferase reporter line increased proportionally as the parasite population increased, with a high correlation coefficient, R^2, of 0.99 as shown in Figure 3.7 below. This indicates that luciferase activity in the reporter line under the *PfSir2A* promoter should be equivalent to the parasite numbers.

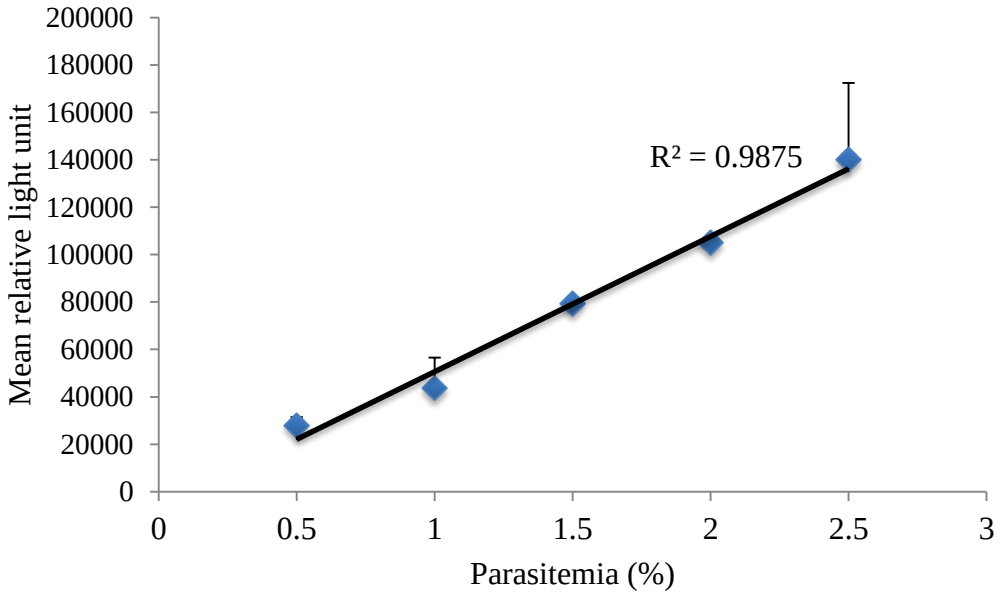

Figure 3.7: Mean light units of 3D7 *PfSir2A* luciferase reporter line at increasing parasitaemia. Mean light units are mean of three technical replicates, while error bars are standard deviation.

3.3.2 Bioluminescence signal throughout the IDC of the reporter line

Characterization of the 3D7 *PfSir2A* luciferase reporter line was conducted by determining relative luciferase expression across 10 time-points over a 47 hr period, with highly synchronized parasites from the ring stage of about 0 - 7 hpi. This characterization captured promoter activity changes during its IDC. Luciferase expression under the *PfSir2A* promoter begins at the very young ring stage and peaks at the schizont stage (Fig. 3.8A). This pattern of expression is broadly similar to steady state mRNA pattern of the *PfSir2A* endogenous gene (Fig. 3.8B, Otto, Wilinski et al. 2010) shown alongside the characterization of the temporal change of *PfSir2A* promoter activity. Generally, there was little *PfSir2A* expression from the rings stage (as represented in the panel of images) up until ~30 hpi for both graphs, however, after 30 hpi promoter activity (luciferase expression) and *PfSir2A* expression dramatically increases in the late trophozoite/schizont stages. This indicates that the expression levels of luciferase closely mimicked endogenous promoter activity, independent of *PfSir2A* gene expression in the wild-type parasite, and could potentially be responsive in a similar manner to host stress factors. A well-characterized luciferase expressing line, Dd2luc, expressing luciferase under the *Pfpcna* promoter, was characterized (Fig. 3.9A) alongside 3D7 *PfSir2A* luciferase reporter line. This showed a similar pattern of luciferase expression throughout its IDC as previously published (Fig. 3.9B, Hasenkamp, Wong et al. 2012), with expression peaking at trophozoite stage.

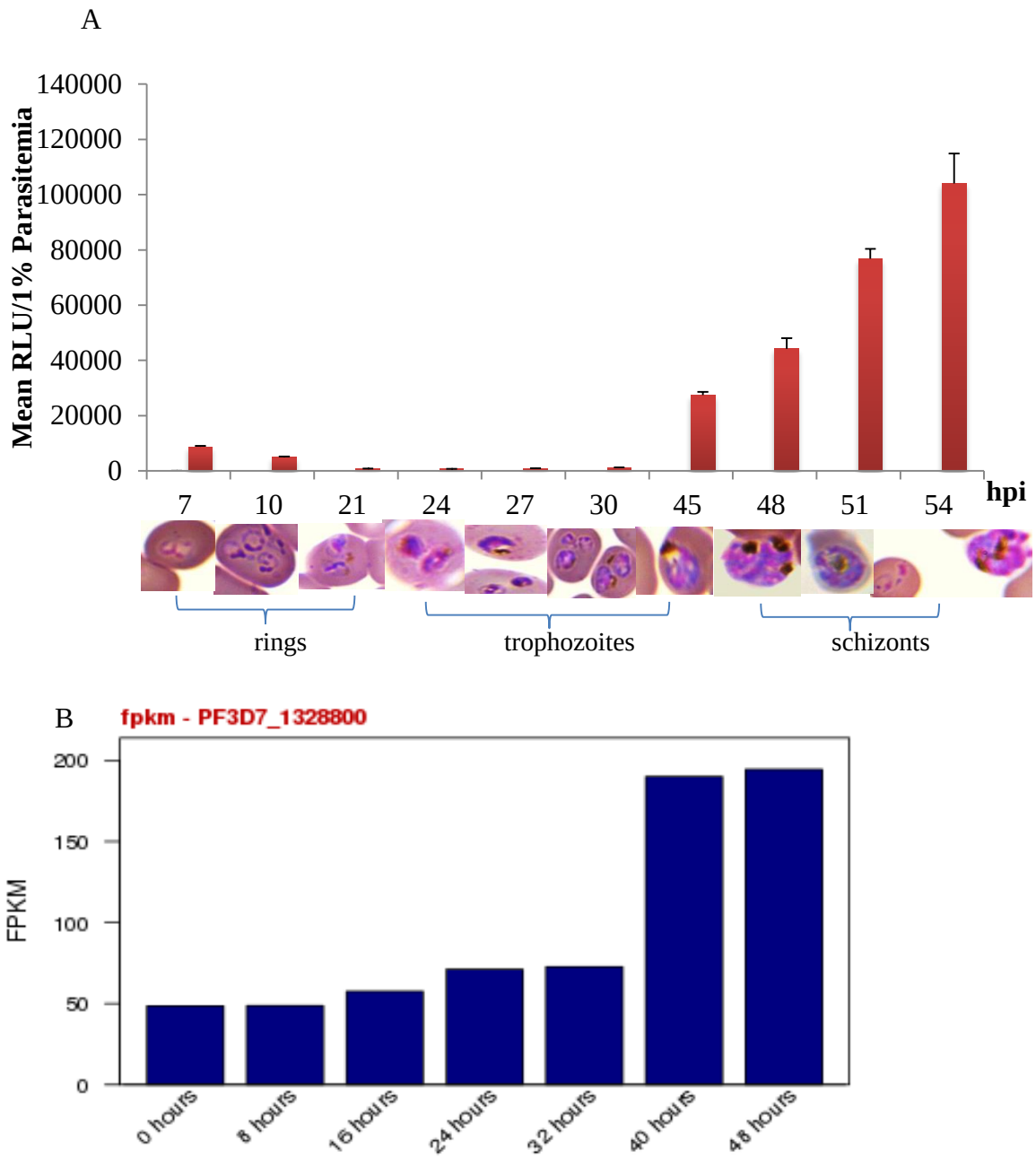

Figure 3.8: Temporal bioluminescence pattern throughout the IDC of a 3D7 line expressing luciferase under the control of *PfSir2A* promoter. A. Luciferase expression in 3D7 *PfSir2A* luciferase reporter line over one asexual life cycle demonstrating temporal changes in its various stages (shown in the panel of images). Mean light units are mean of three technical replicates and error bars are standard deviation of technical replicates from the mean. **B.** Temporal changes in the expression of *PfSir2A* gene (PF3D7_1328800) throughout the IDC of 3D7 wild type as published in PlasmoDB by Otto *et al*. 2010 (Otto, Wilinski et al. 2010). FPKM is Fragments Per Kilobase of transcript per Million mapped reads. RLU = relative light unit.

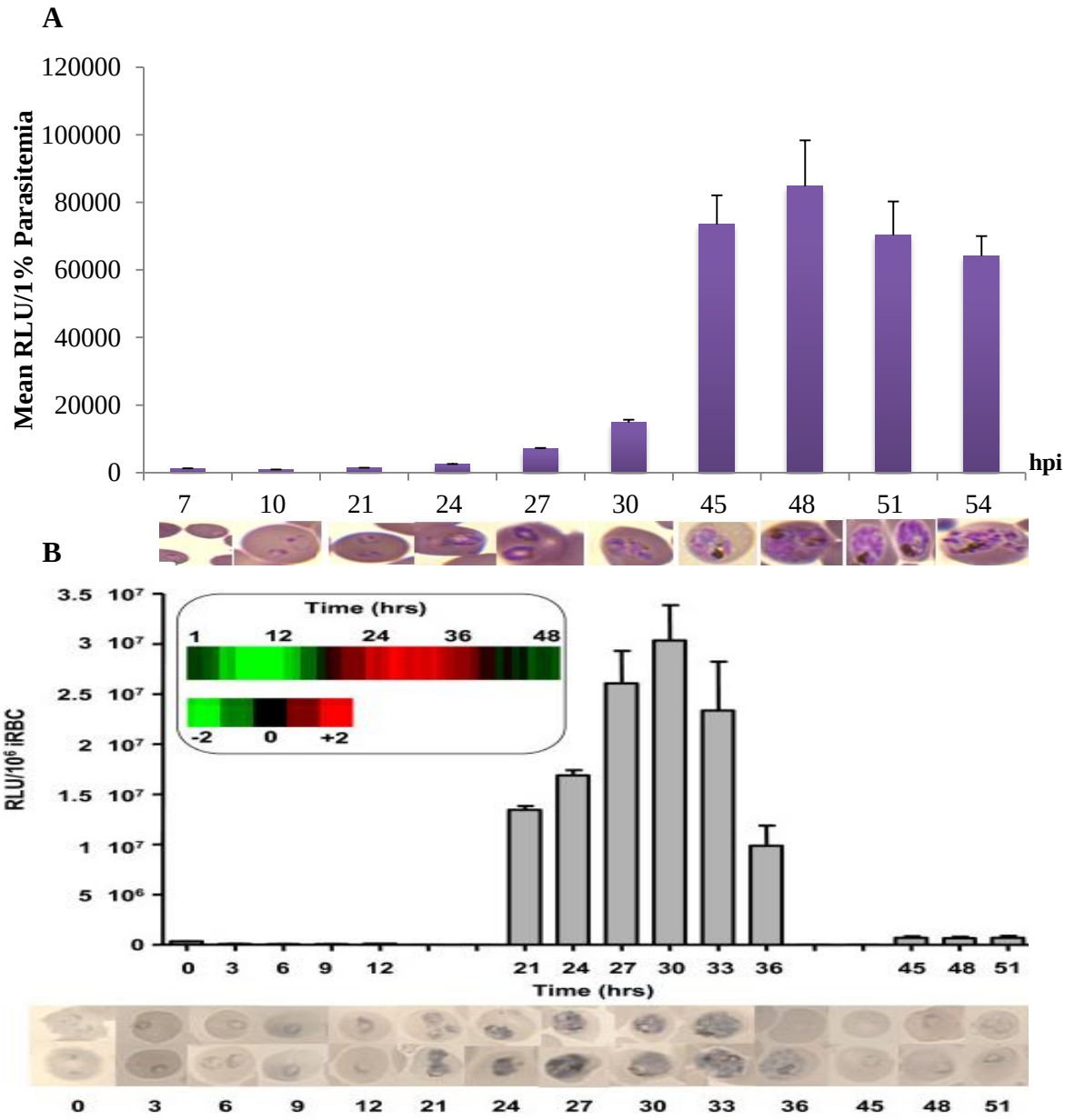

Figure 3.9: Temporal bioluminescence pattern of the previously characterized Dd2 lines expressing luciferase under the control of *Pfpcna* promoter. A. Luciferase expression in Dd2luc over one asexual life cycle demonstrating temporal changes in expression mimicking the promoter activity of *Pfpcna*. Mean light units are mean of three technical replicates and error bars are standard deviation of technical replicates from the mean. **B.** Temporal changes of *Pfpcna* promoter activity throughout the IDC of Dd2 using a luciferase reporter construct as earlier published (Hasenkamp, Wong et al. 2012).

In Figure 3.9A, parasite staging differed from that earlier reported (Fig. 3.9B) as in this report the parasites had reinvaded and matured into rings at 45 hpi. In this report, at 7 hpi, we actually have parasites that are 0 – 7 hours old because the sorbitol synchronization was performed 7 hrs after Percoll synchronization. The experiments began 48 h after sorbitol synchronization and lasted for a further 48 h. Parasite synchrony will dramatically reduce in the 96 h leading to some mismatch of the fine stage-specific expression. It is important to note that the level of expression at maximum for endogenous *Pfpcna* is 10 times that of endogenous *PfSir2A*, but the data transgenic line indicated that the luciferase expression from *PfSir2A-luc construct* was higher by 19,278 RLU.

3.3.3 Bioluminescence signal after stress in trophozoites

Having characterized the *PfSir2A-luc* reporter line and confirmed that the *PfSir2A* promoter appeared to be temporally regulated in a similar way as the promoter in the laboratory, we proceeded to use this line to investigate the response of this promoter to stress conditions. The average bioluminescence signal from two biological replicate experiments after exposure of trophozoite-staged 3D7 *PfSir2A-luc* and Dd2 *Pfpcna-luc* reporter lines to host stress factors for 2 and 6 h are shown in Figure 3.10. A 70-76% decrease in bioluminescence was observed, compared to the control, for the 3D7 *PfSir2A-luc* reporter line (hereon referred to as PfSir2A-luc). This decreased bioluminescence (24 – 30% cf control) was similar when heat shock was applied either alone or in combination with high lactate. A longer exposure of the parasites to stress did not dramatically decreased luciferase activity for both the heat shocked parasites alone (70%) or in combination with lactate (73%). This indicated that there may be a decreased *PfSir2A* promoter activity in parasites exposed to the stress, but other explanations were also possible. A decreased protein synthesis, protein degradation, thermo-instability or a combination of these may provide an explanation for the more than 50% loss in luminescence. Luciferase has a half-life of 1.5 h in *P. falciparum*

(Hasenkamp, Sidaway et al. 2013) so 2h and 6h stress exposure should allow substantial turnover of the existing enzyme. Paradoxically, exposure to high lactate increased bioluminescence, although this finding was not statistically significant, and an in-depth investigation of this observation was done and is presented in chapter 7.

A greater decrease in bioluminescence of the control reporter line, Dd2 *Pfpcna-luc* reporter line (hereon referred to as Pfpcna-luc), was observed after 6 h with a range of 84 -87 %, after heat shock alone and with lactate. This decrease was more pronounced in parasites exposed to heat shock alone. A 20% decrease in bioluminescence was also observed after 6 h of stress with high lactate alone.

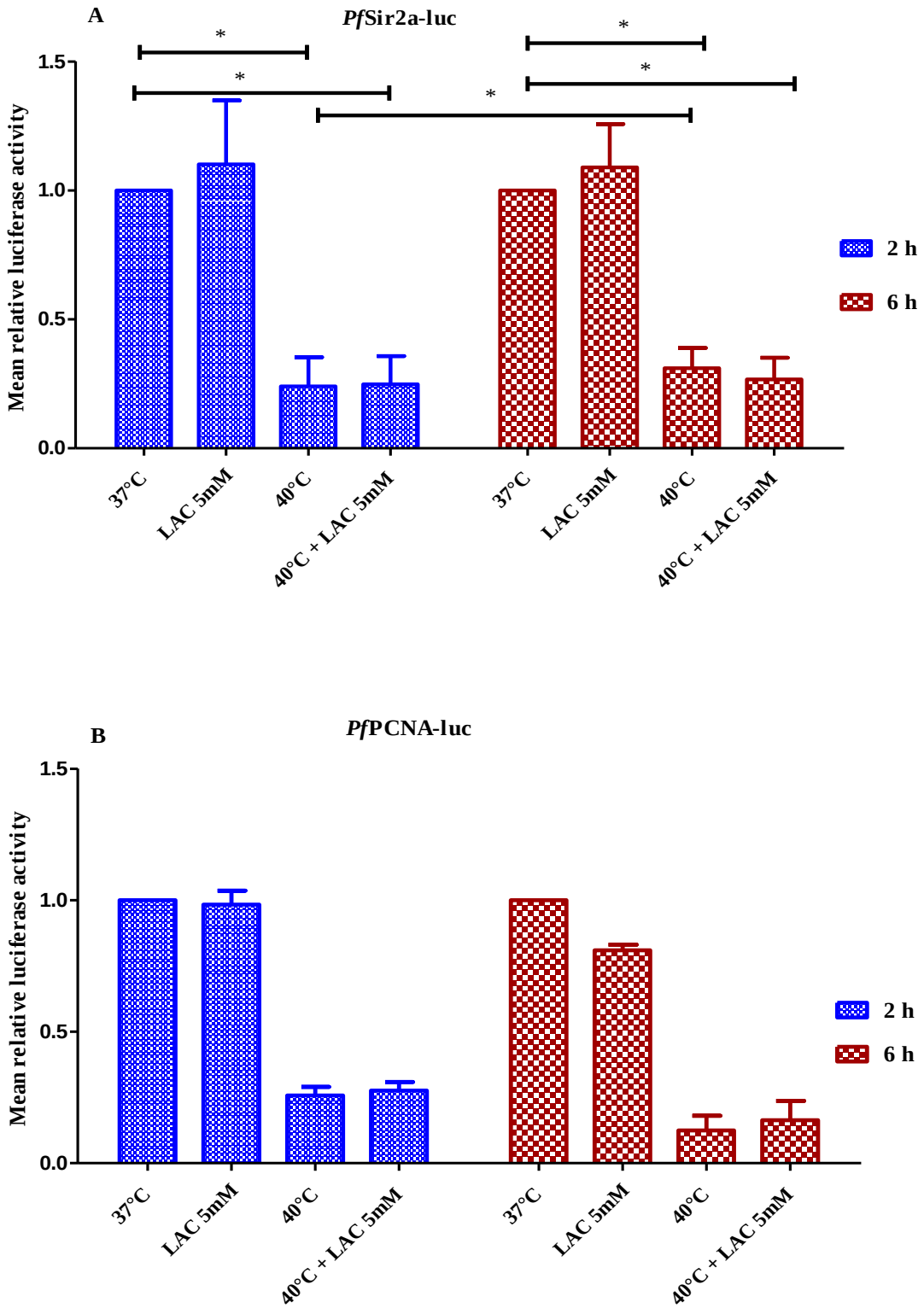

Figure 3.10: **Alteration of luciferase activity after exposure of PfSir2A-luc and Pfpcna-luc trophozoites to high lactate and heat shock stress for 2 and 6 h.** (Figure legend on the next page)

Mean relative luciferase activity is the mean of four or two independent biological replicate luciferase activities for *PfSir2A-luc* line (n = 12) or *Pfpcna-luc* line (n = 6), respectively, each derived as a mean of bioluminescence from three technical replicates relative to the untreated control. The raw bioluminescence data from technical replicates were normalized to 1% parasitaemia before being used. Error bars are SEM. *p < 0.05 Kruskal-Wallis test with Dunn's post test of normalized raw bioluminescence data. It is important to mention that the second biological replicate experiment with *Pfpcna-luc* was performed with unknowingly partially degraded LAS, and this is why the data did not reach statistical significance.

3.3.4 Changes in *Fluc* expression after stress in trophozoites

In an attempt to verify if the decreased bioluminescence after heat shock was due to a reduction in the corresponding mRNA transcript, quantitative real-time PCR experiment on the stored RNA from one of the biological replicate experiments shown in Figure 3.10 was done. At 2 h time point, a small (~2x) but significant increase in luciferase transcript for heat shock alone and in combination with high lactate was seen (Fig. 3.11). The expression of endogenous *PfSir2B* was slightly, but significantly, increased after heat shock alone and in combination with lactate, whereas that of endogenous *PfSir2A* was not significantly increased. The expression of *Hsp70* was significantly increased, as expected, after heat shock alone and in combination with lactate (Fig. 3.11). Therefore, the decreased bioluminescence did not tally with the increased luciferase mRNA transcript at this time point. A similar result was seen with Pfpcna-luc at 2 h, appendix VI. This implies possible degradation of the translated luciferase as an alternative explanation. Although *Hsp70* expression was induced after stress, it apparently did not protect the transgenic luciferase protein from denaturation.

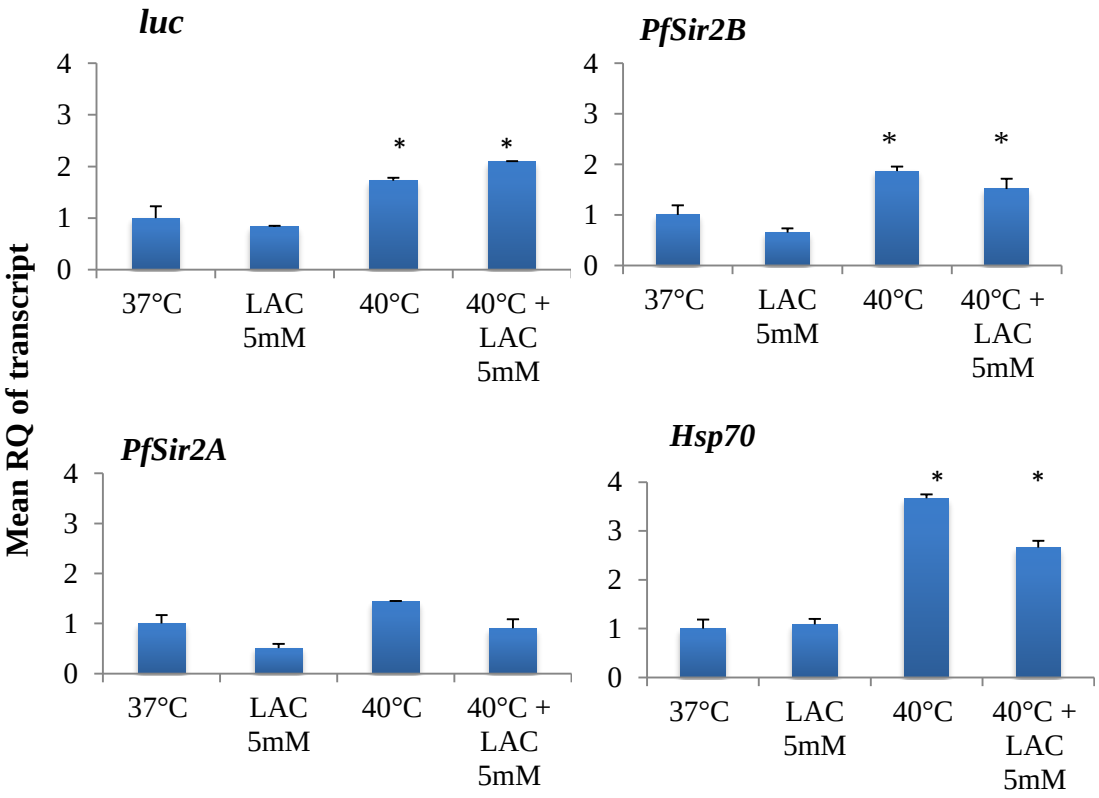

Figure 3.11: **Alteration in *Hsp70, PfSir2A, PfSir2B and Fluc* transcript levels in trophozoites-staged 3D7 *PfSir2A-luc* reporter lines after 2 h of stress.** The heading of each graph is the transcript under investigation. Mean RQ = mean relative quantity of three technical replicates from one biological experiment (n = 3). Error bars are standard deviation of technical replicates from the mean. Anderson-Darling test for normality indicated that the data is not normal for *Hsp70* and *Fluc* data, but *PfSir2A* and *PfSir2B* data were normally distributed. *$p < 0.05$, Kruskal-Wallis test of the relative copy number (RCN), derived from $2(^{-\Delta Cq})$.

The RTPCR was repeated on RNA samples from parasites exposed to 6 h stress, as per Figure 3.11, but the results were inconsistent with that of Figure 3.11. We had lost the heat shock response. A second pair of RTPCR primers for *Fluc* was designed and this did

entirely improve the consistency of the RTPCR data as the heat shock response was only seen for the parasites exposed to the combined stress. Marked differences were seen in the results when compared to those after the 2 h stress (Fig. 3.12). Most importantly, a strong upregulation of *Hsp70* was not seen. Upregulation was maximally ~1.5-fold and there was no significant upregulation at all after heat shock alone. This raised the possibility that the *Hsp70* transcriptional response is quite quickly downregulated again after prolonged heat stress. Nevertheless, the picture regarding luciferase was similar: transcript was upregulated (consistent with a slight upregulation of endogenous *PfSir2A* in most conditions) despite the loss of bioluminescence signal. This reinforced possible degradation as an explanation for the loss of bioluminescence after heat shock.

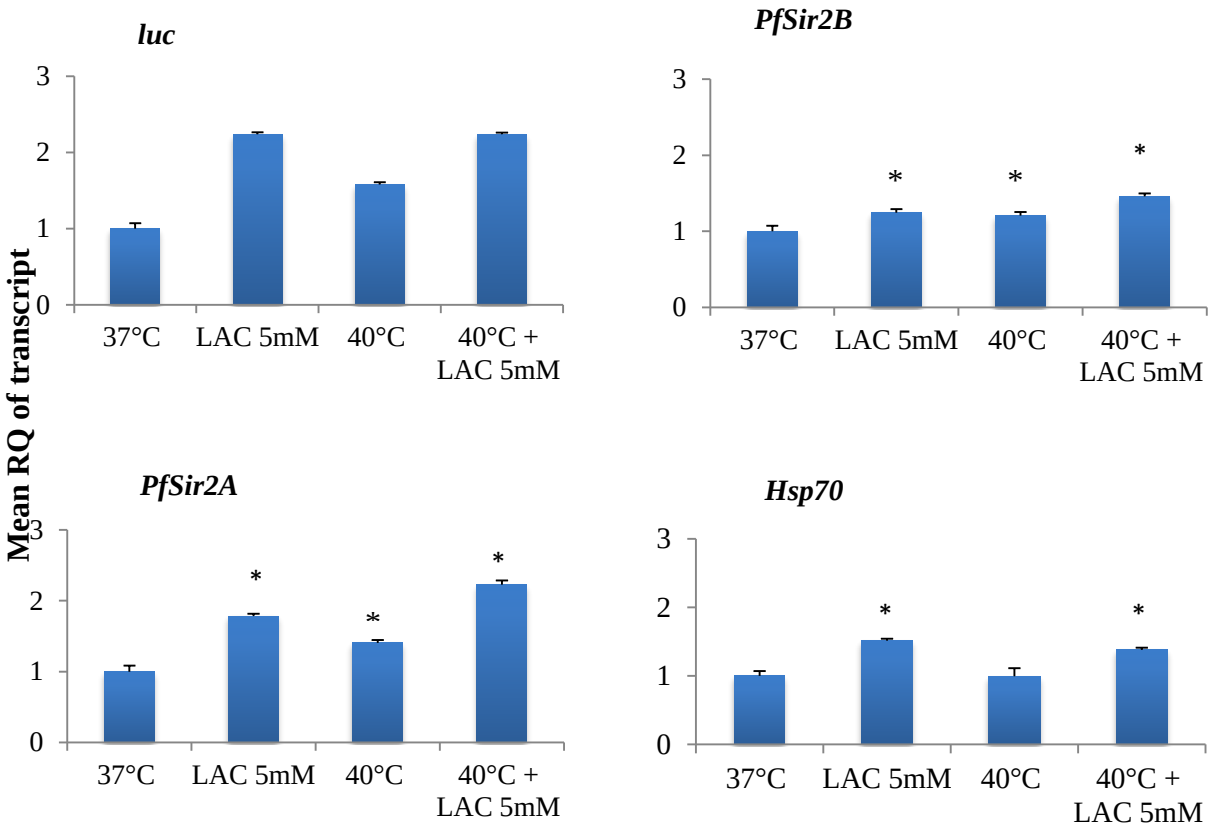

Figure 3.12: Alteration in *Hsp70, PfSir2A, PfSir2B and Fluc* transcript levels in trophozoites-staged 3D7 *PfSir2A-luc* reporter lines after 6 h of stress. The heading of each graph is the gene under investigation. Mean RQ = mean of three technical replicates from one biological experiment (n = 3). Error bars are standard deviation of technical replicates from the mean. Anderson-Darling test for normality indicated that the data is normal (except for LUC of which Kruskal-Wallis test showed not statistical significance). *p < 0.05 ANOVA of the relative copy number (RCN), derived from $2^{(-\Delta Cq)}$.

3.3.5 Bioluminescence after stress in schizonts

We next explored whether the luciferase reporter would behave similarly regardless of the parasite stage in the IDC. A similar drop in bioluminescence was observed for schizont-staged parasite reporter line exposed to stress (Fig. 3.13). The decrease in bioluminescence of the control reporter line, schizont-staged Pfpcna-luc, was also similar but significantly smaller than that of the PfSir2A-luc line at 6 h with a decrease ranging from 51 – 75% of luciferase

activity compared to the untreated group. However, it is notable that the drop in bioluminescence was reduced for the schizonts compared to the trophozoites.

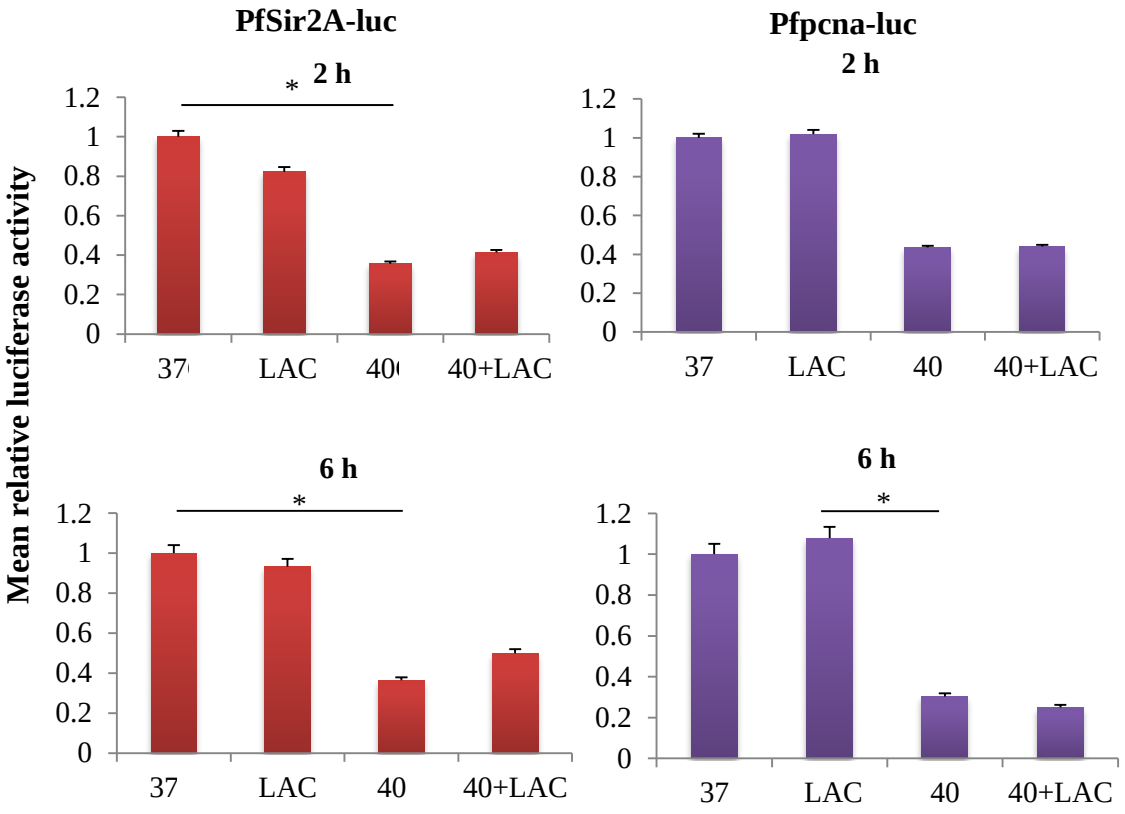

Figure 3.13: **Alteration of luciferase activity after exposure of PfSir2A-luc and Pfpcna-luc schizonts to high lactate and heat shock stress for 2 and 6 h**. Mean relative luciferase activity is the mean of three technical replicates (n=3). The raw bioluminescence data from technical replicates were normalized to 1% parasitaemia before being used. Error bars are SD. *p < 0.05, Kruskal-Wallis test with Dunn's post test of normalized raw bioluminescence data. 37 = 37°C, 40 = 40°C, LAC = Lactate at 5 mM and 40+LAC is the combination of both stresses.

The mRNA transcripts were analysed for 3D7luc using qRT-PCR (appendix VII) but the data showed a downregulation of *Hsp70* after heat shock at 40°C. This was not consistent with the upregulation of *Hsp70* seen in heat shocked trophozoites, and raised some concern

about the accuracy of the experiment. However, it is possible that the *Hsp70* gene is simply less sensitive to heat-induced upregulation at the schizont stage than it is at the trophozoite stage.

3.3.6 Bioluminescence after stress in ring stage parasite

Finally, the experiment was repeated in ring stage parasites, which were predicted to be least sensitive to heat stress. There was 80% and 83% reduction in luciferase activity after 2 h of heat shock and in combination with lactate, with a similar reduction (~90%) after prolonged (6h) stress (Fig. 3.14). A similar result was seen with Pfpcna-luc but only the 2 h time point was investigated.

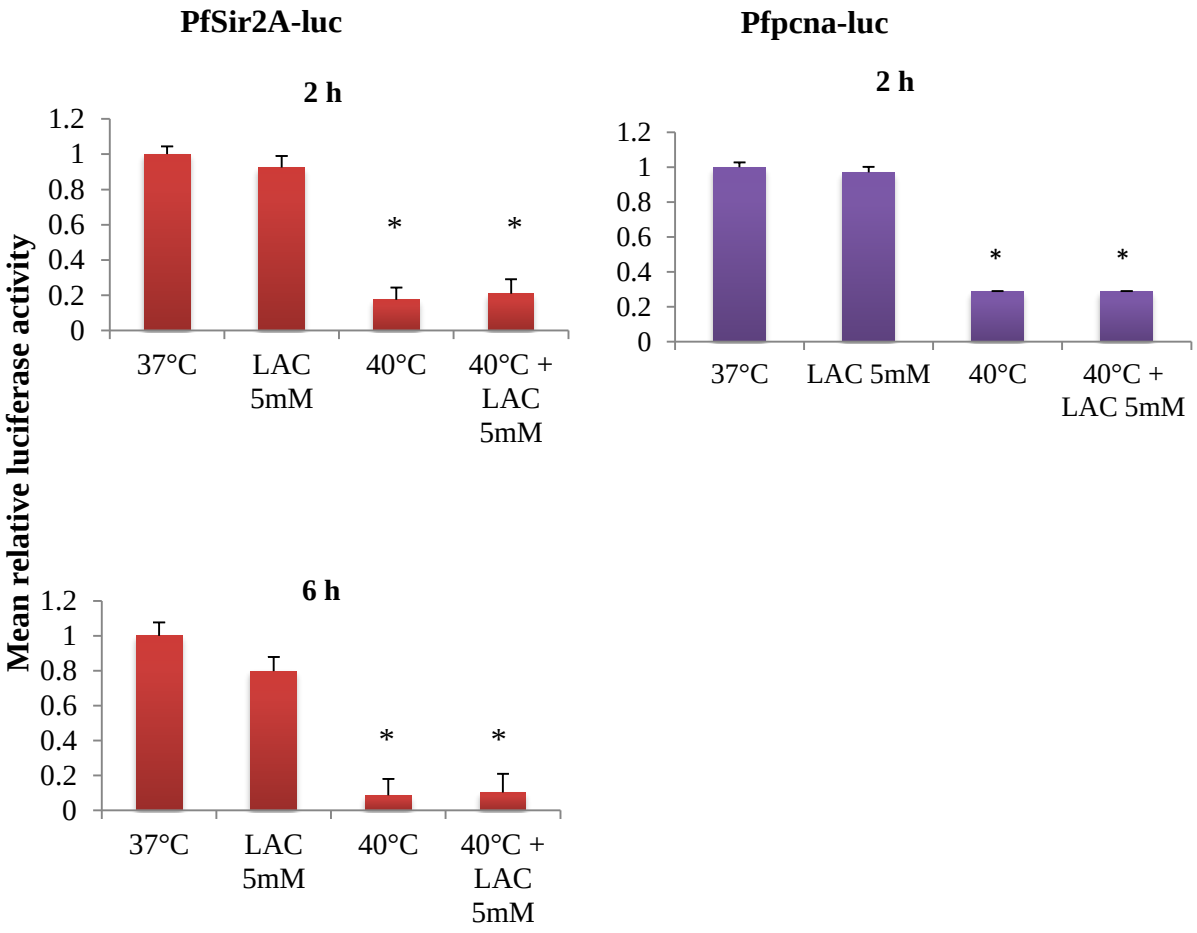

Figure 3.14: Alteration of luciferase activity after exposure of PfSir2A-luc and Pfpcna-luc rings to high lactate and heat shock stress for 2 and 6 h. Mean relative luciferase activity is the mean of technical replicate in one biological replicate experiment (n=3). The raw bioluminescence data from technical replicates were normalized to 1% parasitaemia before being used. Error bars are SD. *p < 0.05, Kruskal-Wallis test with Dunn's post test of normalized raw bioluminescence data, compared to the control culture.

3.3.7 Recovery of stressed trophozoite-staged *PfSir2A-luc* reporter line

The experiments shown in sections 3.3.3 – 3.3.6 strongly suggested that the luciferase reporter enzyme was destroyed by heat stress, independent of any changes in its transcription. If this was so, production of functional enzyme might be expected to recover once heat stress was removed. Experiments were therefore conducted to see if this occurred. Recovery was assessed by microscopy, bioluminescence and malaria SYBR Green 1-based fluorescence

methods after 48 h of culture without the stress, under normal conditions. A biological duplicate set of experiments were performed on the trophozoite stage for 2 and 6 h and the parasites sub-cultured for 48 h after the media was completely changed. Recovery was then assessed by determining the relative luciferase activity and Survival rate (from the SYBR Green-1 fluorescence reads) of the parasite cultures (Fig. 3.15).

A marked recovery of luciferase activity was seen for trophozoite-staged 3D7 *PfSir2A-luc* reporter line heat shocked at 2 (75%) and 6 h (44%), with greater recovery for parasites heat shocked for a shorter time. This maybe a reflection of growth as the SYBR read does indicate a greater biomass for the parasites heat shocked for a short time compared to those exposed for a longer time. However, the SYBR read was impacted by the presence of background fluorescence from the nucleic acid of dead parasites and it may give a false higher parasite biomass. This will especially be evident in the 2 h data that shows a slight discrepancy between the luciferase activity and the survival. At 6 h there is a larger discrepancy and the background fluorescence may not account for this alone. Nonetheless, these experiments may indicate that luciferase degradation did contribute to the drop in bioluminescence and that the enzyme is newly synthesized when stress is removed. A similar result was seen for parasites exposed to the combined stress, although these parasites showed a lesser recovery.

Survival rates as measured by SYBR (quantifying parasite DNA) were not very different between those parasites heat shocked alone or in combination with high lactate, despite the different recovery rate of bioluminescence (Fig. 3.15). Survival rate was down by about 12-13% for parasite exposed to heat shock alone and in combination with high lactate for 2 h. Longer exposure to these stresses decreased growth rate by 20% or 23% for parasites heat shocked alone or in combination with lactate, respectively. Therefore, as expected,

greater stress had a greater impact on parasite viability, but the majority of parasites survived both periods of stress.

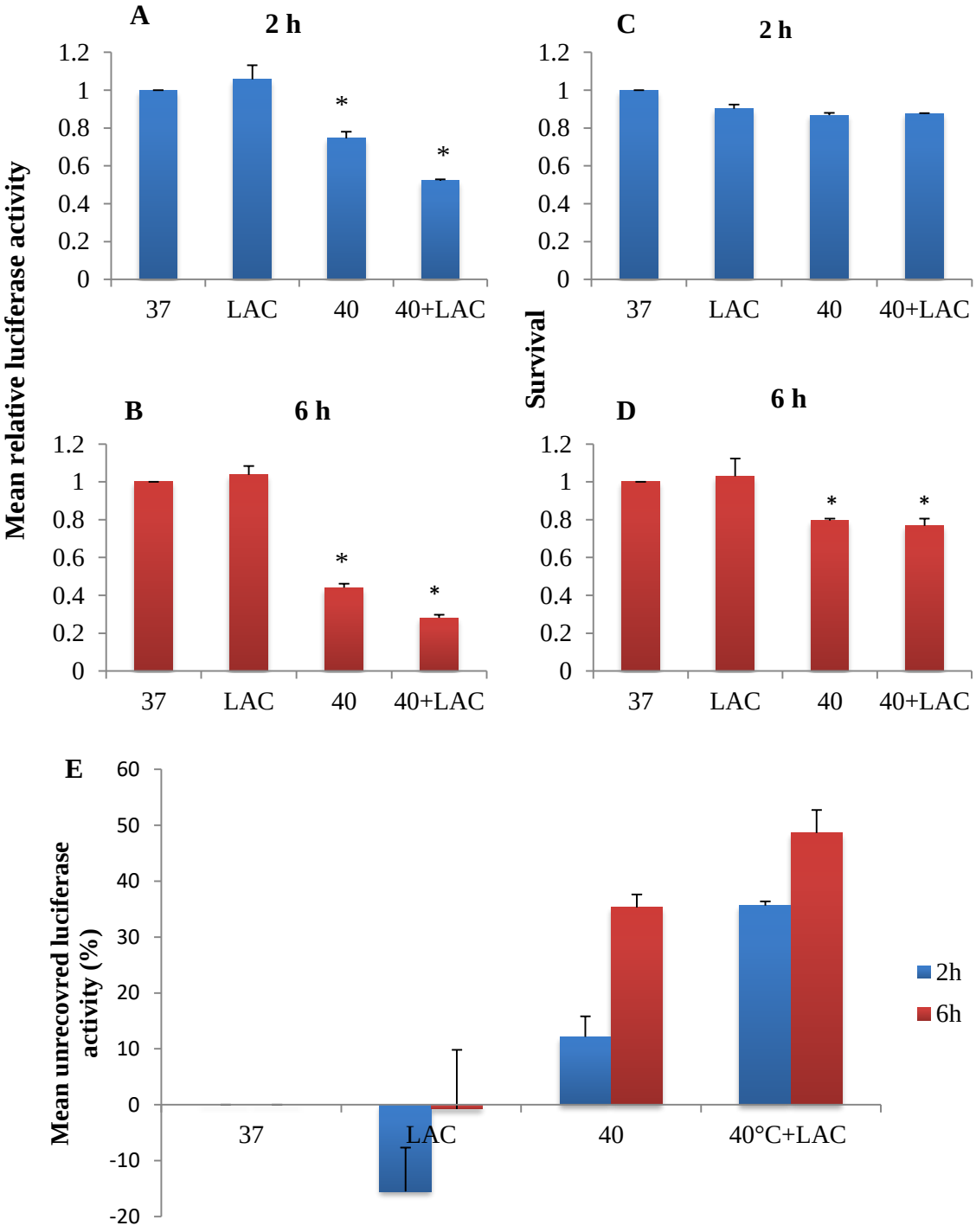

Figure 3.15: Parasite (PfSir2A-luc trophozoite) luciferase recovery and survival 48 h post stress. (Figure legend is in the next page)

A & B represents the mean luciferase activity after 48 h of recovery from high lactate and heat shock stress for 2 h (blue chart) and 6 h (red chart). **C & D** represents the mean SYBR read after 48 h of recovery from high lactate and heat shock stress for 2 h (blue chart) or 6 h (red chart). Chart represents the mean of two independent biological replicates, n = 6. Error bars are SEM. *p < 0.05 Kruskal-Wallis of raw bioluminescence or fluorescence reads. **E.** Represents the mean percentage of unrecovered luciferase activity post recovery of PfSir2A-luc trophozoites from high lactate and heat shock stress for 2 and 6 h. The percentage unrecovered luciferase activity was obtained by subtracting the relative luciferase activity from the relative SYBR read and multiplying by 100. There is a background fluorescence background. Error bars are propagated SEM. 37 = 37°C, 40 = 40°C, LAC = Lactate at 5 mM and 40+LAC is the combination of both stress.

In addition to the SYBR green readings, growth rate was also assessed by parasite counting via microscopy. Growth rate as determined by microscopy (Fig. 3.16) indicated no dramatic decrease in growth rate that would account for the loss of bioluminescence, with about 10% reduction for the 2 h heat shocked parasite. Therefore, microscopy was highly consistent with the SYBR method and indicated that most parasites survived the stress.

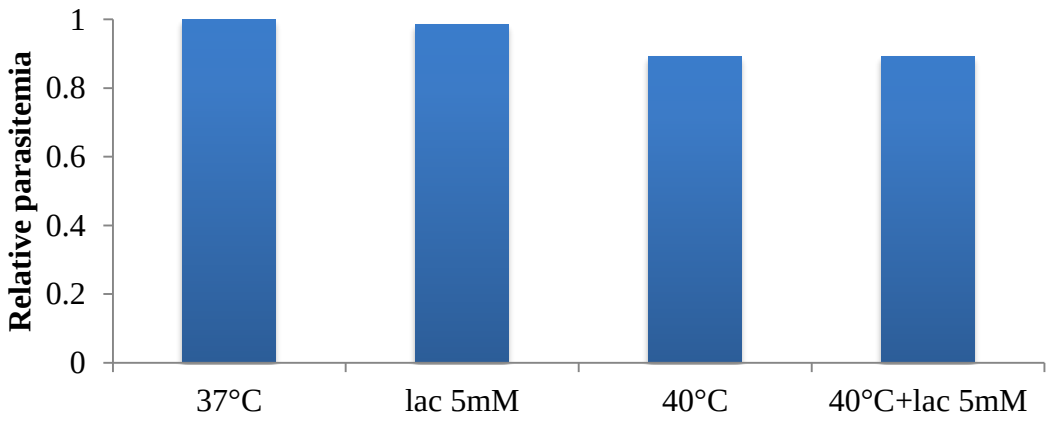

Figure 3.16: Growth rate of trophozoite-staged *PfSir2A-luc* transfected lines as determined by microscopy 48 h post stress for 2h. (Figure legend on the next page)

Growth rate is represented as relative parasitaemia which is the ratio of the parasitaemia of the treatment group to that of the control from a single count.

Therefore, parasite death generally accounted for less than half of the loss in luciferase activity. The incomplete recovery of luciferase activity could have several explanations besides parasite death. One is a loss of the *Fluc* transgene, although drug selective pressure was maintained throughout. Another is an incomplete re-synthesis of the degraded protein within 48 h, although previous work has suggested a fast turnover of luciferase in parasites (Hasenkamp, Wong et al. 2012).

3.4 Discussion

The promoter activity of *PfSir2A* in response to host stress factors, high temperature and high blood lactate, was investigated here using a luciferase reporter transgene. This was done by constructing a luciferase reporter plasmid and transfecting *P. falciparum* 3D7 with the reporter construct. The resulting reporter line was then characterized before being used in this study. The goal was to get an independent readout of the changes in the level of sirtuin expression in parasites exposed to two host factors in severe malaria that were found to correlate in malaria patients with high expression of sirtuins, in the infecting parasite isolates. High expression of one of the sirtuins, *PfSir2A*, was in turn found to correlate well with high expression of upsB type severe-disease-associated *var* gene group (Merrick, Huttenhower et al. 2012). This work aimed to increase our understanding of how the parasite is able to recognise an adverse host condition and respond by altering its sirtuins and *var* expression, thus selecting for phenotypes that might survive better in the adverse host environment. The sirtuins have been shown to be important in ensuring mutually exclusive expression of a single *var* gene *in vitro*-cultured (Duraisingh, Voss et al. 2005; Tonkin, Carret et al. 2009).

We were able to reconstitute temporal changes in *PfSir2A* expression (Fig. 3.8) throughout the IDC of the parasite using a *Fluc* transgene. The *PfSir2A-luc* reporter line showed stage-specific luciferase expression that is synonymous to the endogenous expression of *PfSir2A* (Otto, Wilinski et al. 2010). Expression was low at ring stage and increased as the parasite increased in size with peak expressions at the schizont stage. A positive control, *Pfpcna-luc* reporter line that had previously been characterized, did show the same stage-specificity in luciferase expression as published (Hasenkamp, Wong et al. 2012), with expression peaking at the trophozoite stage and falling at the schizont stage. The bioluminescence of the *PfSir2A-luc* line was also proportional to the percentage parasitaemia, with a high correlation of 0.99. This meant that any change in bioluminescence should reflect the parasite numbers at any particular life cycle stage.

Initial experiments indicated a transcription-independent reduction of luciferase activity, irrespective of the promoter upstream of the luciferase gene, in *P. falciparum* parasite lines stressed by heat shock, either alone or in combination with high lactate. The expressed luciferase protein, although rapidly turned over with a half-life of 1.5 h in *P. falciparum* (Hasenkamp, Sidaway et al. 2013), appeared to be turned over at even a higher rate, and/or degraded or denatured, in parasites exposed to the heat shock. Thermal degradation of luciferase has been reported in pGL3 *luc* transgenic adenocarcinoma cells exposed to heat (43°C) for 45 min with a 40% reduction in relative luciferase activity (Harrison, Garden et al. 2006). An earlier report on the terminal degradation of luciferase in Drosophila and mouse cells ascribed degradation to denaturation, and the half-life of luciferase was reduced from 200 min at 37°C to 4 min at 42°C in mouse cell (Nguyen, Morange et al. 1989). This clearly makes *Fluc* unsuitable for use in reporter assays that require application of mild heating, as thermal degradation will obscure any useful analysis, but we did not take this into consideration or anticipate this as we were applying a milder heat (40°C). Luciferase,

however, has a longer half-life in live mammalian cells (2h) or their lysates (3h) (Ignowski, Schaffer 2004) than it does in *Plasmodium* (1.5 h) (Hasenkamp, Sidaway et al. 2013). Induced *Hsp70* under stress is known to protect critical cellular proteins from denaturation (reviewed (Murphy 2013)), but it did not protect the luciferase enzyme in this study, probably because it was not a native protein.

This decrease in luciferase activity is not indicative of either the *PfSir2A* promoter or *Pfpcna* promoter activity, as preliminary findings showed that the luciferase transcript levels increased in response to heat shock and the combined stress. Its levels were higher on prolonged heat shock (Fig. 3.11 & 3.12) and the trend was similar to that of endogenous *PfSir2A*. Additionally, subsequent evidence showed a recovery of luciferase activity after 48 h. Recovery was, however, halved after exposure to heat shock (alone or in combination with lactate) for 6 h versus 2 h. Recovery of luciferase activity has been reported in the same study involving pGL3 luc transgenic adenocarcinoma cells, with a significant recovery beginning after 4 h and almost 100% recovery at 12 h (Harrison, Garden et al. 2006), but death rate of the cells was not reported. Here, we did not perform a close time point recovery assay as it was not the aim of our study, but we did not see a 100% recovery of luciferase activity even after 48 h of subculture. This may be due to the difference in the cell lines (human versus *Plasmodium*), the heat application for a longer time and the background fluorescence we did not account for in the SYBR growth assay.

Luciferase assay measures the amount of ATP from viable cells and SYBR green assay measures the fluorescence resulting from the binding of nucleic acid by SYBR green 1 dye. This assay is limited by it non-specific binding to other nucleic acid apart from double stranded (ds) DNA from viable cells. It also binds dsDNA form dead cells which can remain intact for several days. The SYBR green assay was backed up by the microscopic counts which estimates the parasitaemia from a thin blood smear and could be subjective. The

limitation from subjectivity can be reduced by counting a large number of red blood cells, up to 3000 erythrocytes. Nevertheless, this is the first report on degradation of luciferase in *P. falciparum* under the *PfSir2A* promoter by mild heating.

In our study we were focused on changes in the level of gene expression, which was underestimated by our assay model due to the thermal instability of the luciferase protein. It is likely that, as it occurs in mammalian systems, thermally denatured firefly luciferase could be refolded through an ATP-dependent process that is mediated by Hsp90, Hsp70, p60 and other factors, but the failure to refold would result in proteolysis (Schneider, Sepp-Lorenzino et al. 1996). In any case, the degradation of luciferase protein hindered the investigation of changes in the expression of *PfSir2A* when *P. falciparum* was exposed to two stress factors, high body temperature and high blood lactate, both of which were found to correlate well with high expression of sirtuins in a field study (Merrick, Huttenhower et al. 2012). Our findings here are largely preliminary but it can be suggested that future experimentation with this assay system could look into shortening the time of exposure to heat shock. A one-hour exposure which is shorter than the half-life of luciferase may produce meaningful result although luciferase should have a shorter half-life under mild heating. The contribution of sirtuins to the epigenetic selection of *Plasmodium* phenotypes in severe malaria was not, therefore, successfully clarified in this investigation.

Chapter 4: Comparative study of the changes in sirtuin and *var* expression in cultured *P. falciparum* parasites upon stress

4.1 Overview of the study

Plasmodium encodes two NAD^+-dependent deacetylase paralogues, PfSir2A and PfSir2B. These proteins deacetylate the lysine tails of histone residues contributing to silencing of inactive *var* genes. They are indispensable in the control of *var* expression as a disruption of their genes leads to a loss of mutually exclusive expression of *var* genes (Duraisingh, Voss et al. 2005; Tonkin, Carret et al. 2009). This is predicted to be immunologically disadvantageous for the parasite's survival in its host. In a single *P. falciparum* parasite, only one or a few of the ~60 *var* genes is normally expressed during the ring stage. *Var* genes are expressed after the merozoites have invaded a RBC, with maximum expression somewhere around 10 hpi and a second increase occurring again around 22 hpi as demonstrated for the parent strain of 3D7, NF54 (Dahlbäck, Lavstsen et al. 2007). The expressed *var* genes encodes PfEMP-1 that enables parasites older than 18 h to sequester in post capillary venules and remain out of circulation for 30 h. This increases the adhesion of the iRBC to endothelial cells of blood vessels, thus enabling the parasite evade the host defence mechanisms, including clearance by the spleen and immune responses.

P. falciparum in human infections tend to grow in synchronous cycles and thus it is repeatedly exposed to heat shock every 48 h at the end of its intraerythrocytic development cycle (IDC) when merozoites are released (Bartoloni, Zammarchi 2012) along with malaria toxins and haemoglobin metabolites (Gazzinelli, Kalantari et al. 2014). Damage to parasite proteins and other macromolecules as a result of heat shock and other stress is cushioned by the PfHsp90 multi-chaperone complex, which includes PfHsp70. PfHsp70 is a well-conserved abundantly expressed protein across all *Plasmodium* species. The growth promoting effect of prior heat shock was shown to be dependent on PfHsp90 multi-chaperone complex (Pavithra,

Banumathy et al. 2004) and inhibition of this complex inhibits parasite growth ((Banumathy, Singh et al. 2003), reviewed in Acharya, Kumar et al. 2007). This complex may also be a defining factor for the pathogenesis of malaria (Pallavi, Acharya et al. 2010). PfHsp70 is induced on heat stress (Oakley, Kumar et al. 2007; Zininga, Achilonu et al. 2015). There are six *PfHsp70*-like genes (Shonhai, Boshoff et al. 2007). They are abundantly expressed at 37°C during the IDC, but upon exposure to heat (41°C was used in this study) their expression is induced (Oakley, Kumar et al. 2007).

In a study that increased our understanding of *var* gene regulation in Gambian children with severe malaria, a relationship was reported between two host stress factors; fever and high blood lactate; high expression of *PfSir2*, and expression of severe-disease-associated *var* genes. Severe malaria was shown to correlate with a transcriptional response of *Plasmodium* sirtuins to host-stress factors. The upregulation of sirtuins could lead to an alteration of *var* gene expression to those *var* genes associated with the severe disease (Merrick, Huttenhower et al. 2012). This implicated the epigenetic process in the progress from uncomplicated to complicated malaria, and it may indicate that in severe disease an impairment in the epigenetic regulation of mutually exclusive expression of *var* gene expression occurs (Duraisingh, Voss et al. 2005), possibly leading to upregulation of a number of disease-associated *var* genes. Similar disrupted mutually exclusive *var* gene expression is seen when either of the sirtuin genes are knocked-out (Duraisingh, Voss et al. 2005; Tonkin, Carret et al. 2009).

A 2 h heat shock at 41°C has previously been shown to increase the expression of *PfSir2A* by 2.4-fold, and this treatment also led to the increased expression of five *var* genes by an average of 2.8-fold, as measured using microarray analysis from a non-clonal population possibly expressing multiple *var* genes prior to heat shock (Oakley, Kumar et al. 2007). No published data currently exist on the *var* expression phenotypes that occur after

exposure to the other stress factor identified in the Gambian study above, i.e. high blood lactate or ideally a combination of the two stress factor as occurs in the severe disease.

Research in this chapter attempts to establish a causal link of the two host-stress factors above, and increased sirtuin expression and high expression of *var* gene types associated with severe malaria. Changes in the relative level of sirtuin and *var* gene expression in parasites exposed to high temperature (40°C) and high lactate (5 mM), were assessed alone and in combination. The expression of *PfSir2A, PfSir2B* and *Hsp70* or *var* genes, relative to three or five endogenous control genes, were measured by RT-qPCR. The resulting relative levels of expression were normalized to the levels seen in parasites not under any stress. Importantly, measurements were made first in the lab-adapted 3D7 (sections 4.3.3 and 4.3.4) and then in three recently lab-adapted field isolates from Africa (sections 4.3.7 and 4.3.8), aiming to mimic as closely as possible the parasites from Gambian patients in which the original observations were made (Merrick, Huttenhower et al. 2012). These experiments were conducted because detailed studies on the regulation of *P. falciparum var* genes upon encounter with host stress environment are needed to increase our understanding of the epigenetic process in severe disease states.

4.2 Methodology

4.2.1 Culturing, synchronization and stress treatment of parasites, RNA harvest, purification and cDNA synthesis, RT-PCR for changes in gene expression

The parasites used for this study were the following wild-type (WT) parasites: *P. falciparum* 3D7 laboratory strain (MR4) and 3 Kenyan patient field strains from the European Malaria Reagent Repository (http://www.malariaresearch.eu/content/plasmodium-falciparum-clones-and-lines), identified as 9775, 3518 and 10668. We have no information of the medical history of the patients from whence they were isolated from.

Parasites were cultured as previously described in section 2.1. For the experiments with the field strains, we altered our method of culturing as previously reported (Radfar, Méndez et al. 2009) due to our inability to obtain highly synchronous, reasonably high and healthy parasite populations. This method enabled us to grow high parasite populations without stressing them as the parasite's culture media was changed twice per 24 h at the late trophozoite/early schizont stages and once per 24 h at ring stages. Fresh blood, washed every week, was also added at around 40 hpi, and the cultures transferred to a shaker, prior to reinvasion. This sometimes required splitting the culture into two or three culture flasks. The parasites were grown at ~ 1% haematocrit and brought up to 4% haematocrit prior to stress application. *P. falciparum* grows better when cultured at about 1-2% haematocrit (Ménard 2013). For all parasite cultures double sorbitol synchronization was performed as previously described in section 2.2 depending on the stage of the parasite needed. The parasites were subjected to stress factors as described previously in 2.3. Post-stress growth assessment by microscopy was conducted as discussed in section 2.3 and SYBR Green 1-based fluorescence growth assessment was conducted, as highlighted in section 2.4, at 48 h for trophozoites or schizont stages, or 72 h for ring stages. iRBCs were counted using a counting grid, against up to 3000 erythrocytes, where possible, or at least 5 fields of view (5 different fields). The RNA was harvested, purified and converted to cDNA, which was then used for RT-qPCR in order to assess changes in sirtuin and *var* gene expression in response to host stress. All these methods were described in sections 2.5 and 2.6. In addition, to the primers in section 2.5, primers were used for the major *var* gene groupings as earlier described (Rottmann et al., 2006), as well as the conserved acidic terminal segment (ATS) of all *var* genes and two ring-stage expressed genes as endogenous control genes: skeleton-binding protein (SBP1) and membrane-associated histidine-rich protein 1 (MAHRP 1), designed using the Snapgene

software, as the original one used in this paper was closer the 5’ end (Merrick, Huttenhower et al. 2012). These primer sets are presented in Table 4.1 below.

Table 4.1: Primers used for detection of *var* gene groups, ATS of *var* genes and ring-specific control genes

Gene/gene group	Fwd Primer	Rev Primer	Product Size (bp)
upsA1	TTGGGRAATBTGTTAGTTAYRGCAA	CTGCAAAACTKCGWGCAAG	110-120
upsA2	AACCCATCTGTRRATGATATACCTATGGA	GTTCCAASGATCCATTRGATGTATTA	100
upsA3	AGGTAATGTTTTAGATGATGGTAT	ACCAGAATATACATTATTTGATACATA	160
upsB1	CATCCGCCATGCAAGTATAA	CGTGCACGATTTCGATTTTT	260
upsB2	ATCAAGGTAATTTCATACATATGTGATA	GTCCGTGCACGATTTCGATTTT	190
upsC1	CACATCGATTACATTTTAGCGTTT	TGTGGTAATATCATGTAATGG	106
upsC2	GTAGCGACAACCACGRYATCATGG	CATTGTTAACATAGTCTACCATTA	120
upsE	CACGACATTAACAATACATGCAGA	CATTGCATTCACAGACATTGG	184
ATS	CCCATACACAACCAAYTGGA	TTCGCACATATCTCTATGTCTATCT	
SBP1 PF3D7_0501300	CACTTGCAACTACCGAATTA	GTAAAGCTTCTTGAGCCATT	183
MAHRP 1 PF3D7_1370300	GATGATCAAACTGATGGTGA	TGGCTTTATGTTCACTCTTG	205

A different DNase treatment and cDNA synthesis kit, QuantiTect® reverse Transcription Kit (QIAGEN GmbH, Germany) containing the wipe out buffer (WO), was used for experiments on the trophozoite and ring-staged parasites as there were a number of issues with the consistent effectiveness of DNase treatment using DNase 1 and also issues with availability of iScript™ cDNA synthesis kit from our supplier. Comparatively, QuantiTect® reverse Transcription Kit did give a better yield as shown in Figure 4.1B, below, and the WO in the kit was 100% efficient (Fig. 4.1A).

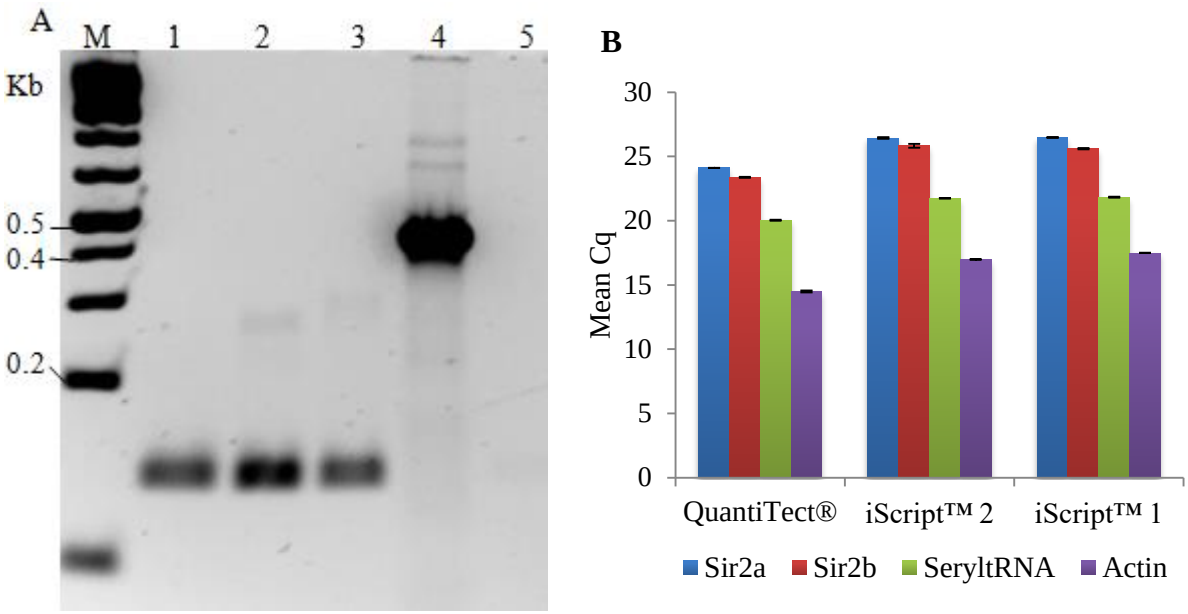

Figure 4.1 Comparison of QuantiTect® wipe out buffer (WO) and iScript™ DNase 1. A is the gel electrophoresis of gDNA check after treatment with WO buffer versus DNase 1. Lanes are labelled 1= wipe out buffer, 2 = 2µl of DNase1, 3 = 1µl of DNase 1, 4 = gDNA (as control) and 5 = negative control. WO gave one discrete band size after amplification of the exon region of DNA. Amplification of resulting cDNA from RNA will be smaller due to splicing of the introns. There is presence of other fainter mid-size b and apart from the required PCR product after treatment with DNase 1. **B** is the mean Cq after RTPCR of cDNA synthesized from RNA treated with the DNase from the two different kits. QuantiTect® reverse Transcription Kit contained the WO buffer, while iScript™ 2 or 1 cDNA synthesis kit contained the DNase 1 enzyme which was used at 2 or 1 µl. The slightly lower Cq for QuantiTect® reverse Transcription Kit means an increased yield of RNA transcript of the genes under study compared to the iScript™ cDNA synthesis kit. Values are mean of three technical replicates and error bars are standard deviation from the mean.

Biological duplicate experiments were performed for most experiments, and a biological triplicate experiment for the trophozoite-staged 3D7. All biological replicate studies were done more than 2 weeks apart except for the ring-staged strain 10668. It is

important to note that all biological replicate experiments were done with the same DNase and reverse transcriptase enzymes. DNase 1 and iScript™ cDNA synthesis kit was used for the schizonts-staged experiments, while WO buffer and QuantiTect® reverse Transcription Kit was used for all other experiments.

4.2.2 Statistical analysis

Relative copy number (RCN) of the target gene calculated as $2^{(-\Delta Cq)}$ as described in section 2.7 were tested for normality, using Anderson-Darling test for normality, of which majority of the data set did not follow a normal distribution. Therefore, statistical significance was determined by using the Kruskal-Wallis with Dunn's post test. For the very few data sets that followed a normal distribution, ANOVA was used to assess significance level with Dunnett multiple comparisons or Games-Howell pairwise comparisons depending on the equality of their variances.

4.3 Results

4.3.1 Effect of high lactate and high temperature on viability and growth of 3D7 Trophozoites

We carried out our investigations first on the trophozoite stage, as this stage is markedly affected by mild heat shock, probably due to increased metabolic activity compared to all other asexual stages (Oakley, Kumar et al. 2007). This stage is also most likely to be affected by chemical changes in its environment (Desai, Krogstad et al. 1993). Growth was determined 48 h after exposure of the parasite to each stress, and the survival rate calculated as per the equation in section 2.4. Parasite cultures used here were mainly early trophozoites as, depicted in the staging Figure, with a starting parasitaemia of 2-4% before stress.

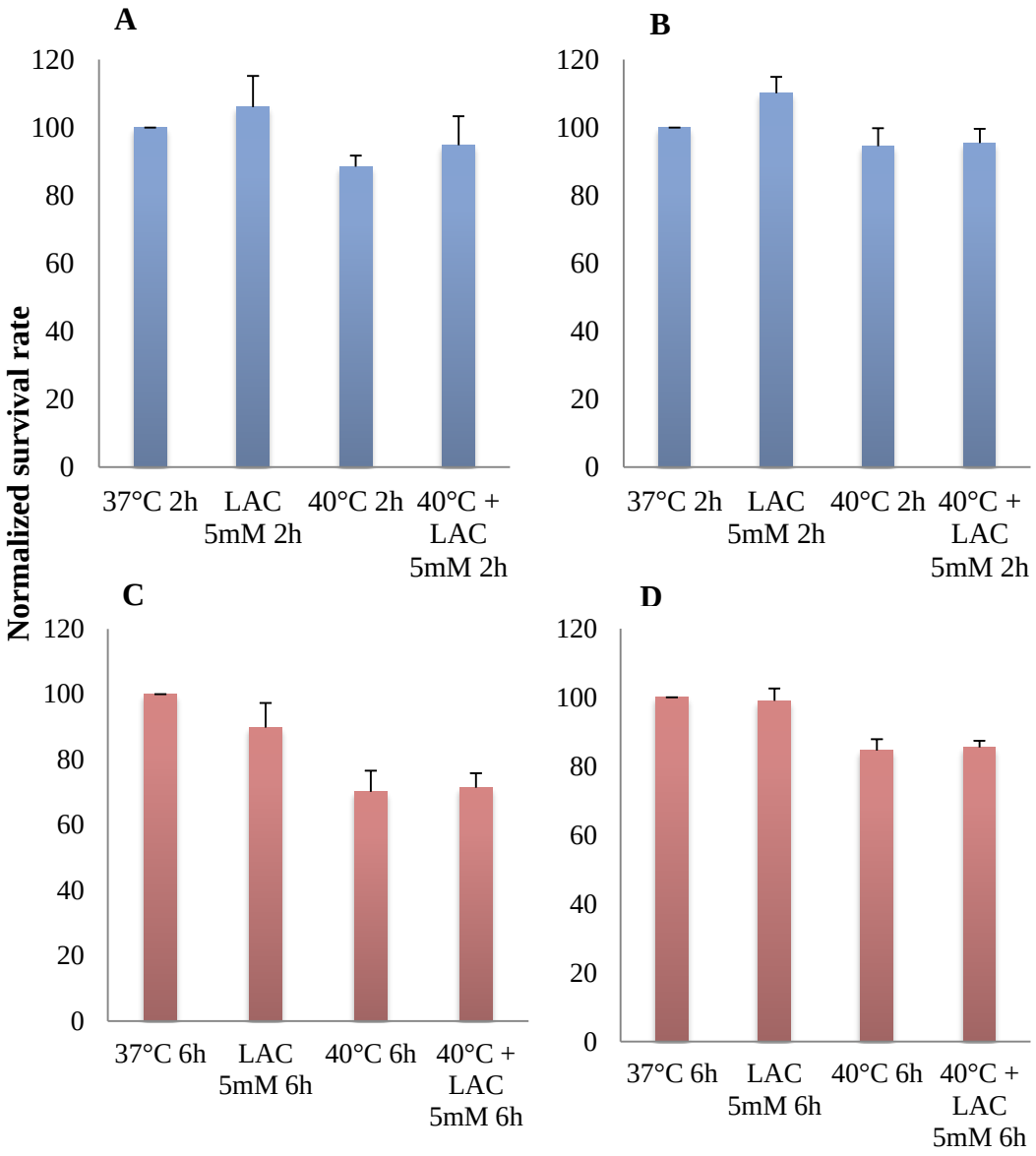

Figure 4.2 Post-stress survival of trophozoite-staged 3D7 *P. falciparum*. A & B are the mean survival rates calculated using the growth measurements by microscopy and SG 1-based fluorescence growth assessment, respectively; 48 h post 2 h of stress. **C & D** are the mean survival rates calculated using the growth measurements by microscopy and SG 1-based fluorescence growth assessment; 48 h post 6 h of stress. The mean survival rates are from biological duplicate experiments for the SG 1-based fluorescence growth assessment or biological triplicate experiments and the error bars are their SEM.

Little death of the parasites occurred after 2h exposure to heat shock alone and in combination with lactate, as assessed by microscopy and SYBR Green-1 based assay, and compared to the unstressed parasites (Fig. 4.2A & B). Prolonged (6 h, Fig. 4.2C & D) exposure to all stress decreased parasite viability with a 1-10% decrease after lactate alone and 15-30% decrease after heat shock either alone and in combination with lactate. The relatively similar growth rate for both stress groups indicates that lactate alone contributes little or nothing to the impact of heat shock on parasite survival after stress. The higher end of the growth decrease is as assessed by microscopy while the SYBR Green-1 gave a much smaller decrease. The underrepresentation of parasite death is due to the method used in our SYBR assay which does not account for dead parasites, as explained in section 2.4. However, microscopy can be subjective and a huge number of parasites have to be counted to give a more accurate count. The parasites were considered dead when they did not appear like the rings/trophozoite or schizont stages, but rather like slightly bigger than merozoite purple round structures with no chromatin dot. Merozoites were excluded from the count in order to avoid counting them as dead parasites.

4.3.2 Effect of high lactate and high temperature on the survival of 3D7 schizonts

3D7 parasites at 40 ± 4 hpi, corresponding to the schizont stage of the parasite, were exposed to stress for 2 and 6 h. Counting and staging was done after stress and the culture was allowed to recover for 48 h under normal conditions. Only microscopy was used to assess the post-stress survival of schizont-stage *P. falciparum* 3D7 (section 2.4), as we had not decided to include SYBR-Green-1 assay in our routine assessment. The schizont-staged parasites looked the same before the stress experiments but after the stress experiments, staging profiles indicated very different proportions of parasite stages for the two biological replicate experiments, with the second biological replicate having a greater number of parasites that had just reinvaded whereas the first biological replicate showed a greater proportion of

remaining schizonts, particularly after the heat shock treatment, as shown in Figure 4.3A & B. As a result of this, the parasitaemia were not merged and subsequent data from the two experiments were presented separately.

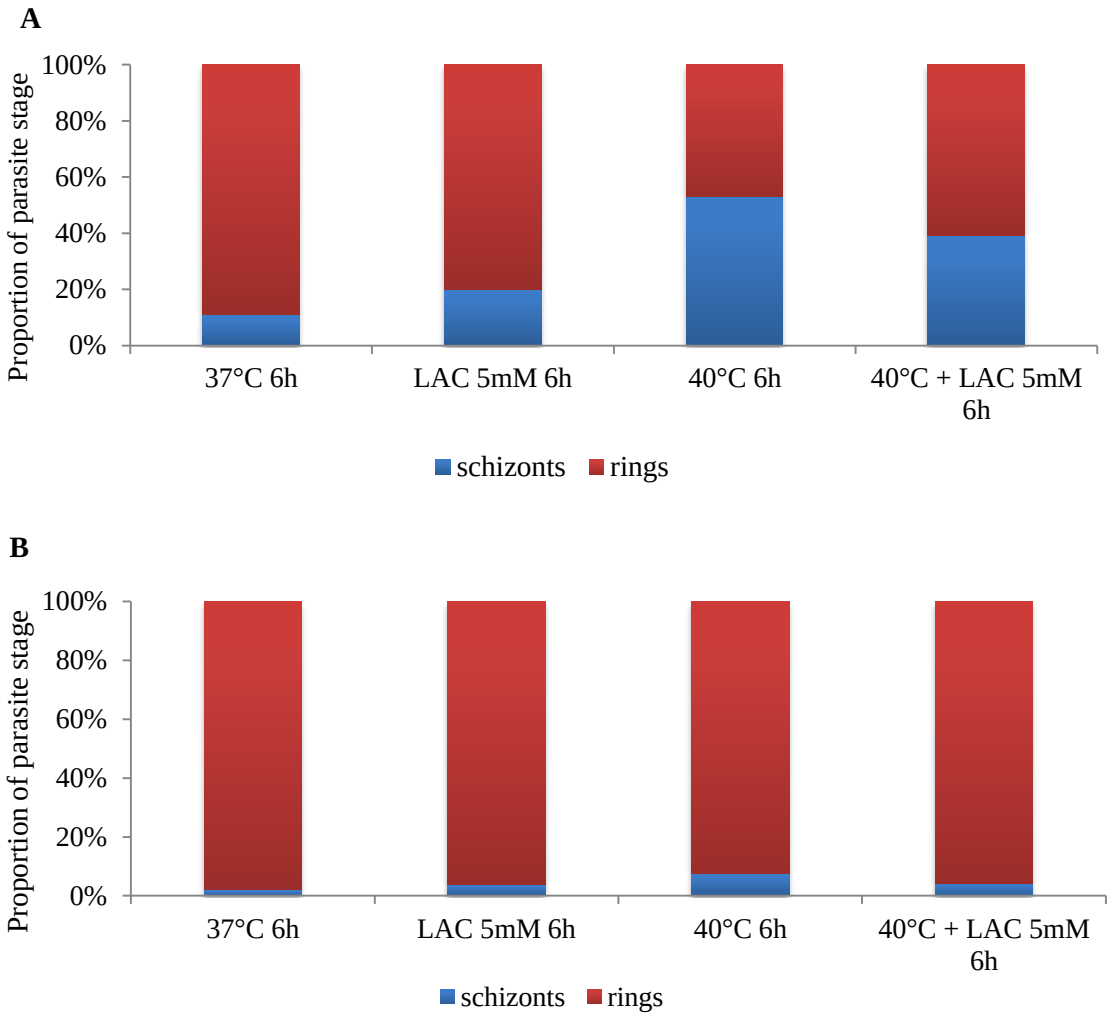

Figure 4.3: Post 6 h stress staging of 'schizont-staged biological replicates'. A is the 1st biological replicate staging at 46 ± 4 h schizont after 6 h of stress. **B** is the 2nd biological replicate staging at 46 ± 4h schizonts after 6 h of stress. Chart is the proportion of schizont or rings at the end of the stress period. More rings had reinvaded after the 2nd biological replicate had been exposed to the 6 h of stress, even though they were relatively of the same staging profile before the stress. It appeared that the second biological replicate had a faster growth.

There was no apparent death after 2 h exposure to lactate, but 40% and 50% of the parasites died after exposure to heat shock alone and in combination with lactate, respectively, compared to the unstressed parasites (Fig. 4.4A). For the slightly older parasite population in the second experiment, lactate exposure for 2 h slightly reduced parasite survival (Fig. 4.4C) but again a greater effect occurred after heat shock and combined stress. Prolonged (6 h) exposure to all stresses decreased parasite survival further compared to the 2 h stress (Fig. 4.4B); slightly (4%) for the lactate stress but 55 and 57% after exposure to heat shock and heat shock plus lactate. In the second experiment, consistent, severe reductions in growth were seen after heat shock treatment but there was, surprisingly, a slight increase in growth after lactate treatment (Fig. 4.4D). Again, the relatively similar growth rate for both the heat shocked and combined-stress groups indicated that lactate alone contributes little or nothing to the impact of heat shock on parasite survival after stress.

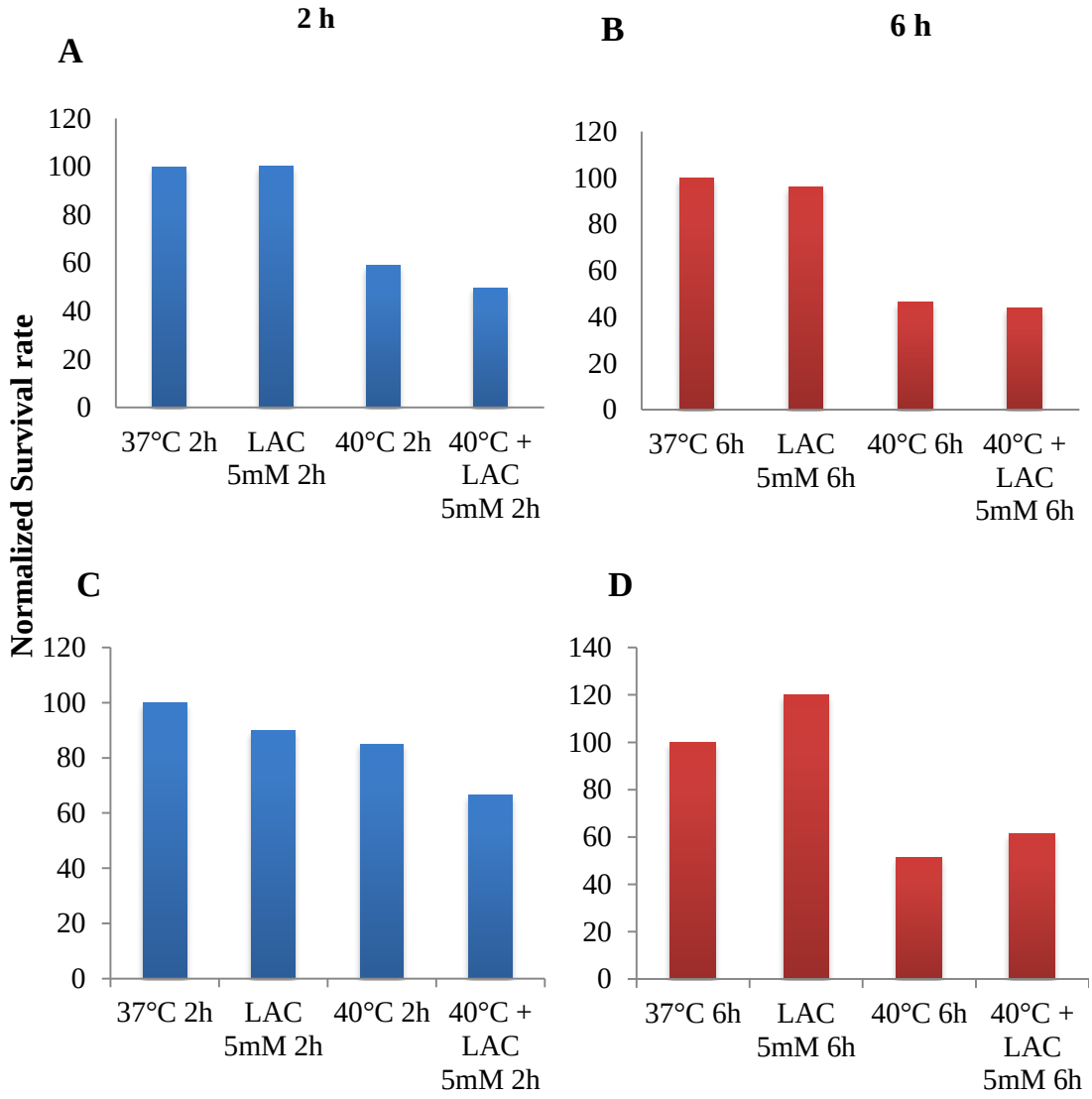

Figure 4.4: 48 h post stress survival of schizonts, assessed by microscopy. Two 'biological replicate experiments' are reported separately as staging post stress indicated that they had different profiles. **A & B** are survival of schizont-staged parasites from the 1st biological replicate experiment with a starting parasitaemia of 1.1% before stress. Parasite counts were single counts against 3000 RBC and reported for the parasites stressed for 2 h (blue chart) or 6 h (red chart). **C & D** are survival of schizont-staged parasites from the 2nd biological replicate experiment with a starting parasitaemia of 3.19% before stress. Parasite counts were single counts from 5 fields of view and reported for the parasites stressed for 2 h (blue chart) or 6 h (red chart).

4.3.3 Changes in sirtuin expression of 3D7 trophozoites after stress

The majority of the parasites used for this study were early trophozoites as mentioned earlier in section 4.3.1 and shown in Figure 4.5.

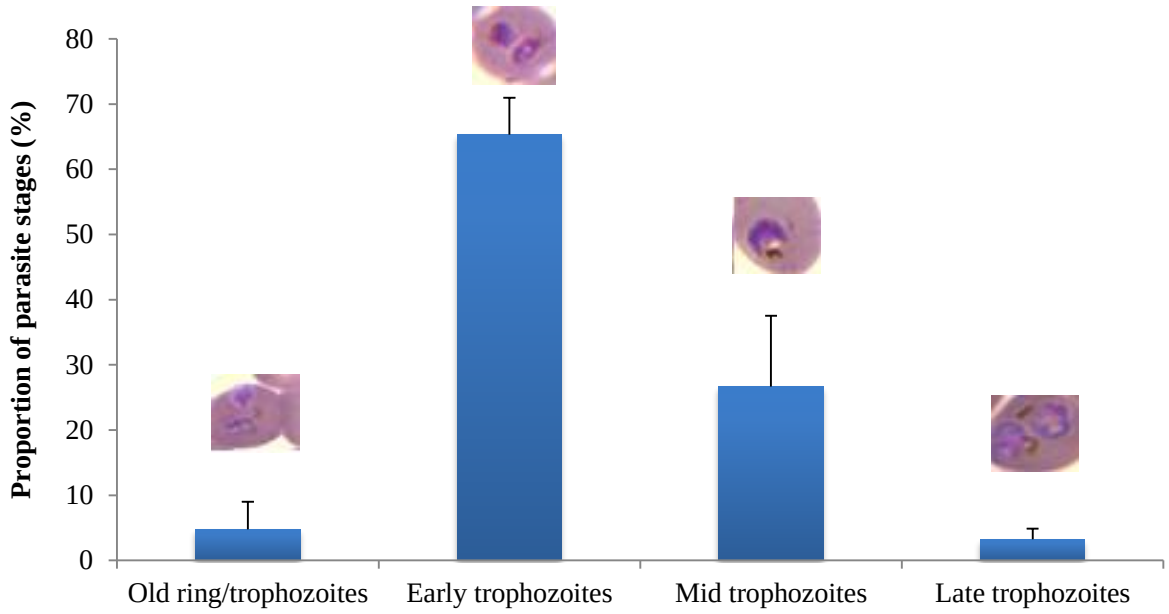

Figure 4.5: Mean percentage proportion of parasite stages from three biological replicates. Starting parasitaemia for the 1st, 2nd and 3rd biological replicates were 2%, 3.2% and 2.5% respectively. The bars are mean percentage of specific parasite sub-stages (represented in the pictures) in the entire population. Error bars are SEM of each biological replicate proportion from the mean.

Transcriptional responses of trophozoite-staged 3D7 through their sirtuins after exposure to 5mM lactate and/or 40°C stress for 2 h and 6 h were quantified (Fig. 4.6). This was derived using the $2^{(-\Delta\Delta Cq)}$ method to calculate the relative quantity, RQ, for each biological replicate and the mean RQ from all replicates was represented on the graphs. Error bars are SEM. The mean relative copy number, RCN, from all the biological replicates, was derived from $2^{(-\Delta Cq)}$, see section 2.7, and also plotted in Figure 4.7.

After 6 h of lactate stress (Fig. 4.6 A-C) there was a slight increase in *Hsp70* expression. There was also a slight decrease in *PfSir2A*. In response to high temperature of 40°C for 2 h, 3D7 trophozoites increased by 3.4-fold their expression of *Hsp70*. After 6 h, there was a 5.9-fold increase in *Hsp70* expression and this was statistically significant. Expression of *PfSir2A* was slightly increased at 2 h but there was little change at 6 h. Expression of *PfSir2B* was also slightly increased (2.27-fold) at 2 h with this increase reaching statistical significance (2.00-fold) at 6 h. Exposure to the combined stress, as would occur in most severe malaria cases, increased the expression of *Hsp70* at 2 h (2.8-fold) and at 6 h (4.6-fold) (all to a lesser degree that was not statistically significant than after heat shock alone). *PfSir2A* was increased to the same level as after heat shock alone at 2 and 6 h but this response was not statistically significant. *PfSir2B* was slightly increased to similar levels at 2 h and 6 h.

In summary, there was a more than 2-fold significant increase in *Hsp70* occurred upon 6 h of heat shock. A 2-fold or less significant increase in *PfSir2B* also occurred upon exposure to heat shock alone for 6 h, and in *Hsp70* upon exposure to lactate for 6 h. Trophozoite-staged 3D7 overall made little transcriptional response to high lactate of 5 mM. Prolonged mild heat, as obtainable in severe malaria, led to an increase in the expression of *PfSir2B* and *Hsp70* and these responses were slightly decreased after the combined stress.

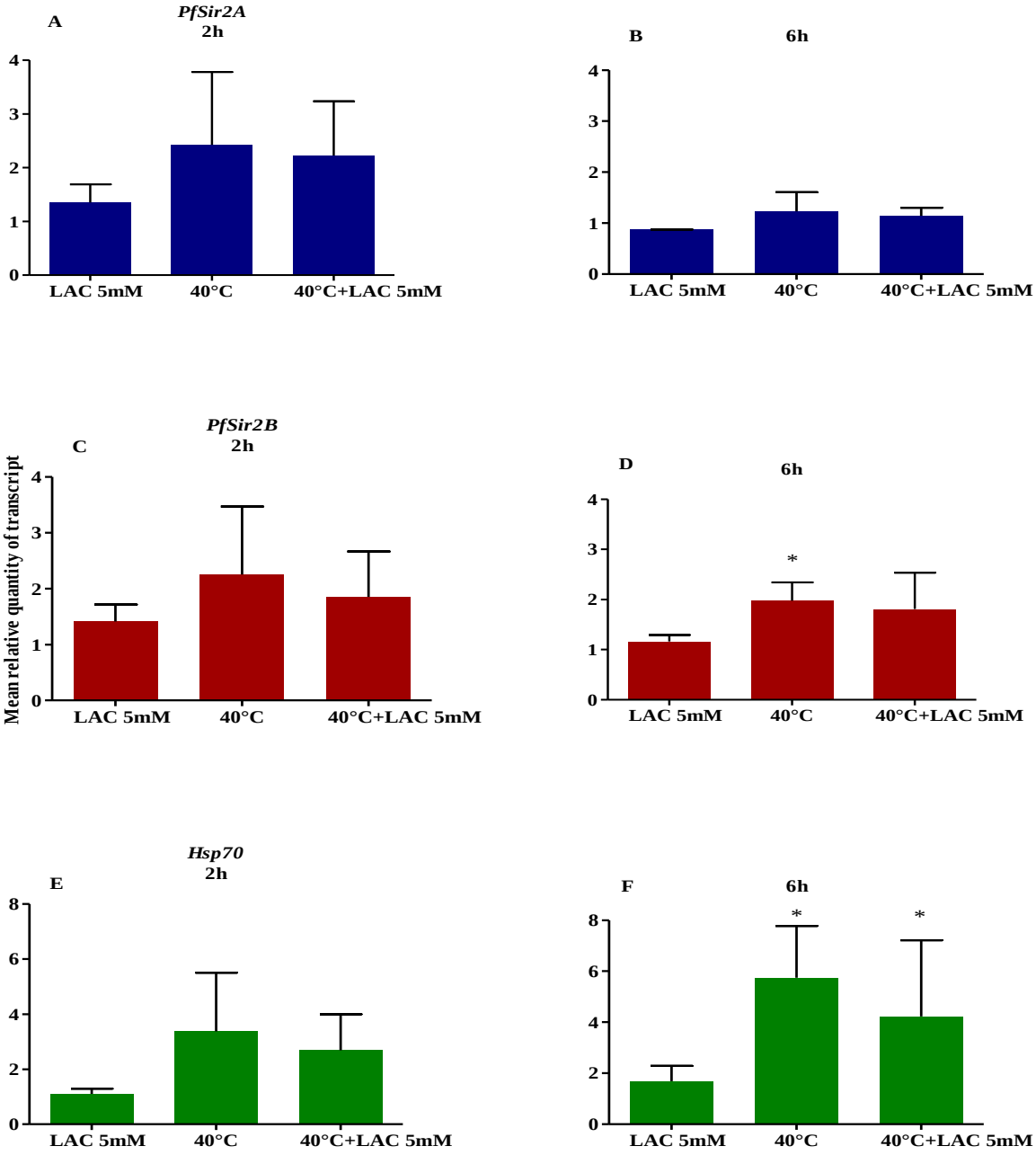

Figure 4.6: Transcriptional response of trophozoite-staged 3D7 after stress. The quantity of transcripts relative to that of a control culture for *PfSir2A* at 2 (**A**) and 6 h (**B**), *PfSir2B* at 2 (**C**) and 6 h (**D**), *Hsp70* at 2 (**E**) and 6 h (**F**), after the exposure of 3D7 to 5 mM lactate and/or 40°C from independent biological triplicate experiments. The different coloured bars represent the gene being measured: *PfSir2A* (blue bars), *PfSir2B* (red bars) and *Hsp70* (green bars). Error bars are SEM. *$p < 0.05$ Kruskal-Wallis test with Dunn's post test of the relative copy number (RCN), derived from $2^{(-\Delta Cq)}$.

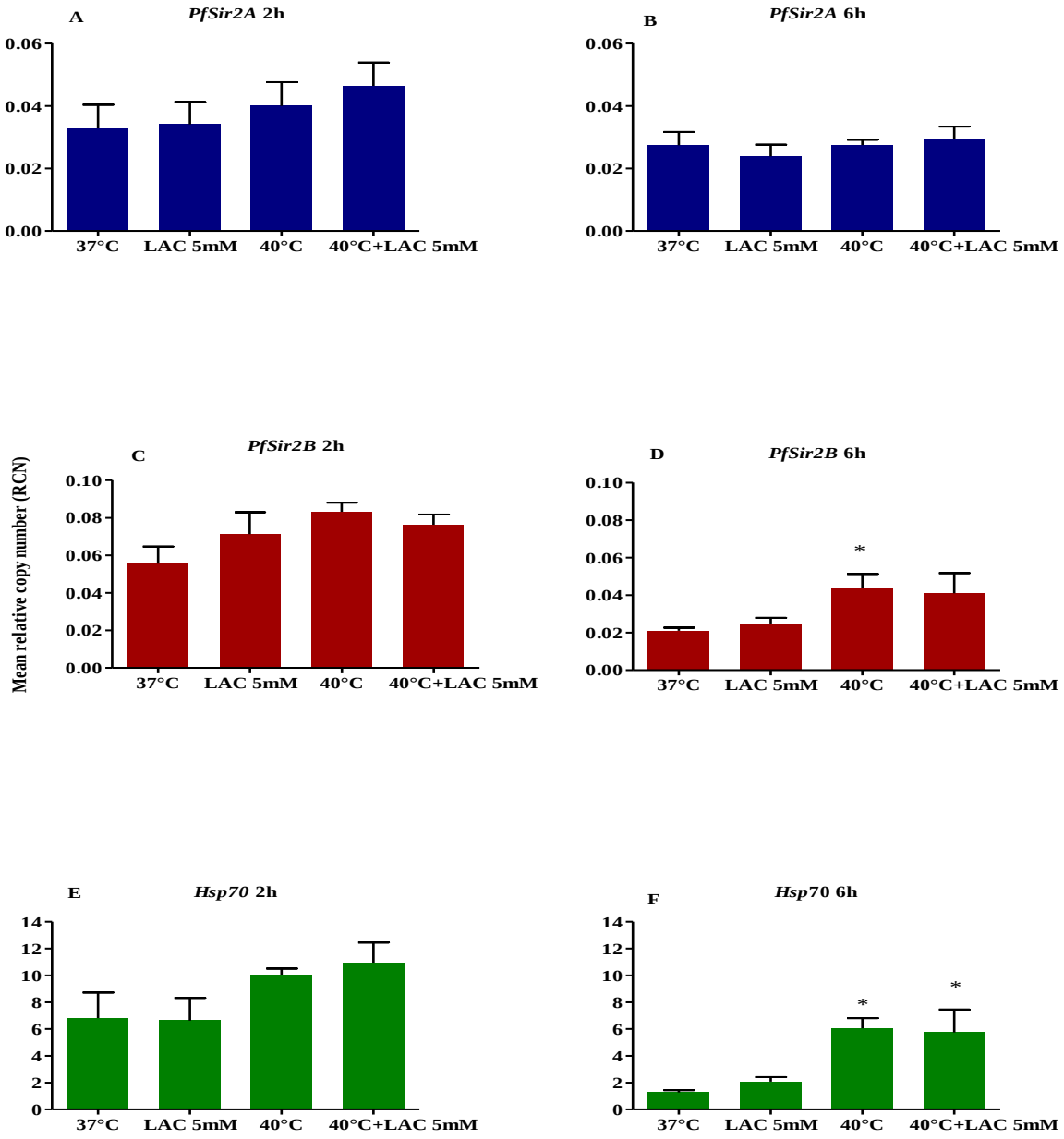

Figure 4.7: Mean Relative Copy Number (RCN) of expressed *PfSir2A*, *PfSir2B* & Hsp*70*

The **r**elative copy number (RCN), derived from $2^{(-\Delta Cq)}$, of *PfSir2A* at 2 (**A**) and 6 h (**B**), *PfSir2B* at 2 (**C**) and 6 h (**D**), *Hsp70* at 2 (**E**) and 6 h (**F**), after the exposure of 3D7 to no stress (37°C),.' 5 mM lactate and/or 40°C from independent biological triplicate experiments. The different coloured bars represent the gene being measured: *PfSir2A* (blue bars), *PfSir2B* (red bars) and *Hsp70* (green bars). Error bars are SEM. *p < 0.05 Kruskal-Wallis test with Dunn's post test.

There were large differences in the normalized Cq of target genes in the stressed parasites and unstressed control parasites between biological replicates (Fig. 4.7) and this may affect the magnitude of the alteration of gene expression upon stress, relative to the control. These differences were more evident after 6 h of stress for *Hsp70* and *Sir2B* ($p = 0.008$ and 0.005, respectively, test for equal variances). However, statistical analysis accounts for this variability. The difference in the pattern of expression of the endogenous control genes between biological replicate may play a role in the variations of expression of the target genes under study. However, it is also important to note that there was a similar pattern of expression of each endogenous control in individual experiments. We next looked at the transcriptional response in the older parasite schizont stage after exposure to the same stress the trophozoites had been exposed to.

4.3.4 Changes in sirtuin expression in 3D7 schizonts after stress

In the previous section the transcriptional response of the trophozoite-staged parasites via their sirtuin genes were measured after exposure to stress conditions. There were some consistent trends towards upregulated gene expression but few of these reached statistical significance across independent experiments. Therefore, we explored whether parasites at the schizont stage – which, as shown in Figure 4.4, showed more death after heat shock than trophozoites- might also show transcriptional responses of a greater magnitude.

Figure 4.8 shows that, unlike trophozoites, schizonts did have a less subtle response to prolonged lactate exposure. Prolonged lactate exposure caused a slight upregulation in the expression of *PfSir2A*, and also a nonsignificant increase in *PfSir2B* and *Hsp70* (Fig. 4.8 A, B). There was a 5-fold (significant) heat shock response in *Hsp70* at 2 h and a 2.5-fold response at 6h, but expression of *PfSir2B* and *PfSir2A* was unchanged after 2 h and only *PfSir2A* showed any upregulation after 6 h (fig 4.8 C, D). The combined stress caused a reduced response in *Hsp70* compared to heat shock alone but the response was still

significant. Surprisingly, *PfSir2A* was actually downregulated 0.7-fold, while *PfSir2B* remained unchanged (Fig. 4.8E, F). All heat shock responses were > 2-fold and significant. Of note, these data clearly show little error when compared to previous Figures: this is because a single experiment is shown, with error bars representing only the variation between technical replicates of RTPCR, rather than variation between independent biological replicates. This was because the two schizont-stage experiments done proved to have non-comparable staging (see Fig. 4.3).

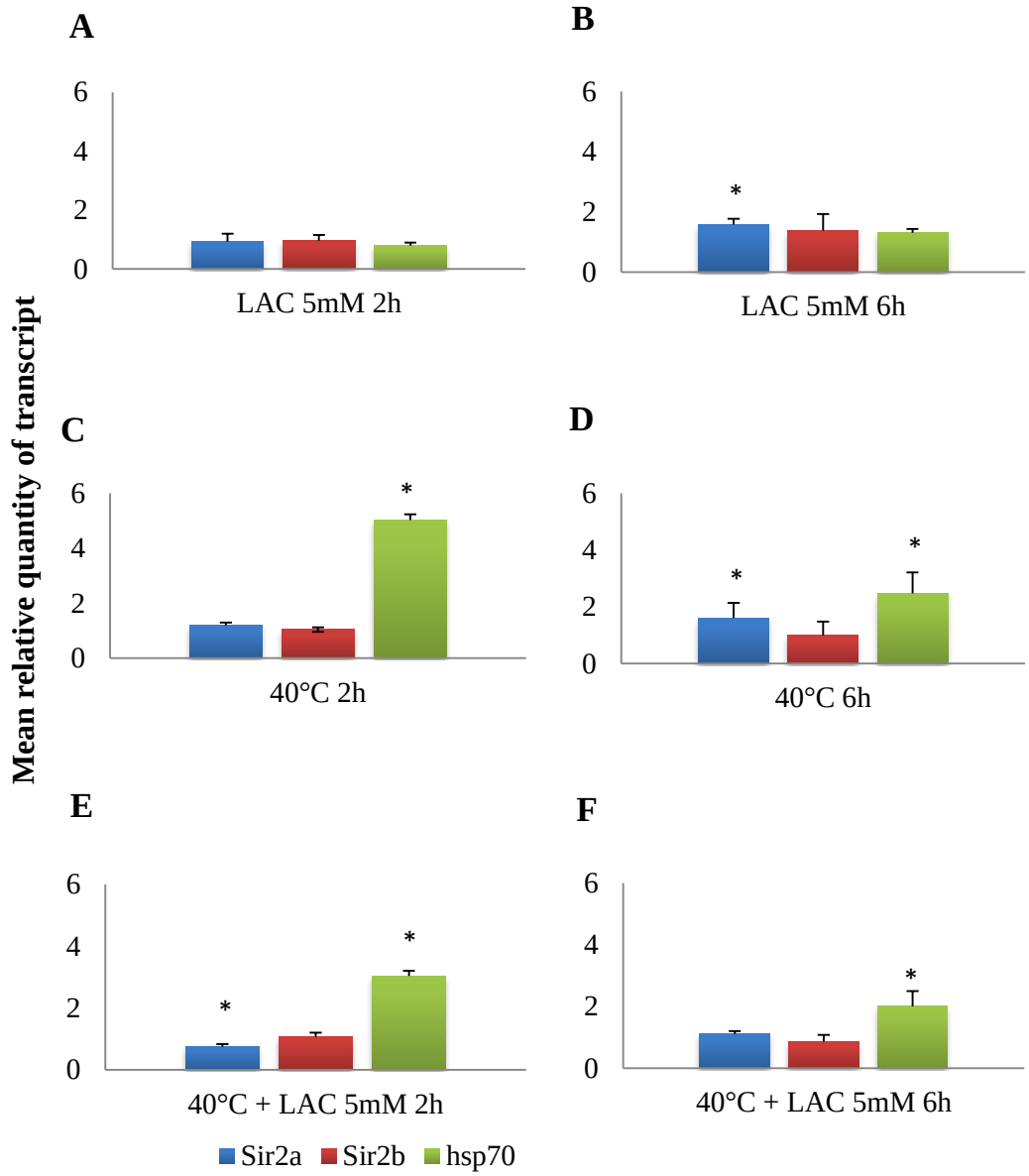

Figure 4.8: **Transcriptional response of schizont-staged 3D7 ('1st Biological Replicate') after stress. Q**uantity of transcripts is relative to that of a control culture for *Hsp70*, *Sir2A* and *Sir2B* after high lactate at 5 mM for 2 (**A**) and 6 h (**B**), high temperature at 40°C for 2 (**C**) and 6 h (**D**), high temperature at 40°C combined with high lactate at 5 mM for 2 (**E**) and 6 h (**F**). The different coloured bars represent the gene being measured. *$p < 0.05$, Kruskal-Wallis test or ANOVA of RCN significantly different from the control. Error bars are Confidence Intervals derived from subtracting RQ from RQmax for high bar and RQmin from RQ for low bar. RQmax/min calculated by the StepOne Software.

A second experiment using slightly older schizonts enabled us to establish what the ring's response may look like after an initial heat shock of the parent parasites, as more of the parasites had reinvaded at the end of the 6 h experiment compared to the first schizont experiment (Fig. 4.3). Of note is that most of the fold changes in expression of the genes under study here are significantly different from the control. There was little change in the *Hsp70* upon lactate stress at 2 and 6 h (Fig. 4.9 A, B) and the same was true for target genes under study except for *PfSir2A,* which was slightly downregulated at 2 h only. Conversely, there was a downregulation of *Hsp70*, *PfSir2A* and *PfSir2B,* upon heat shock (Fig. 4.9 C, D), but this was not sustained and expression was increased on prolonged heat shock. For the combined stress, we see the same trend, although we have a greater upregulation of *PfSir2A* about a fold more than heat shock alone. Overall, it appears that schizonts, like trophozoites, are capable of making a heat shock response in *Hsp70,* but unlike the trophozoites there is a consistent increase in *PfSir2A* not *PfSir2B* after heat shock alone, despite a more severe death after heat shock.

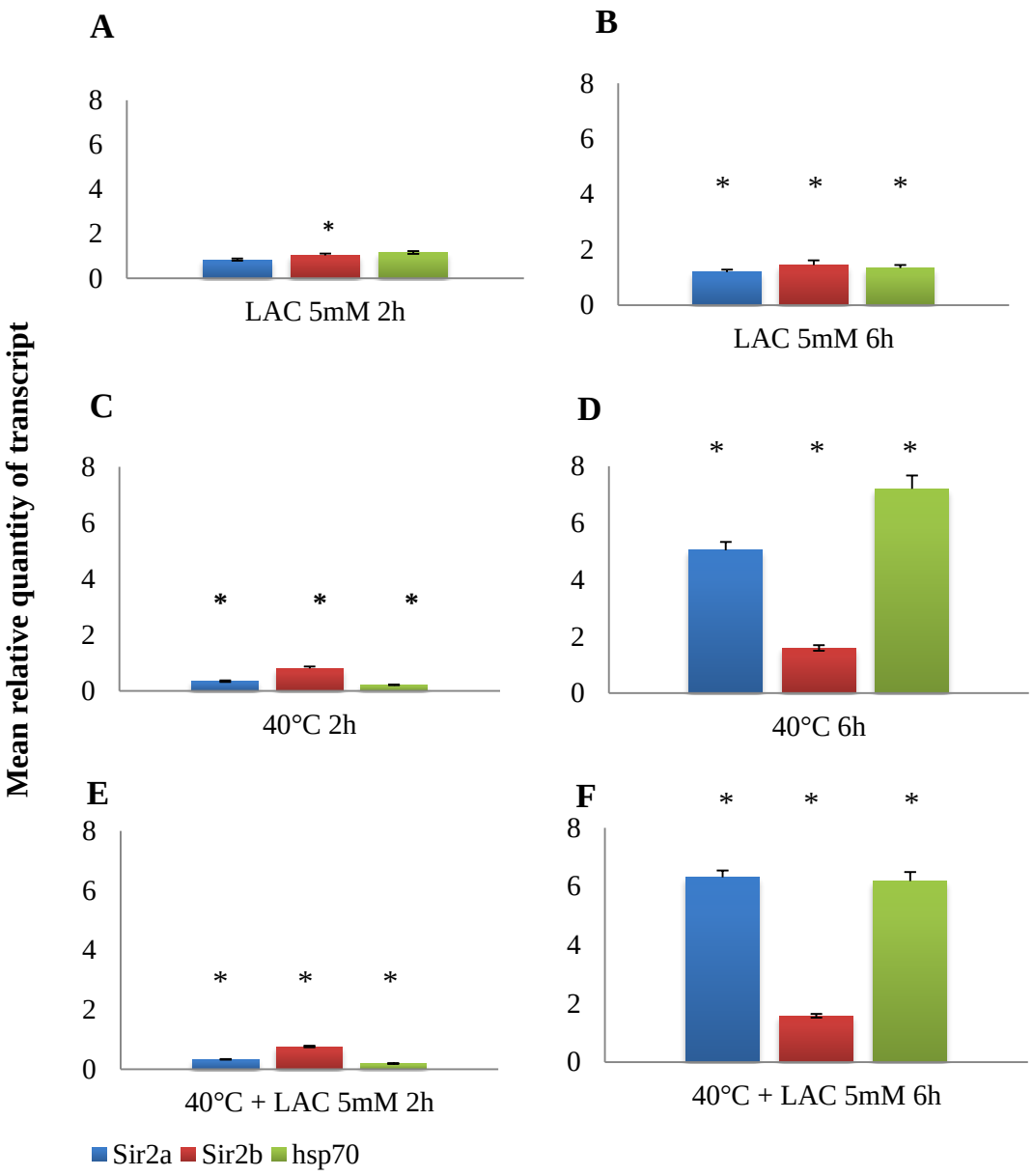

Figure 4.9: **Transcriptional response of schizont-staged 3D7 ('2nd Biological Replicate') after stress.** Quantity of transcripts is relative to that of a control culture for *Hsp70*, *Sir2A* and *Sir2B* after high lactate at 5 mM for 2 (**A**) and 6 h (**B**), high temperature at 40°C for 2 (**C**) and 6 h (**D**), high temperature at 40°C combined with high lactate at 5 mM for 2 (**E**) and 6 h (**F**). The different coloured bars represent the gene being measured. *$p < 0.05$, Kruskal-Wallis test or ANOVA of RCN significantly different from the control. Error bars are Confidence Intervals derived from subtracting RQ from RQmax for high bar and RQmin from RQ for low bar. RQmax/min calculated by the StepOne Software.

4.3.5 Effect of high lactate and high temperature on the survival of 3 culture-adapted patient field strains: *P. falciparum* 3518, 9775 and 10668 Trophozoites

In the previous two sections, the transcriptional responses of sirtuin genes following exposure of lab-adapted strain of *P. falciparum* 3D7 to stress were assessed. However, the link between stress and sirtuin expression was first observed not in 3D7, but in field isolates of *P. falciparum* directly from human patients (Merrick, Huttenhower et al. 2012). In this study although 3D7 clearly retained the ability to mount an *Hsp70* upregulation in response to heat shock, they gave a limited transcriptional response in their sirtuins. We were thus concerned that this limitation may presumably be due to their long adaptation in stable *in vitro* culture conditions. Therefore, the experiments were repeated in three field isolates from Kenya that had been adapted to *in vitro* culture much more recently. The rationale was that these lines may more closely resemble the original field isolates in Merrick 2012.

As a first experiment, the three Kenyan field isolates were tested for their survival after exposure to stress conditions. Each viability study was done as a follow up 48 h after exposure of the parasite to each stress. Parasite used here were mainly early trophozoite. Freshly lab-adapted field strains have been shown to have lower multiplication rates than long term-adapted laboratory strains and this was observed especially for *P. falciparum* 3518, and may be important for their survival. 9775 grew faster than 3D7 and the other field strains. The asexual life cycle for all field strains seem to be slightly longer than 48 h for a while during the first few weeks of culturing before we used them for the stress experiments.

The survival of *P. falciparum* 3518 exposed to 2 h of lactate stress did not significantly change compared to the control (Fig. 4.10). Heat shock alone led to about 19% significant decrease in growth rate, with a combined stress causing a similar significant (21%) decrease. SYBR Green-1 based assessment of growth rate 48 h after stress did corroborate the microscopic counts to an extent. From this assessment however, lactate exposure resulted in

an increase in growth (as measured by SYBR-Green-1) after 2 h which was significant (~11%) but not sustained after 6 h exposure. The heat shock alone and with lactate stress did not negatively affect survival after 2 h or 6 h, although there was a downward trend. Again, the reason for the underrepresentation of parasite death in the SYBR assay has been explained in section 2.4. Prolonged stress thus had a greater deleterious effect on parasite growth as seen with 3D7.

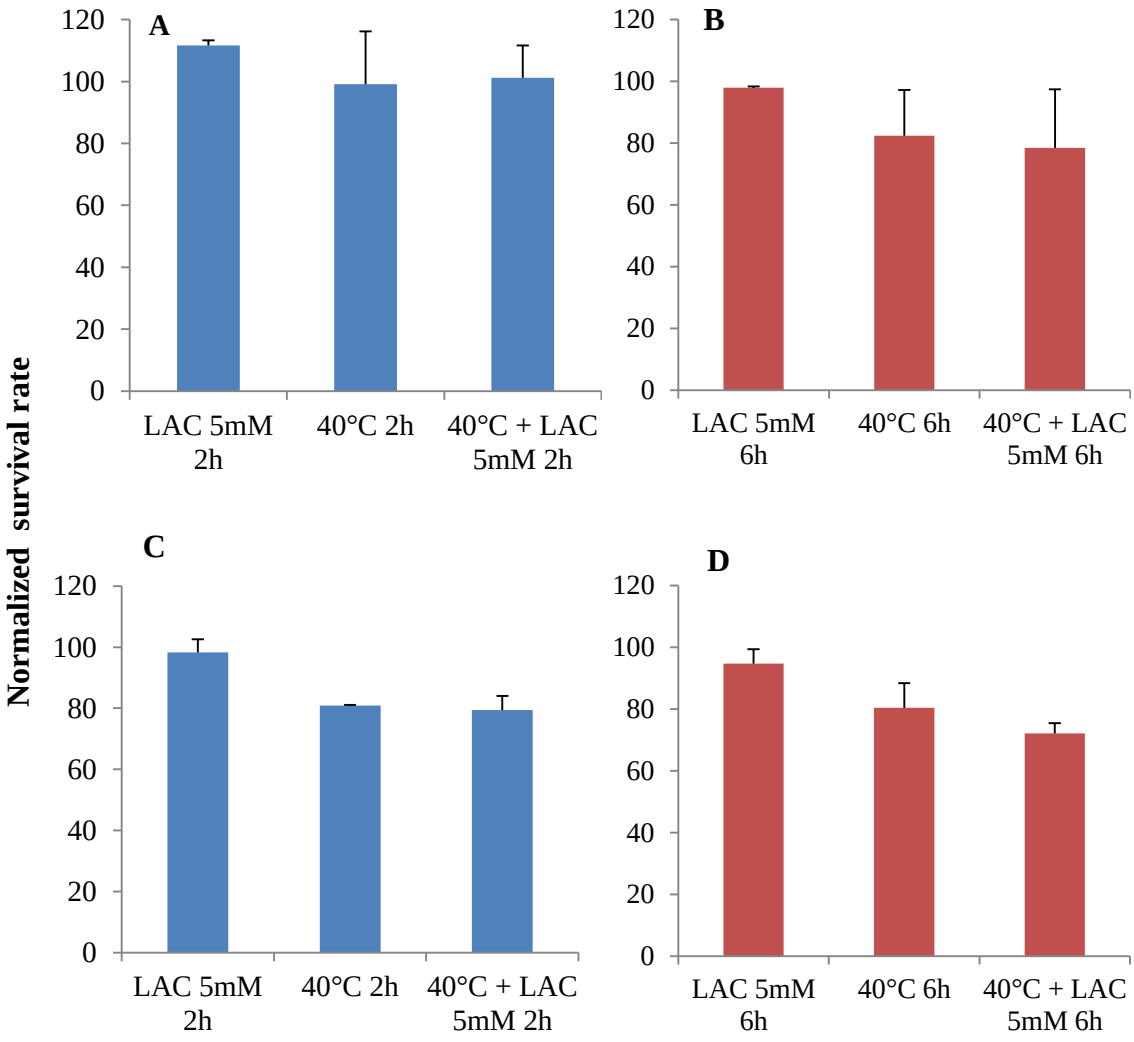

Figure 4.10: **Post-stress survival of trophozoite-staged 3518 by microscopy and DNA content via SYBR-Green-1 based assay.** Survival of strain 3518 at 48 h after stress treatment for 2 h or 6 h at the trophozoite stage, relative to growth of a control culture, measured via DNA content in a SYBR-Green-1 based assay, **A & B** or microscopy, **C & D**, respectively for the time points. Data are from two biological replicate experiments. Microscopy is from a single count, n = 2, while each SG 1 read is the mean of three technical replicates, n = 6. The mean survival rate from each biological replicate experiment was calculated and merged to get a pooled mean of biological replicates before being presented on the graphs. Error bars are SEM.

The remaining two field strains, 9775 and 10668 were assessed for survival only by their DNA content, although Figure 4.10 shows that this is less sensitive than microscopy. Figure 4.11 shows that 9775 was affected by 2 h heat exposure similarly to 3518, but was more severely affected after 6h. As with 3515, lactate had little effect on parasite survival.

P. falciparum 10668 was relatively unaffected by stress after a 2 h exposure. Prolonged heat stress, however, caused a significant decrease in survival, as seen in all strains examined.

Summarily, strain 3518 and 10668 showed similar heat shock response to 3D7, with a maximum of ~30% death upon prolonged stress, while, half of the 9775 culture was killed off by prolonged heat shock. Of the three parasite field strains, *P. falciparum* 9775 could grow the fastest and to a higher parasitaemia without crashing under the optimized normal culture conditions that were adopted for theses field strains.

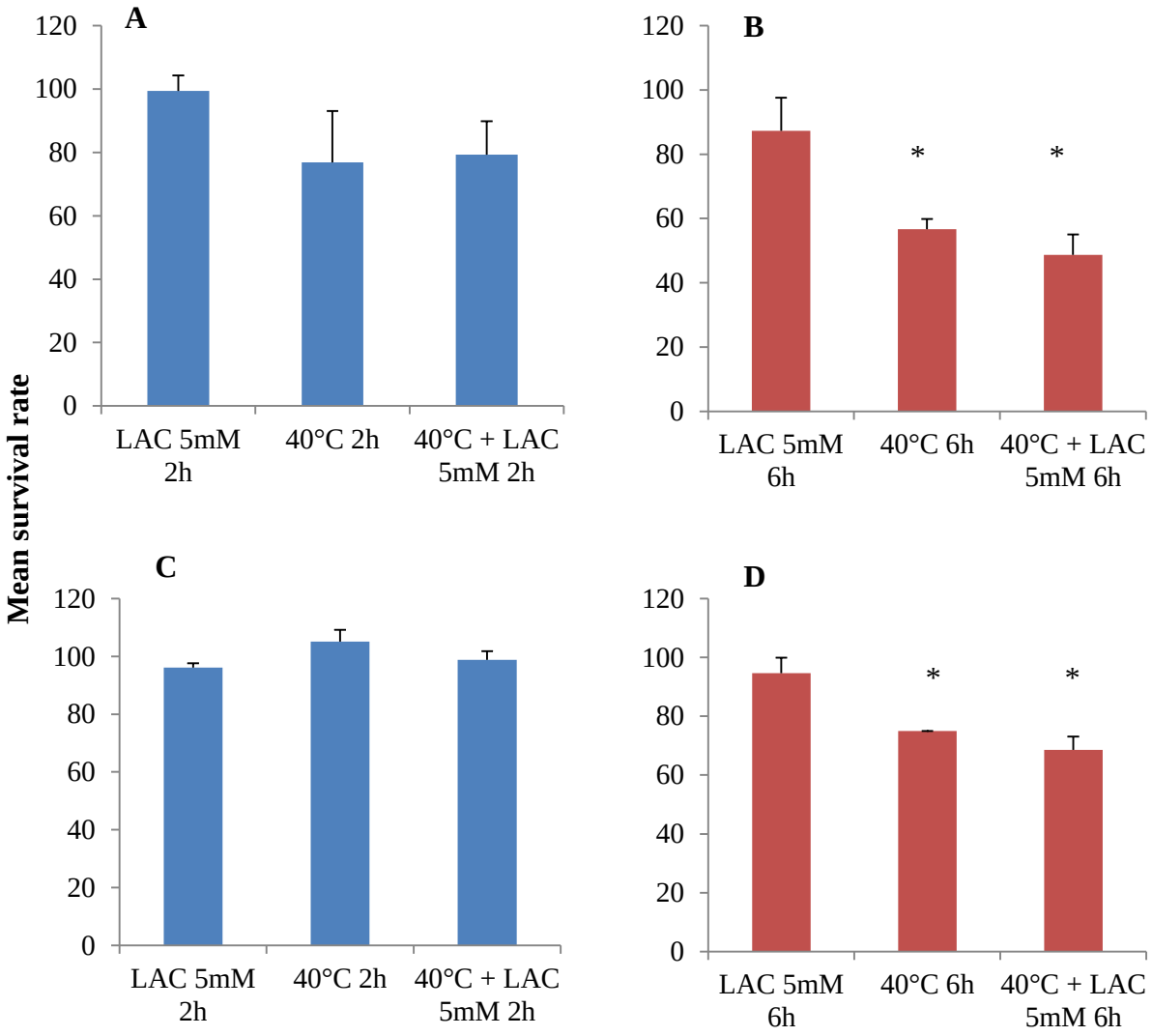

Figure 4.11: Post-stress survival of trophozoite-staged 9667 and 10668 by DNA content via SG 1-based fluorescence growth assessment. Survival of strain 9775 at 48 h after stress treatment for 2 h (**A**) & 6 h (**B**). Survival of strain 10668 at 48 h after stress treatment for 2 h (**C**) & 6 h (**D**). Data are from two biological replicate experiments. Each biological replicate experiment was conducted in three technical replicates. The mean survival rate from each biological replicate experiment was calculated and merged to get a pooled mean of biological replicates before being presented on the graphs. *$p < 0.05$, Kruskal-Wallis test with Dunn's post test of raw fluorescence reads.

4.3.6 Effect of high lactate and high temperature on the survival of 3 culture-adapted field strains: *P. falciparum* 3518, 9775 and 10668 0-4 h rings

In the previous section, the trophozoite stage of the field strain were shown to be equally or more sensitive than 3D7 to stress. However, we wished to also establish the sensitivity of their ring stage to stress. This strategy was adopted partly because 3D7 at trophozoites and schizonts showed limited transcriptional sirtuin response and partly because the Merrick *et al*. study assessed transcriptional response to these stress only in rings (Merrick, Huttenhower et al. 2012), as this is the only available stage in the circulation of human malaria patients. Thus, the response of parasite to the stress via their sirtuins may be best reproduced in cultured ring stages of the field strains. The release of merozoites triggers the fever response, although this is not a perfectly synchronous event. Therefore, the early rings together with remaining schizonts are most likely to be exposed to heat shock. Sequestration and metabolism of trophozoites and schizonts do contribute to acidosis; so all parasite stages are probably equally exposed to elevated lactate. For these reasons, all remaining experiments in this chapter were conducted on ring stages as well as trophozoites of the field strains.

Parasites used here were mainly rings, with a ratio of rings to schizonts determined before the stress experiment. Each viability study was done as a follow up 72 h after exposure of the parasite to each stress. The parasitaemia and SYBR reads were converted to survival rate (equation in section 2.4).

The survival of *P. falciparum* 9775 rings as assessed by SYBR-Green-1 assessment was increased by 5% (non-significant) after lactate stress, reduced by 26% after heat shock and by 25% after the combined stress (Fig. 4.12 A). However, by microscopy there was a 12% reduction after lactate stress, a 49.5% reduction after heat shock and a 55% reduction after combined stress (Fig. 4.12 B). The picture for 10668 was very comparable to that for

9775 (Fig. 4.12 A & B), with only slight change in survival after lactate stress and marked death after heat shock. In strain 3518, ring stages were more resistant to stress than either 10668 or 9775, with only slight growth reduction after heat shock. This is consistent with this strain being the most resistant to heat shock at trophozoites as well.

Based on SYBR-Green 1 assessment, young rings of *P. falciparum* 3518, 9775 and 10668 are clearly less affected by heat shock and 5mM lactate than their trophozoites. This is likely because the trophozoite stage is much more metabolically active than the ring stage. However, we see again that 9775 is the most affected by stress compared to other strains, and that 3518 was most resistant to stress.

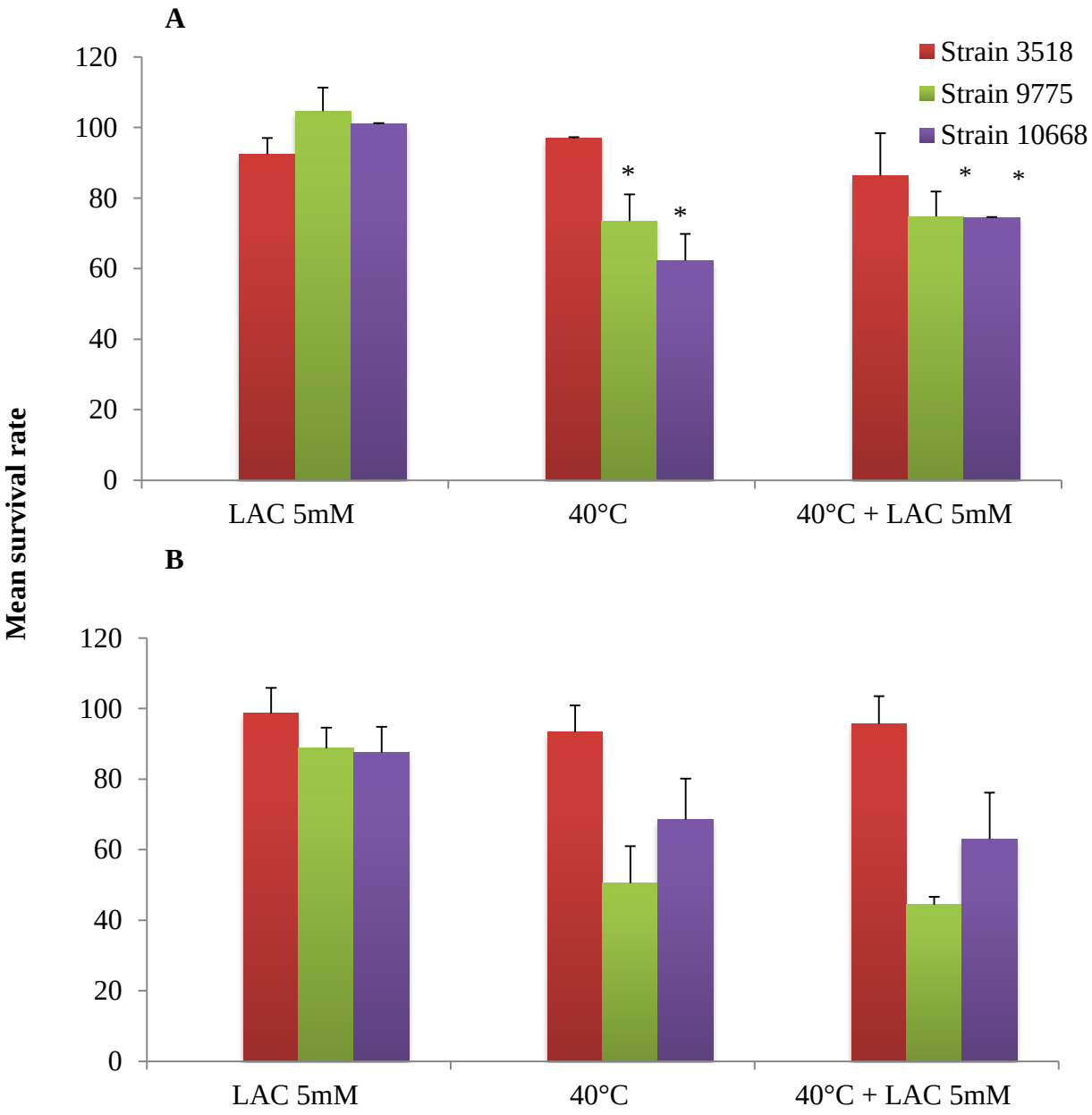

Figure 4.12: Post-stress survival of ring-staged field strains by SG 1-based fluorescence growth assessment and microscopy. A is growth measurements of by SG 1-based fluorescence growth assessment 72 h post 6h of stress. **B** is growth measurements by microscopy 48 h post 6 h of stress. Data are from two biological replicate experiments. For each biological replicate experiment microscopy is from a single count while each SYBR-Green-1 read is the mean of three technical replicates. Error bars are SEM. *p < 0.05, Kruskal-Wallis test with Dunn's post test of raw fluorescence reads. Counts were done per 5*100 squares (5 different fields) using a counting grid.

4.3.7 Changes in sirtuin expression in the trophozoites of the 3 culture-adapted field strains after stress

Having established the relative survival of the three field stains after stress at both trophozoite stages and rings, we proceeded to assess their transcriptional response to stress. This section deals with transcription in trophozoites and the next sections deals with the rings. The majority of the parasites used to study the transcriptional response of the field strains were early trophozoites (Fig. 4.13).

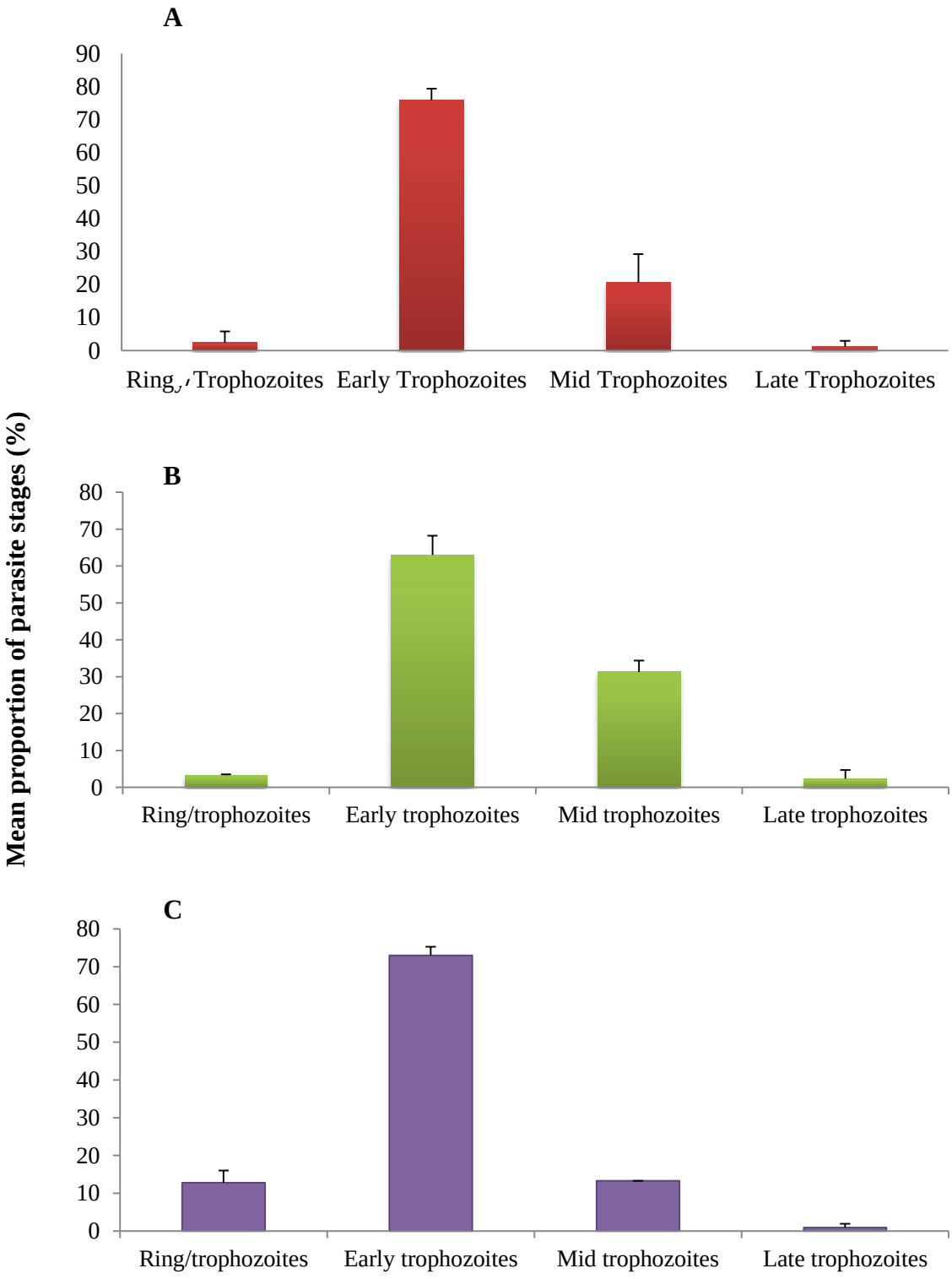

Figure 4.13: Proportion of parasite stages in strains 3518, 9775 and 10668 before stress. The red bar is *P. falciparum* 3518 (**A**) **(**3.45% and 2%), green is 9775 (**B**) **(**7.3% and 3.96%) and purple is 10668 (**C**) **(**7.5% and 7.8%). Chart represents the mean of two biological replicate experiments with parasitaemia in brackets. Error bar is SEM.

For strain 3518, after lactate stress (Fig. 4.14A - F) there was no significant change in *Hsp70* expression after 2 h ($p = 0.112$) and 6 h ($p = 0.191$) (Fig. 4.14A & B). There was no significant change in the expression of *PfSir2A* (Fig. 4.14C & D) and *PfSir2B* after 2 h and 6 h. Following lactate stress in strain 9775, there was no change in *Hsp70*, *PfSir2A* and *PfSir2B* expressions after 2h and 6h. Finally, in trophozoite-staged 10668 there was almost no transcriptional response to lactate. The results after the lactate stress were not markedly different from that seen in 3D7 except that 3D7 did increase its expression of *Hsp70* significantly after 6 h of lactate stress.

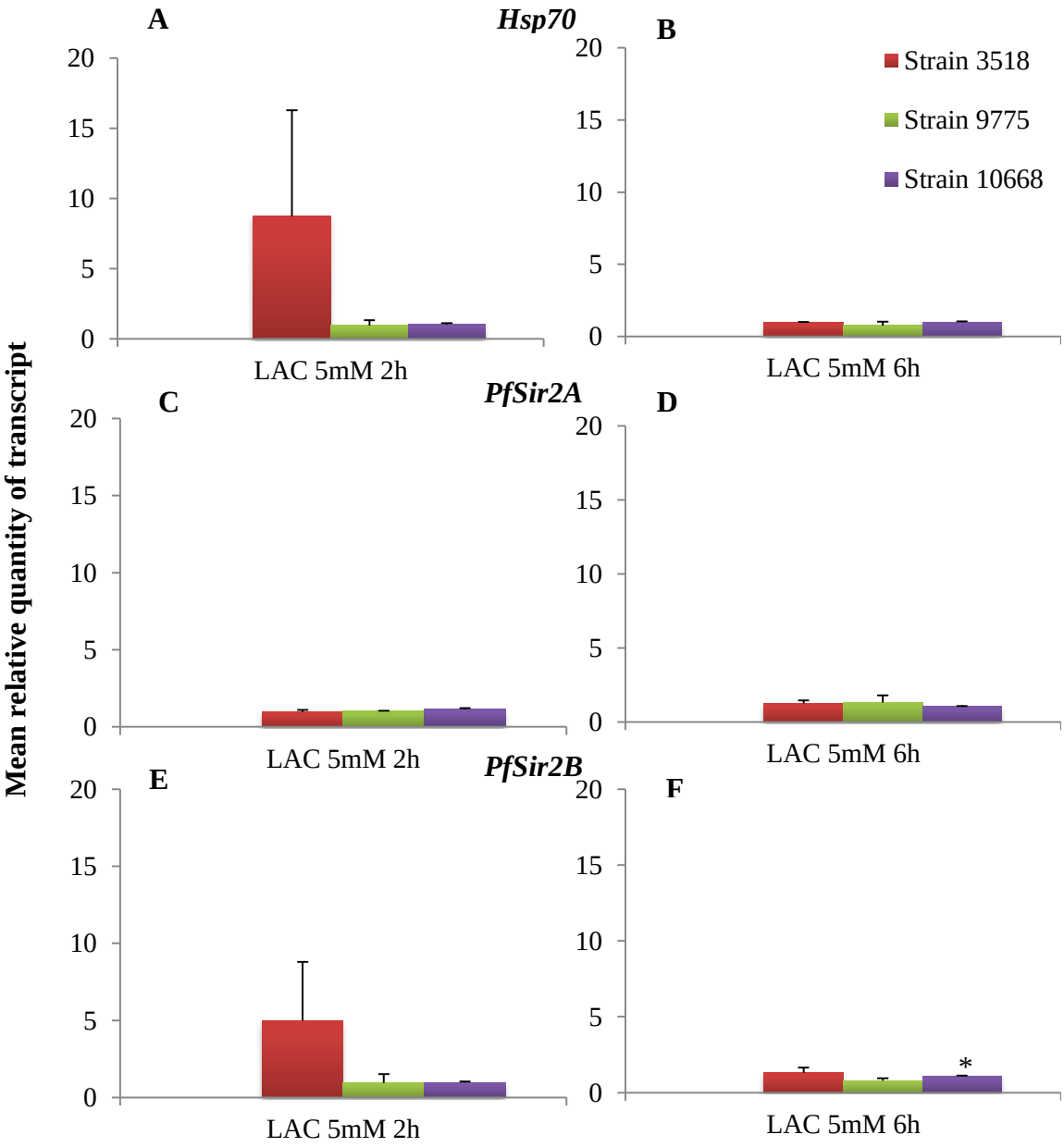

Figure 4.14: Transcriptional response of trophozoite-staged field strains after lactate stress. Mean RQ = mean of $2^{(-\Delta\Delta Cq)}$ from two biological replicate experiments. Error bars are SEM from the pooled mean. Quantity of transcript are relative to quantities in a control culture for *Hsp70* after 2 (**A**) and 6 h (**B**), *PfSir2A* after 2 (**C**) and 6 h (**D**) and *PfSir2B* after 2 (**E**) and 6 h (**F**). *p < 0.05 Kruskal-Wallis test with Dunn's post test of the relative copy number (RCN), derived from $2^{(-\Delta Cq)}$. and represented in appendix VIII.

In response to high temperature of 40°C (Fig. 4.15A - F), strain 3518 trophozoites did not increase their expression of *Hsp70* (Fig. 4.15A & B), *PfSir2A* (Fig. 4.15C & D) and *PfSir2B* (Fig. 4.15E & F) significantly, after 2 h and 6 h. For strain 9775, heat shock led to the significant increase in the expression of *Hsp70*, at 2 h (6.2-fold) and 6 h (6.7-fold) ($p = 0.0005$ for both). There was no change in the expression of *PfSir2A* after 2 h and 6 h of stress. Expression of *PfSir2B* was significantly increased after 2 h (1.7-fold, $p = 0.0185$), but not after 6 h of stress. Strain 10668 showed a similar response as strain 9775, but the expression of *Hsp70* was lower at 2 h (5.2-fold) and was down-regulated at 6 h (3.3-fold). Its *PfSir2A* expression was significantly slightly increased only after 6 h, while its *PfSir2B* expression was increased after 2 ($p = 0.0004$) and 6 h ($p = 0.0005$), but never by more than 2-fold.

In response to heat shock *Hsp70* was generally upregulated in all the trophozoite strains, including 3D7 ($p < 0.0001$, $n = 27$). *PfSir2B* expression was generally increased only after 2 h of heat shock ($p = 0.0031$, $n = 27$). Overall, there was reduced transcript levels of *Hsp70* and *PfSir2B* after 6 h compared to after 2 h in response to heat shock ($p = 0.000$, $n = 27$).

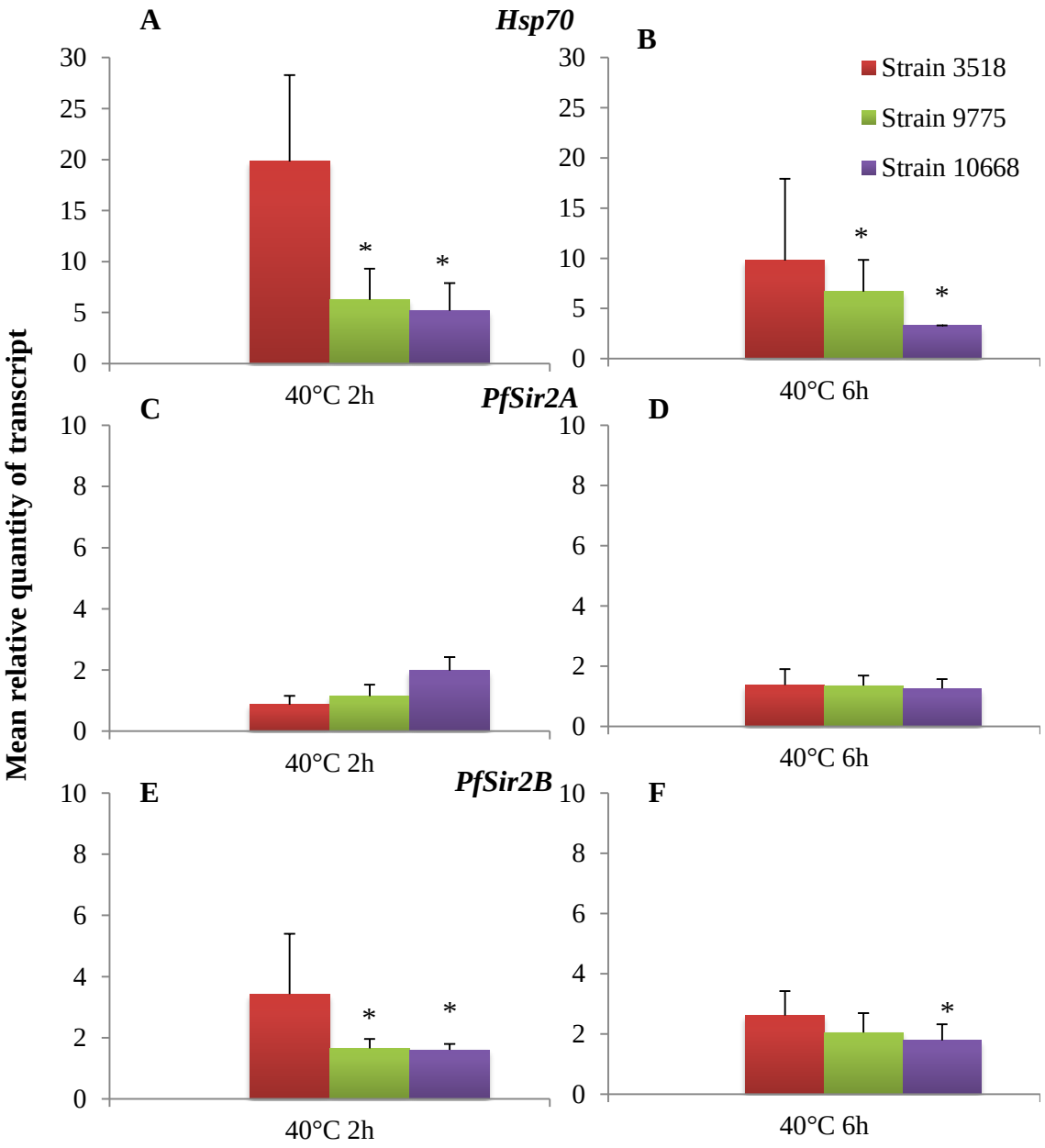

Figure 4.15: Transcriptional response of trophozoite-staged field strains after heat shock stress. Mean RQ = mean of $2^{(-\Delta\Delta Cq)}$ from two biological replicate experiments. Error bars are SEM from the pooled mean. Quantity of transcript are relative to quantities in a control culture for *Hsp70* after 2 (**A**) and 6 h (**B**), *PfSir2A* after 2 (**C**) and 6 h (**D**) and *PfSir2B* after 2 (**E**) and 6 h (**F**). *p < 0.05 Kruskal-Wallis test with Dunn's post test of the relative copy number (RCN), derived from $2^{(-\Delta Cq)}$. and represented in appendix VIII.

Exposure to the combined stress (Fig. 4.16A - F), as is obtainable in most severe malaria cases, increased the expression of *Hsp70* after 2 h of stress for strain 9775 and 10668 and this response was downregulated on prolonged stress (6 h). *PfSir2B* was significantly increased at 2 h and 6 h for strain 10668. There was no significant difference in their responses after the combined stress compared to heat shock alone.

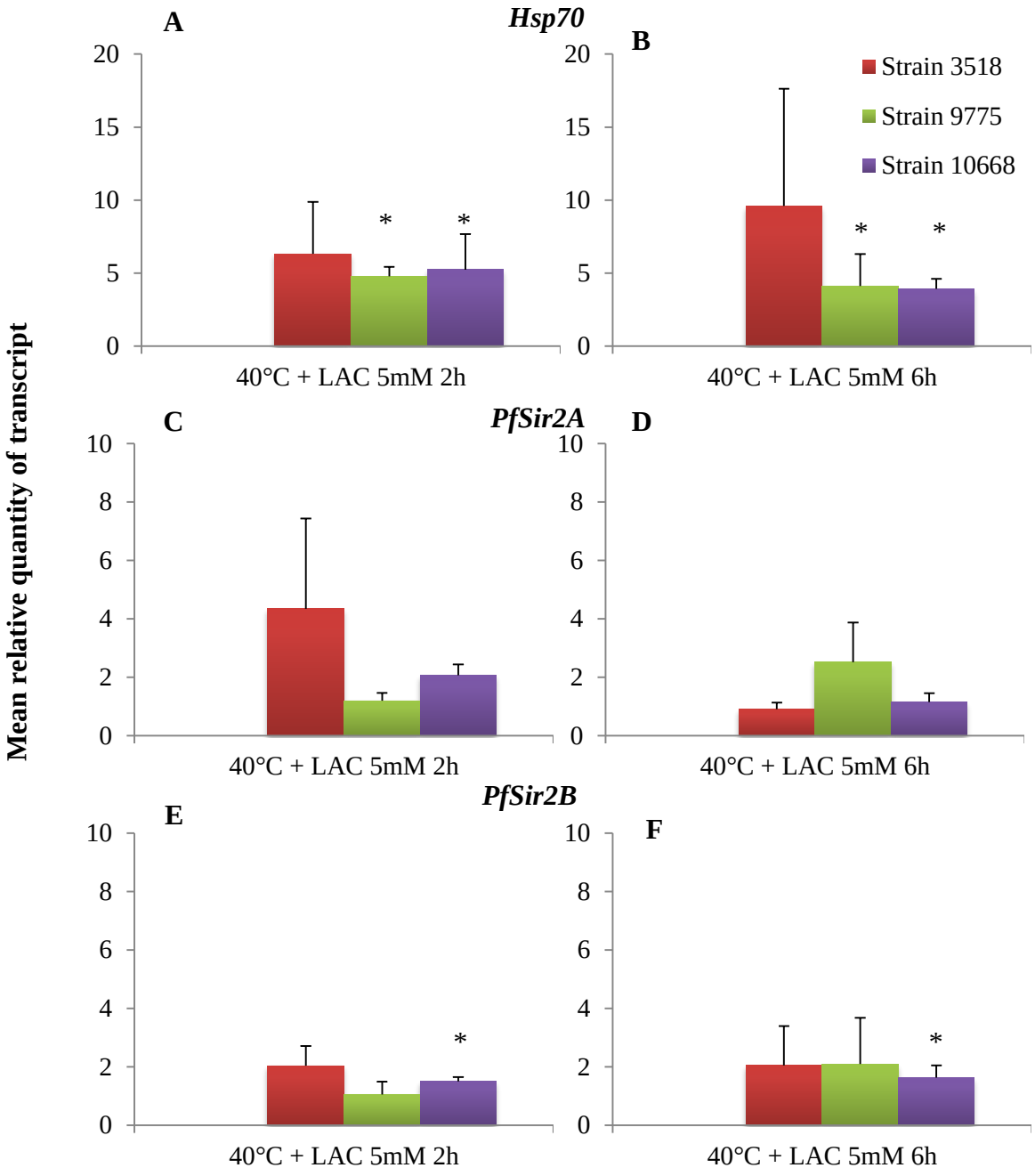

Figure 4.16: Transcriptional response of trophozoite-staged field strains after combined lactate and heat shock stress. Mean RQ = mean of $2^{(-\Delta\Delta Cq)}$ from two biological replicate experiments. Error bars are SEM from the pooled mean. Quantity of transcript are relative to quantities in a control culture for *Hsp70* after 2 (**A**) and 6 h (**B**), *PfSir2A* after 2 (**C**) and 6 h (**D**) and *PfSir2B* after 2 (**E**) and 6 h (**F**). *p < 0.05 Kruskal-Wallis test with Dunn's post test of the relative copy number (RCN), derived from $2^{(-\Delta Cq)}$. and represented in appendix VIII.

Overall, the transcriptional responses seen in sirtuins in the three recently-adapted field strains were not very different from those seen in 3D7. Trophozoites of all strains responded strongly to heat shock in upregulating *Hsp70* (a range of 3.33 to 6.68 folds), while there was a general trend to moderate upregulation of sirtuins, consistently *PfSir2B* (2-fold or less). There was no transcriptional response to lactate in the field strains.

4.3.8 Altered sirtuin expression in the rings may select for the expression of severe disease-associated *var* gene subsets after stress

As explained previously, the same stress experiments were conducted on ring-stage parasites. The data did not have a direct precedence from prior comparable experiments in 3D7. Furthermore, since this is the stage at which *var* genes are expressed, these experiments allowed the simultaneous measurement of sirtuin and *var* expression under stress conditions. The majority of the parasites used for the two biological replicate per parasite strain in this study were young rings (2 ± 2 hpi), with parasitaemia and ratio of rings to schizonts as follows: 3518 **(**10:1 {2%} and 16:1 {4%}), 9775 **(**8:1{3.1%} and 9:1{4.1%}) 10668 **(**3:1{2.49%}). The ring-staged field strains were exposed to 5 mM lactate and/or 40°C stress for 6 h, and allowed to recover for 10 h. Their transcriptional responses both directly after stress and after 10 h recovery were analysed. The same experiments were carried out in biological duplicates on all strains except 10668 because staging at 16 h indicated that its second biological replicate was not tightly synchronized, with schizonts seen up until 16 h (i.e. after 10 h recovery, post stress). This meant that the second replicate was more contaminated with schizonts rather than rings, which is particularly problematic because schizonts contain more RNA than rings per parasite.

For strain 3518, after lactate stress, there was little or no change in *Hsp70*, *PfSir2A* and *PfSir2B* expression after 6h, or upon recovery (Fig. 4.17). Following lactate stress, strain 9775 again showed no transcriptional response. For the one biological replicate of 10668

transcriptional response show that after lactate stress, *Hsp70* (2.2-fold) was significantly increased but this response was lost upon recovery. *PfSir2A* (0.3-fold) and *PfSir2B* (0.75-fold) were downregulated significantly after stress but returned to baseline levels.

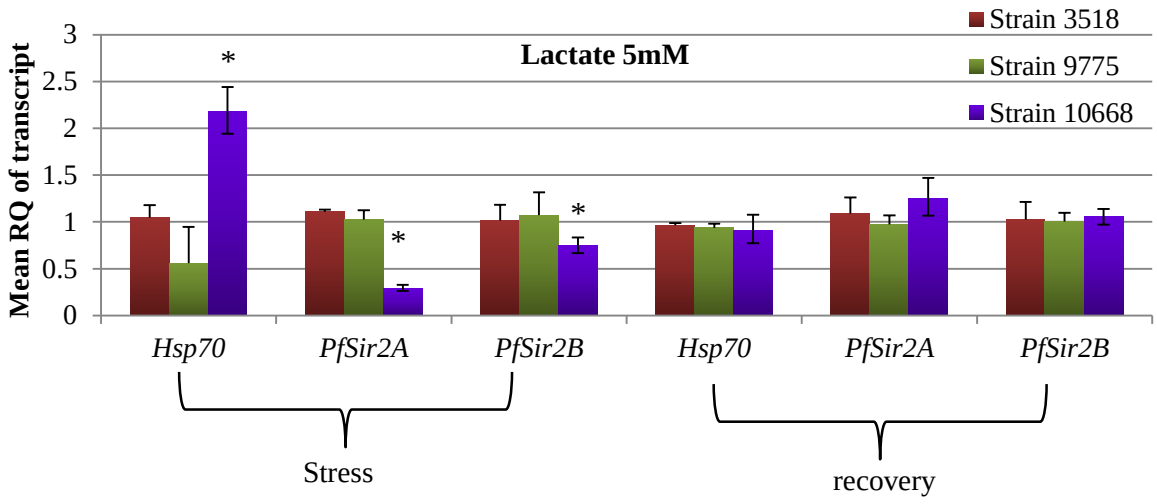

Figure 4.17: Transcriptional response of ring-staged field strains after lactate stress. Relative quantity of transcripts for *Hsp70*, *Sir2A* and *Sir2B* in parasites immediately after 6h of 5mM lactate ('stress') and after a further 10 h of recovery ('recovery'), relative to transcript quantities in a control culture. Mean RQ = mean of $2^{(-\Delta\Delta Cq)}$ from two biological replicate experiments (except for 10668). Error bars are SEM or CI for 10668. *p < 0.05 Kruskal-Wallis test with Dunn's post test of the relative copy number (RCN), derived from $2(^{-\Delta Cq})$, n = 6 but n = 3 for 10668.

P. falciparum parasites switch continuously between different *var* genes, thus in a parasite population different *var* genes may be expressed. *Var* genes are expressed primarily in ring stage parasites and are downregulated at later stages. We set out to investigate if there was a direct causal link between the stress factors and *var* expression following changes in sirtuin expression upon the same stress. Primers to *var* gene groups ups A1, A2, A3, B1, B2, C1, C2 and E as previously described in the methods were used. The RNA used for this study was from the ring-staged parasites already subjected to stress. Figure 4.18A and B shows the

expression of all *var* gene groups after exposure to lactate (6 h) and on recovery (10 h), respectively for all field strains. Strain 3518 did not respond to lactate stress.

The 9775 strain of *P. falciparum*, unlike 3518, responded to lactate stress (Fig. 4.18 A), by increasing its expression of *var* genes A3 and predominantly B2. The ATS region, representing the total *var* gene expression was also significantly increased. On recovery, no *var* gene is selectively upregulated.

The experiment with the third *P. falciparum* strain 10668, gave its own unique *var* gene group profile, however, the data is not conclusive as it is from one biological replicate because the second one had some staging defect. For the presented replicate experiment there was not any obvious issue with the parasite biology as even the SBP1/MARHP ring-specific endogenous control levels were 2 or more Cqs lower than the level of seryltRNA--ligase endogenous control gene. After lactate stress, its response was similar to that of 3518 (Fig. 4.18). The Cq values of its *var* genes on recovery were obtained as technical duplicates and so statistical test were not performed for the recovery data since n was less than 3.

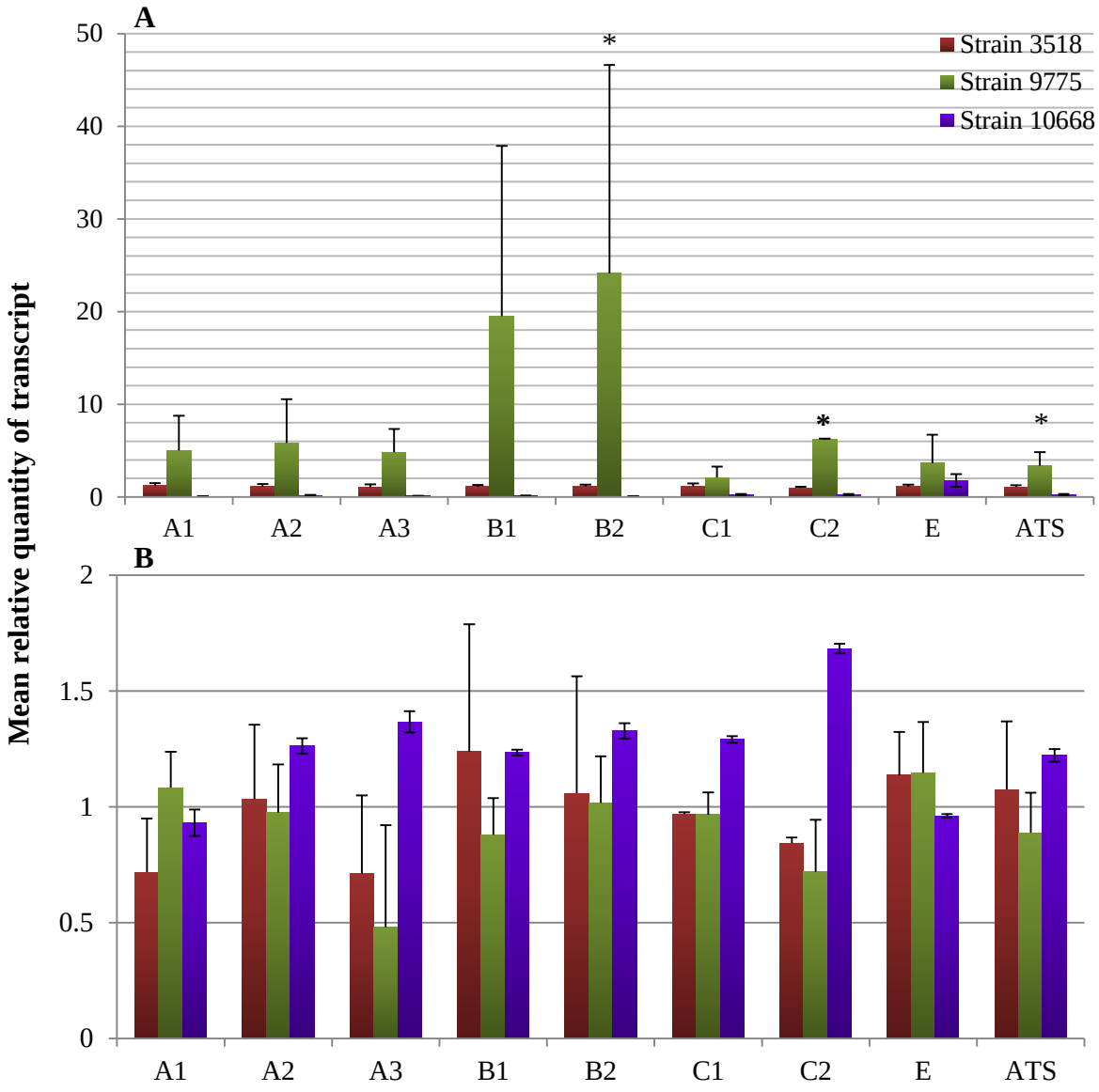

Figure 4.18: *Var gene* response of ring-staged field strains after lactate stress. Corresponding relative quantities of *var* gene group transcripts from the same parasite with sirtuin responses that are shown in Fig. 4.17, are depicted in **A.** immediately after stress and **B.** after 10 h of recovery. Mean RQ = mean of $2^{(-\Delta\Delta Cq)}$ from two biological replicate experiments (except for 10668). Error bars are SEM or CI for 10668. *p < 0.05 Kruskal-Wallis test with Dunn's post test of the relative copy number (RCN), derived from $2(^{-\Delta Cq})$, n = 6 but n = 2 for 10668.

In response to high temperature of 40°C (Fig. 4.19), 3518 rings significantly increased (2.7-fold) their expression of *Hsp70* and this remained significantly upregulated on recovery. Expression of *PfSir2A* did not change significantly at 6 h but it was significantly more after recovery (1.7-fold). Expression of *PfSir2B* showed little decrease. Strain 9775 did not respond to heat shock contrary to strain 3518. *PfSir2A*, however, was slightly increased to 1.5 fold: a similar response to that seen in 3518, but it did not reach statistical significance here. Interestingly, there was a significant decrease in *PfSir2B* expression upon stress, and a return to baseline levels upon recovery: strain 3815 showed the same trend in *PfSir2B*, which reached statistical significance here in strain 9775. In response to high temperature of 40°C, strain 10668 increased its expression of *Hsp70* (5.2-fold) which was still up, significantly after recovery. *PfSir2A* was increased significantly (1.5-fold) and was significantly downregulated upon recovery while *PfSir2B* was significantly downregulated upon stress and then slightly significantly increased upon recovery.

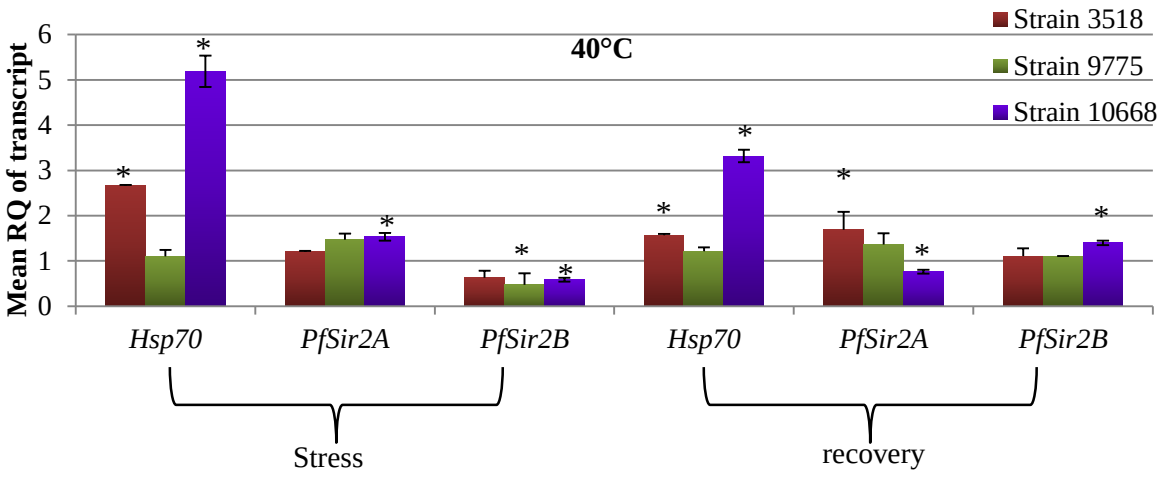

Figure 4.19: Transcriptional response of ring-staged field strains after heat shock. Relative quantity of transcripts for *Hsp70*, *Sir2A* and *Sir2B* in parasites immediately after 6h of heat shock ('stress') and after a further 10 h of recovery ('recovery'), relative to transcript quantities in a control culture. Mean RQ = mean of $2^{(-\Delta\Delta Cq)}$ from two biological replicate experiments (except for 10668). Error bars are SEM or CI for 10668. *p < 0.05 Kruskal-Wallis test with Dunn's post test of the relative copy number (RCN), derived from $2(^{-\Delta Cq})$, n = 6 but n = 3 for 10668.

For *P. falciparum* 3518 after heat shock (Fig. 4.20A), the predominant statistically significant increase was in upsA1 *var* gene group (6.6-fold increase), upsA2, A3, B1, C1 and C2 were also upregulated. However, after recovery (Fig. 4.20B), upsC2 was predominantly upregulated (12-fold), but this did not reach statistical significance. There was an accompanying increase in *var* expression globally, represented by the ATS region. The relative expression of the ATS region was increased from 1.8-fold during stress to 3.7-fold on recovery. This implies that heat shock can cause an increase in the expression of severe-disease-associated *var* genes, with a potential switch to predominantly an alternate *var* gene group after the stress was removed. For strain 9775, heat shock (Fig. 4.20A) predominantly led to more than 2-fold increase in the expression of the same *var* gene group predominantly

expressed upon lactate stress, upsB2, but this did not reach statistical significance. Recovery led to an increased expression of the total *var* ATS region with a switch to predominantly *var2csa*. After heat shock (Fig. 4.20), the total *var* levels were increased in strain 10668, with a predominant expression of *var2csa*. upsE (*var2csa*) was further increased, 5.5-fold, on recovery, but B1 and C1 were the predominant *var* group (6 & 6.2-fold) with the total *var* level increasing. However, statistical tests were not performed on these data as n for the heat shock data was less than 3.

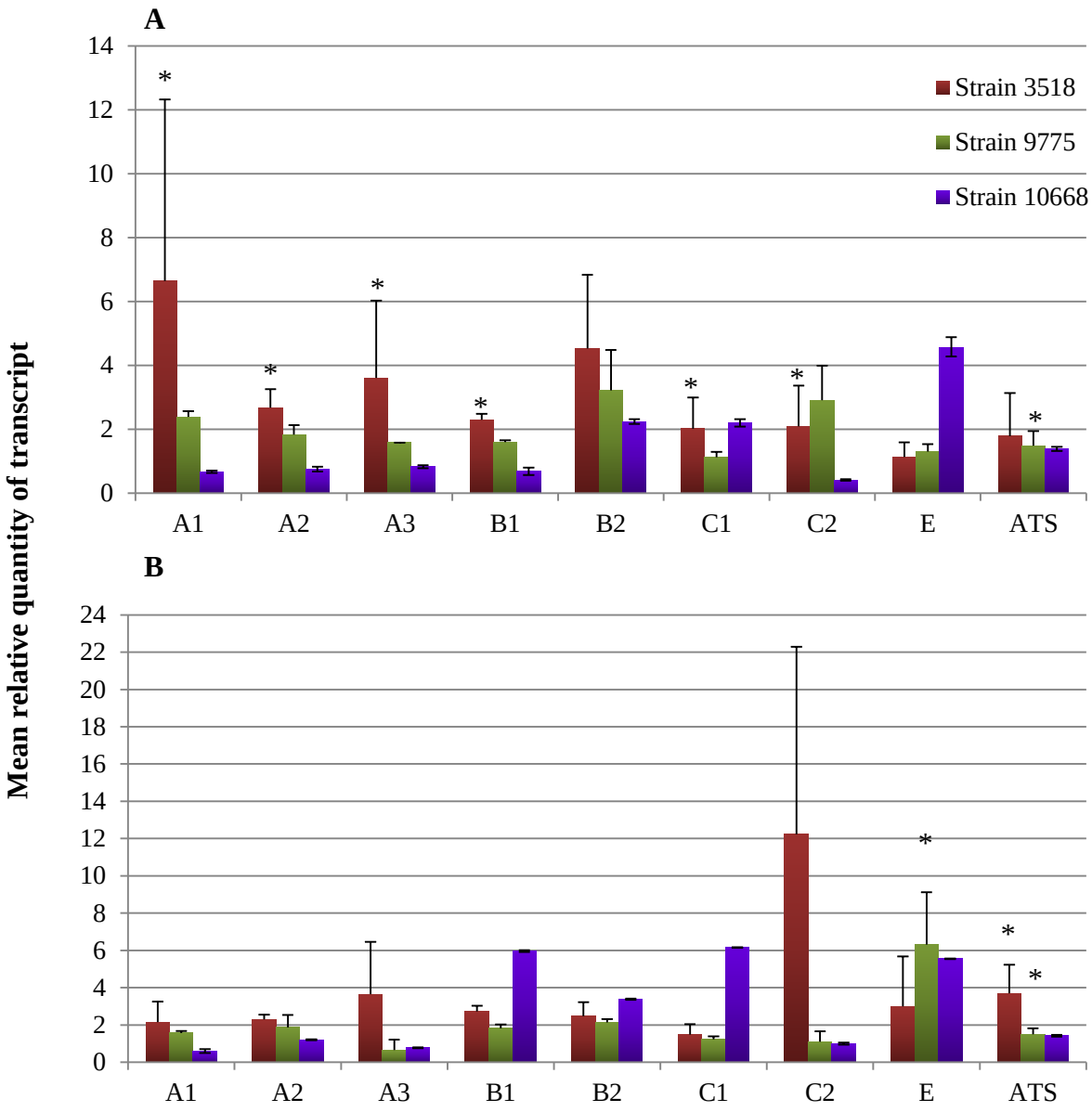

Figure 4.20: *Var* gene response of ring-staged field strains after heat shock. Corresponding relative quantities of *var* gene group transcripts from the same parasite whose sirtuin responses were shown in Fig. 4.19, are depicted in **A.** immediately after stress and **B.** after 10 h of recovery. Mean RQ = mean of $2^{(-\Delta\Delta Cq)}$ from two biological replicate experiments (except for 10668). Error bars are SEM or CI for 10668. *$p < 0.05$ Kruskal-Wallis test with Dunn's post test of the relative copy number (RCN), derived from $2(^{-\Delta Cq})$, n = 6 but n = 2 for 10668.

Exposure of strain 3518 to the combined stress led to a significant increase in the expression of *Hsp70* (2.7-fold, a level similar to that upon heat shock alone) (Fig. 4.21). *PfSir2A* was increased to the same level as after heat shock alone, with response increasing upon recovery (1.6-fold), but this did not reach statistical significance. Similar to heat shock alone, *PfSir2B* showed very little change. For 9775 the combined stress led to very similar transcriptional pattern as the heat shock alone. Exposure of strain 10668 to the combined stress led to a similar response as heat shock alone in *Hsp70* and *PfSir2B*, whereas *PfSir2A* was very slightly downregulated upon stress.

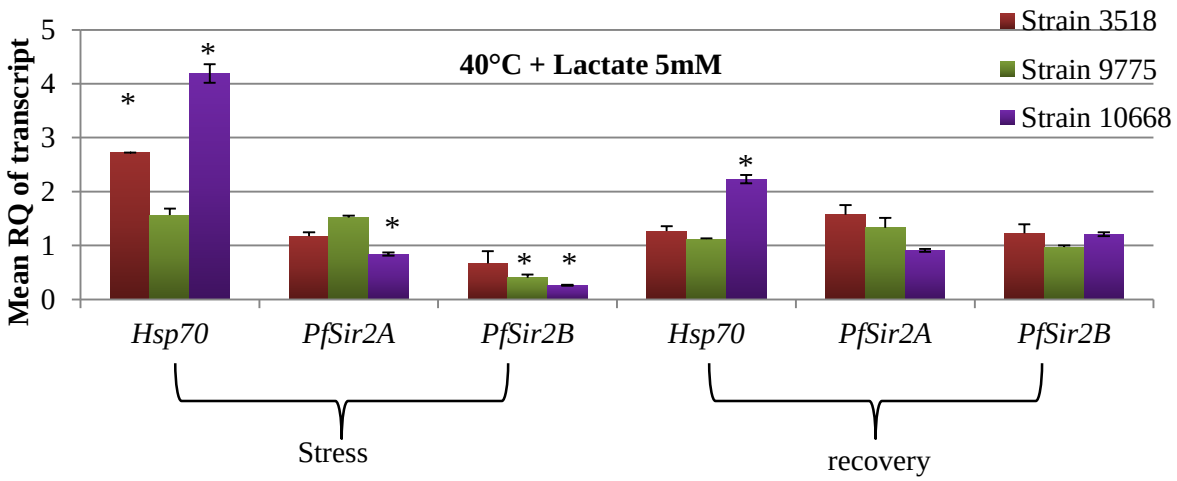

Figure 4.21: Transcriptional response of ring-staged field strains after heat shock combined with lactate stress. Relative quantity of transcripts for *Hsp70*, *Sir2A* and *Sir2B* in parasites immediately after 6h of heat shock and 5mM lactate ('stress') and after a further 10 h of recovery ('recovery'), relative to transcript quantities in a control culture. Mean RQ = mean of $2^{(-\Delta\Delta Cq)}$ from two biological replicate experiments (except for 10668). Error bars are SEM or CI for 10668. *p < 0.05 Kruskal-Wallis test with Dunn's post test of the relative copy number (RCN), derived from $2(^{-\Delta Cq})$, n = 6 but n = 3 for 10668.

The combined stress (Fig. 4.22) caused an upregulation of *var* groups A1, C1 and predominantly C2 in strain 3518. No *var* group expression was significantly altered on recovery, but there was an upregulation of total *var* expression levels (ATS) upon recovery. For strain 9775, after the combined stress was applied (Fig. 4.22), there was no significantly expressed *var* gene group. The total *var* gene level was increased on recovery. Following combined stress, strain 10668 with a similar trend as its heat shock response.

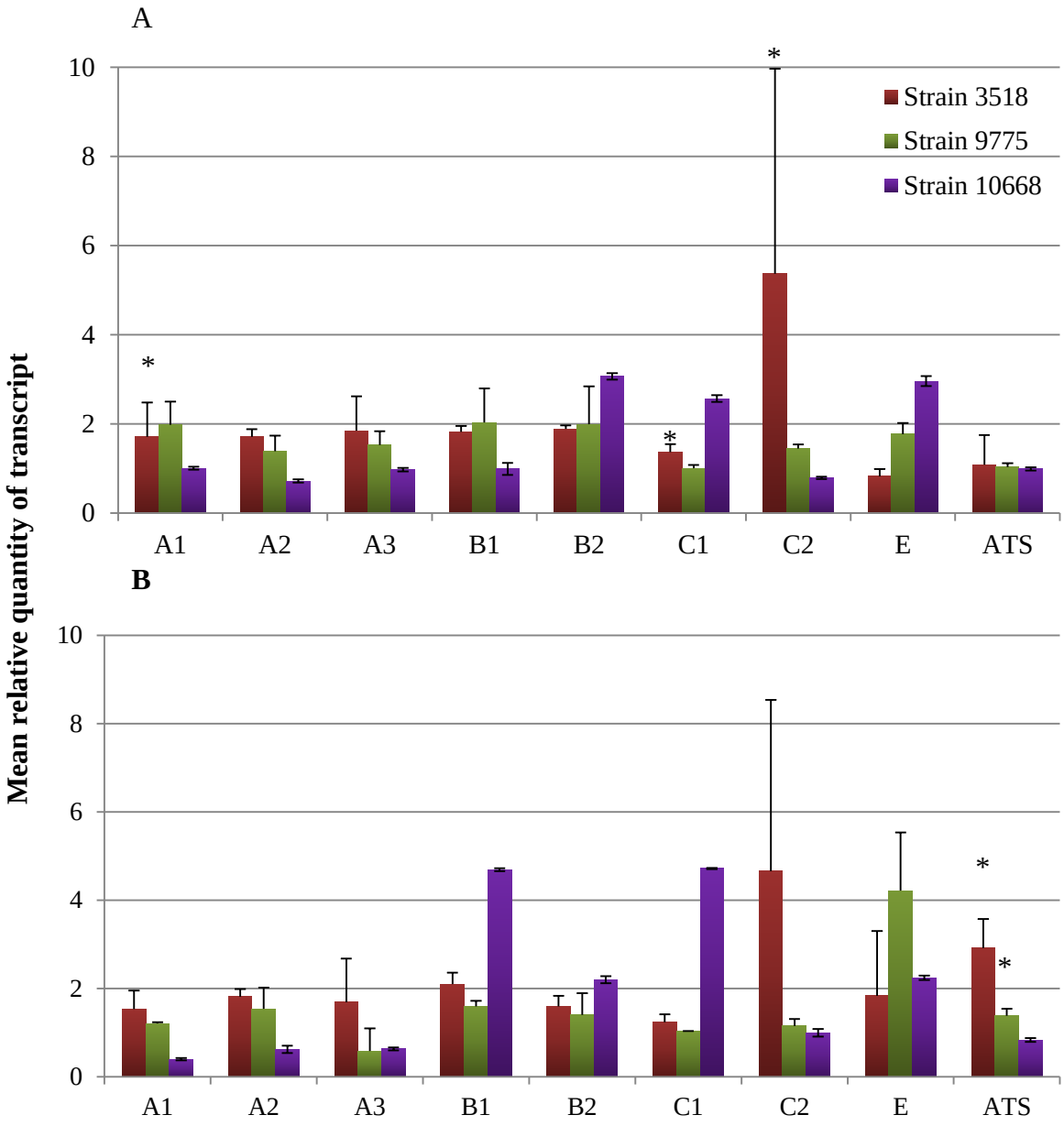

Figure 4.22: *Var gene* response of ring-staged field strains after heat shock combined with lactate stress. Corresponding relative quantities of *var* gene group transcripts from the same parasite whose sirtuin responses were shown in Fig. 4.21, are depicted in **A.** immediately after heat shock and **B.** after 10 h of recovery. Mean RQ = mean of $2^{(-\Delta\Delta Cq)}$ from two biological replicate experiments (except for 10668). Error bars are SEM or CI for 10668. *p < 0.05 Kruskal-Wallis test with Dunn's post test of the relative copy number (RCN), derived from $2(^{-\Delta Cq})$, n = 6 but n = 2 for 10668.

The pattern of expression of *PfSir2B* was overall essentially the same ($p < 0.0001$, $n = 15$) as that seen in two field strains with a consistent pattern of reproducible transcriptional change after heat shock and in combination with lactate, but never after lactate stress alone. There was a general trend for upregulation of *PfSir2A* ($p = 0.014$, $n = 15$). The rings of the field strains overall responded to heat shock by increasing their expression of *Hsp70* ($p = 0.000$, $n = 30$), both after stress and upon recovery. There was no significant difference in the response to heat shock compared to the combined stress. The level of the ATS of *var* genes was consistently increased, generally, after 10 h of recovery from heat shock or the combined stress ($p = 0.007$). This was due to the responses in strains 3518 and 9775 compared to strain 10668 ($p = 0.000$). There was an inconsistent response to lactate stress.

4.4 Discussion

This chapter investigated the changes that may occur in *P. falciparum*'s expression of the major regulators of its *var* gene expression, PfSir2A and B, upon changes in the host environment during severe malaria. Several aspects of the parasite's response to high temperature and high lactate were explored. *In vitro* cultured parasites were used in order to isolate these factors from the whole-body environment of the human host and to allow controlled manipulation of each putative stress condition. The parasites used were firstly the laboratory strain 3D7, which is very well characterized but has been in culture for many decades (potentially losing some aspects of host responsiveness), and secondly three recently-culture-adapted African strains. Two main elements were then investigated: a. transcriptional changes in sirtuin genes after stress at various cell cycle stages, and b. transcriptional changes in *var* genes after stress at the ring stage (the peak stage for expression of *var* genes).

4.4.1 Changes in the expression of *Hsp70* and the sirtuins after stress

Trophozoites of all *P. falciparum* strains responded to heat shock rapidly, as expected; with the least response from *P. falciparum* 3518 and the most response from strain 9775

based on the significant upregulation in the *Hsp70* gene that was elicited after exposure to heat shock at 40°C. Prolonged heat shock majorly led to a reduction in the heat shock response, except with 3D7, which only reached significant levels after this prolonged heat shock, Table 4.2. *Hsp70* has been shown to negatively feedback on its expression in human cells (Mosser, Duchaine et al. 1993; Rabindran, Wisniewski et al. 1994; Shi, Mosser et al. 1998). This delayed downregulation of heat shock response exhibited by *P. falciparum* 3D7 points to its inability to rapidly respond to environmental changes, possibly due to its long term culture *in vitro*. Similar increase in expression of *Hsp70* was seen after exposure to the combined stress but the magnitude was lower than was seen after heat shock alone, except in *P. falciparum* 10668. There was an interesting hint that lactate may suppress the magnitude of the heat shock response. It is unclear why this should be as 3D7 did respond to lactate by increasing its *Hsp70* expression, although to a very low magnitude. One possible explanation could be an interference of heat shock response arising from the increased influx of lactate following changes in membrane fluidity. Such changes in membrane fluidity have been shown to occur in mammalian cells (Feder, Hofmann 1999) during mild heat changes (Bromberg, Weiss 2016). However, this does not occur in all organisms (Rütgers, Muranaka et al. 2017).

Table 4.2: Summary of sirtuin responses in the strains of *P. falciparum* trophozoites

VARIABLE	RELATIVE QUANTITY OF TRANSCRIPT IN THE TROPHOZOITE STRAINS AFTER EXPOSURE TO STRESS											
	3D7			3518			9775			10668		
	1	2	3	1	2	3	1	2	3	1	2	3
Hsp70 2h	1.11	3.37	2.69	8.73	19.80	6.34	0.95	6.24*	4.79*	1.02	5.01*	5.06**
HSP70 6H	1.68	5.74**	4.23*	0.99	9.77	9.60	0.77	6.68**	4.12*	1.01	3.33*	4.17**
Sir2A 2h	1.35	2.42	2.23	0.97	0.87	4.34	1.03	1.15	1.20	1.12	1.95	2.04
SIR2A 6H	0.87	1.23	1.14	1.26	1.37	0.91	1.32	1.35	2.51	1.07	1.25	1.23
Sir2B 2h	1.41	2.26	1.85	4.99	3.42	2.03	0.95	1.65*	1.05	0.97	1.60**	1.49*
SIR2B 6h	1.17	1.98*	1.81	1.31	2.61	2.04	0.79	2.05	2.09	1.11	1.78**	1.73**

1 is lactate 5mM, 2 is 40°C heat shock, while 3 is the combined stress (lac + 40°C), *p<0.05 Kruskal-Wallis with Dunn's post test, number of asterisk show greater difference from the control culture.

Concerning the sirtuins, there was little or no change in the expression of *PfSir2A* upon lactate stress, Table 4.2. Concerning heat shock stress, only one field strain (10668) responded to heat shock by slightly increasing its expression of *PfSir2A,* a response that has been previously reported in an asynchronous parasite population of 3D7 (Oakley, Kumar et al. 2007). However, there was a general trend in most of the strains to upregulate *PfSir2A*- by 2-fold or less-when trophozoites were heat shocked but this does not reach significant levels. This relatively modest change maybe due to the level of heat shock which was higher in the Oakley et al. study; 41°C vs the 40°C used here. There was also differences in the parasite population; asynchronous vs synchronous population used here. For *PfSir2B,* overall, *P. falciparum* trophozoites responded to heat shock by increasing *PfSir2B* expression but this response was not generally sustained on prolonged stress, except for one strain. Transcript levels were reduced on prolonged stress suggesting a negative feedback regulation as occurs

for *Hsp70*. The response to the combined stress was similar to that of heat shock alone. We propose that *P. falciparum* trophozoites increase their expression of *PfSir2B* as a response to host fever, probably to maintain silencing of inactive *var* genes.

Only the rings of strain 10668 transiently increased its *Hsp70* expression in response to lactate, Table 4.3. This was equally seen for the trophozoites of 3D7. Heat shock proteins have been shown to be upregulated in non-heat shock stress but the inconsistency of this response in our data means that firm conclusions cannot be drawn. The heat shock response was minimal, as expected for this parasite stage, compared to the response by the trophozoites, (except for 10668 strains, which showed the same response as its trophozoites). The magnitude of responses was generally reduced on recovery; 10 h after heat stress was removed. Equally, response via *Hsp70* to the combined stress was lower than the response of the trophozoites and also the response to heat shock alone. This again suggests modulation of heat shock response by lactate in ring stages as well as in trophozoites. Concerning the sirtuins in ring stages, there was an overall trend to increase or decrease the expression of *PfSir2A* or *PfSir2B* after stress or on recovery.

Table 4.3: Summary of sirtuin responses in the field strains of *P. falciparum* rings

VARIABLE	RELATIVE QUANTITY OF TRANSCRIPT IN THE RINGS STRAINS AFTER EXPOSURE TO STRESS								
	3518			**9775**			**10668**		
	1	**2**	**3**	**1**	**2**	**3**	**1**	**2**	**3**
HSP70 6H	1.05	2.45*	2.51*	0.56*	1.10	1.57	2.18*	5.17*	4.18*
HSP70 R	0.97	1.57**	1.27	0.94	1.22	1.12	0.91	3.31*	2.23*
SIR2A 6H	1.02	1.12	1.08	1.03	1.47	1.52	0.29*	1.53*	0.84*
SIR2A R	1.09	1.70*	1.57	0.98	1.37	1.13	1.25	0.76*	0.91
SIR2B 6H	0.92	0.57	0.60	1.08	0.48**	0.41**	0.75*	0.59*	0.26*
SIR2B R	1.03	1.12	1.23	1.00	1.10	0.97	1.05	1.40*	1.21

1 is lactate 5mM, 2 is 40°C heat shock, 3 is the combined stress (lac + 40°C) and R is recovery. *P<0.05 Kruskal-Wallis with Dunn's post test, number of asterisk show greater difference from the control culture.

Overall, our findings point to the fact that it is possible for the parasites to respond rapidly within a short window to environmental changes by altering their sirtuin expression significantly. This response may wane on prolonged exposure, or on removal of the stress, suggesting a homeostatic feedback. Trophozoites increased their expression of *PfSir2B*. By contrast, rings decrease their *PfSir2B* expression after stress and increased their expression of *PfSir2A* after stress or on recovery.

The *Plasmodium* sirtuins have previously been shown to have a strong association with high temperature occurring in severe malaria (Merrick, Huttenhower et al. 2012, Abdi, Warimwe et al. 2016). Lactate too has been shown to have such association (Merrick, Huttenhower et al. 2012) but it can frequently occur with high temperature in severe malaria, and, it can also be consistently high and not periodic like high temperature during the course of a malaria infection. It is therefore possible that the lactate/sirtuin-expression association

that was found in human patients may be coincidental because we could not reproduce any causal association *in vivo*. On the contrary, lactate may modulate heat shock responses but this is not supported by statistical analysis. Inflammatory responses may impact sirtuin levels indirectly by causing a fever. Other host factors may also alter sirtuin expression in the parasite.

Rings were also less responsive to heat shock, as has been demonstrated previously, than the trophozoites (Kwiatkowski 1989; Thomas, Sedillo et al. 2016). This is justifiable as DNA replication begins at the trophozoite stage and thus the protein machinery needed for this stage must be protected from denaturation/degradation. It is expected that the ring-staged parasites will be more resistant to environmental changes and indeed that they may respond strategically to ensure survival. They are also less metabolically active compared to the trophozoites. The rings exposed to heat shock had a higher survival compared to trophozoites and there were strain specific differences in the parasites' survival, Table 4.4. Strain 9775 was most affected by heat shock while 3518 was the least affected. Among the trophozoite stages, strain 9775 was also the most affected, with a ~50% survival on prolonged heat shock. The length of heat shock did increase the detrimental effect of this stress upon all strains, as expected. Lactate had little or no effect on the parasites' survival, alone or in combination with heat shock. This contrasts with a previous publication showing that lactate retards parasite growth (Hikosaka, Hirai et al. 2015) but in this study the effect was only significant at or above 10mM concentration, which is markedly higher than the 5mM level used here.

Table 4.4: Summary of the survival of the *P. falciparum* stages after stress

STRAIN	STRESS	PARASITE STAGE SURVIVAL (DURATION OF EXPOSURE)		
		Trophozoite (2h)	**Trophozoite (6h)**	**Rings (6h)**
3D7	**1**	110.1	99.1	N/A
	2	94.5	84.5	N/A
	3	95.4	85.5	N/A
3518	**1**	111.7	97.9	92.5
	2	99.2	82.4	96.9
	3	101.2	78.4	86.4
9775	**1**	99.4	87.3	104.7
	2	76.9	56.6**	73.5*
	3	79.3	48.7**	74.8*
10668	**1**	96.1	94.6	101
	2	105.1	75*	62.3**
	3	98.8	68.6**	74.4

1 is lactate 5mM, 2 is 40°C heat shock, while 3 is the combined stress (lac + 40°C). Survival is as measured by SYBR Green I assessment. *P<0.05 Kruskal-Wallis with Dunn's post test, number of asterisk show greater difference from the control culture.

4.4.2 Modification of sirtuin expression in the rings may select for the expression of particular *var* gene subsets after stress

Exon 1 of *var* genes has extensive nucleotide diversity and encodes the external part of PfEMP-1 (Cockburn, Mackinnon et al. 2004). Therefore, this external part of PfEMP-1 can be varied as the parasite switches to another *var* gene in an attempt to conceal itself from recognition by the prevailing host antibodies in the human environment. In the absence of pressure from the antibodies field strains cultured, *in vitro*, for a long time, switch to chromosome central (mostly upsC type) *var* genes (Frank, Dzikowski et al. 2007). However, the field strains used in this study were recently lab-adapted and may retain their ability to switch *var* expression in response to simulated changes in the host environment.

Transcription of the active *var* involves removal of histone silencing marks, loss of PfHP1 and relocation of the active *var* away from the perinuclear repressive centres (Mok,

Ribacke et al. 2008; Duraisingh, Voss et al. 2005; Brancucci, Bertschi et al. 2014). No one has been able to show how the switch from one *var* to the other occurs, but a number of theories have been proposed, and it may be slow or fast. In this chapter, we looked to detect *var* transcription profile of an unselected population immediately after stress and after a 10 h recovery in one asexual cycle. We demonstrated a general upregulation of various *var* gene subsets as well as upregulation of the total *var* transcript quantity after stress, Table 4.5. It is possible that this enables the parasite to survive in the stress environments, mostly heat shock, by increasing PfEMP1 expression, cytoadherence, and hence protection of late-stage parasites, leading to increased growth of the population. After 10 h without heat stress, strain 9775 predominantly expressed *var2csa*.

Table 4.5: Summary of *var* responses in the strains of *P. falciparum* rings

VARIABLE	RELATIVE QUANTITY OF TRANSCRIPT IN TWO RINGS STRAINS AFTER STRESS AND ON RECOVERY 'R'											
	3518 6h			**3518 R**			**9775 6h**			**9775 R**		
	1	**2**	**3**	**1**	**2**	**3**	**1**	**2**	**3**	**1**	**2**	**3**
upsA1	1.19	7.13**	2.17*	0.72	2.17	1.55	5.02	2.39	1.98	1.08	1.56	1.21
upsA2	1.07	3.80*	2.54	1.03	2.28	1.81	5.84	1.84	1.39	0.97	1.86	1.54
upsA3	1.08	4.32**	2.38	0.69	3.35	1.58	4.83	1.58	1.53	0.48	0.65	0.59
upsB1	1.10	3.57**	2.80	1.09	2.73	2.12	19.52	1.60	2.04	0.88	1.82	1.60
upsB2	1.12	5.87	2.87	1.06	2.48	1.59	24.11*	3.21	2.00	1.02	2.13	1.41
upsC1	1.15	2.65**	1.97*	0.97	1.49	1.24	2.09	1.13	1.01	0.97	1.22	1.02
upsC2	0.95	2.35*	5.72*	0.84	12.21	4.65	6.73**	2.77	1.45	0.72	1.10	1.15
upsE	1.10	1.45	1.16	1.14	3.02	1.84	3.89	1.25	1.77	1.14	6.30*	4.22
ATS	1.08	2.045	1.30	1.07	3.69**	2.91*	3.56	1.43*	1.03	0.89	1.50*	1.39*

1 is lactate 5mM, 2 is 40°C heat shock, while 3 is the combined stress (lac + 40°C), *$p<0.05$ Kruskal-Wallis with Dunn's post test, number of asterisk show greater difference from the control culture.

There may possibly be some kind of order of switching to a different *var* from that previously activated in a previous asexual cycle and this switch may be preceded by a downregulation of *PfSir2B* or an upregulation of *PfSir2A*. Indeed, a loss of *PfSir2A* has been shown to lead to a slower switching rate for a while (Merrick, Dzikowski et al. 2010). Increased expression of *PfSir2A* correlated well with increased expression of upsB *var* in a previous study (Merrick, Huttenhower et al. 2012) but this correlation was not statistically reproduced in the one strain that predominantly upregulated its group B *var* genes. Some reasons for this may include the lack of the whole human environment which presents with other interfering factors and the possibility that lab-adapted Kenyan strains behave differently to in-patient Gambian strains. However, strain specific differences in the regulation of *var* gene expression by the sirtuins have been observed (Tonkin, Carret et al. 2009; Merrick, Jiang et al. 2015). A balance between the two sirtuins may be required to regulate the *var* genes as when the *PfSir2B* was downregulated the *PfSir2A* was upregulated in the rings immediately after stress (Table 4.3).

Furthermore, although some of the *var* genes groups elevated has equally been shown to be elevated upon stress (Oakley, Kumar et al. 2007) and are associated with severe malaria (Rottmann, Lavstsen et al. 2006; Merrick, Huttenhower et al. 2012; Kalmbach, Rottmann et al. 2010; Abdi, Fegan et al. 2014; Storm, Jespersen et al. 2019), one strain increasingly expressed upsC *var* gene group. Group C *var* gene has rarely been associated with severe malaria (Kalmbach, Rottmann et al. 2010; Abdi, Warimwe et al. 2016).

Adaptation in parasite phenotypes has been demonstrated to occur by natural selection acting upon a heterogeneous population. It is not, per se, an immediate direct transcriptional response but it requires a population of transcriptionally-heterogeneous parasites from which to select (Rovira-Graells, Gupta et al. 2012). Here, we investigated whether stress conditions can produce changes in a particular direction within that heterogeneous population. We were

able to capture an immediate transcriptional response of a majority of the population of each parasite strain, despite heterogeneous responses, with the general trend being to upregulate total *var* transcription. In relation to this study it is easy to see why transcriptional response to the applied stressors from some subset of parasite lines will vary depending on the pre-existing transcriptional state of the population, thus presenting a pattern that may not be consistent amongst biological replicates.

The ultimate biological result of increased *var* expression (predicted to be an increase in surface-expressed PfEMP1) was not measured in the study, but has been shown to correlate in some other study (Dahlbäck, Lavstsen et al. 2007). However, *P. falciparum* specific J-dots contain exported *Hsp70* and may be involved in the transport of PfEMP-1 (Külzer, Rug et al. 2010). Maybe an increased content of *Hsp70* in the heat shocked parasite lines may increase the export of more (and maybe different) expressed PfEMP-1.

It is important to note the limitations of the study presented here. Limitations include that variation in fold induction of genes between biological replicates was observed. Even more so, there was experiment-to-experiment variation in the relative copy number of the genes under study transcribed by the unstressed parasites. Indeed, variability between biological replicates does genuinely occur in some models (Willems, Leyns et al. 2008). A highly synchronous culture obtained using magnetic column isolation methods may reduce variability in future investigations (Duffy, Avery 2017). In addition, primer efficiency differing between biological replicates and primer efficiency differing for each treated sample may have affected the results, although all RTPCR assays were conducted in a consistent manner. The primer for *var* upsC2 consistently gave a low Cq, ~22, for the no-template control, even after the primer concentration was reduced corresponding to unusually high background for this primer set. The Cq of the samples were thus nearer to this and it was therefore necessary each time to verify the RTPCR product by agarose gel electrophoresis.

These findings have increased our understanding of the epigenetic process of virulence gene regulation in severe disease, however, a parasite population expressing a defined binding phenotype or specific subset of var genes will be most useful in establishing and confirming if host stress, especially heat shock, alters the expression of sirtuins and *var* genes in *P. falciparum* rings. We are a step closer to the identification of relevant factors in the asexual parasite forms that enable survival in the adverse host conditions including immune pressure and high temperature.

Chapter 5: Preliminary experiments measuring sirtuin protein activity on *P. falciparum* native histone

5.1 Overview of study

In chapter 3 transcript level and protein level were indirectly matched in the unstressed parasites throughout its life cycle using the *PfSir2A-luc* reporter line. However, due to thermal instability of the luciferase protein under heat shock we could not determine how protein levels changed under stress. In chapter 4, we showed that trophozoites of all *P. falciparum* strains used in this study significantly and consistently increased their expression of *PfSir2B* under heat shock, while rings mostly decreased their expression of *PfSir2B* and increased their expression of *PfSir2A*. However, this transcript level may or may not translate to increased/decreased enzyme activity. For *Hsp70*, mRNA and protein level were shown to be different when comparing differential changes following heat shock, with a 7.4-fold increase in mRNA level compared to 3.7-fold increase in protein level (Oakley, Kumar et al. 2007). Protein level and mRNA level may generally correlate with a discrepancy in their abundances manifesting majorly as a delay (Le Roch, Johnson et al. 2004) of about 11 h during which post-translational modifications and degradation probably occurs (Foth, Zhang et al. 2011).

P. falciparum sirtuins are class III histone deacetylase or deacylase enzymes that require NAD+ for their deacetylase activity. The 30kDa PfSir2A deacetylates H3 (9Ac, 14Ac) (Merrick, Duraisingh 2007) and also removes other acyl residues from the lysine 9 position (Zhu, Zhou et al. 2012). It also deacetylates H4 (5Ac, 16Ac). It is, however, a bifunctional enzyme, which in addition ADP-ribosylates histones, BSA and itself, with increased modification of itself in the presence of these substrates (Merrick, Duraisingh 2007). 10 years on after PfSir2B was shown to cooperate with PfSir2A in the epigenetic silencing of *var* genes, its biochemical characteristics have yet to be clearly described. It has been shown to

have a similar catalytic domain as PfSir2A, pointing to similarity it their mechanism of action. However, it has a different substrate-binding pocket suggesting that it may bind different cellular substrates than acetyl groups (Tonkin, Carret et al. 2009); and probably some other activating epigenetic marking(s). PfSir2B may undergo post translational modification (PTM) by ADP-ribosylation, as has been demonstrated for recombinant PfSir2A, and this may have an effect on its activity (Merrick, Duraisingh 2007). PTMs of either the sirtuins or their substrates may occur upon stress and this may be an adaptive mechanism (Zhang, Bhattacharya et al. 2015). For example, Leishmania Sir2RP1, has been shown to interact with hsp83, without affecting the acetylated status of this heat shock protein (Adriano, Vergnes et al. 2007). Thus it is possible that the sirtuins may interact with another protein without altering the acetylation status of the protein, suggesting a possibility of an alternative mechanism through which any perceived sirtuin-mediated effect can be achieved.

In this chapter, an attempt was made to measure sirtuin enzyme activity in stressed and unstressed parasites directly, at the protein level, rather than measuring transcriptional changes. There is no precedent for the assay done here. There is equally no commercial antibody available for detecting the presence of *P. falciparum* sirtuins. However, as in any other research, we had to move from known knowns, known unknowns and thence to unknown unknowns (Merrick, Duraisingh 2010). The approach used in this study was a considerably simpler alternative to cloning and transfecting a Nano luciferase reporter line, which might be more stable than Fluc reporter line but would require up to 6 months of work, due to the time required to genetically modify *P. falciparum*. An assay using endogenous parasite lysate as our sirtuin source from both stressed and unstressed parasites was developed and thus used to determine changes in its biochemical deacetylase activity on native histones under stress.

5.2 Methodology

5.2.1 Extraction of parasite histones

10-20 ml cultures of the 3D7 or NF54 strain at 5% parasitaemia containing mainly the trophozoite and schizont asexual parasite stage were incubated with 5mM Sodium butyrate for 2 h at 37°C. Sodium butyrate, known to inhibit histone deacetylase (HDAC) I and II classes of histone deacetylases leading to hyperacetylation. The infected red blood cells (iRBCs) were then lysed with equal volume of 0.2% saponin in 1XPBS on ice for 5 min and washed with 1XPBS. The resulting pellet was re-suspended in 1 ml ice-cold lysis buffer (20 mM HEPES pH 7.8, 10 mM KCl, 1 mM EDTA, 1 mM DTT, 0.65% Nonidet P-40, and 1 mM PMSF) and incubated on ice for 5 min. The mixture was centrifuged at 2500 g for 5 min. The supernatant, containing cytoplasmic proteins, was discarded and the pellet, containing nuclear proteins, washed twice with lysis buffer. The washed pellet was re-suspended in 1 pellet volume of extraction buffer (20 mM HEPES pH 7.8, 800 mM KCl, 1 mM EDTA, 1 mM DTT, 1 mM PMSF, 1% Complete Protease Inhibitor (PI) cocktail (Roche Applied Science, UK) and shaken vigorously at 4°C for 30 min. This mixture was subsequently spun at 13,000 g in a 1.5 ml eppendorf tube for 30 min. The supernatant, containing nuclear proteins apart from histones, was discarded. 10 pellet volumes of ice cold 0.5 M HCl was added to the resulting pellet and mixed in the eppendorf tube. The tube was incubated on ice for 1 h with frequent agitation. At the end of the hour the mixture was centrifuged at 12000 g for 2 min. The supernatant was stored in another eppendorf tube and the acid extraction repeated using the resulting pellet. All the supernatants were pooled and the contained histones were precipitated with trichloroacetic acid at a final concentration of 20% (g/100ml) of the final volume of the combined supernatants. This was incubated for 1 h on ice and then spun at 14000 rpm (top speed) for 10 min at 4°C. The supernatant was discarded and the pellet washed with ice-cold acetone after a brief incubation on ice for 15 min. The mixture was spun

at 14000 rpm for 10 min at 4°C and the precipitated histones were allowed to dry briefly for 2 min. The histones were stored at -80°C, after solubilisation in distilled deionized water containing 1% Roche's PI, or as a solid, dry precipitate.

5.2.3 SDS-PAGE and western blotting

Sodium Dodecyl Sulphate-Polyacrylamide Gel Electrophoresis (SDS-PAGE) and western blotting were done using the protocol for *P. falciparum* proteins (Cooper 2002). Briefly, SDS-PAGE reducing sample buffer (2X Laemmli buffer, Table 5.1) was made without the addition of the β-mercaptoethanol and stored. β-mercaptoethanol was added just before the 2X Lamelli buffer was used. An equal volume of 2X Lamelli buffer was added to the histone solution and the mixture was heated at 90°C for 5 min in a heating block so as to denature the histones.

Table 5.1: Composition of 2X Laemmli buffer

Component	**Amount**
0.5 M Tris-HCl pH 6.8	9.6 ml
Glycerol	10 ml
SDS	2 g
0.1 M EDTA	3.25 ml
bromophenol blue	10 mg
β-mercaptoethanol	1 ml

Samples were run on an SDS- 15% polyacrylamide gel and any unused samples were stored at -20°C for several weeks. The gel was made of SDS- 15% polyacrylamide separating gel (Table 5.2) and a top layer of stacking gel (Table 5.3). SDS- 15% polyacrylamide separating gel was prepared and cast using the sandwich-clamp assembly and electrophoresis

unit by Bio-Rad (MiniProtean II), and allowed to polymerize for 45 min. The stacking gel was then poured on the separating gel and combs inserted. This was equally allowed to polymerize for 30 - 45 min.

Table 5.2: Composition of SDS- 15% polyacrylamide separating gel

Component	**Amount**
1.5 M Tris-HCl pH 8.8	2.5 ml
H_2O	2.35 ml
30% acrylamide stock	5 ml
10% SDS	100 µL
10% ammonium persulphate	50 µL
TEMED	5 µL

Table 5.3: Composition of stacking gel

Component	**Amount**
0.5 M Tris-HCl pH 6.8	2.5 ml
H_2O	6.0 ml
30% acrylamide stock	1.2 ml
10% SDS	250 µL
10% ammonium persulphate	50 µL
TEMED	5 µL

The glass plate and gel were removed from the clamp assembly and put into the electrophoresis tank and balanced, if needed, with a dummy gel assembly. The inner chamber

of the tank surrounded by the gel assembly was filled with 1XTris-glycine electrophoresis buffer (a 10X concentration is shown in Table 5.4) first to ensure there was no leakage through the tank before filling the entire tank to the required mark. The denatured histone was loaded into well(s) and run alongside PageRuler™ Plus Pre-Stained Protein Ladder (Thermo Scientific, UK) at 200 V for ~45 min.

Table 5.4: Composition of 10XTris-glycine electrophoresis buffer

Component	**Amount**
Tris-base	30 g
Glycine	145 g
SDS	10 g
H_2O	To 1 L

Western blotting was performed using 0.45 (which worked for the protein size under investigation) and 0.2 (the correct pore size for the protein under investigation) µm nitrocellulose blotting membrane (Amersham™ Protran™ 0.2 µm NC), 1xTris-glycine transfer buffer (10X = 30 g Tris-base, 145 g glycine). The whole blot was incubated for 1 h at room temperature in 25 ml of blocking buffer (5% low-fat (1%) milk (Marvel, Premier Foods, UK), in PBS-Tween (1% Tween 20 in 1XPBS)), with gentle rocking, at the end of which blots were washed with PBS-Tween for 5 min after an initial rinsing. Then the membrane was cut into 4 strips down from the 'loaded well position' and each strip incubated with these dilutions of primary antibodies in the blocking buffer as follows: rabbit anti-H3 (Abcam, UK), 1: 5,000; rabbit anti-H4 (Abcam, UK), 1: 1,000; rabbit anti-AcH3 (Lys9,14) (CST, UK), 1: 1,000; and rabbit anti-AcH4 (Lys5,8,12,16) (Abcam, UK), 1: 20,000. Each strip was washed again in PBS-Tween and washed trice in blocking buffer. They were incubated with

secondary horseradish peroxidase-linked Goat Anti Rabbit IgG (Abcam, UK) for 45 min and subsequently washed in PBS-Tween trice for 10 min each time. Chemiluminescent detection was done using ECL (Pierce, Rockford IL, USA) for 1 min, after reassembling the strips and protein ladder. The blot was wrapped face down with saran wrap and viewed using FluorChem M (Protein Simple, USA) in the dark room.

5.2.4 Preparation of parasite lysate

A number of methods were used to prepare the parasite lysate in order to evaluate deacetylase activity of sirtuins on the parasite's hyperacetylated histones. Most sirtuins are present in the nucleus with some others present in the cytoplasm or mitochondria and can translocate to the nucleus (Religa, Waters 2012). Histidine tagged recombinant (r)PfSir2A was found to be located in the nucleus (Merrick, Duraisingh 2007), so PfSir2A is primarily located in the nucleus, but PfSir2B could be present in either the nuclear or the cytoplasmic protein fractions of the parasite. The sodium butyrate added to the parasite while preparing the histones prevents HDAC I and II activity but not HDAC III activity. The methods were;

1. A method outlined in Voss *et al.* 2002 (Voss, Mini et al. 2002). This method is similar to the method used for extracting histones described earlier except that we collected and stored the cytoplasmic fraction after parasite lysis and the nuclear fraction after extraction and then discarded the histone containing pellet. The method was done with or without DTT and EDTA while optimizing for sirtuin extraction. Both the cytoplasmic and nuclear extracts were used immediately or stored at -80°C until needed. It is possible that we discarded some sirtuin with the histone pellet as has been shown for the recombinant form of the protein. As PfSir2A has previously been suspected to be resistant to extraction with 800 mM KCl from chromatin (Merrick, Duraisingh 2007), we decided to increase our success rate by using a similar but slightly different method below that employed a reduced amount of KCl in the nuclear extraction buffer.

2. A method published in Cui *et al*. 2007 (Cui, Miao et al. 2007). This method is similar to method 1 but the HEPES, EDTA and DTT are half the concentration used in method 1 for the lysis buffer, PMSF is replaced with a 1% protease inhibitor cocktail, Nonidet P-40 is omitted, 1.5 mM $MgCl_2$ is included and 100 µl of this buffer is used. In addition, the lysate mixture is spun at 10000 g for 2 min. The method was done with or without DTT and EDTA while optimizing for sirtuin extraction. For nuclear extraction, KCl was reduced to 200mM, while DTT and EDTA were halved, PMSF was excluded, and 10% glycerol and 0.5% Nonidet P-40 were added. The mixture was vortexed at high speed (instead of grinding with a homogenizer) and centrifuged 10,000 g for 10 min at 4°C. Both the cytoplasmic and nuclear extracts were used immediately or stored at -80°C until needed. The *Fluc PfSir2A* transfected line made in chapter 3 was also included in this method and the resulting extract glowed at about 1500 RLU even after 3 h on ice, in addition to the time spent processing the parasite fractions, indicating that lysis and probably extraction worked at least for obtaining active luciferase enzyme and therefore hopefully also for obtaining sirtuin enzymes.

3. A method designed for immunoprecipitation of active protein kinases from parasite extract which unlike method 1 and 2 does not separate nuclear and cytoplasmic fractions (Ménard 2013). Briefly, after saponin lysis, equal volume of lysis buffer (25 mM Tris–HCl pH 7.5, 150 mM NaCl, 25 mM MgCl2, 5 mM NAD^+ (instead of 10 mM ATP), 0.5 mM EDTA, with or without 1% Nonidet P-40 (NP-40), 0.5% Triton X-100, 1% protease inhibitor cocktail, 1 mM PMSF) was added to the pellet and re-suspended. The mixture was incubated on ice for 30 min, sonicated for 3 s and centrifuged at 14,000 rpm for 30 min at 4°C. The lysate was used immediately or stored at -80°C until needed.

4. A method specifically designed for recovery of *P. falciparum* native proteins and active enzymes (Ménard 2013). Culture of iRBCs was washed twice with RPMI and re-suspended in 1 volume of ddH2O. It was frozen at -20°C and thawed at room temperature. 2

volumes of (2% Triton X-100, 2 M non-detergent sulfobetaine (NDSB) 201 (Merck, UK), 10 mM Tris buffer) were added. The mixture was incubated at room temperature for 30 min. The mixture was then pelleted at 14000 rpm for 30 min at 4°C. The lysate was used immediately or stored at -20°C until needed.

5. A snap freeze of parasite pellet in PBS (containing protease inhibitor cocktail) with liquid nitrogen, and then thaw at 37 °C with a heat block (freeze/thaw repeated five times).

6. Use of 1XCell Lysis buffer or Passive Lysis buffer (Promega, UK), originally used to liberate luciferase enzymes from parasites or 4% SDS in 1 M Tris HCl pH 7.5.

7. 2 M NDSB 201 was subsequently added to the nuclear extraction buffer from methods 1 and 2.

5.2.5 Measurement of HDAC III deactetylase activity of the parasite lysate

Hyperacetylated histones were treated with parasite lysate and the histone deacetylation was measured as a reduction in the density of the band from the acetylated histones. The reaction solution was made up with components (5 mM HEPES pH 7.6, 50 mM KCl, 0.05% Nonidet P-40, 1 mM Sodium Butyrate, 5% Sucrose, 0.05 mM DTT) as suggested in the literature (Tanny, Kirkpatrick et al. 2004) to which other variable components were added in a 20 µL reaction. Individual master mixes are itemized in Table 5.5.

Table 5.5: Reaction master mixes for determination of HDAC III activity

Component	**Control 1**	**Test Reaction**	**Control 2[a]**	**Control 3[b]**
Reaction solution	1.1 µl	1.1 µl	1.1 µl	1.1 µl
Histone	1* µg	1 µg	1 µg	1 µg
Parasite lysate		5 (or 10) µl	5 µl	5 µl
SAHA (2.5mM)	+	+	+	-
NAD^+ (500 or 1000 nM)	+	+	-	+
H_2O up to	20 µl	20 µl	20 µl	20 µl

Suberoylanilide hydroxamic acid (SAHA) was included in most reactions to inhibit HDAC I and II activity. [a]This was included to determine if there was any deacetylation activity due to above mentioned HDACs in the reaction mixture, despite the addition of SAHA. [b]This was included in some cases to determine if the activity of the sirtuins was inhibited by the DMSO used to dissolve SAHA, as the reaction mixture already contained sodium butyrate which together with SAHA inhibits the activity of HDAC I and II. SAHA and NAD^+ were from Sigma, UK. * 5 µg was initially used but because we had no way of quantifying our sirtuin in the lysate, we decided to maximize the activity of the sirtuin by reducing the amount of substrate to 1 µg. 5 µl of the parasite lysate was used as suggested in the method 2 of extraction but this was subsequently increased to 10 µl for longer reaction duration of 6 h to 48 h.

Nuclear or cytoplasmic extract were tested alone or in combination, and also reactions were carried out with or without NAD^+/SAHA. The reactions were incubated at 30 or 32°C for 20 min, 1 h, 3 h, 6 h, 24 h and 48 h. Components of the reactions were separated using SDS polyalycramide gel electrophoresis, blotted on nitrocellulose membrane and antibodies

were used to probe for separated proteins as described in 5.2.3. Ponceau S staining (Sigma, USA) was used to visualize total protein, by immersing the membrane in sufficient stain for 5 min, rinsing with distilled water until the background was clear and air drying. The membrane was subsequently visualized using the FluorChem M (Protein simple, USA). The pH of the various components of the reaction master mixes was also determined to rule out any intervening effect of extreme pH conditions on the stability of the sirtuins.

5.3 Results

5.3.1 Detection of H3, H4, AcH3 and AcH4

The native parasite histone 3, 4 and their acetylated versions were detected using the above mentioned antibodies and are presented in Figure 5.1. The acetylated form of the native histone is roughly of the same size because acetylation adds only an infinitesimal weight to the weight of the native histone and so the size differences cannot be resolved on the gel. H3 was about 17 KDa, H4 ~ 14KDa, AcH3 ~ 17KDa and AcH4 about 14 KDa.

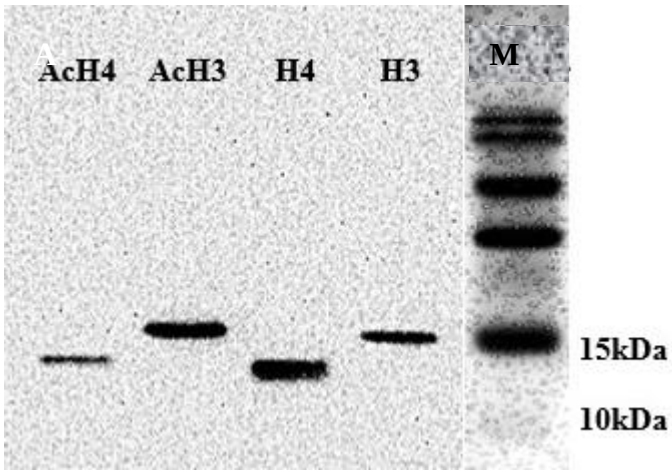

Figure 5.1: Unmodified and acetylated histones, H3 and H4in *P. falciparum*. The picture of this western blot was taken by using the Chemiluminescence protocol in the FluorChem M Protein Simple machine. Bands are acetylated histone H4 (AcH4), acetylated histone H3 (AcH3), unmodified histone H4 and H3. AcH4 is acetylated at positions 5, 8, 12 & 16 of its

lysine residue, while AcH3 is acetylated at positions 9 & 14 of its lysine residue. There is no loading control and Coomassie staining. A chemi with markers module, appendix IX a, shows that the marker lane was correctly aligned.

5.3.2 HDAC III activity of parasite lysate at different time points

Figure 5.2 (panel A-H) shows the various attempts to determine the HDAC III activity of the sirtuins (present in the parasite lysates) on hyperacetylated parasite histones AcH3Lys9, 14. This readout was chosen because recombinant PfSir2A has been shown to deacetylate H3 lysine residues more efficiently than H4 (Merrick, Duraisingh 2007). After incubations of less than 24 h, no consistent deacetylation was detected and there are several possible reasons for this. Most importantly, although rPfSir2A has been shown to work in this assay (Merrick, Duraisingh 2007) it has never been performed with total parasite extract. There may be substances interfering with the activity of sirtuins in the reaction mixture.

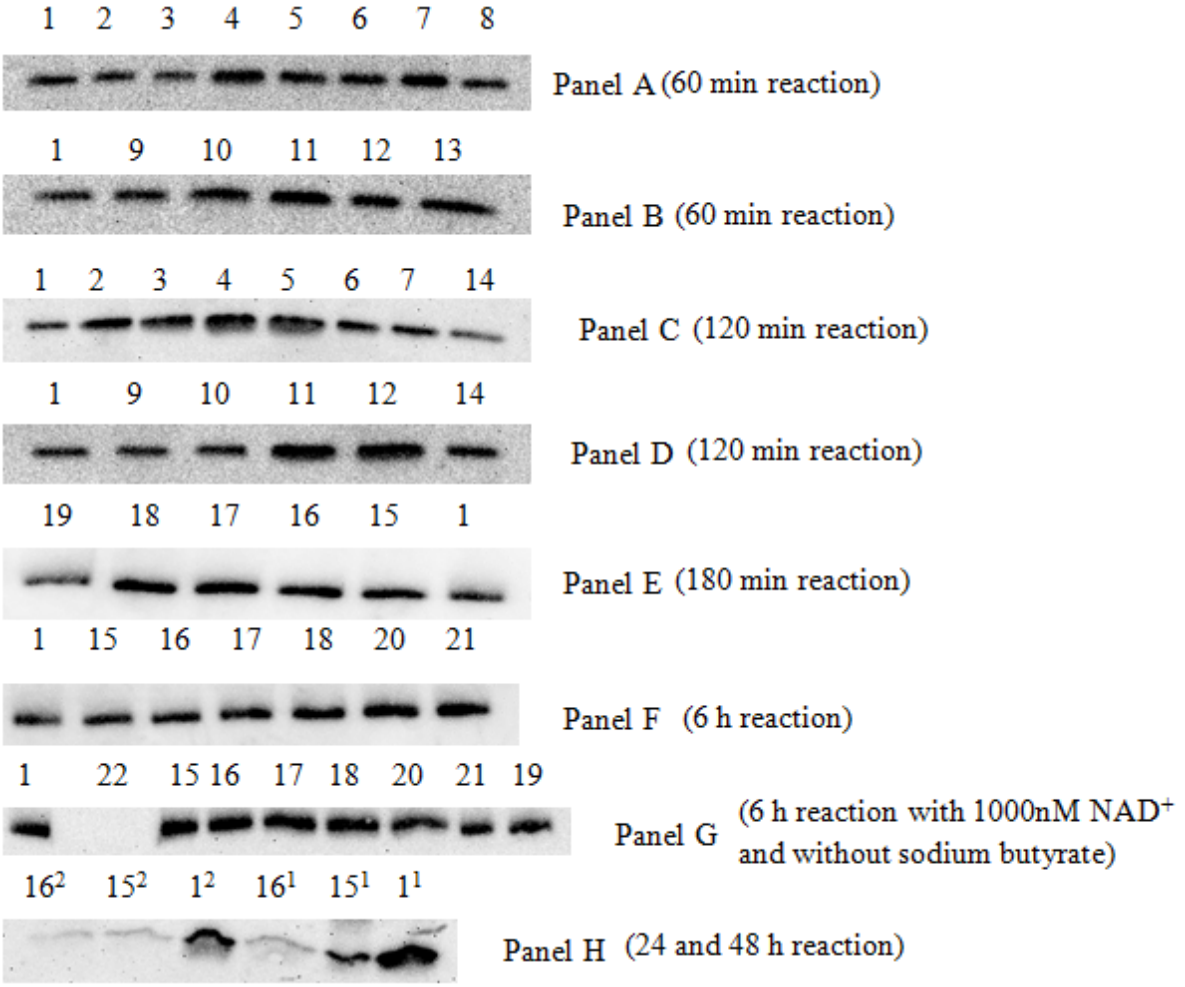

Figure 5.2: Immunoblotting of AcH3 following a reaction of *P. falciparum* lysate (possibly containing sirtuins) and their native histones, *in vitro*, at different time points. See sections 5.2.4 for the extraction methods and 5.2.5 for the composition of the test reaction and controls. Lanes interpretations are: 1 = histone alone, control 1, 2 = method 2 nuclear extract test reaction, 3 = method 2 nuclear extract control 2 reaction, 4 = method 1 nuclear extract test reaction, 5 = method 1 nuclear extract control 2 reaction, 6 = method 3 test reaction, 7 = method 3 control 2 reaction, 8 = method 1 nuclear extract control 3 reaction,, 9 = method 2 combined extract test reaction, 10 = method 2 combined extract control 2 reaction, 11 = method 1 combined extract test reaction, 12 = method 1 combined extract control 2 reaction, (continues on the next page)

13 = method 1 combined extract control 3 reaction, 14 = method 3 control 3 reaction, 15 = method 3 with NP-40 test reaction, 16 = method 3 with NP-40 control 2 reaction, 17 = method 3 without NP-40 test reaction, 18 = method 3 without NP-40 control 2 reaction, 19 = histone from a 60 min parallel experiment with method 3 extract, 20 = method 3 with NP-40 control 3 reaction, 21 = method 3 without NP-40 control 3 reaction and 22 = method 3 extract. [1]24 h reaction. [2]48 h reaction. Unaltered images are in appendix IX b.

The method 3 whole parasite lysate (Figure 5.2 panel H) appeared to deacetylate AcH3 Lys9,14, but incubation times of 24 - 48 h were required. This is much longer than was required for rPfSir2A to deacetylate AcH3, but comparable with the time required for rPfSir2A to act on synthetic substrate (Merrick, Duraisingh 2007). ≥ 24 h may be required because sirtuin expression in the parasites is low, so a more concentrated lysate and up to 24 h incubation time is needed for any meaningful NAD^+-dependent deacetylase activity to be detected using parasite lysate. It may also be that even the relatively low sirtuin amounts in cells cannot be efficiently extracted in enzymatically-active form. The incubation time may affect the histone stability, with longer incubation reducing stability, evidenced by the lower density of the 48 h band (Fig. 5.2 panel H). Also, SAHA may not be necessary as there was no difference at 48 h with or without it, suggesting minimal HDAC I/II activity, and it may even be inhibitory because of the use of DMSO to solubilize it. However, this is only a preliminary, unconfirmed finding.

Subsequently, we were able to detect the loading control H4 band following immunoblotting of reactions between extractions from method 1 and 3 containing NDSB 201. The Ponceau S-stained and chemiluminescent blots are shown below in Figure 5.3A and B. The Ponceau S-stained blot showed multiple bands as it detects total protein. On subsequent incubation with the primary/secondary antibodies the H4 loading control band was detected however it indicated uneven loading. In addition, the detection of multiple bigger bands

bigger than AcH3 may suggest that polymerization of the proteins or some kind of instability occurred on addition of NDSB 201.

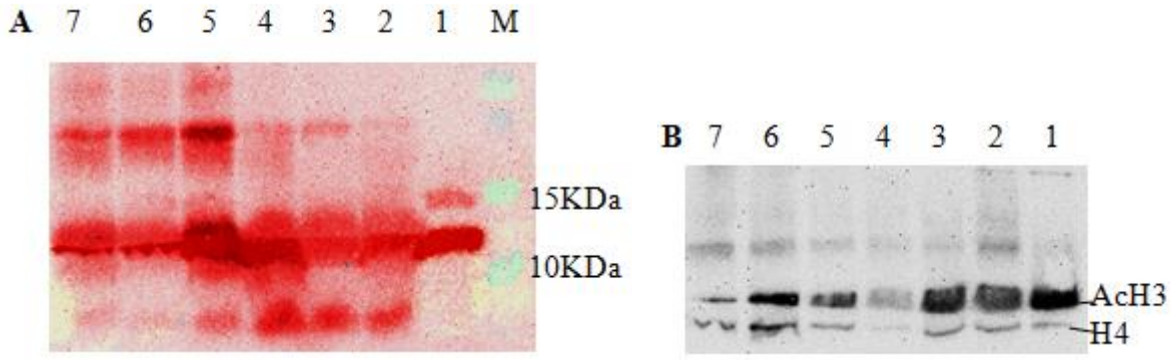

Figure 5.3: Ponceau S staining and immunoblot after the reaction of the parasite extracts from method 1 and 2 containing NDSB and histone at 24 h using in an attempt to detect H4 as loading control. A. Ponceau S staining showing total protein. **B.** Western blot showing the detection of the H4 loading control. Lanes are: 1 = histone, 2 = method 2 combined extract test reaction, 3 = method 2 combined extract control 2 reaction, 4 = method 2 combined extract control 3 reaction, 5 = method 1 nuclear combined test reaction, 6 = method 1 combined extract control 2 reaction and 7 = method 1 combined extract control 3 reaction. The proximity of the AcH3/H3 band and AcH4/H4 band may lead to the lower band being cut off during probing for this control histone H4 band.

In an attempt to investigate the presence of reaction conditions or components that are possibly interfering with the activity of the sirtuin in the reaction mixture, we measured the pH of the histone substrate solution, parasite lysate in solution following extraction with the various outlined methods, and finally, the reaction solution. After series of failed experiments, we discovered that the pH of the histone solution was in the acidic range (Table 5.6) and so we had to wash it twice after precipitation with TCA. The pH of extracts and the reaction mixture (Table 5.6) indicated that method 1 and 2 were in the best pH range needed to

preserve the activity of the possibly extracted sirtuins, while the method 3 extract was acidic and may denature the sirtuin proteins. However, the pH of the reaction solution prior to adding the individual reactants was slightly basic and should cushion any acidic effect from the slightly acidic histone extract as it also contained buffers.

Table 5.6: pH of extracts and reaction mixture used

Reaction components	**pH**
Reaction solution	7.5
Histone alone	5 (decided to wash twice with acetone)
Method 1 Lysate+ histone +NAD+ + SAHA	6.5
Method 3	5.5-6
Method 2 Cytoplasmic extract	7.0-7.5
Method 2 Nuclear extract	6.5
NDSB 201 extract	8.0

5.4 Discussion

Numerous attempts to detect sirtuin deacetylase activity using western blotting were unsuccessful due to a perceived poor activity of the sirtuins contained in the parasite lysate, if indeed they were present at all in stable quantities. In addition, we were unable to persistently probe for a loading control (i.e. total histone protein) due to the proximity of the location of the control to the acetylated histone. If time constraints had not precluded further work, it would have been necessary to strip and reprobe the blots to consistently obtain this control. Perhaps, the prior hyperacetylation of histones *in vivo* before extraction used in this assay may have altered the net acetylation status of the histones and prompted more sirtuin-mediated deacetylation *in vivo*, thus limiting the availability of substrate that can be

deacetylated *in vitro*. However, it was previously shown that histones prepared from parasites in this way could be efficiently deacetylated by rPfSir2A (Merrick, Duraisingh 2007). The numerous components of the reaction mixture may interfere with the in vitro deacetylase activity of sirtuins or reduce their mobility. A simple reaction of parasite lysate and histone with NAD^+ in a buffered solution with a protease inhibitor may have been adequate for its deacetylase activity.

PfSir2A has been shown to have weak deacetylase activity, using the recombinant protein, compared to its hydrolysis of long and medium chain fatty acyl lysine residues, with a demyristoylase activity of more than 390 magnitudes higher than its HDAC activity. The very powerful assay used in this study could not detect deacetylase activity on total parasite protein but deacylation of longer fatty acyl groups were detected (Zhu, Zhou et al. 2012). Its ability to remove fatty acyl groups was suggested to play a more relevant physiological function in the parasite. Indeed, the myristoyl group can bind to the hydrophobic pocket for acetyl groups as has been demonstrated for some other sirtuins, contributing to the entire observed biological activity, which cannot be attributed to deacetylation alone. This has been elegantly reviewed (Bheda, Jing et al. 2016). Therefore, it may be that the histone deacetylase activity of at least PfSir2A, although detectable in recombinant protein, is actually a minor component of its natural *in vivo* activity, and that extracted parasite protein is poor at deacetylating histones.

Var gene silencing does occur via the deacetylase activity of sirtuins (albeit beyond our limit of detection in these assays) but deacylation may be a more measurable activity, although the physiological relevance of this protein modification is yet to be elucidated. There is no limitation from the parasite stage used here as although PfSir2A expression is stage specific, like its mRNA expression it is abundantly expressed in the trophozoite and schizonts stages compared to its ring stage (Dhaneswar Prusty, 2008). Thus, the enzymatic

readout used here would have told us only of the endpoint of the sirtuin deacetylase activity, which may not directly correlate with protein quantity, as more of the protein may be involved in deacylation. Furthermore, it may have revealed if more of the sirtuin protein will be available for deacetylation upon stress (applied in this study).

Further research can focus on the use of histidine or GFP-tagged rPfSir2 to readily detect alterations of protein levels after stress but this will require the use of proteins that are not endogenous and so may not truly reflect the effect of such stress on the native protein expression due to exclusion of the native regulatory elements. Alternatively, the alteration of sirtuin levels after stress can be analysed by measuring the quantity of protein expressed. This can be done by using polyclonal antibodies to PfSir2, but such antibodies are not commercially available and will need to be raised in animals. There are ethical considerations for the use of animal models and such investigation will take some time. Future research should also be aimed at establishing the impact of their deacylase activity on *var* gene regulation.

Chapter 6: Host stress and gametocyte production

6.1 Overview of the study

Gametocytes produced by *P. falciparum* are a sexual differentiation developmental stage used by the parasite to ensure its continual transmission via its vector to another human host. Its life cycle Gametocyte production is an important virulence strategy, with immature gametocytes likely being less susceptible to phagocytosis than the more virulent asexual stage (Joice, Nilsson et al. 2014). Sometime, during the blood-stage asexual cycling in the host, some of the parasites develop into gametocytes through a process called gametocytogenesis. The commitment to become a gametocyte may be made just prior to schizogony, following activation of the euchromatic *pfap2-g* locus that encodes the PfAP2-G protein. Brancucci *et al*., have demonstrated that sexual commitment occurs exactly between 32 - 40 hpi (Brancucci, Bertschi et al. 2014). Alternatively, it may occur within cycle where the ring-stage is rerouted to begin PfAP2-G expression (Bancells, Llorà-Batlle et al. 2019). The protein directly activates the transcription of early gametocyte genes with its level correlating well with the level of gametocyte formation (Kafsack, Rovira-Graells et al. 2014).

Gametocytes of *P. falciparum* take 10 - 12 days to mature (Josling, Williamson et al. 2018) with the more rigid immature stages I - IV virtually absent from the blood circulation (Fig. 6.1). Like mature asexual blood stages of the parasite, immature gametocytes sequester in the spleen, brain, lungs, gut, heart and fat. However, most of them have been found to sequester in the bone marrow. These gametocytes develop from merozoites that develop in erythroid precursor cells. Older but still immature gametocytes extravasate in the bone marrow and develop until they reach stage IV (Joice, Nilsson et al. 2014; De Niz, Meibalan et al. 2018).

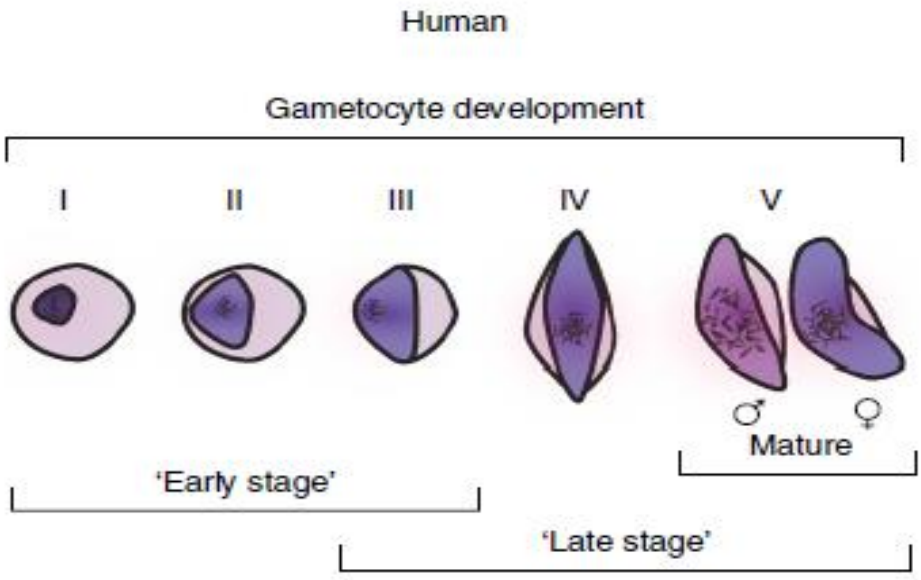

Figure 6.1: Stages of gametocyte development in humans (Delves, Straschil et al. 2016).

PfAP2-G is a member of the ApiAp2 major transcriptional regulatory proteins in *P. falciparum* (Kafsack, Rovira-Graells et al. 2014) and is bi-stably expressed. Its expression is epigenetically switched on by the eviction of *P. falciparum* Heterochromatin Protein 1 (PfHP1) from its gene locus (Brancucci, Bertschi et al. 2014) by gametocyte development 1 (GDV1) protein (Filarsky, Fraschka et al. 2018). *P. falciparum* histone deacetylase 2 (PfHDA2) also controls the low frequency of gametocytogenesis (Coleman, Skillman et al. 2014). Coincidentally, PfHP1 and PfHDA2 also participate in the silencing of *var* gene expression. It has been hypothesized that the epigenetic silencing of *pfap2-g* promotes continuous asexual cycling and antagonizes sexual conversion (Brancucci, Bertschi et al. 2014). Therefore, gametocytogenesis, like *var* gene switching, is another epigenetically-controlled process that affects parasite virulence and could potentially be regulated by epigenetic modulators that are responsive to stress in the human host.

A number of triggers for commitment have been identified and include nutrient-depleted media, presence of reticulocytes and antimalarial drugs (Josling, Williamson et al. 2018). The effect of nutrient-depleted media on gametocytogenesis was indirectly observed in a demonstration that the length of parasite exposure to a severe malaria environment led to a greater proportion of gametocyte formation (Joice, Nilsson et al. 2014). In the presence of spent media *P. falciparum* also responds transcriptionally by increasing its expression of GDV1 (Filarsky, Fraschka et al. 2018). In addition, it has been suggested that the unique environment of an immature RBC may signal an invading merozoite to begin gametocytogenesis (Gardiner, Trenholme 2015). However, only spent media has been used routinely to trigger gametocyte formation *in vitro* (Josling, Williamson et al. 2018). The exact factor(s) in nutrient-depleted media that signals gametocytogenesis remain under study. Parasite-secreted extracellular vesicles in spent media can increase gametocytogenesis but are not essential for the formation of gametocytes (Brancucci, Gerdt et al. 2017). A depleted lysophosphatidylcholine (LysoPC), as demonstrated in nutrient-depleted conditioned media has been shown to enhance gametocytogenesis *in vitro* in a dose dependent manner, by acting upstream of *ap2-g* activation and changing the metabolic status of *P. falciparum* (Brancucci, Gerdt et al. 2017; Josling, Williamson et al. 2018).

We hypothesize that *P. falciparum* may also respond to high lactate and/or heat shock host stress factors by modulating gametocytogenesis directly or indirectly. Gametocyte formation commitment can be triggered in the face of increasingly adverse host physiological conditions. As it is a virulence survival strategy, the goal maybe to evade the harsh environment experienced by the asexual form of the parasite, due to heat shock and lactic acidosis.

6.2 Methodology

6.2.1 Culturing of parasites and gametocyte induction

Parasite strains used were the laboratory strain, NF54, and the three patient field strains; 3518, 9775 and 10668; of *P. falciparum*. They were cultured as described earlier in section 2.1 prior to induction of gametocytogenesis. The method for induction of gametocytogenesis was as described by (Delves, Straschil et al. 2016) for production of functionally viable gametocytes synonymous with the stochastic low frequency gametocytogenesis that occurs in nature. However, a mixture of Albumax II and serum rather than serum alone was used to induce gametocytogenesis, and the serum was not filtered through a 0.2 µm filter unit, it was just heat inactivated. Seed cultures at different percentages of ring-stage parasitaemia and at 4% (vol/vol) haematocrit (HC; day 0) were used in this study. Other asexual parasite stages were present in the seed cultures although these do not substantially affect the resultant yield of mature gametocytes. The medium was replaced daily for 14 subsequent days without the addition of fresh erythrocytes. Asexual parasitaemia increased between days 1 and 4 after culture induction to a peak. Stress, thought to be naturally produced by the high parasitaemia, induces gametocyte formation (Chaubey, Grover et al. 2014). Early-stage gametocytes were observed on day 7. By day 8, gametocytes were beginning to elongate, and by day 14 morphologically distinguishable, mature stage V gametocytes were present. During the period of gametocyte induction, the temperature of the parasite culture was not allowed to fall below ~37°C during media changes and making of blood smears. Parasitaemia was determined as described in 2.1, while gametocytemia was determined using a similar method.

6.2.2 Gametocyte induction and stress treatment

In a second experiment we investigated how stress factors high temperature and high lactate for 6 h can perturb the basal level of gametocytogenesis in *P. falciparum* 3518, the only field strain that produced gametocytes in this study.

6.3 Results

6.3.1 Induction of gametocyte production in *P. falciparum* field strains

Preliminary experiments showed that the NF54 control line was able to produce gametocytes easily at 3.1% parasitaemia with 50% rings. The D-shaped form seen on day 7 and elongation beginning on day 8. Gametocytogenesis was complete on day 14. However, parallel experiments with the field strains failed to produce gametocytes at this parasitaemia and for this length of time: they were equally able to reach very high parasitaemia before growth arrest, but with no gametocyte formation.

After several trials, a parasitaemia of 6% with 50% rings were used to induce gametocyte formation in all strains in parallel. *P. falciparum* 3518 was the only field isolate that produced gametocytes, Figure 6.2 B and its stage V gametocytaemia was lower than that of the control, NF54, as shown in Figure 6.2 C.

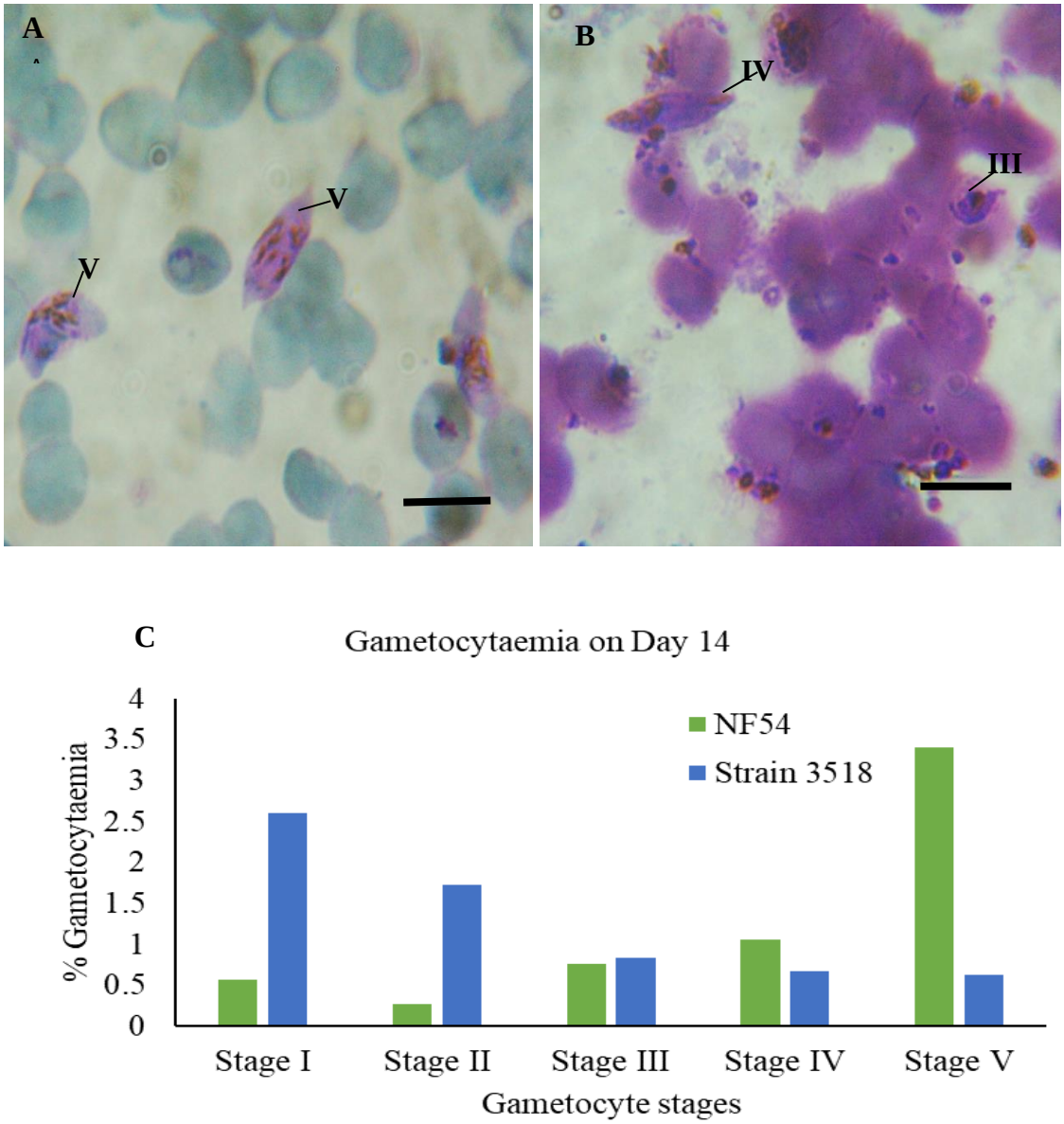

Figure 6.2: Day 14 of induction of gametocytogenesis in *P. falciparum* strains. A. Strain NF54 at 1000 x magnification, with mostly stage V gametocytes seen. Black scale bar is 10.3 µm. **B.** Strain 3518 is at 1000 x magnification and has less gametocyte than NF54 and they appear to be younger (stages III (5 µm) and IV (10.7 µm) mostly seen) than those of NF54. Black scale bar indicates the sizes. **C.** Gametocytaemia by stages of strain 3518 and NF54 laboratory strain. Gametocyte count is against up to 3000 erythrocytes and is from a single count of one biological replicate experiment.

6.3.2 Changes in gametocytaemia of *P. falciparum* 3518 after stress treatment

P. falciparum 3518 was subjected to high lactate 5 mM or heat shock at 40°C alone and in combination. The percentage gametocytemia was determined in two biological replicate experiments as shown in Figure 6.3. The starting parasitaemia was 2.1% rings in 4.2% blood stages for the first biological replicate and 2.4% rings in 2.8% blood stages for the second parasitaemia. The decision to use a lower parasitaemia from the high cap used to induce gametocytemia was made to prevent the parasite from being stressed at all prior to exposure to the host's stress factors. However, we could not get the parasitaemia of the biological duplicate to be very similar. Different percentage gametocytemia (representing mainly stages III to V) was observed between biological replicates, with a lower percentage for the second replicate likely due to a lower proportion of older blood stage (0.4% of older stages in the second replicate vs 2.1% of older stages in the first replicate) asexual forms impacting the magnitude of nutrient turnover and waste production in the culture media. In addition, the two replicate experiments were not done in parallel and so they were both cultured with a different batch of serum. The serum may also have an effect on the ability of the second biological replicate to produce gametocyte, as far less gametocytes were produced even in the control experiment. Thus the results from both biological replicates were presented separately.

Exposure to stress caused a decrease in gametocyte production, Fig. 6.3, but, since there would be a decrease in parasitaemia after the stress, this could have an effect on the gametocytaemia. From chapter 4 we could assume that the stress can lead to up to 50% reduction in survival, thus accounting for a proportional decrease in gametocytaemia. However, this does not account for the more than 90% reduction in gametocytaemia. For the second biological replicate there is little change in gametocytaemia with about 30% reduction after exposure to the combined stress.

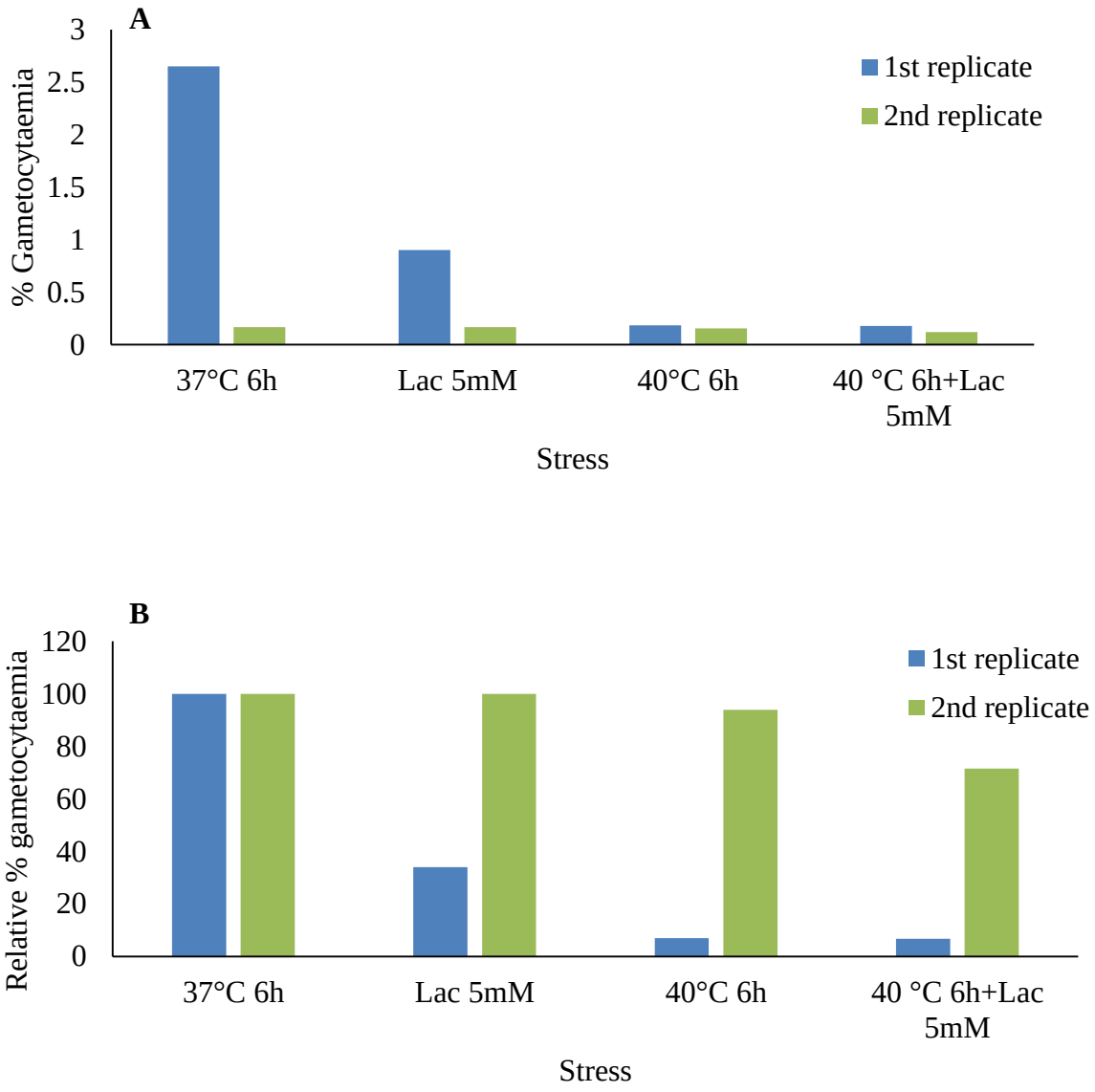

Figure 6.3: Differing impact of high temperature 40°C and/or high lactate on the ability of *P. falciparum* 3518 to produce gametocytes. Gametocytaemia (**A**) differs for the 2 independent biological replicate experiments. Gametocytaemia was evaluated by single count against up to 1000 erythrocytes in a thin smear. The relative percentage gametocytaemia (**B**) were calculated relative to the control for each biological replicate experiment.

6.4 Discussion

It is common for laboratory parasite isolates to lose their ability to make gametocytes. 3D7, for example, is a poor gametocyte producer. Field strains have also been shown to lose their ability to make gametocytes on prolonged *in vitro* culturing (Ponnudurai, Meuwissen et al. 1982). There are also *P. falciparum* strains that do not produce gametocytes at all. Naturally occurring non-gametocyte producers, F12 line and GNP-A4, which have lost their ability to produce gametocytes, both have mutations in their *pfap2-g*; with a stop codon upstream of or within the AP2 DNA-binding domain. However, mutations occurring in the coding region do not lead to encoding a defective AP2-G. Laboratory deletions of the *ap2-g* gene led to no gametocyte production and such resulting strains usually replicate asexually at a higher magnitude that the parent gametocyte producer (Kafsack, Rovira-Graells et al. 2014). Therefore, it is possible that *P. falciparum* 9775 and 10668 strains have lost their ability to produce gametocyte or are non-gametocyte producers. On the other hand, the ability to produce gametocytes has been shown to differ among parasite strains and with their environment. An optimized induction method for high through-put assays has been described previously by Brancucci *et al*. 2015, where condition media (spent media from a high parasitaemic culture) was added to fresh parasite cultures at 28 hpi for 24 h, and then assayed after 38 h to determine early gametocytogenesis (Brancucci, Goldowitz et al. 2015). However, the research targeted early gametocyte production and so there was no regimen for addition of the conditioned media (CM) up to stage V maturation. 3518 and NF54 did produce gametocytes, and exposure to the stresses under study had a negative impact on the ability of 3518 to produce gametocytes. The degree of this effect was however not reproducible but there was a general trend of reduced gametocytaemia especially on exposure to heat shock and/or lactate stress.

The effect of heat shock and high lactate levels on gametocytogenesis *in vitro* cannot, however, be directly linked to what happens *in vivo* during severe malaria as the parasite is repeatedly exposed to heat shock and may be exposed to high lactate for a prolonged time. The decreased gametocytogenesis can partially be ascribed to the reduced turnover of nutrients and waste product in the media due to the stress heat shock killing off the older blood stage forms more rapidly than occurred in the control. This was evident in the second biological replicate experiment, leading to little difference in relative gametocytaemia as there were fewer older parasite blood forms compared to the first replicate. It is also important to note that *in vivo*, gametocytes hide out mainly in the bone marrow where they may be exposed to different environmental niches from the general circulation. Therefore, other host factors apart from those under study may have an effect on gametocyte production.

Additionally, the heat shock temperature used here may be too subtle, or the length of exposure too short, to induce any reproducible change in gametocytogenesis. Repeated heat shock maybe needed. *P. falciparum* has been shown to be resistant to heat shock-induced death on repeated exposure, thus the residual resistant population may be more informative in deciphering the effect of heat shock on gametocytogenesis. This eliminates the survival bias.

Furthermore, a more striking effect would have been observed if conditioned media was used instead of the normal culture media for daily media changes (Brancucci, Goldowitz et al. 2015). Nevertheless, overall, this chapter cannot draw reliable conclusions about the effect of high temperature and high lactate upon gametocytogenesis: a topic that still merits further study. It may be necessary to investigate and understand the effect of parasite survival after stress and different serum batches on gametocytaemia before reliable experiments can be designed. It is certainly necessary to maintain a similar ratio of rings to other older parasite asexual stages, a 1:1 may be optimal. In a more complex experiment where cultures are stimulated to convert to gametocyte after repeated stress exposures, a design more analogous

to the conditions that may be experienced in human malaria patients, the true effect of host stress on gametocytaemia may be revealed.

Chapter 7: Effect of physiological and non-physiological concentration of lactate on parasite survival

7.1 Overview of the study

Respiratory distress is one of the few severe malaria syndromes that highly predict a negative prognosis for severe malaria (Sypniewska, Duda et al. 2017). It is a clinical manifestation of metabolic acidosis, which is principally caused by deficit in the consumption of protons by the mitochondrial metabolism, tricarboxylic acid cycle. These protons are released following ATP hydrolysis to ADP with concomitant energy release (Fig. 7.1). Some protons are consumed when lactate is produced from pyruvate in a reaction catalysed by lactate dehydrogenase during glycolysis. Thus, lactate production helps to prevent acidosis and regenerate NAD^+ for phase 2 of glycolysis. Hyperlactatemia has, coincidentally, been implicated in metabolic acidosis but has been demonstrated to be an indirect indicator of metabolic acidosis (extensively reviewed in Robergs, Ghiasvand et al. 2004). Nevertheless, it has a high prognostic value for severe malaria in children and adults but it occurs more in children (Krishna, Waller et al. 1994; World Health Organization 2014; Dabadghao, Singh et al. 2015), with lactate level dropping a little or increasing in children who eventually die despite medical interventions (Krishna, Waller et al. 1994). Lactatemia could be mild (> 1.5 mM), moderate (> 3 mM) or severe (> 5 mM). Hyperlactatemia in severe malaria is defined as ≥ 5 mM (Severe Malaria. 2014). Its occurrence as well as a reduced pH of < 7.35 is defined as metabolic acidosis.

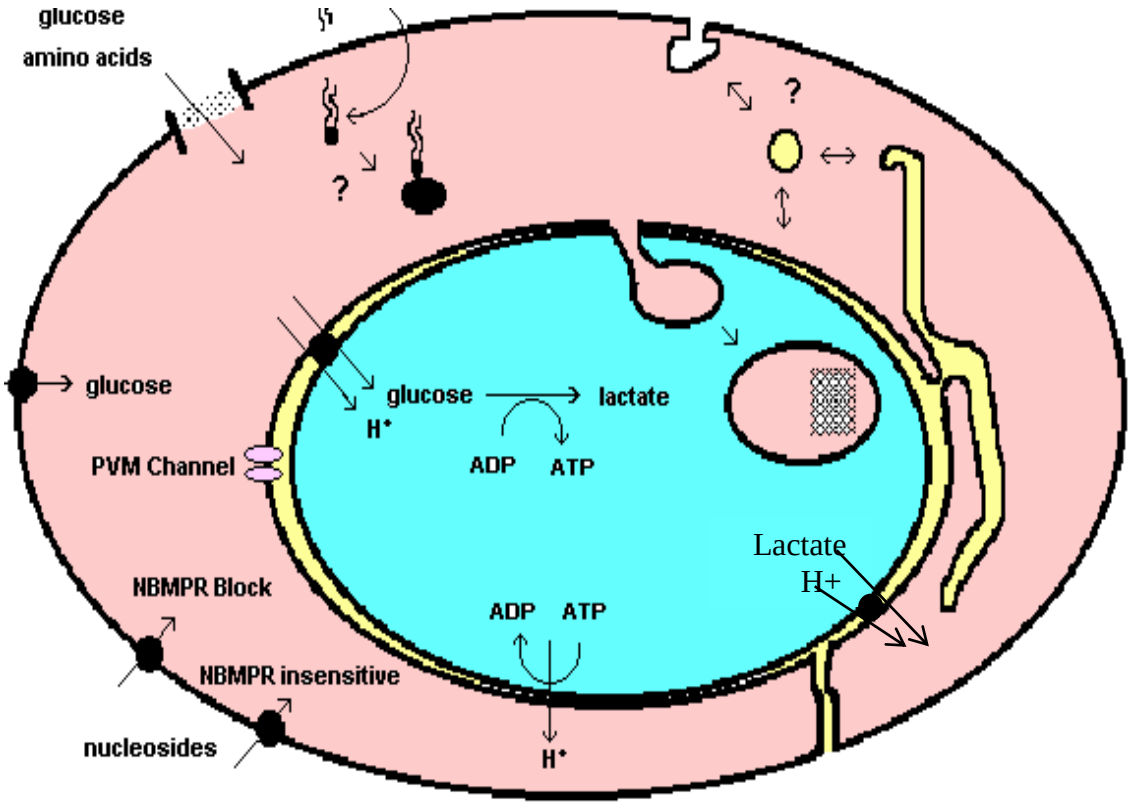

Figure 7.1: Metabolism of *P. falciparum* in a red blood cell (Wiser 1999). The diagram is from the Wiser 1999 but the efflux of lactate and H^+ through a symporter was an added modification for the purpose of this introduction.

During the IDC, *P. falciparum* undergoes intensive anaerobic metabolism. It uses large amounts of glucose to produce energy with concomitant release of large amounts of lactate and H^+ ions as by-products. These cross its membranes into the parasitophorous vacuole (PV) via a H^+/lactate symporter (Elliott, Fau et al. 2001), a saturable monocarboxylate transporter (MCT) (Wu, Rambow et al. 2015; Marchetti, Lehane et al. 2015). PfFNT is an MCT that is now a target of antiplasmodial compounds (Hapuarachchi, Cobbold et al. 2017). This helps the parasite to prevent cytotoxic accumulation of lactate and a detrimental drop in its pH by actively removing H^+ ions together with lactate; thus maintaining osmotic pressure and redox status, and preventing pH-induced denaturation of the protein machinery network of the parasite (Elliott, Fau et al. 2001). The lactate then exits the

PV through its porous membrane and enters the cytosol of the iRBC. It exits this cytosol via normal channels or new parasite-induced channels in the iRBC membranes (Desai, Krogstad et al. 1993; Kirk, Horner et al. 1994; Ginsburg, Stein 2004). There is also influx of L-lactate in a similar way as efflux depending on the pH gradient (Cranmer, Fau et al. 1995).

P. falciparum principally produces L-lactate rather than D-lactate (Vander Jagt, Hunsaker et al. 1990). Contribution of the parasite to the overall lactate blood level may be small because in addition to the lactate produced by the parasite, the skeletal muscle and the kidney produces L-lactate in severe malaria, due to a shift towards glycolysis. This shift arises from the reduction of oxygen reaching various tissues, arising from an occluded microvasculature. A compromised microcirculation occurs as a result of sequestered iRBCs containing mature forms of the parasite. Partially rigid iRBC/RBC may not be able to squeeze through the partially occluded venules (Ishioka, Ghose et al. 2016). Lactate levels are associated with parasite burden in severe malaria and may lead to respiratory distress syndrome. However, other factors that may contribute to increased blood lactate include induction of inflammatory responses (Casals-Pascual, Kai et al. 2006) and anaemia (English, Sauerwein et al. 1997), which maybe a mere association considering that the normal RBC produces ATP only through glycolysis.

The iRBC has been shown to produce from 5 to > 100x more lactate than the uninfected RBC with a drastic increase after a medium change, indicating an efflux down the concentration gradient (Jensen, Conley et al. 1983; Zolg, Macleod et al. 1984). The transport of lactate is also H^+ ions (pH) dependent (Cranmer, FAU et al. 1995). However, *P. falciparum* has been shown to survive best at a pH between 7.2 and 7.45 and a lactate level below 12 mM (Jensen, Conley et al. 1983). Lactate or lactic acid have been shown to have an inhibitory effect on parasite growth due to accumulation (Pfaller, Krogstad et al. 1982; Zolg, Macleod et al. 1984), or supplementation, significantly at levels > 10 mM (Hikosaka, Hirai et al. 2015).

Lactate concentration below 12 mM has been found to be optimal for the growth of *P. falciparum*, with daily media change required (Jensen, Conley et al. 1983) or twice daily (Zolg, Macleod et al. 1984) in order to maintain the level of lactate below this level during *in vitro* culture.

We thus investigated the effect of supplemental high lactate levels using *in vitro* static culture, and also the effect of non-physiologically-attainable lactate concentrations of up to 60 mM on parasite survival at normal host body temperature (37°C) and in the presence of heat shock (40°C), in this chapter. This was a follow up on chapter 4, which sought to establish whether there is a causal relationship between high blood lactate and high expression of sirtuins and *var* genes, shown to be associated in the severe malaria disease (Merrick, Huttenhower et al. 2012). High blood lactate is a reflection of parasite burden and a worsening pathology. The investigations here were equally a follow up on the reduced crashing of parasite culture, confirmed by microscopy, after exposure to 5 mM lactate alone or with heat shock, compared to the control and heat shock alone. This was observed in the two luciferase transfected *P. falciparum* lines in chapter 3 under two different promoters.

7.2 Methodology

7.2.1 Malaria SYBR-Green-1 Fluorescence (MSF) growth assay

Synchronous seed cultures of trophozoite-staged *P. falciparum* 3D7 (at 1, 0.7 and 0.1% parasitaemia) were exposed to varying concentrations of sodium L-lactate and growth was monitored over time using the Malaria SYBR-Green-1 Fluorescence (MSF) protocol as earlier described (Smilkstein, Sriwilaijaroen et al. 2004). Here, 100 µl of incomplete media was added to the edge wells to prevent evaporation of the culture medium in the testing wells. 200 µl complete media was added in the first triplicate well containing 2x the highest concentration of lactate to be used in the assay. 100 µl complete media was added to other

testing wells. Two-fold dilutions were done by transferring 100 µl from well to well, starting from the first testing well, and discarding the last bit. 100 µl of iRBCs at 4% haematocrit were added in the testing wells except the negative control. A chloroquine control (0% growth) containing a supra-lethal dose of chloroquine (1-2 mM (i.e. ~50x EC50) was included and also contained iRBCs. A positive control (100% growth) without added lactate or drug was included. The plate wells were incubated for 48 h or up to 144 h. A 1:5000 dilution of SYBR Green-1 in MSF lysis buffer (20 mM Tris pH 7.5, 5mM EDTA, 0.008% wt/v saponin and 0.08% v/v Triton X-100) was made, and 100 µl of this was transferred to a black Corning 96 – well plate. 100 µl of the content of each well in the cultured plate was then mixed well with the diluted SYBR Green solution. The black plate was incubated in the dark for 1 h at room temperature, after which the fluorescence signal was measured using a plate reader at Excitation (Ex) Wavelength (λ) of 485 nm and Emission (Em) Wavelength (λ) of 528 nm, for the Tecan Infinite 200 Pro plate reader (Tecan, Switzerland), and Ex λ of 490 nm and Em λ of 510-570 nm for the Glomax-Multi Detection System (Promega, UK). Percentage parasite growth was determined as follows: $\frac{(f-cb)}{pc-cb}\ x\ 100$, where *f* is the mean fluorescence from the testing wells, *cb* is the mean fluorescence from the chloroquine control and *pc* is the mean fluorescence from the positive control.

7.2.2 Determination of schizogony

In other to determine any possible mechanism of lactate induced alteration of parasite growth an investigation of the effect of lactate on schizogony was conducted. Here, a seed culture of early to mid-trophozoite staged *P. falciparum* 3D7 was exposed to either 5mM lactate for 16 h or no lactate supplementation and then the number of merozoites, rings and total number of schizonts were determined by counting the number of merozoites in mature schizonts in a thin blood smear using microscopy, section 2.1.

7.2.3 Determination of lactate mediated protection from heat shock and death due to waste accumulation and nutrient depletion

Experiments were also conducted by culturing the parasites under heat shock conditions, with or without lactate supplementation in the culture media, in order to assess changes in growth or increased survival attributable to potential lactate protection as observed in *P. falciparum* luciferase transgenic lines cloned in Chapter 3 and wild-type parasites in Chapter 4. Here, two ring-staged *P. falciparum* strains (NF54 and 3D7) at 0.5 % parasitaemia were exposed to heat shock at 40°C, with or without lactate at 5mM concentration for 6 h. A control with no treatment was also included. Afterwards, the treated cultures were left to complete another round of reinvasion and growth assessment was carried out by SYBR Green 1-based fluorescence method, Section 7.2.1.

A second experiment was carried out to assess the possible lactate-mediated protection of parasite from death due to nutrient depletion and waste accumulation. Here, trophozoite-staged *P. falciparum* 3D7 at 0.8 % parasitaemia were exposed to lactate at 5 and 10mM for 6 h or continually. Two controls that were not exposed to the lactate were also included, one for the 6 h duration of exposure and another for the continual exposure. The culture media was completely changed for the cultures that were to be exposed for 6 h only including the control. All cultures where left to grow until there was evidence of death in the control (at 96 h) due to over growth of the cultures. Growth of each treatment was assessed at 24, 48 and 96 h using the SYBR Green 1-based fluorescence method, Section 2.4.

7.2.4 Graphical presentation and statistical analysis

Percentage parasite growth from technical or biological replicate were averaged and represented on an XY graph with a connecting line joining all data points as it was unsuitable to use any specific fitting including the semi-log line and the log[inhibitor] vs. response fit. Raw fluorescence values were used to determine statistical significance. Normal distribution

was determined using Anderson darling, after which data that were normally distributed were analysed using 2-Sample T-test or ANOVA, while non-normal data were analysed using Mann-Whitney Test

7.3 Results

7.3.1 Effect of different lactate concentrations on one cycle of growth of *P. falciparum* 3D7

Following the observation of a subtle growth increase of parasites exposed to lactate briefly for 2 or 6 h in Chapter 3 or 4, we decided to investigate if this effect was real. To this end, 1% starting culture of *P. falciparum* 3D7 was exposed to varying concentrations of L-lactate continually for 48 h in the culture media used routinely to grow this parasite. There was indeed a slight growth increase of about 7% at 0.47 mM lactate concentration (Fig. 7.2). There was no significant growth change at lactate concentrations up to 7.5 mM (log 0.875061). However, concentration above 7.5 mM led to a significant growth inhibition. Here, the parasite was continually exposed without any media change to remove the lactate produced by the parasite during the 48 h incubation. About 90% of the parasites died after a 48 h exposure to 60 mM.

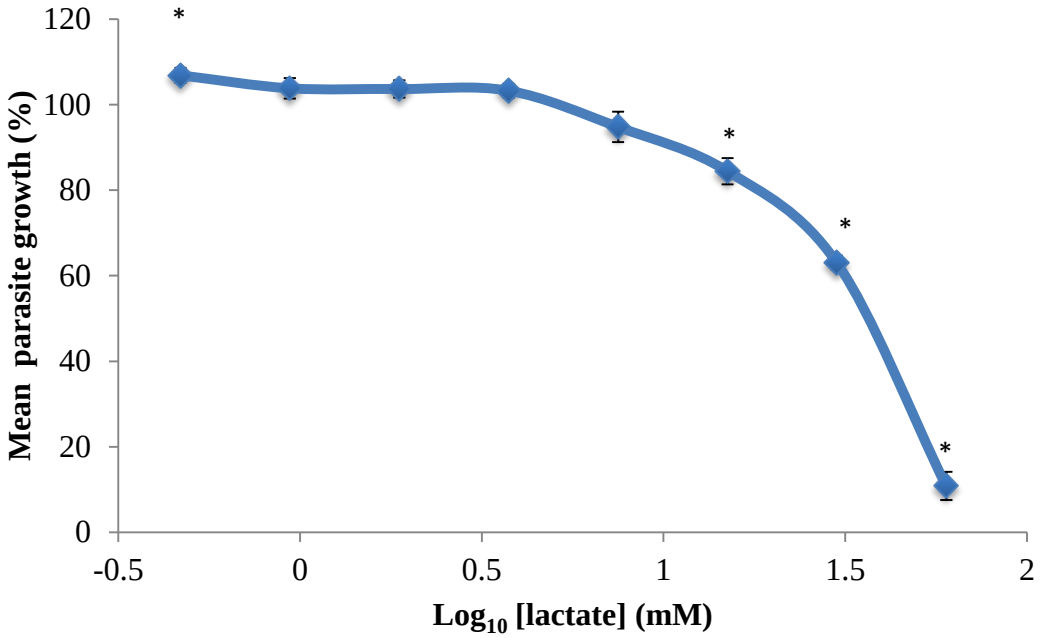

Figure 7.2: Relative percentage growth after exposure to increasing L-Lactate concentrations for 48 h. The mean growth rate is the mean of two independent biological replicate studies. Each biological replicate was done in technical triplicate, n = 6. Mean growth rate from each biological replicate was determined from technical replicates. Error bars are SEM. * $p<0.05$, significantly different from the control culture using Mann-Whitney test of normalized fluorescence units. The lactate concentration was diluted two-fold from 120 mM in complete RPMI media.

We confirmed that the above observed effect was due solely to sodium L-Lactate and not to pH changes as when this salt of a weak acid was added to the heavily-buffered parasite culture media it (as expected) had little effect on pH of the media, appendix X and as previously reported (Hikosaka, Hirai et al. 2015). Indeed, there was less than 0.4 unit change in pH with additions up to 120 mM lactate.

Figure 7.2 suggested that relatively low lactate levels of < 15 mM had no detrimental effect on parasite growth. Therefore, we further examined the effect of lactate concentrations up to 15 mM on parasite growth, and showed that different starting culture parasitaemia produced different effects. When the starting culture was 1%, as was used in the previous section, there was no significant change in parasite growth (red graph of Fig. 7.3). However, when the starting culture was 0.7%, there was a significant increase in growth at 1.875, 3.75 and 7.5 mM (log 0.875061) (blue graph of Fig. 7.3).

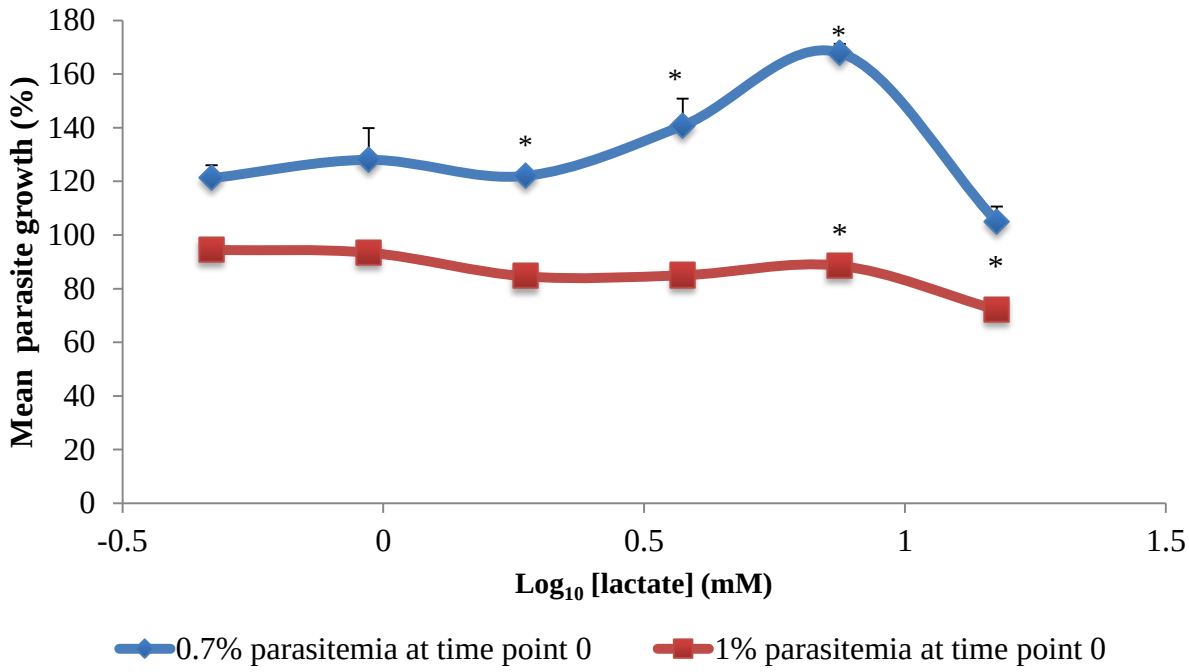

Figure 7.3: Relative percentage growth after exposure to limited increasing L-lactate concentrations for 48 h. Data shown are from one biological replicate experiment, analysed on two different plate readers. Experiment with the Glomax done at 0.7% parasitaemia (blue graph). Experiment with the Tecan was at 1% parasitaemia (red graph). Mean growth rate was determined from technical triplicates, n = 3. Error bars are SD. * $p<0.05$, significantly different from the control culture using 2 – Sample t - test of normalized fluorescence units.

7.3.2 Effect of different lactate concentrations beyond the 1st cycle growth of *P. falciparum* 3D7

The cultures in Figure 7.3 (blue graph) were allowed to go through one further cycle to determine if the growth enhancing effect of lactate will still be maintained. Death following nutrient-depletion did ensue as evident from microscopy and the fluorescence reads however, the growth enhancing effect was maintained (Fig. 7.4) similar to the observation after one cycle.

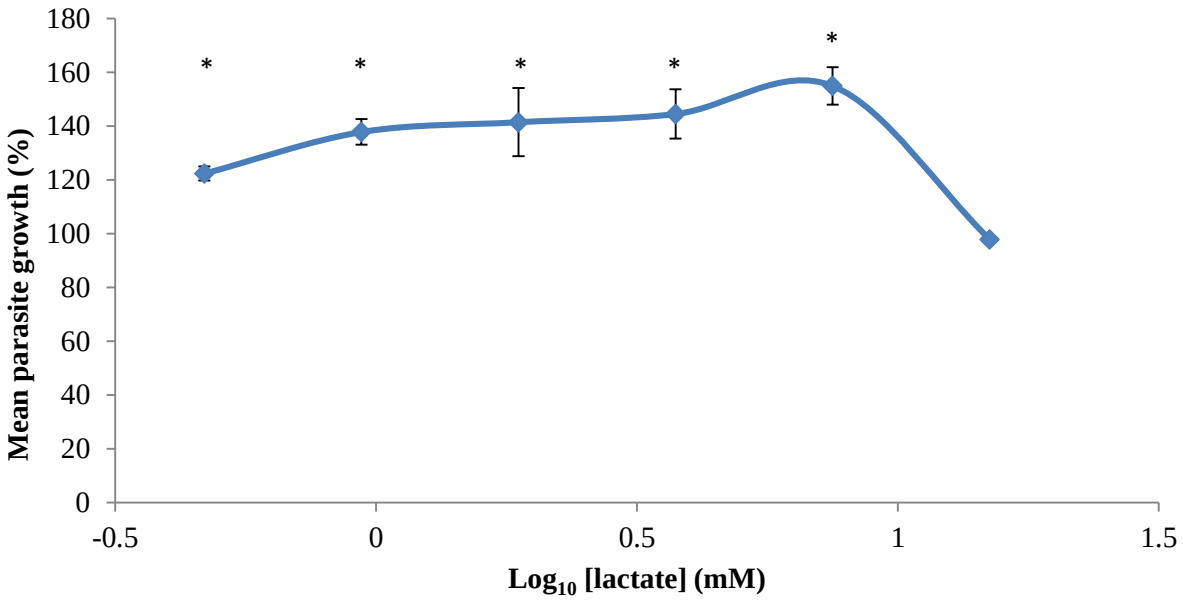

Figure 7.4: Relative percentage growth rate after exposure to limited increasing L-Lactate concentrations for 96 h. Mean growth rate was determined from technical triplicates, n = 3. Error bars are SD. * $p<0.05$, significantly different from the control culture using Mann-Whitney test of normalized fluorescence units.

Starting with a seed culture of 0.1% parasitaemia, the effect of lactate up to 60 mM on parasite growth was determined at 48, 96 and 144 h. Lactate accumulates in static cultures following glucose metabolism (Pfaller, Krogstad et al. 1982, Zolg, Macleod et al. 1984) and may contribute to any effect of the added lactate. This was to clarify if the inhibitory effect observed in Figures 7.2 and 7.3 was due only to the high parasitaemia of the starting culture. The parasites in the lower parasitaemia culture are exposed to much less lactate, following glucose metabolism, in addition to the supplemented lactate.

A lactate-concentration-dependent increase in growth was observed at 48 h from 0.235 mM up to 30 mM (Fig. 7.5). This was in contrast to the growth inhibitory effect observed in Figures 7.2 and 7.3 at 15 mM and above. Similar growth enhancement was seen at 96 h, but the increase was much less than at 48 h and all the parasites died at 60 mM lactate, as was seen in Figure 7.3 with a 1% starting parasitaemia after 48 h. At 144 h there was no growth increase, and parasite growth was inhibited at 30 mM (20%) and completely at 60 mM (Fig. 7.5). Lactate thus enhances parasite growth up to a concentration that increases as parasitaemia decreases, consistent with lactate being beneficial only up to a certain point, which can be reached both by supplemental L-lactate and through parasite metabolism.

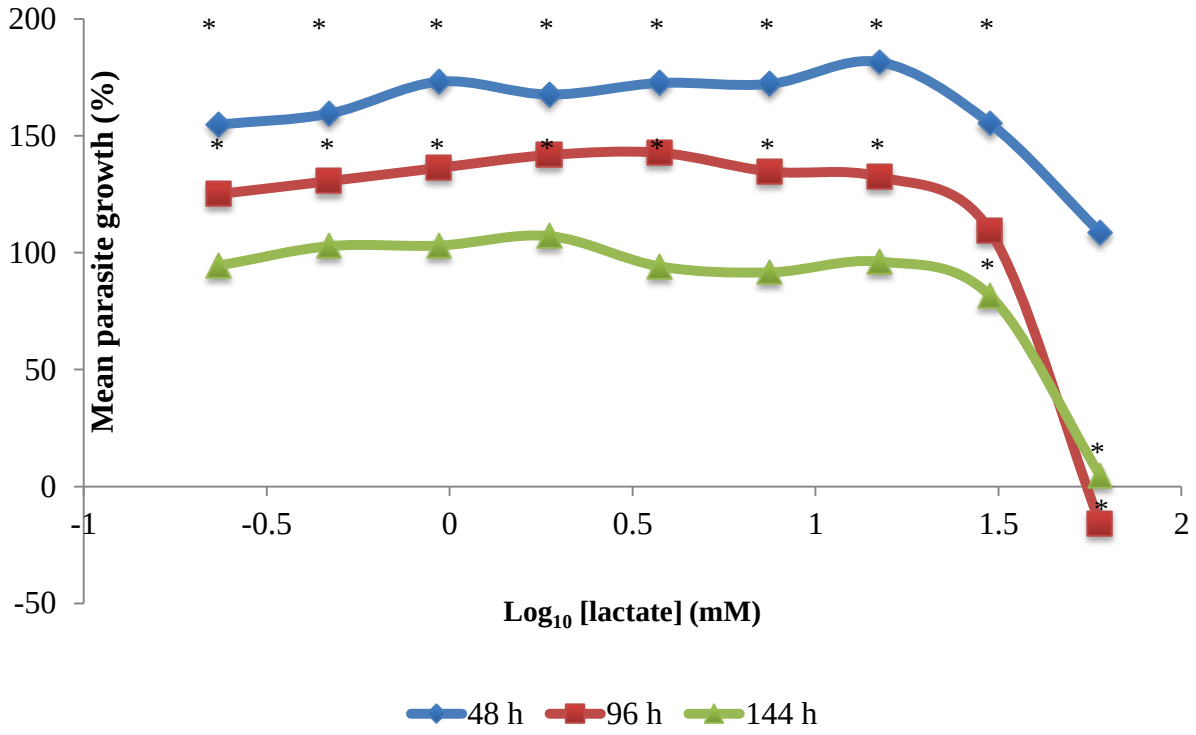

Figure 7.5: Relative percentage growth after exposure to increasing L-Lactate concentrations up to 60mM for 48, 96 and 144 h. The starting parasitaemia was at 0.1%. Parasitaemia of the positive controls at 48, 96 and 144 h were 1%, 3.4% and 11.07%. Parasite media was completely changed before introducing the lactate containing media. Mean growth rate was determined from technical triplicates, n = 3. Error bars are SD. * $p<0.05$, significantly different from the control culture using 2 – Sample t - test of normalized fluorescence units.

7.3.3 Effect of high lactate on schizogony

In an attempt to investigate the mechanism by which lactate might stimulate increased parasite growth we determined the average number of merozoites from 15 schizonts of parasites exposed as synchronized early trophozoite-staged parasites to 5 mM lactate for 16 h, a concentration that subtly or significantly increased parasite growth in chapter 4 and here, depending on the parasitaemia of the exposed culture. The parasites were exposed at 24 ± 8 hpi and contained about 80% of the required (trophozoite) stage. The number of merozoite

nuclei in the segmented schizonts was determined and compared to a non-lactate exposed control and the percentage schizonts and rings were also determined (Fig. 7.6A), as some of the schizonts had undergone lysis but some few schizonts had not segmented distinctively.

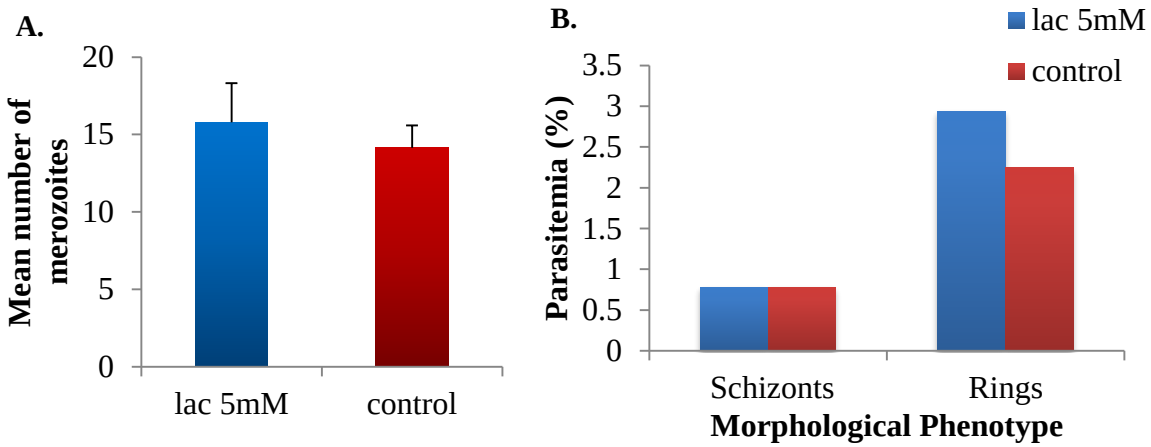

Figure 7.6: Increased schizogony and developmental enhancement after exposure of trophozoite-staged 3D7 to 5 mM lactate for 16 h. Parasites were exposed to lactate and no lactate at 1% parasitaemia. **A.** Mean merozoites per schizont. One biological replicate experiment and merozoites count is from the same number of schizonts for both groups, number of schizont counted is 15. Error bars are SD of the mean merozoite per schizont. **B.** Percentage schizont and rings. % schizonts and rings are per > 1000 erythrocytes from a singular count.

The mean number of merozoites in parasite exposed to 5 mM lactate is not significantly higher than that of the control as a result of the wide variation in merozoites numbers. Furthermore, the percentage of rings from the lactate treated schizonts was higher than that of the control, but the percentage of schizonts remained the same (but less than the parasitaemia of the trophozoite-staged seed culture used for both conditions). This suggested that 5 mM lactate may enhance schizogony and the invasion of merozoites.

7.3.4 Lactate-mediated protection of parasites from nutrient depletion and waste accumulation

Following a series of attempt to recover the lost bioluminescence signal in chapter 3, the ring-staged luciferase reporter lines (at 12 - 16 hpi) were cultured for 72 h after exposure to potential stress (lactate with or without heat shock) for only 2 h. Accidentally, there was some death in the control and test cultures resulting from overpopulation (crashing, with nutrient depletion and/or waste accumulation occurring), but the test cultures appeared to survive better when exposed to high lactate alone and in combination with heat shock (Fig. 7.7). This was confirmed by microscopy (data not shown) and luciferase activity with the PfSir2A-luc line generally appearing to survive better than the Pfpcna-luc control line. There was an increased survival of parasites exposed to lactate compared to parallel cultures exposed to no lactate for both lines or only heat shock for the PfSir2A-luc line.

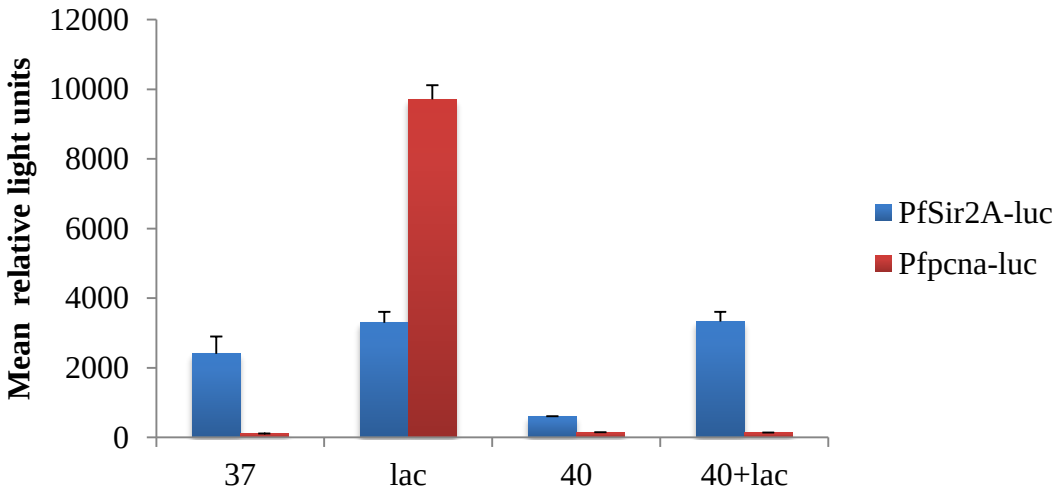

Figure 7.7: Potential Protection of Rings from heat shock (PfSir2A-luc) and nutrient depletion and waste accumulation (both strains) by 5 mM lactate for 2 h. 3D7luc and Pfpcna-luc stressed for 2 h and allowed to recover for 72 h to determine growth rate and viability. The media was not completely changed after the stress experiment (at about 0.5% parasitaemia) but all cultures were diluted 1:5 before recovery and so the lactate concentration was at 1mM before recovery. The parent parasite line of Pfpcna-luc has been shown to have a higher growth rate than 3D7, the parent parasite line of PfSir2A-luc and that is why its control crashed more even though both culture had a 0.5% starting parasitaemia. Error bars are standard deviation of raw light units.

Thus, we decided to investigate if lactate may exert a protective effect from death due to nutrient depletion and waste accumulation. In Figure 7.8, the starting parasitaemia of the 3D7 seed culture was 0.8% of mostly trophozoites in 4% haematocrit, and all cultures were exposed to 5 mM or 10 mM lactate or no lactate for 6 h and left to recover for up to 96 h or continually to these concentrations of lactate for up to 96 h. The included control for the two sets of experiment indicated that the parasites were dying from waste accumulation and nutrient depletion at the 96 h time point.

Continuous exposure to lactate did not protect the parasites from crashing but brief lactate exposure did (Fig. 7.8); but, this effect was not statistically significant. However, the parasites exposed to 5 mM lactate grew significantly higher compared to the control after 48 h (Fig. 7.8A), consistent with our previous findings. This may be due to the small growth increase on brief exposure compared to continuous lactate exposure, which can easily be overshadowed by experimental error.

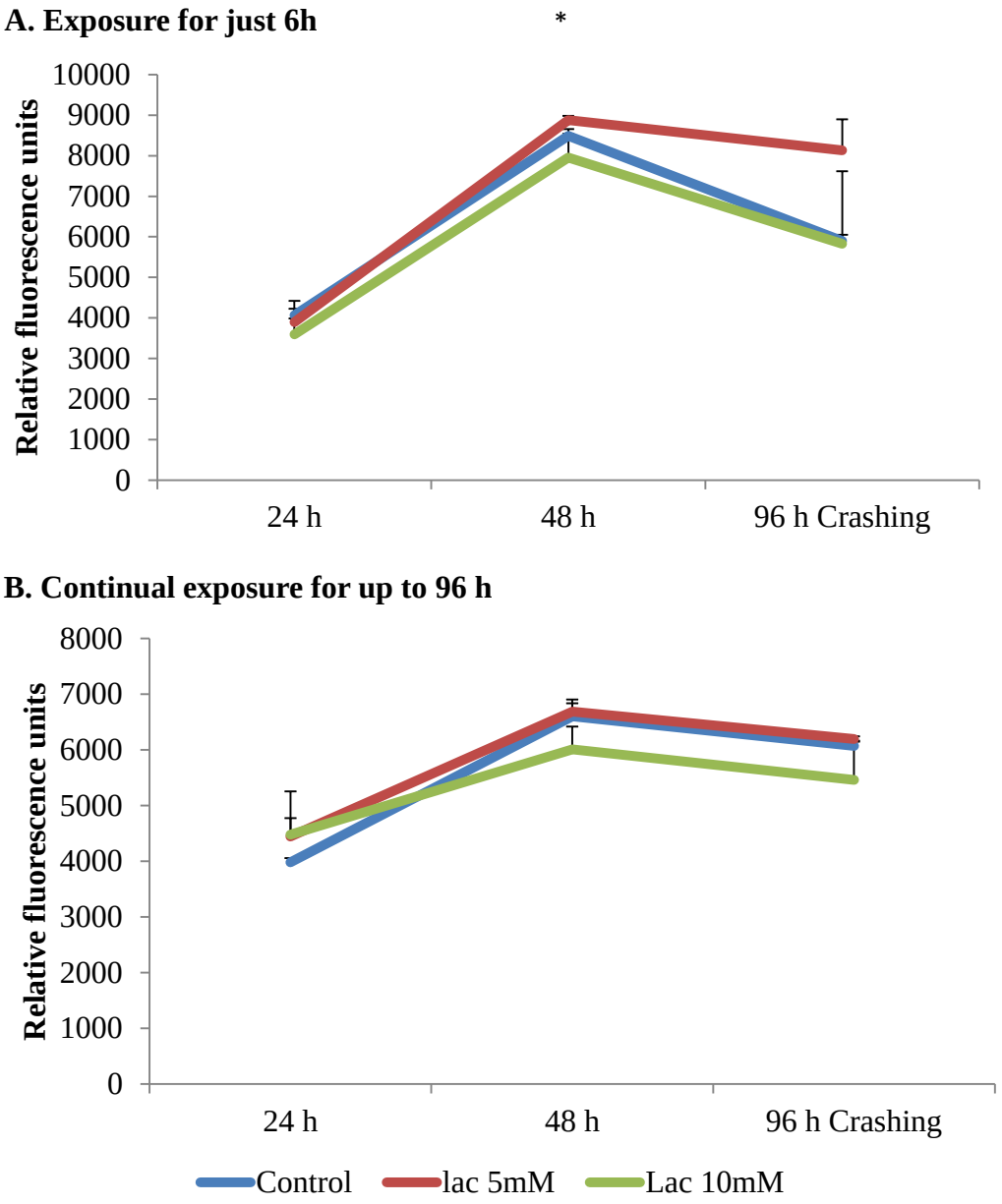

Figure 7.8: Growth of synchronized early trophozoite-staged *P. falciparum* 3D7 after exposure to 5 mM and 10 mM L-lactate for 6 h or continuously for up to 96 h. Fluorescence read by SYBR Green-1, represented as Relative Fluorescence units (RFL). 1 biological replicate; n = 3 technical replicates. Error bars are SD.* $p<0.05$ using normalized fluorescence units.

In the continuously-exposed parasites (both 5 and 10 mM), at 24 h, when the parasites were schizonts/early rings, parasite multiplication increased compared to other treatments. The control, both washed and unwashed, and that exposed to 5 mM lactate for a short time were on similar level of survival, while parasites exposed to 10 mM lactate for a short time had the least survival.

As the parasites mature from rings to trophozoites at 48 h, the expected accumulation of toxins, including lactate produced by the trophozoite parasites at 48 h, eventually impaired the maturation on continuous exposure to lactate (5 and 10 mM) and spent media in the control that was unwashed. Parasites exposed to the highest lactate concentration had the least survival. Their previous growth increase at 24 h was overtaken by parasites briefly exposed to 5mM & 10mM lactate, and the washed control. Brief exposure to 5mM lactate gave the best survival and this was significant compared to the washed control. Trophozoites/early schizonts produce more lactate and are most inhibited by accumulated lactate metabolically.

Most importantly, after another round of ‘multiplication and maturation’, parasites exposed to 5mM lactate crashed less, while others crashed in a similar manner to almost the level exhibited by parasite continually exposed to lactate or spent media at 48 h. The fluorescence read for the parasites that crashed less is statistically different from that of the control parasites left in their spent media for 96 h (not shown on the graph).

7.3.5 Lactate-mediated protection from heat shock is strain specific

In chapter 4 of this thesis, it was observed that trophozoite-staged 3D7 at parasitaemia of ~2.6% treated with heat shock in the presence of 5mM lactate, for 6 h, survived better than a parallel population without lactate. This suggested the possibility that high lactate may provide some protection against heat shock. In addition, a similar effect was observed when ring-staged 3D7 luciferase expressing lines were exposed to the same stress (Fig. 7.7).

Here, ring-staged *P. falciparum* NF54 and 3D7, both at 0.5% parasitaemia, were exposed to heat shock alone and in combination with lactate for 6 h and then their growth was assessed at 72 h (Fig. 7.9). A negative chloroquine control representing 100% was used to normalize the fluorescence reads of the heat shocked group and the combined treatment group. There was no growth increase on exposure to lactate for 6 h, compared to no lactate and heat shock for both strains. Both the brief exposure and particularly the parasitaemia of the starting cultures exposed to the severe-malaria-defining 5 mM lactate concentration may have limited the influence of the total lactate in the lactate-supplemented media, as the parasite's metabolism will contribute to the actual lactate concentration. There was a significant reduction in growth rate of parasites exposed to heat shock alone and in combination with lactate for both strains. However, 3D7 exposed to the combination of heat shock and lactate survived better (Fig. 7.9 A), significantly compared to those exposed to heat shock alone. This effect was not observed for NF54; rather there was a significant growth reduction (Fig. 7.9 B). This indicates that this may be a strain specific effect.

A. Post-stress growth assessment of 3D7

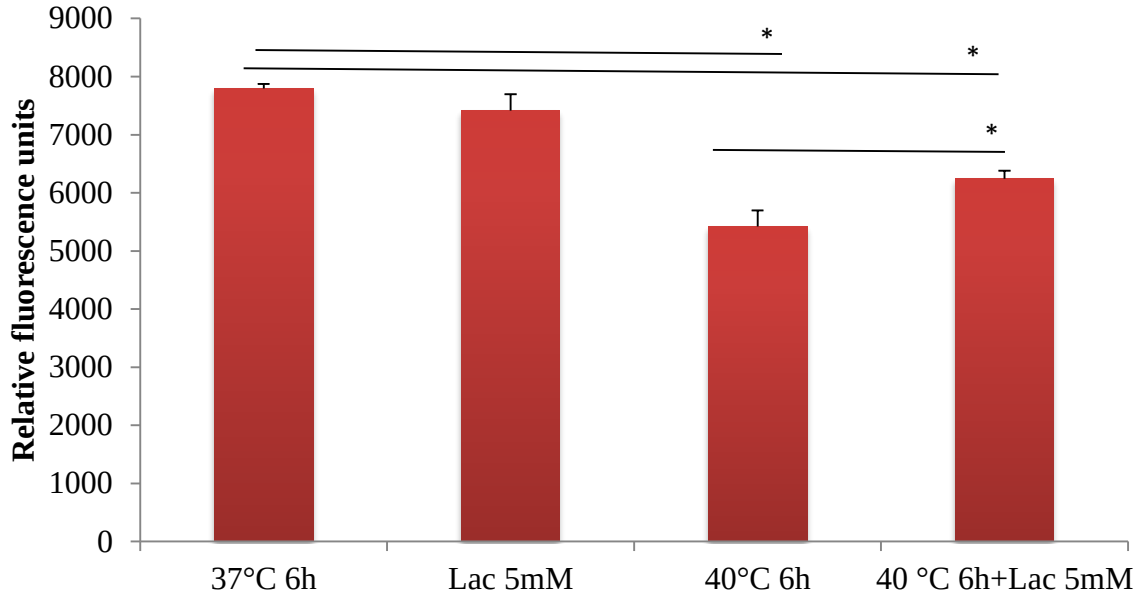

B. Post-stress growth assessment of NF54

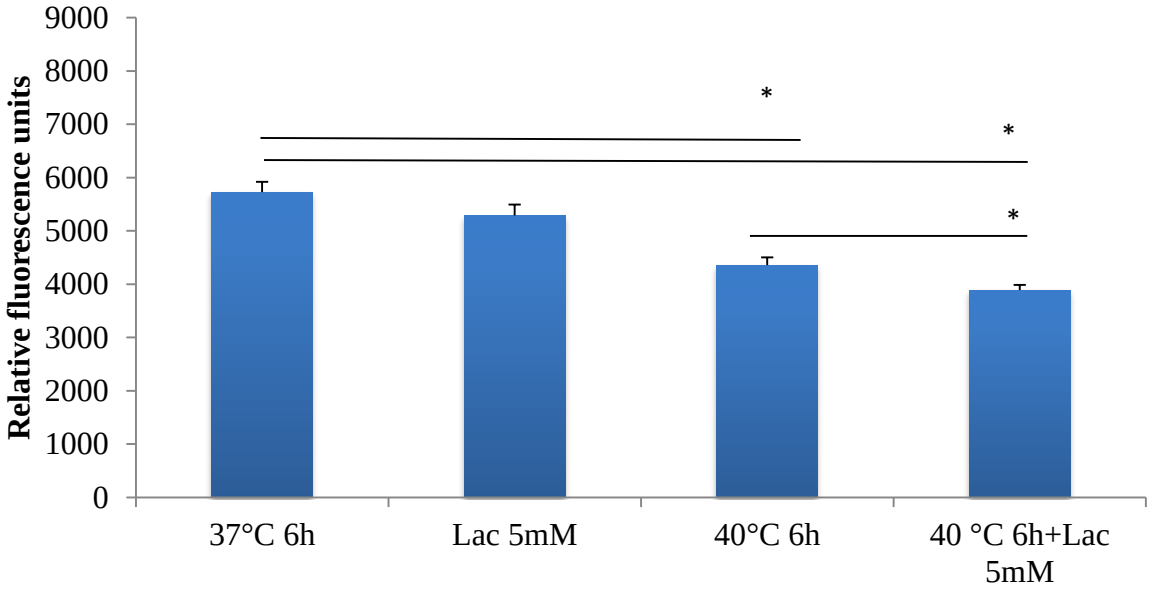

Figure 7.9: Post-stress relative percentage growth after exposure of two 12-16 h old ring-staged *P. falciparum* strains to heat shock and/or 5mM L-lactate for 6 h. One biological replicate experiment, n = 3 technical replicate. Fluorescence reads by SYBR Green-1 are the mean relative fluorescence units of 3 technical replicates. Error bars are SD.* $p<0.05$ ANOVA of normalized fluorescence units.

7.4 Discussion

Lactate was shown to have a growth-enhancing effect but this was dependent on the parasitaemia of the starting culture and thus that of the next generation(s). This may simply be viewed as a cumulative effect as lactate production increases with parasitaemia, as demonstrated (Pfaller, Krogstad et al. 1982), and lactate below 12 mM has been shown to be optimal for parasite growth (Jensen, Conley et al. 1983). At high parasitaemia, accumulation of lactate and other waste products may negatively impact parasite growth (Hikosaka, Hirai et al. 2015). The novel finding here, however, is that lactate at lower levels may actually enhance parasite growth (Fig. 7.3 and 7.5).

At 1% parasitaemia starting culture, the effect of lactate was inhibitory at ≤ 15 mM when the asexual parasites were allowed to go through one lifecycle. This suggests a cumulative effect from the total lactate in culture, both the added lactate as well as that produced by the parasite during development. In addition, this may be similar to the build-up of lactate due to renal insufficiency in the severely ill malaria patient (Day, Fau et al. 2000), an accumulation that is detrimental to both the parasite and host.

On the contrary, when the parasitaemia of the seed culture was < 0.5%, lactate concentrations that previously caused no change or were growth-inhibitory were observed to increase parasite growth after 1 and 2 cycles. This was true up to 30 mM lactate, but not at 60 mM lactate concentration. The salient question, therefore, is why the additional lactate should enhance parasite growth. A previous study demonstrated that a subset of parasite populations from malaria patients may rely on alternative pathways of energy production where they use alternative carbon sources like lactic acid and glycerol (Daily, Scanfeld et al. 2007). One is tempted to suggest that this may be a means of increased survival in the waste laden environment of the parasite here. In addition, lactate may well prevent intracellular acidification as it does not reduce pH in an electrolyte system and will be co-transported with

H+ ions to the extracellular region, with acidosis resulting only when the lactate is overwhelmed (Ginsburg, Stein 2004; Elliott, Fau et al. 2001).

An enhancement of the parasite's replicative fitness, subsequent invasion of RBCs and development of merozoites to rings may all be possible mechanisms of the growth enhancing effect of lactate, as shown for the 5 mM concentration. However, the findings in Figure 7.6 did not significantly support this suggestion. One is, however, tempted to speculate that the observed increased number of merozoites may occur because the parasites detect an apparent increase in the nutrient availability in the culture media, manifesting as increased lactate turnover. This is similar but opposite to the effect brought about by calorie restriction, which leads to reduced merozoites per schizonts and is mediated by KIN signalling kinase (Mancio-Silva, Slavic et al. 2017). This is a potential mechanism of the lactate growth-enhancing effect, previously reported (Jensen, Conley et al. 1983; Zolg, Macleod et al. 1984) and subtly observed in chapters 3 and 4. Indeed, the inhibitory effect of 30 and 60 mM lactate concentration has been attributed to a decreased schizogony and even the size of the schizonts at 60 mM (Hikosaka, Hirai et al. 2015). Logically, it can be speculated that the reverse may be the case for an enhancing effect. However, this remains to be thoroughly investigated.

P. falciparum has previously been thought to have a defunct TCA cycle during its asexual stage but recent evidence suggests that this stage alternatively uses its TCA cycle (MacRae, Fau et al. 2013) probably incorporating lactate as the primary source of carbon for this cycle as recently demonstrated for cancerous (Faubert, Li et al. 2017; Chen, Mahieu et al. 2016) and normal mammalian cells (Hui, Ghergurovich et al. 2017). (Lactate can probably be recycled in the heart of mammals (Nielsen, Clemmesen et al. 2002).) The study by Daily *et. al.*, referenced above, has suggested that *P. falciparum* genes, associated with oxidative phosphorylation, respiration and fatty acid metabolism, as well as invasion, are induced in a subset of the parasite population from the venous blood of malaria-infected patients, thus

indicating their ability to use alternative energy sources in lower oxygen containing host niches (Daily, Scanfeld et al. 2007). Furthermore, a recent study has shown that although gametocytes do consume the same quantity of glucose as asexual parasite stage, they produce much less lactate, pointing to the fact that they may use their resulting lactate from glycolysis (Lamour, Straschil et al. 2014).

In addition, earlier studies on the parasite's production and tolerance of lactate suggest that glucose utilization as measured by the amount of lactate produced accounts for two-third or a half of the starting glucose level (Jensen, Conley et al. 1983; Zolg, Macleod et al. 1984). This presents two scenarios. Firstly, that glucose utilization by the asexual blood stage parasite may involve some other pathway apart from glycolysis, where lactate is not an end product. And, secondly, lactate may be recycled through some other metabolic pathway. To this end, one is tempted to suggest that the parasite may be able to adapt to the hypoglycaemic host environment and use alternative sources of carbon to survive.

Concerning the possibility that lactate exposure reduces parasite crashing, a non-significant increased survival was seen after the parasites exposed to 5 mM lactate for 6 h were allowed to grow to very high parasitaemia, at which point their multiplication index drops (Zolg, Macleod et al. 1984). The possibility of lactate enhancing parasite survival warrants further investigation with more biological replicates as this is not yet confirmed in our study. This concentration of lactate was also shown to protect 3D7 from heat shock but not NF54 and this is also only a preliminary report that needs to be replicated. If the effect is real, however, it may contribute to *P. falciparum* survival during waves of fever that otherwise would have killed the parasite. Indeed, lactate has previously been shown to regulate adaptation to stress in humans (Nalbandian, Takeda 2016).

Hyperparasitemia in severe malaria has been defined as ≥ 4% in children with the presence of other co-morbidities, and > 10% in adults. In this study, a normal physiological level of lactate, ≤ 1.5 mM, and markedly higher than this too, introduced as supplement in cultured parasites, has been shown to enhance parasite survival. This does not take into account the lactate produced by the uninfected RBCs and the parasites during glucose metabolism, which will introduce additional lactate surpassing this level. It also does not take into account the difference between a static *in vitro* culture and a dynamically metabolising human body, which must of course be considerable. It can, however, be suggested that a pre-existing hyperlactatemia condition prior to a human blood stage infection might increase the multiplication rate of the parasite. Such pre-existing condition may be due to a compromised liver or renal function or coinfection with another microbe.

The impact of hyperlactatemia on severe malaria prognosis is high. Lactate from sequestered parasites may damage the blood brain barrier in severe malaria via the G-protein coupled (GPR81) receptors as hypothesized by Mariga *et. al*. It was suggested that lactate may excessively down-regulate cAMP by binding to GPR81 in the endothelial cells and astrocytes (Mariga, Kolko et al. 2014; Morland, Lauritzen et al. 2015). Lactate binding to GPR81 has been demonstrated in other cell types (Wagner, Kania et al. 2017; Ranganathan, Shanmugam et al. 2018). In addition, similar levels of lactate in the blood and the cerebrospinal fluid have been reported (Krishna, Waller et al. 1994). Expression of monocarboxylate transporter (MCT)-like genes coding for lactate/proton symporters are enhanced at the trophozoite stage following lactate supplementation (Hikosaka, Hirai et al. 2015), and this may be needed to prevent growth inhibition.

In this study, using an *in vitro* static culture system, exponential growth of parasites was shown to be modulated by lactate, with a positive modulation at low parasite burden and a negative modulation at high parasite burden. We hypothesize that increasing lactate might

have increased the proton buffering capacity of the *in vitro* culture system, which reduced the onset of acidosis during prolonged culture especially with a low parasite burden, thus enhancing parasite survival. But, there may be a threshold where its capacity was overwhelmed and the accumulated lactate or pyruvate (its conversion to lactate may be inhibited by excess lactate) would then be detrimental to parasite survival as a result of a perturbed cytosolic redox. More so, lactate may enhance the ability of the parasite to survive environmental stress. However, the exact mechanism through which lactate enhances parasite survival and growth needs to be determined.

Chapter 8: General discussion and summary of findings

8.1 Discussions

This is the first study to establish a causal link between increased expression of *P. falciparum* sirtuins, especially *PfSir2B*, and high body temperature, by the application of heat shock at 40°C to parasites *in vitro*. Host high body temperature and high blood lactate have previously been shown to be associated with up-regulated sirtuin expression in Gambian field isolates of *Plasmodium falciparum* causing a severe disease (Merrick, Huttenhower et al. 2012). High body temperature alone has been shown to be marginally positively associated with the expression of the sirtuins (Abdi, Warimwe et al. 2016). However, it was not known if these two host factors can actually lead to increased sirtuin expression. This study has thus clarified this.

A reduced parasite survival occurred upon heat shock, as equally demonstrated by Oakley and colleagues (Oakley, Kumar et al. 2007). Mature trophozoites and schizonts were more affected than rings as has previously been shown (Kwiatkowski 1989; Thomas, Sedillo et al. 2016). The parasite strain with the least survival induced the highest expression of *Hsp70*, which can be translated into the cytoprotective protein. Recurrent exposure to high temperatures, mimicking tertian malaria fever, has been shown to synchronize the parasites by limiting their development to older stages. However, these parasites go on to develop normally when returned to normal body temperature (Kwiatkowski 1989) which was observed when the parasites in our study were allowed to recover and grow for another asexual cycle.

On the contrary, subtle increases in parasite growth upon lactate stress were evident at up to 6 h of exposure, and confirmed on continual exposure for one or two cycles in a concentration-dependent manner up to 30mM. This lactate-mediated enhanced growth was equally dependent on the parasitaemia of the starting culture, thus suggesting a subtle effect due to a difference in nutrient depletion. In severe malaria, hyperlactatemia is predominantly determined by increased lactate production and not decreased lactate disposal with dramatic increase in the transport of lactate into iRBC as has previously been demonstrated (Ginsburg, Stein 2004; Cranmer, Fau et al. 1995). The highest lactate recorded in severe disease is 13.42 mM (Agbenyega, Baffoe-Bonnie et al. 2000), and we showed that this concentration can enhance parasite growth, but at parasite levels markedly lower than that reported for severe malaria. One possible mechanism may be through increase in merozoites per schizonts, although this needs to be clarified. We were also able to show that lactate may enhance parasite survival upon heat shock. In addition, *P. berghei* asexual stages have recently been shown to carry out TCA cycle with glutamine as the carbon source (Srivastava, Philip et al. 2016) and it is possible that *P. falciparum* similarly metabolises a range of carbon sources.

In vitro vs *in vivo* growth conditions, as shown in Figure 8.1, differ and may reveal some differences in the parasite biology from what has been previously demonstrated, including epigenetic control of *var* genes and the switching of *var* gene expression. The included high lactate and high temperature among the parasite growth conditions in our study, revealed an altered sirtuin expression and probably a perturbed *var* transcription, primarily, upon heat shock stress.

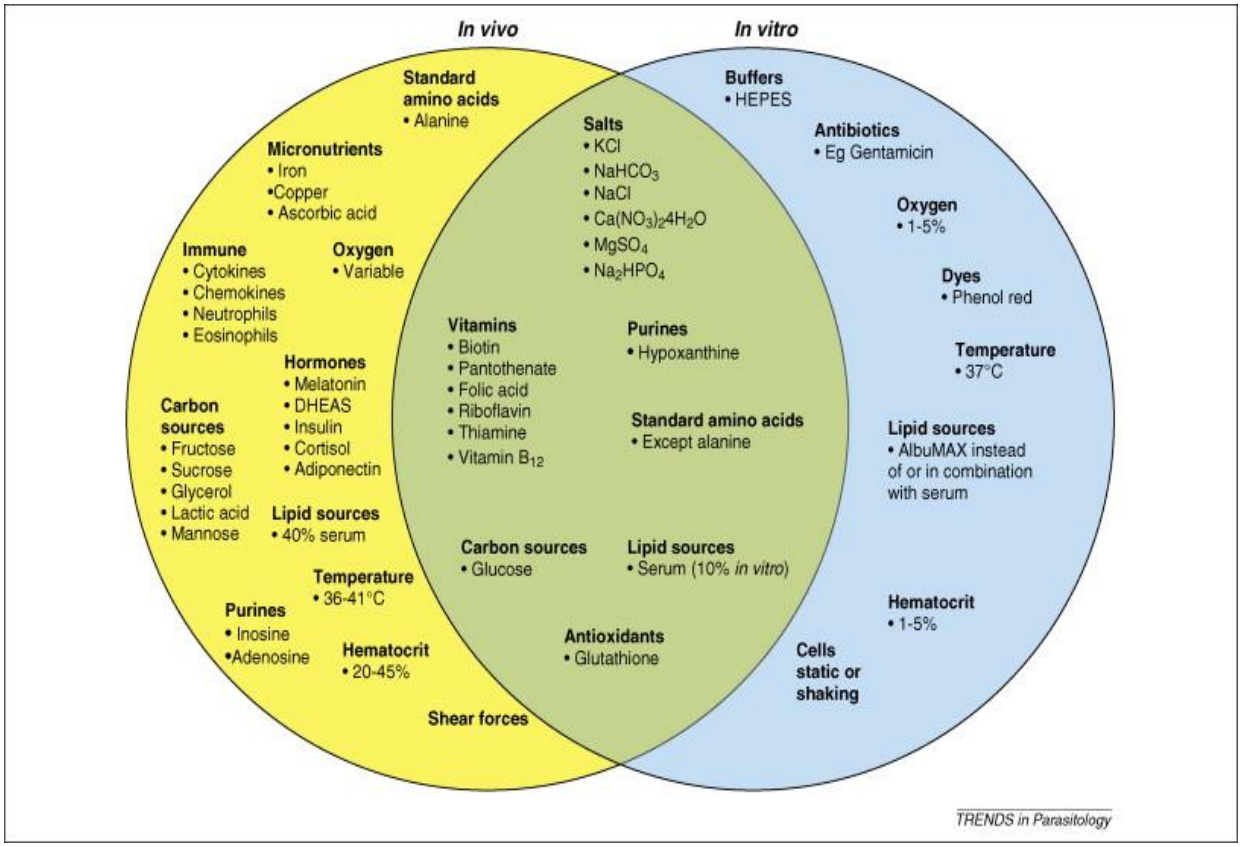

Figure 8.1: Difference in environmental conditions experienced by *P. falciparum* during *in vivo* and *in vitro* growth (LeRoux, Lakshmanan et al. 2009)**.** *P. falciparum* is exposed to different environmental conditions *in vitro* compared to *in vivo*.

Heat shock protein-70 expression was rapidly highly induced in trophozoite-staged field isolates compared to the laboratory strain 3D7, which had a delayed heat shock response that began after 2 h but was significant after 6 h, whereas the field strains began to downregulate their response by 6 h. Prolonged heat shock generally led to a reduction in the heat shock response of the trophozoites, because *Hsp70* negatively feedbacks on its expression (Mosser, Duchaine et al. 1993; Rabindran, Wisniewski et al. 1994; Shi, Mosser et al. 1998). There was greater heat shock response in trophozoites than rings possibly because DNA replication begins at the trophozoite stage and the protein machinery needed for this stage has to be protected from denaturation/degradation. Only one ring-staged parasite strain increased its *Hsp70* expression upon heat shock to similar levels as its trophozoites; other strains were not equally responsive.

The trophozoites consistently increased their expression of *PfSir2B* after heat shock (Fig. 4.6 and 4.15). However, the rings responded by increasing their *PfSir2A* expression (either immediately or upon recovery), while *PfSir2B* was actually down-regulated in the rings of *P. falciparum* strains and then increased (back to baseline or higher) upon 10 h of recovery (Fig. 4.19 and 4.20). Generally, lactate appeared to modulate heat shock response, but this was not statistically significant in parasites exposed to the combined stress. There was no consistent response to lactate alone across all strains tested.

Heat shock (and for only one strain, high lactate) also led to the predominant expression of severe disease-associated *var* genes. Subsets of *var* genes were expressed in response to host stress in a strain-specific manner. A particular *var* gene group tended to be predominantly expressed upon stress, especially heat shock but this was not the same group in all the strains. This predominant *var* may have been epigenetically marked in the strain, and may possibly correspond to gaps in the patient's antiPfEMP1 antibodies from which the isolates were obtained. However, since the field isolates had all been adapted to culture, at least for weeks/months, any epigenetic signatures from the in-patient situation may well have decayed.

Subsets of *var* genes, some of which are frequently associated with severe malaria, were predominantly expressed upon stress and included: groups A, B and E *var genes*. Group C *var* gene, which is rarely associated with severe malaria, was also predominantly expressed by one of the strains after exposure to the combined stress (Fig. 4.20). It has been demonstrated that upsA *var* genes tend to have a faster switching off rate on culturing of patients isolates for a short time (Peters, Fowler et al. 2007), even in the next cycle (Bachmann, Predehl et al. 2011) and have a low probability of being activated (Fastman, Noble et al. 2012), however, they reached a higher level (Fig. 4.20) in our study after exposure to heat shock stress.

Upon recovery for 10 h one of the strain predominantly upregulated a var2csa, which was not previously increased immediately after stress. This suggest that a different *var* gene may have been selected but due to the presence of different phenotypes in the unselected population we cannot confirm this finding. Selection of a different *var* gene may involve rapid deacetylation of the acetyl residues on histones binding the predominantly expressed *var* genes by the sirtuins upon stress or upon recovery. One strain downregulated *PfSir2B* upon stress but upregulated it upon recovery, while downregulating *PfSir2A*. *PfSir2A* has been shown to have a significant clear relationship with the increased expression of upsB type of severe-disease-associated *var* genes in the same (Merrick, Huttenhower et al. 2012) and with upsA, upsB/A and upsC2 in a more recent study (Abdi, Warimwe et al. 2016). Thus, an alteration of the quantity of *PfSir2A* and *PfSir2B* may be needed to determine which *var* will be predominantly expressed and switching may have some order with activation of a different *var* group than was previously activated.

The total amount of *var* gene was increased upon recovery from stress, potentially a mechanism enabling parasites to cytoadhere more efficiently away from the circulating antibodies following an immune response induced fever. *Plasmodium* immune evasion in chronic infections may also involve a low *var* gene expression (Abdi, Warimwe et al. 2016) but this was not observed in this study. Patient isolates cultured for 10 days do show significant downregulation of all *var* genes (Peters, Fowler et al. 2007) and this may be why we did not observe any dramatic change in total *var* gene level as measured by priming for the ATS region. In addition, this region may differ for field strains from that of 3D7, leading to imperfect detection of this transcript. The levels of *var* gene upregulation were higher in this study than reported previously (Oakley, Kumar et al. 2007). This may be because heat shock was applied for longer in our study (6 h vs 2 h) and field strains are more responsive than laboratory strains. The expressed *var* genes encode PfEMP-1 that enables parasites older

than 18 h sequester in post capillary venules and remain out of circulation for 30 h. An increased content of *Hsp70* in the heat shocked parasite line may increase the presentation of more and maybe different, expressed PfEMP-1, as exported Hsp70 (PfHsp70-x) may be involved in the presentation of PfEMP1 (Külzer, Charnaud et al. 2012).

A selective upregulation of *var* genes enables the parasites to adapt or resist the adverse host conditions and continuously establish a chronic infection. The association of febrile temperatures with high *var* expression may be causal. Immune response can lead to high body temperature in the host and the parasite may sense this as a signal of the host immune status, thus altering its sirtuin and *var* genes accordingly. PfHDAC1 has been shown to co-migrate with Hsp-70-1 and 90, indicating a possible interaction of PfHDAC1 with heat shock proteins (Engel, Norris et al. 2019); other PfHDACs may interact with these proteins too. However, high lactate is a reflection of the high parasite biomass, and the degree of microvessel obstruction due to sequestration, of the already naturally selected parasites. In a possible positive-feedback loop, parasite increase in biomass may actually be enhanced by lactate, as demonstrated in our preliminary report here but lactate does appear to dampen the parasite's response to heat shock.

Although febrile episodes limit the exponential multiplication of the parasite with the advertent aim of reducing the development of hyperparasitemia as occurs in severe malaria, subsequent episodes may promote the parasite's accelerated development from rings to trophozoites (Pavithra, Banumathy et al. 2004). In addition, fever was earlier demonstrated to induce cytoadherence of rings and trophozoite stages *in vitro*, potentially reducing parasite clearance, a virulence strategy indeed (Udomsangpetch, Pipitaporn et al. 2002). These indicate an ability of the parasite to alter its form in the face of an adverse host condition. This study tried to intensify our understanding of how the parasite is able to survive the adverse host environment and establish a chronic severe disease.

An attempt to corroborate our findings on the ability of parasites to respond to heat shock by moderately increasing their sirtuins, the sirtuin promoter activity was investigated using a transgenic line (3D7 expressing *Fluc* under the *PfSir2A* promoter). However, this experiment failed probably due to denaturing of the luciferase protein upon mild heat shock as has previously been suggested in Drosophila and mouse cells lines, although the heating was more extreme (42°C) (Nguyen, Morange et al. 1989). The firefly luciferase reporter is thus unsuitable for experiments also requiring mild heating. Perhaps some regulatory elements within the 3'UTR of *hsp86*, which was used as the 3'UTR for the *Fluc* transgene, are responsive to heat shock and this also affected the luciferase mRNA stability or transcript level in the heat shocked parasites, as demonstrated for the 3'UTR region of a different gene elsewhere (Wong, Hasenkamp et al. 2011; Hu, Zhu et al. 2009). We were able to recover most of the denatured luciferase after the parasites has been allowed to reinvade for another cycle.

8.2 Contribution to science

In summary, heat shock specifically increased the expression of *Plasmodium falciparum* sirtuins and subsets of severe-disease-associated *var* genes upon stress. However, *PfSir2B* expression was downregulated in the ring stage upon stress. There was a predominantly expression of a *var* gene group upon stress or recovery. There was equally an increased total *var* transcript upon recovery. Upregulation of a particular *var* gene subset or total *var* gene levels may thus manifest as a strategy to cope with host stress. The strain with least response to heat shock, at its trophozoite stage, was the only gametocyte producer amongst the field strains and grew the slowest under *in vitro* conditions. These may be the defining features of a very virulent strain, or alternatively of a strain that has undergone only minimal changes during culture adaptation. The association of high lactate concentration with the sirtuins and *var* genes appears to be coincidental; however, lactate does positively impact

parasite growth at low parasitaemia (and at least one strain did respond transcriptionally to lactate stress). Firm conclusions cannot be drawn from the findings in this thesis due to the challenge of producing enough experimental replicates. The highest number of biological repeat was three with each biological repeat having three technical replicate. This gives a sample number of at most 9. Ideally the sample number should be at least 15 to give a conclusive evidence, but there were challenges in carrying out sufficient biological repeats with the cell culture system. There is also the issue of variability between biological repeats and expression in the different strains thus preventing us from drawing any firm conclusion. Taking this into account, the relationship between *Plasmodium* sirtuin and *var* gene expression, and high body temperature in the host may still be coincidental, warranting further investigation as other host factors may be at play in the field.

8.3 Future direction

Figures 4.8 & 4.9 showed an increased expression of *PfSir2A* upon heat shock of the late schizont. This implies that *PfSir2A* may be increasingly synthesized and mobilized for silencing of *var* in the new merozoite progeny different from the *var* that may have been epigenetically marked. Stressing the late stages and harvesting the subsequent rings may therefore give a more reproducible substantial increase in sirtuin and *var* gene expression. Also, conducting transcriptomics 48 h after stress may provide a deepened insight into epigenetic regulation on encounter of a host stress environment. It is good to note that we had a more consistent and less varying result between biological replicates when the parasite population was kept fairly constant (see e.g. experiment on strain 10668 trophozoites (appendix VIII c). However, it was difficult to get the parasite populations to be the same as well as achieve a similar staging for biological replicates. Technical replicates could be sacrificed for a greater number of biological replicates. A nuclear run-on assay that measures

the frequency of transcription initiation may be suitable for in-depth studies of transcriptional changes.

Different transcriptional phenotypes can be seen in different genetically-identical mutant clones (Bryant, Regnault et al. 2017). So maybe panning would have been more appropriate to streamline phenotypic variations that may complicate establishment of the cause and effect relationship. We were unable to establish if sirtuin activity can be enhanced upon heat shock following the very modest statistically significant upregulation of their mRNA. Host stress may also directly impact induction of gametocytogenesis, fostering transmission and future studies can focus on investigating this possibility.

An understanding of *var* gene regulation can theoretically identify means of hindering parasite switching to another *var* gene that will provide advantage against immune pressure in the immune naïve patient. In the absence of PfSir2A parasites have been previously shown to have diminished *var* switching (Merrick, Dzikowski et al. 2010), and reasonably a slower switching may give an immune naïve patient some time to build up immunity to the frequently occurring parasite phenotype(s). Therefore, the studies in this thesis could inform and ultimately be relevant for the development of anti-disease or anti-chronicity interventions against malaria.

References

ABDI, A.I., FEGAN, G., MUTHUI, M., KIRAGU, E., MUSYOKI, J.N., OPIYO, M., MARSH, K., WARIMWE, G.M. and BULL, P.C., 2014. *Plasmodium falciparum* antigenic variation: relationships between widespread endothelial activation, parasite PfEMP1 expression and severe malaria. *BMC Infectious Diseases,* **14**, pp. 170-170.

ABDI, A.I., HODGSON, S.H., MUTHUI, M.K., KIVISI, C.A., KAMUYU, G., KIMANI, D., HOFFMAN, S.L., JUMA, E., OGUTU, B., DRAPER, S.J., OSIER, F., BEJON, P., MARSH, K. and BULL, P.C., 2017. *Plasmodium falciparum* malaria parasite *var* gene expression is modified by host antibodies: longitudinal evidence from controlled infections of Kenyan adults with varying natural exposure. *BMC Infectious Diseases,* **17**(1), pp. 585.

ABDI, A.I., WARIMWE, G.M., MUTHUI, M.K., KIVISI, C.A., KIRAGU, E.W., FEGAN, G.W. and BULL, P.C., 2016. Global selection of *Plasmodium falciparum* virulence antigen expression by host antibodies. *Scientific Reports,* **6**, pp. 19882.

ACHARYA, P., KUMAR, R. and TATU, U., 2007. Chaperoning a cellular upheaval in malaria: Heat shock proteins in *Plasmodium falciparum*. *Molecular and Biochemical Parasitology,* **153**(2), pp. 85-94.

ADAMS, Y., KUHNRAE, P., HIGGINS, M.K., GHUMRA, A. and ROWE, J.A., 2014. Rosetting *Plasmodium falciparum*-infected erythrocytes bind to human brain microvascular endothelial cells *in vitro*, demonstrating a dual adhesion phenotype mediated by distinct *P. falciparum* erythrocyte membrane protein 1 domains. *Infection and Immunity,* **82**(3), pp. 949.

ADRIANO, M., VERGNES, B., PONCET, J., MATHIEU-DAUDE, F., DA SILVA, A.C., OUAISSI, A. and SERENO, D., 2007. Proof of interaction between *Leishmania* SIR2RP1 deacetylase and chaperone HSP83. *Parasitology Research,* **100**(4), pp. 811-818.

AGBENYEGA, T., ANGUS, B.J., BEDU-ADDO, G., BAFFOE-BONNIE, B., GUYTON, T., STACPOOLE, P.W. and KRISHNA, S., 2000. Glucose and lactate kinetics in children with severe malaria. *The Journal of Clinical Endocrinology & Metabolism*, **85**(4), pp. 1569-1576.

ALMELLI, T., NDAM, N.T., EZIMEGNON, S., ALAO, M.J., AHOUANSOU, C., SAGBO, G., AMOUSSOU, A., DELORON, P. and TAHAR, R., 2014. Cytoadherence phenotype of *Plasmodium falciparum*- infected erythrocytes is associated with specific PFEMP-1 expression in parasites from children with cerebral malaria. *Malaria Journal*, **13**(1), pp. 333.

AMIT-AVRAHAM, I., POZNER, G., ESHAR, S., FASTMAN, Y., KOLEVZON, N., YAVIN, E. and DZIKOWSKI, R., 2015. Antisense long noncoding RNAs regulate *var* gene activation in the malaria parasite *Plasmodium falciparum*. *Proceedings of the National Academy of Sciences of the United States of America*, **112**(9), pp. E982.

AMULIC, B., SALANTI, A., LAVSTSEN, T., NIELSEN, M.A. and DEITSCH, K.W., 2009. An upstream open reading frame controls translation of *var2csa*, a gene implicated in placental malaria. *PLoS Pathogens*, **5**(1), pp. e1000256; e1000256-e1000256.

ANSTEY, N.M., RUSSELL, B., YEO, T.W. and PRICE, R.N., 2009. The pathophysiology of vivax malaria. *Trends in Parasitology*, **25**(5), pp. 220-227.

AUTINO, B., CORBETT, Y., CASTELLI, F. and TARAMELLI, D., 2012. Pathogenesis of malaria in tissues and blood. *Mediterranean Journal of Hematology and Infectious Diseases*, **4**(1), pp. e2012061-e2012061.

AVALOS, J.L., BOEKE, J.D. and WOLBERGER, C., 2004. Structural basis for the mechanism and regulation of Sir2 enzymes. *Molecular Cell*, **13**(5), pp. 639-648.

AVRIL, M., BERNABEU, M., BENJAMIN, M., BRAZIER, A.J. and SMITH, J.D., 2016. interaction between endothelial protein C receptor and intercellular adhesion molecule 1 to

mediate binding of *Plasmodium falciparum*-infected erythrocytes to endothelial cells. *mBio*, **7**(4), pp. e00615-16.

AZASI, Y., LINDERGARD, G., GHUMRA, A., MU, J., MILLER, L.H. and ROWE, J.A., 2018. Infected erythrocytes expressing DC13 PfEMP1 differ from recombinant proteins in EPCR-binding function. *Proceedings of the National Academy of Sciences of the United States of America*, **115**(5), pp. 1063-1068.

BACHMANN, A., PREDEHL, S., MAY, J., HARDER, S., BURCHARD, G.D., GILBERGER, T., TANNICH, E. and BRUCHHAUS, I., 2011. Highly co-ordinated *var* gene expression and switching in clinical *Plasmodium falciparum* isolates from non-immune malaria patients. *Cellular Microbiology*, **13**(9), pp. 1397-1409.

BALAJI, S., BABU, M.M., IYER, L.M. and ARAVIND, L., 2005. Discovery of the principal specific transcription factors of Apicomplexa and their implication for the evolution of the AP2-integrase DNA binding domains. *Nucleic Acids Research*, **33**(13), pp. 3994-4006.

BANCELLS, C. and DEITSCH, K.W., 2013. A molecular switch in the efficiency of translation reinitiation controls expression of *var2csa*, a gene implicated in pregnancy-associated malaria. *Molecular Microbiology*, **90**(3), pp. 472-488.

BANCELLS, C., LLORÀ-BATLLE, O., PORAN, A., NÖTZEL, C., ROVIRA-GRAELLS, N., ELEMENTO, O., KAFSACK, B.F.C. and CORTÉS, A., 2019. Revisiting the initial steps of sexual development in the malaria parasite *Plasmodium falciparum*. *Nature Microbiology*, 4(1), pp. 144-154.

BANNISTER, L. and MITCHELL, G., 2003. The ins, outs and roundabouts of malaria. *Trends in Parasitology*, **19**(5), pp. 209-213.

BANUMATHY, G., SINGH, V., PAVITHRA, S.R. and TATU, U., 2003. Heat shock protein 90 function is essential for *Plasmodium falciparum* growth in human erythrocytes. *Journal of Biological Chemistry,* **278**(20), pp. 18336-18345.

BARTOLONI, A. and ZAMMARCHI, L., 2012. Clinical aspects of uncomplicated and severe malaria. *Mediterranean Journal of Hematology and Infectious Diseases,* **4**(1), pp. e2012026-e2012026.

BARUCH, D.I., GORMELY, J.A., MA, C., HOWARD, R.J. and PASLOSKE, B.L., 1996. *Plasmodium falciparum* erythrocyte membrane protein 1 is a parasitized erythrocyte receptor for adherence to CD36, thrombospondin, and intercellular adhesion molecule 1. *Proceedings of the National Academy of Sciences of the United States of America*, **93**(8), pp. 3497.

BERGER, S.S., TURNER, L., WANG, C.W., PETERSEN, J.E.V., KRAFT, M., LUSINGU, J.P.A., MMBANDO, B., MARQUARD, A.M., BENGTSSON, D.B.A.C., HVIID, L., NIELSEN, M.A., THEANDER, T.G. and LAVSTSEN, T., 2013. *Plasmodium falciparum* expressing domain cassette 5 type PfEMP1 (DC5-PfEMP1) bind PECAM1. *PloS One*, **8**(7), pp. e69117; e69117-e69117.

BERI, D., RAMDANI, G., BALAN, B., GADARA, D., POOJARY, M., MOMEUX, L., TATU, U. and LANGSLEY, G., 2019. Insights into physiological roles of unique metabolites released from *Plasmodium*-infected RBCs and their potential as clinical biomarkers for malaria. *Scientific Reports,* **9**(1), pp. 2875.

BERNABEU, M., DANZIGER, S.A., AVRIL, M., VAZ, M., BABAR, P.H., BRAZIER, A.J., HERRICKS, T., MAKI, J.N., PEREIRA, L., MASCARENHAS, A., GOMES, E., CHERY, L., AITCHISON, J.D., RATHOD, P.K. and SMITH, J.D., 2016. Severe adult malaria is

associated with specific PfEMP1 adhesion types and high parasite biomass. *Proceedings of the National Academy of Sciences of the United States of America,* **113**(23), pp. E3270.

BHEDA, P., JING, H., WOLBERGER, C. and LIN, H., 2016. The substrate specificity of sirtuins. *Annual Review of Biochemistry,* **85**(1), pp. 405-429.

BISWAS, A.K., HAFIZ, A., BANERJEE, B., KIM, K.S., DATTA, K. and CHITNIS, C.E., 2007. *Plasmodium falciparum* uses gC1qR/HABP1/p32 as a receptor to bind to vascular endothelium and for platelet-mediated clumping. *PLoS Pathogens,* **3**(9), pp. 1271; e130-1280.

BOZDECH, Z., LLINÁS, M., PULLIAM, B.L., WONG, E.D., ZHU, J. and DERISI, J.L., 2003. The Transcriptome of the intraerythrocytic developmental cycle of *Plasmodium falciparum*. *PLOS Biology,* **1**(1), pp. e5.

BRANCUCCI, N.B., BERTSCHI, N., ZHU, L., NIEDERWIESER, I., CHIN, W., WAMPFLER, R., FREYMOND, C., ROTTMANN, M., FELGER, I., BOZDECH, Z. and VOSS, T., 2014. Heterochromatin protein 1 secures survival and transmission of malaria parasites. *Cell Host & Microbe,* **16**(2), pp. 165-176.

BRANCUCCI, N.M.B., GERDT, J.P., WANG, C., DE NIZ, M., PHILIP, N., ADAPA, S.R., ZHANG, M., HITZ, E., NIEDERWIESER, I., BOLTRYK, S.D., LAFFITTE, M.C., CLARK, M.A., GRURING, C., RAVEL, D., BLANCKE SOARES, A., DEMAS, A., BOPP, S., RUBIO-RUIZ, B., CONEJO-GARCIA, A., WIRTH, D.F., GENDASZEWSKA-DARMACH, E., DURAISINGH, M.T., ADAMS, J.H., VOSS, T.S., WATERS, A.P., JIANG, R.H.Y., CLARDY, J. and MARTI, M., 2017. Lysophosphatidylcholine regulates sexual stage differentiation in the human malaria parasite *Plasmodium falciparum*. *Cell JID - 0413066,* **171**(7), pp. 1532-1544.

BRANCUCCI, N.M.B., GOLDOWITZ, I., BUCHHOLZ, K., WERLING, K. and MARTI, M., 2015. An assay to probe *Plasmodium falciparum* growth, transmission stage formation and early gametocyte development. *Nature Protocols,* **10**(8), pp. 1131-1142.

BRANCUCCI, N.M.B., WITMER, K., SCHMID, C. and VOSS, T.S., 2014. A *var* gene upstream element controls protein synthesis at the level of translation initiation in *Plasmodium falciparum*. *PloS One,* **9**(6), pp. e100183.

BROMBERG, Z. and WEISS, Y., 2016. The role of the membrane-initiated heat shock response in cancer. *Frontiers in Molecular Biosciences,* **3**, pp. 12.

BROWN, T.A. and BROWN, T., 2016. Gene cloning and DNA analysis: an introduction. John Wiley & Sons, pp. 3-20

BRYANT, J.M., REGNAULT, C., SCHEIDIG-BENATAR, C., BAUMGARTEN, S., GUIZETTI, J. and SCHERF, A., 2017. CRISPR/cas9 genome editing reveals that the intron is not essential for *var2csa* gene activation or silencing in *Plasmodium falciparum*. *mBio*, **8**(4), pp. e00729-17.

BULL, P.C., LOWE, B.S., KORTOK, M., MOLYNEUX, C.S., NEWBOLD, C.I. and MARSH, K., 1998. Parasite antigens on the infected red cell surface are targets for naturally acquired immunity to malaria. *Nature Medicine*, **4**(3), pp. 358-360.

BUNNIK, E.M., POLISHKO, A., PRUDHOMME, J., PONTS, N., GILL, S.S., LONARDI, S. and LE ROCH, K.,G., 2014. DNA-encoded nucleosome occupancy is associated with transcription levels in the human malaria parasite *Plasmodium falciparum*. *BMC Genomics,* **15**(1), pp. 347-347.

BUSTIN, S. and HUGGETT, J., 2017. qPCR primer design revisited. *Biomolecular Detection and Quantification,* **14**, pp. 19-28.

CARLOS, B.C., FOTORAN, W.L., MENEZES, M.J., CABRAL, F.J., BASTOS, M.F., COSTA, F.T.M., SOUSA-NETO, J.A., RIBOLLA, P.E.M., WUNDERLICH, G. and FERREIRA, M.U., 2016. Expressed *var* gene repertoire and variant surface antigen diversity in a shrinking *Plasmodium falciparum* population. *Experimental Parasitology*, 170, pp. 90-99

CASALS-PASCUAL, C., KAI, O., LOWE, B., ENGLISH, M., WILLIAMS, T.N., MAITLAND, K., NEWTON, C.R.C.J., PESHU, N. and ROBERTS, D.J., 2006. Lactate levels in severe malarial anaemia are associated with haemozoin-containing neutrophils and low levels of IL-12. *Malaria Journal*, **5**(1), pp. 101.

CHAAL, B.K., GUPTA, A.P., WASTUWIDYANINGTYAS, B.D., LUAH, Y. and BOZDECH, Z., 2010. Histone deacetylases play a major role in the transcriptional regulation of the *Plasmodium falciparum* life cycle. *PloS Pathogens*, **6**(1), pp. e1000737.

CHAN, J., FOWKES, F.J.I. and BEESON, J.G., 2014. Surface antigens of *Plasmodium falciparum*-infected erythrocytes as immune targets and malaria vaccine candidates. *Cellular and Molecular Life Sciences*, **71**(19), pp. 3633-3657.

CHAKRABARTY, S.P., SAIKUMARI, Y.K., BOPANNA, M.P. and BALARAM, H., 2008. Biochemical characterization of *Plasmodium falciparum* Sir2, a NAD+-dependent deacetylase. *Molecular and Biochemical Parasitology*, **158**(2), pp. 139-151.

CHAUBEY, S., GROVER, M. and TATU, U., 2014. Endoplasmic reticulum stress triggers gametocytogenesis in the malaria parasite. *The Journal of Biological Chemistry JID - 2985121R*, **289**(24), pp. 16662-16674.

CHEN, Y.,JR, MAHIEU, N.G., HUANG, X., SINGH, M., CRAWFORD, P.A., JOHNSON, S.L., GROSS, R.W., SCHAEFER, J. and PATTI, G.J., 2016. Lactate metabolism is associated with mammalian mitochondria. *Nature Chemical Biology*, **12**(11), pp. 937-943.

CHILDS, R.A., MIAO, J., GOWDA, C. and CUI, L., 2013. An alternative protocol for *Plasmodium falciparum* culture synchronization and a new method for synchrony confirmation. *Malaria Journal*, 12, pp. 386-386.

CHOI, S., KEYES, M.K. and HORROCKS, P., 2006. LC/ESI-MS demonstrates the absence of 5-methyl-2'-deoxycytosine in *Plasmodium falciparum* genomic DNA. *Molecular and Biochemical Parasitology*, **150**(2), pp. 350-352.

CHOOKAJORN, T., DZIKOWSKI, R., FRANK, M., LI, F., JIWANI, A.Z., HARTL, D.L. and DEITSCH, K.W., 2007. Epigenetic memory at malaria virulence genes. *Proceedings of the National Academy of Sciences of the United States of America*, **104**(3), pp. 899-902.

CLAESSENS, A., ADAMS, Y., GHUMRA, A., LINDERGARD, G., BUCHAN, C.C., ANDISI, C., BULL, P.C., MOK, S., GUPTA, A.P., WANG, C.W., TURNER, L., ARMAN, M., RAZA, A., BOZDECH, Z. and ROWE, J.A., 2012. A subset of group A-like *var* genes encodes the malaria parasite ligands for binding to human brain endothelial cells. *Proceedings of the National Academy of Sciences of the United States of America*, **109**(26), pp. E1772-E1781.

COCKBURN, I.A., MACKINNON, M.J., O'DONNELL, A., ALLEN, S.J., MOULDS, J.M., BAISOR, M., BOCKARIE, M., REEDER, J.C. and ROWE, J.A., 2004. A human complement receptor 1 polymorphism that reduces *Plasmodium falciparum* rosetting confers protection against severe malaria. *Proceedings of the National Academy of Sciences of the United States of America*, **101**(1), pp. 272-277.

COETZEE, N., SIDOLI, S., VAN BILJON, R., PAINTER, H., LLINÁS, M., GARCIA, B.A. and BIRKHOLTZ, L., 2017. Quantitative chromatin proteomics reveals a dynamic histone

post-translational modification landscape that defines asexual and sexual *Plasmodium falciparum* parasites. *Scientific Reports,* **7**(1), pp. 607.

COLEMAN, B.I., SKILLMAN, K.M., JIANG, R.H.Y., CHILDS, L.M., ALTENHOFEN, L.M., GANTER, M., LEUNG, Y., GOLDOWITZ, I., KAFSACK, B.F.C., MARTI, M., LLINÁS, M., BUCKEE, C.O. and DURAISINGH, M.T., 2014. A *Plasmodium falciparum* histone deacetylase regulates antigenic variation and gametocyte conversion. *Cell Host & Microbe,* **16**(2), pp. 177-186.

COOPER, R.A., 2002. SDS-PAGE and Western Blotting of *Plasmodium falciparum* Proteins. In: D.L. DOOLAN, ed, *Malaria Methods and Protocols. Methods in Molecular Medicine™.* vol 72 edn. Humana Press, pp. 177.

COULSON, R.M.R., HALL, N. and OUZOUNIS, C.A., 2004. Comparative genomics of transcriptional control in the human malaria parasite *Plasmodium falciparum*. *Genome Research,* **14**(8), pp. 1548-1554.

COWMAN, A.F., HEALER, J., MARAPANA, D. and MARSH, K., 2016. Malaria: biology and disease. *Cell,* **167**(3), pp. 610-624.

CRANMER, S.L., FAU, C.A., FAU, G.W. and HALESTRAP, A.P., 1995. Characterization of the enhanced transport of L- and D-lactate into human red blood cells infected with *Plasmodium falciparum* suggests the presence of a novel saturable lactate proton cotransporter. *The Journal of biological chemistry JID - 2985121R,* **270**(25), pp. 15045-15052.

CUI, L. and MIAO, J., 2010. Chromatin-mediated epigenetic regulation in the malaria parasite *Plasmodium falciparum*. *Eukaryotic cell,* **9**(8), pp. 1138-1149.

CUI, L., MIAO, J. and CUI, L., 2007. Cytotoxic effect of curcumin on malaria parasite *Plasmodium falciparum*: inhibition of histone acetylation and generation of reactive oxygen species. *Antimicrobial Agents and Chemotherapy,* **51**(2), pp. 488-494.

CUNNINGTON, A.J., BRETSCHER, M.T., NOGARO, S.I., RILEY, E.M. and WALTHER, M., 2013. Comparison of parasite sequestration in uncomplicated and severe childhood *Plasmodium falciparum* malaria. *The Journal of Infection,* **67**(3), pp. 220-230.

DABADGHAO, V., SINGH, V., SHARMA, D. and MEENA, B., 2015. A study of serum lactate level in malaria and its correlation with severity of disease. *International Journal of Advanced Medical and Health Research,* **2**(1), pp. 28-32.

DAHLBÄCK, M., LAVSTSEN, T., SALANTI, A., HVIID, L., ARNOT, D.E., THEANDER, T.G. and NIELSEN, M.A., 2007. Changes in *var* gene mRNA levels during erythrocytic development in two phenotypically distinct *Plasmodium falciparum* parasites. *Malaria Journal,* **6**, pp. 78-78.

DAILY, J.P., SCANFELD, D., POCHET, N., LE ROCH, K., PLOUFFE, D., KAMAL, M., SARR, O., MBOUP, S., NDIR, O., WYPIJ, D., LEVASSEUR, K., THOMAS, E., TAMAYO, P., DONG, C., ZHOU, Y., LANDER, E.S., NDIAYE, D., WIRTH, D., WINZELER, E.A., MESIROV, J.P. and REGEV, A., 2007. Distinct physiological states of *Plasmodium falciparum* in malaria-infected patients. *Nature,* **450**, pp. 1091.

DANTZLER, K.W., RAVEL, D.B., BRANCUCCI, N.M. and MARTI, M., 2015. Ensuring transmission through dynamic host environments: host-pathogen interactions in *Plasmodium* sexual development. *Current Opinion in Microbiology,* **26**, pp. 17-23.

DAY, N.P., FAU, P.N., FAU, M.N., FAU, C.T., FAU, L.P., FAU, C.L., FAU, S.D., HOLLOWAY P FAU - HIEN, T.T., FAU, H.T. and WHITE, N.J., 2000. The

pathophysiologic and prognostic significance of acidosis in severe adult malaria. *Critical Care Medicine JID - 0355501,* **28**(6), pp. 1833-1840.

DE NIZ, M., HELM, S., HORSTMANN, S., ANNOURA, T., DEL PORTILLO, H., A., KHAN, S.M. and HEUSSLER, V.T., 2015. In vivo and in vitro characterization of a *Plasmodium* liver stage-specific promoter. *PloS One,* 10(4), pp. e0123473-e0123473.

DE NIZ, M., MEIBALAN, E., MEJIA, P., MA, S., BRANCUCCI, N.M.B., AGOP-NERSESIAN, C., MANDT, R., NGOTHO, P., HUGHES, K.R., WATERS, A.P., HUTTENHOWER, C., MITCHELL, J.R., MARTINELLI, R., FRISCHKNECHT, F., SEYDEL, K.B., TAYLOR, T., MILNER, D., HEUSSLER, V.T. and MARTI, M., 2018. *Plasmodium* gametocytes display homing and vascular transmigration in the host bone marrow. *Science Advances,* **4**(5), pp. eaat3775.

DEITSCH, K., DRISKILL, C. and WELLEMS, T., 2001. Transformation of malaria parasites by the spontaneous uptake and expression of DNA from human erythrocytes. *Nucleic Acids Research,* 29(3), pp. 850-853.

DEITSCH, K.W., CALDERWOOD, M.S. and WELLEMS, T.E., 2001. Cooperative silencing elements in *var* genes. *Nature,* **412**(6850), pp. 875-876.

DELVES, M.J., STRASCHIL, U., RUECKER, A., MIGUEL-BLANCO, C., MARQUES, S., DUFOUR, A.C., BAUM, J. and SINDEN, R.E., 2016. Routine in vitro culture of *P. falciparum* gametocytes to evaluate novel transmission-blocking interventions. *Nature Protocols* JID - 101284307, 11(9), pp. 1668-1680.

DESAI, S.A., KROGSTAD, D.J. and MCCLESKEY, E.W., 1993. A nutrient-permeable channel on the intraerythrocytic malaria parasite. *Nature,* **362**(6421), pp. 643-646.

DUFFY, M.F., NOVIYANTI, R., TSUBOI, T., FENG, Z., TRIANTY, L., SEBAYANG, B.F., TAKASHIMA, E., SUMARDY, F., LAMPAH, D.A., TURNER, L., LAVSTSEN, T., FOWKES, F.J.I., SIBA, P., ROGERSON, S.J., THEANDER, T.G., MARFURT, J., PRICE, R.N., ANSTEY, N.M., BROWN, G.V. and PAPENFUSS, A.T., 2016. Differences in PfEMP1s recognized by antibodies from patients with uncomplicated or severe malaria. *Malaria Journal,* **15**(1), pp. 258-258.

DUFFY, M.F., TANG, J., SUMARDY, F., NGUYEN, H.H.T., SELVARAJAH, S.A., JOSLING, G.A., DAY, K.P., PETTER, M. and BROWN, G.V., 2017. Activation and clustering of a *Plasmodium falciparum var* gene are affected by subtelomeric sequences. *The FEBS Journal,* **284**(2), pp. 237-257.

DUFFY, S. and AVERY, V.M., 2017. *Plasmodium falciparum* in vitro continuous culture conditions: A comparison of parasite susceptibility and tolerance to anti-malarial drugs throughout the asexual intra-erythrocytic life cycle. *International Journal for Parasitology. Drugs and Drug Resistance,* **7**(3), pp. 295-302.

DURAISINGH, M.T., VOSS, T.S., MARTY, A.J., DUFFY, M.F., GOOD, R.T., THOMPSON, J.K., FREITAS-JUNIOR, L., SCHERF, A., CRABB, B.S. and COWMAN, A.F., 2005. Heterochromatin silencing and locus repositioning linked to regulation of virulence genes in *Plasmodium falciparum*. *Cell,* **121**(1), pp. 13-24.

DZIKOWSKI, R. and DEITSCH, K.W., 2008. Active transcription is required for maintenance of epigenetic memory in the malaria parasite *Plasmodium falciparum*. *Journal of Molecular Biology,* **382**(2), pp. 288-297.

DZIKOWSKI, R., FRANK, M. and DEITSCH, K., 2006. Mutually exclusive expression of virulence genes by malaria parasites is regulated independently of antigen production. *PloS Pathogens,* **2**(3), pp. e22.

ELLIOTT, J.L., FAU, S.K. and KIRK, K., 2001. Transport of lactate and pyruvate in the intraerythrocytic malaria parasite, *Plasmodium falciparum*. *The Biochemical Journal JID - 2984726R,* **355**(Pt 3), pp. 733-739.

ELPHINSTONE, R.E., RILEY, F., LIN, T., HIGGINS, S., DHABANGI, A., MUSOKE, C., CSERTI-GAZDEWICH, C., REGAN, R.F., WARREN, H.S. and KAIN, K.C., 2015. Dysregulation of the haem-haemopexin axis is associated with severe malaria in a case-control study of Ugandan children. *Malaria Journal,* **14**(1), pp. 511.

ENGEL, J.A., NORRIS, E.L., GILSON, P., PRZYBORSKI, J., SHONHAI, A., BLATCH, G.L., SKINNER-ADAMS, T., GORMAN, J., HEADLAM, M. and ANDREWS, K.T., 2019. Proteomic analysis of *Plasmodium falciparum* histone deacetylase 1 complex proteins. *Experimental Parasitology,* **198**, pp. 7-16.

ENGLISH, M., SAUERWEIN, R.F., WARUIRU, C.F., MOSOBO, M.F., OBIERO, J.F., LOWE, B.F. and MARSH, K., 1997. Acidosis in severe childhood malaria. *QJM: Monthly Journal of the Association of Physicians JID - 9438285,* **90**(4), pp. 263-270.

EPP, C., LI, F., HOWITT, C.A., CHOOKAJORN, T. and DEITSCH, K.W., 2009. Chromatin associated sense and antisense noncoding RNAs are transcribed from the *var* gene family of virulence genes of the malaria parasite *Plasmodium falciparum*. *RNA (New York, N.Y.),* **15**(1), pp. 116-127.

EPP, C., RASKOLNIKOV, D. and DEITSCH, K.W., 2008. A regulatable transgene expression system for cultured *Plasmodium falciparum* parasites. *Malaria Journal*, 7, pp. 86-86.

FAN, Q., AN, L. and CUI, L., 2004. *Plasmodium falciparum* histone acetyltransferase, a yeast GCN5 homologue involved in chromatin remodelling. *Eukaryotic Cell*, **3**(2), pp. 264-276.

FASTMAN, Y., NOBLE, R., RECKER, M. and DZIKOWSKI, R., 2012. Erasing the epigenetic memory and beginning to switch--the onset of antigenic switching of *var* genes in *Plasmodium falciparum*. *PloS One*, **7**(3), pp. e34168; e34168-e34168.

FAUBERT, B., LI, K.Y., CAI, L., HENSLEY, C.T., KIM, J., ZACHARIAS, L.G., YANG, C., DO, Q.N., DOUCETTE, S., BURGUETE, D., LI, H., HUET, G., YUAN, Q., WIGAL, T., BUTT, Y., NI, M., TORREALBA, J., OLIVER, D., LENKINSKI, R.E., MALLOY, C.R., WACHSMANN, J.W., YOUNG, J.D., KERNSTINE, K. and DEBERARDINIS, R.J., 2017. Lactate metabolism in human lung tumors. *Cell*, **171**(2), pp. 358-371.e9.

FEDER, M.E. and HOFMANN, G.E., 1999. HEAT-SHOCK PROTEINS, MOLECULAR CHAPERONES, AND THE STRESS RESPONSE: Evolutionary and ecological physiology. *Annual Review of Physiology*, **61**(1), pp. 243-282.

FILARSKY, M., FRASCHKA, S.A., NIEDERWIESER, I., BRANCUCCI, N.M.B., CARRINGTON, E., CARRIÃ³, E., MOES, S., JENOE, P., BÃ¡RTFAI, R. and VOSS, T.S., 2018. GDV1 induces sexual commitment of malaria parasites by antagonizing HP1-dependent gene silencing. *Science*, **359**(6381), pp. 1259.

FLUECK, C., BARTFAI, R., VOLZ, J., NIEDERWIESER, I., SALCEDO-AMAYA, A., ALAKO, B.T.F., EHLGEN, F., RALPH, S.A., COWMAN, A.F., BOZDECH, Z.,

STUNNENBERG, H.G. and VOSS, T.S., 2009. *Plasmodium falciparum* heterochromatin protein 1 marks genomic loci linked to phenotypic variation of exported virulence factors. *PloS Pathogens,* **5**(9), pp. e1000569.

FOTH, B.J., ZHANG, N., CHAAL, B.K., SZE, S.K., PREISER, P.R. and BOZDECH, Z., 2011. Quantitative time-course profiling of parasite and host cell proteins in the human malaria parasite *Plasmodium falciparum*. *Molecular & Cellular Proteomics*: MCP, 10(8), pp. M110.006411-M110.006411.

FOX, L.L., TAYLOR, T.E., PENSULO, P., LIOMBA, A., MPAKIZA, A., VARELA, A., GLOVER, S.J., REEVES, M.J. and SEYDEL, K.B., 2013. Histidine-rich protein 2 plasma levels predict progression to cerebral malaria in Malawian children with *Plasmodium falciparum* infection. *The Journal of Infectious Diseases,* **208**(3), pp. 500-503.

FRANCISCHETTI, I.M.B., SEYDEL, K.B. and MONTEIRO, R.Q., 2008. Blood Coagulation, Inflammation, and Malaria. *Microcirculation,* **15**(2), pp. 81-107.

FRANK, M., DZIKOWSKI, R., AMULIC, B. and DEITSCH, K., 2007. Variable switching rates of malaria virulence genes are associated with chromosomal position. *Molecular Microbiology,* **64**(6), pp. 1486-1498.

FRANK, M., DZIKOWSKI, R., COSTANTINI, D., AMULIC, B., BERDOUGO, E. and DEITSCH, K., 2006. Strict pairing of *var* promoters and introns is required for *var* gene silencing in the malaria parasite *Plasmodium falciparum*. *Journal of Biological Chemistry,* **281**(15), pp. 9942-9952.

FREITAS-JUNIOR, L., HERNANDEZ-RIVAS, R., RALPH, S.A., MONTIEL-CONDADO, D., RUVALCABA-SALAZAR, O., ROJAS-MEZA, A., MÂNCIO-SILVA, L., LEAL-SILVESTRE, R., GONTIJO, A.M., SHORTE, S. and SCHERF, A., 2005. Telomeric

heterochromatin propagation and histone acetylation control mutually exclusive expression of antigenic variation genes in malaria parasites. *Cell,* **121**(1), pp. 25-36.

FRENCH, J.B., CEN, Y. and SAUVE, A.A., 2008. *Plasmodium falciparum* Sir2 is an NAD+-dependent deacetylase and an acetyllysine-dependent and acetyllysine-independent NAD+ glycohydrolase. *Biochemistry,* **47**(38), pp. 10227-10239.

FRIED, M. and DUFFY, P.E., 1996. Adherence of *Plasmodium falciparum* to chondroitin sulfate A in the human placenta. *Science,* **272**(5267), pp. 1502.

GARDINER, D.L. and TRENHOLME, K.R., 2015. *Plasmodium falciparum* gametocytes: playing hide and seek. *Annals of Translational Medicine,* **3**(4), pp. 45; 45-45.

GARDNER, J.P., PINCHES, R.A., ROBERTS, D.J. and NEWBOLD, C.I., 1996. Variant antigens and endothelial receptor adhesion in *Plasmodium falciparum*. *Proceedings of the National Academy of Sciences of the United States of America,* **93**(8), pp. 3503.

GARDNER, M.J., HALL, N., FUNG, E., WHITE, O., BERRIMAN, M., HYMAN, R.W., CARLTON, J.M., PAIN, A., NELSON, K.E. and BOWMAN, S., 2002. Genome sequence of the human malaria parasite *Plasmodium falciparum*. *Nature,* **419**(6906), pp. 498-511.

GAZZINELLI, R.T., KALANTARI, P., FITZGERALD, K.A. and GOLENBOCK, D.T., 2014. Innate sensing of malaria parasites. *Nature Reviews Immunology,* **14**, pp. 744.

GINSBURG, H. and STEIN, W.D., 2004. The new permeability pathways induced by the malaria parasite in the membrane of the infected erythrocyte: comparison of results using different experimental techniques. *The Journal of Membrane Biology,* **197**(2), pp. 113-134.

GOEL, S., PALMKVIST, M., MOLL, K., JOANNIN, N., LARA, P., R AKHOURI, REETESH, MORADI, N., ÖJEMALM, K., WESTMAN, M., ANGELETTI, D., KJELLIN,

H., LEHTIÖ, J., BLIXT, O., IDESTRÖM, L., GAHMBERG, C.G., STORRY, J.R., HULT, A.K., OLSSON, M.L., VON HEIJNE, G., NILSSON, I. and WAHLGREN, M., 2015. RIFINs are adhesins implicated in severe *Plasmodium falciparum* malaria. *Nature medicine,* **21**, pp. 314.

GOMES, A.P., VITORINO, R.R., COSTA, A.D.P., MENDONÇA, E., GOMES DE, OLIVEIRA, M.G.D.A. and SIQUEIRA-BATISTA, R., 2011. Severe *Plasmodium falciparum* malaria. *Revista Brasileira de Terapia Intensiva,* **23**, pp. 358-369.

GONÇALVES, B.P., HUANG, C., MORRISON, R., HOLTE, S., KABYEMELA, E., PREVOTS, D.R., FRIED, M. and DUFFY, P.E., 2014. Parasite burden and severity of malaria in Tanzanian children. *The New England Journal of Medicine,* **370**(19), pp. 1799-1808.

GOONEWARDENE, R., DAILY, J., KASLOW, D., SULLIVAN, T.J., DUFFY, P., CARTER, R., MENDIS, K. and WIRTH, D., 1993. Transfection of the malaria parasite and expression of firefly luciferase. *Proceedings of the National Academy of Sciences of the United States of America,* **90**(11), pp. 5234-5236.

GUPTA, A.P., CHIN, W.H., ZHU, L., MOK, S., LUAH, Y., LIM, E. and BOZDECH, Z., 2013. Dynamic epigenetic regulation of gene expression during the life cycle of malaria parasite *Plasmodium falciparum*. *PloS Pathogens,* **9**(2), pp. e1003170.

HAPUARACHCHI, S.V., COBBOLD, S.A., SHAFIK, S.H., DENNIS, A.S.M., MCCONVILLE, M.J., MARTIN, R.E., KIRK, K. and LEHANE, A.M., 2017. The malaria parasite's lactate transporter PfFNT is the target of antiplasmodial compounds identified in whole cell phenotypic screens. *PloS Pathogens,* **13**(2), pp. e1006180.

HARRISON, E.M., GARDEN, O.J., ROSS, J.A. and WIGMORE, S.J., 2006. Firefly luciferase terminally degraded by mild heat exposure: Implications for reporter assays. *Journal of Immunological Methods*. 310(1-2), pp.182-5

HASENKAMP, S., SIDAWAY, A., DEVINE, O., ROYE, R. and HORROCKS, P., 2013. Evaluation of bioluminescence-based assays of anti-malarial drug activity. *Malaria Journal*, **12**, pp. 58-58.

HASENKAMP, S., WONG, E.H. and HORROCKS, P., 2012. An improved single-step lysis protocol to measure luciferase bioluminescence in *Plasmodium falciparum*. *Malaria Journal*, **11**(1), pp. 42.

HERDMAN, M.T., SRIBOONVORAKUL, N., LEOPOLD, S.J., DOUTHWAITE, S., MOHANTY, S., HASSAN, M.M., MAUDE, R.J., KINGSTON, H.W.F., PLEWES, K., CHARUNWATTHANA, P., SILAMUT, K., WOODROW, C.J., GHOSE, A., CHOTINAVICH, K., HOSSAIN, M.A., FAIZ, M.A., MISHRA, S., LEEPIPATPIBOON, N., WHITE, N.J., DAY, N.P.J., TARNING, J. and DONDORP, A.M., 2015. The role of previously unmeasured organic acids in the pathogenesis of severe malaria. *Critical Care (London, England)*, **19**(1), pp. 317; 317-317.

HIKOSAKA, K., HIRAI, M., KOMATSUYA, K., ONO, Y. and KITA, K., 2015. Lactate retards the development of erythrocytic stages of the human malaria parasite *Plasmodium falciparum*. *Parasitology International*, **64**(3), pp. 301-303.

HORROCKS, P., PINCHES, R., CHRISTODOULOU, Z., KYES, S.A. and NEWBOLD, C.I., 2004. Variable *var* transition rates underlie antigenic variation in malaria. *Proceedings of the National Academy of Sciences of the United States of America*, **101**(30), pp. 11129-11134.

HORROCKS, P., PINCHES, R.A., CHAKRAVORTY, S.J., PAPAKRIVOS, J., CHRISTODOULOU, Z., KYES, S.A., URBAN, B.C., FERGUSON, D.J.P. and NEWBOLD, C.I., 2005. PfEMP1 expression is reduced on the surface of knobless *Plasmodium falciparum* infected erythrocytes. *Journal of Cell Science,* **118**(11), pp. 2507.

HORROCKS, P., WONG, E., RUSSELL, K. and EMES, R.D., 2009. Control of gene expression in *Plasmodium falciparum* - ten years on. *Molecular and Biochemical Parasitology,* **164**(1), pp. 9-25.

HOWELL, D.P.-., LEVIN, E.A., SPRINGER, A.L., KRAEMER, S.M., PHIPPARD, D.J., SCHIEF, W.R. and SMITH, J.D., 2008. Mapping a common interaction site used by *Plasmodium falciparum* Duffy binding-like domains to bind diverse host receptors. *Molecular Microbiology,* **67**(1), pp. 78-87.

HU, S., ZHU, X., TRIGGS, J.R., TAO, Y., WANG, Y., LICHTENSTEIN, L., BISSONNETTE, M., MUSCH, M.W. and CHANG, E.B., 2009. Inflammation-induced, 3'UTR-dependent translational inhibition of Hsp70 mRNA impairs intestinal homeostasis. *American Journal of Physiology. Gastrointestinal and Liver Physiology,* **296**(5), pp. G1003-G1011.

HUI, S., GHERGUROVICH, J.M., MORSCHER, R.J., JANG, C., TENG, X., LU, W., ESPARZA, L.A., REYA, T., LE ZHAN, YANXIANG GUO, J., WHITE, E. and RABINOWITZ, J.D., 2017. Glucose feeds the TCA cycle via circulating lactate. *Nature,* **551**, pp. 115.

IGNOWSKI, J.M. and SCHAFFER, D.V., 2004. Kinetic analysis and modelling of firefly luciferase as a quantitative reporter gene in live mammalian cells. *Biotechnology and Bioengineering JID - 7502021,* **86**(7), pp. 827-834.

ISHIOKA, H., GHOSE, A., CHARUNWATTHANA, P., MAUDE, R., PLEWES, K., KINGSTON, H., INTHARABUT, B., WOODROW, C., CHOTIVANICH, K., SAYEED, A.A., HASAN, M.U., DAY, N.P., FAIZ, A., WHITE, N.J., HOSSAIN, A. and DONDORP, A.M., 2016. Sequestration and red cell deformability as determinants of hyperlactatemia in falciparum malaria. *The Journal of infectious diseases*, **213**(5), pp. 788-793.

JENINGA, D.M., QUINN, E.J. and PETTER, M., 2019. ApiAP2 transcription factors in apicomplexan parasites. *Pathogens*, 8(2), pp. 47.

JENSEN, A.T.R., MAGISTRADO, P., SHARP, S., JOERGENSEN, L., LAVSTSEN, T., CHIUCCHIUINI, A., SALANTI, A., VESTERGAARD, L.S., LUSINGU, J.P., HERMSEN, R., SAUERWEIN, R., CHRISTENSEN, J., NIELSEN, M.A., HVIID, L., SUTHERLAND, C., STAALSOE, T. and THEANDER, T.G., 2004. *Plasmodium falciparum* associated with severe childhood malaria preferentially expresses PfEMP1 encoded by group A *var* genes. *The Journal of Experimental Medicine*, **199**(9), pp. 1179-1190.

JENSEN, M.D., CONLEY, M. and HELSTOWSKI, L.D., 1983. Culture of *Plasmodium falciparum*: The role of pH, glucose, and lactate. *The Journal of Parasitology*, **69**(6), pp. 1060-1067.

JESPERSEN, J.S., WANG, C.W., MKUMBAYE, S.I., MINJA, D.T.R., PETERSEN, B., TURNER, L., PETERSEN, J.E.V., LUSINGU, J.P.A., THEANDER, T.G. and LAVSTSEN, T., 2016. *Plasmodium falciparum var* genes expressed in children with severe malaria encode CIDRα1 domains. *EMBO Molecular Medicine*, **8**(8), pp. 839.

JIANG, L., MU, J., ZHANG, Q., NI, T., SRINIVASAN, P., RAYAVARA, K., YANG, W., TURNER, L., LAVSTSEN, T., THEANDER, T.G., PENG, W., WEI, G., JING, Q., WAKABAYASHI, Y., BANSAL, A., LUO, Y., RIBEIRO, J.M.C., SCHERF, A.,

ARAVIND, L., ZHU, J., ZHAO, K. and MILLER, L.H., 2013. PfSETvs methylation of histone H3K36 represses virulence genes in *Plasmodium falciparum*. *Nature,* **499**(7457), pp. 223-227.

JING, Q., CAO, L., ZHANG, L., CHENG, X., GILBERT, N., DAI, X., SUN, M., LIANG, S. and JIANG, L., 2018. *Plasmodium falciparum var* gene is activated by its antisense long noncoding RNA. *Frontiers in Microbiology,* **9**, pp. 3117.

JOERGENSEN, L., BENGTSSON, D.C., BENGTSSON, A., RONANDER, E., BERGER, S.S., TURNER, L., DALGAARD, M.B., CHAM, G.K.K., VICTOR, M.E., LAVSTSEN, T., THEANDER, T.G., ARNOT, D.E. and JENSEN, A.T.R., 2010. Surface co-expression of two different PfEMP1 antigens on single plasmodium falciparum-infected erythrocytes facilitates binding to ICAM1 and PECAM1. *PLoS Pathogens,* **6**(9), pp. e1001083; e1001083-e1001083.

JOICE, R., NILSSON, S.K., MONTGOMERY, J., DANKWA, S., EGAN, E., MORAHAN, B., SEYDEL, K.B., BERTUCCINI, L., ALANO, P., WILLIAMSON, K.C., DURAISINGH, M.T., TAYLOR, T.E., MILNER, D.A. and MARTI, M., 2014. *Plasmodium falciparum* transmission stages accumulate in the human bone marrow. *Science Translational Medicine,* **6**(244), pp. 244re5-244re5.

JOSHI, M.B., LIN, D.T., CHIANG, P.H., GOLDMAN, N.D., FUJIOKA, H., AIKAWA, M. and SYIN, C., 1999. Molecular cloning and nuclear localization of a histone deacetylase homologue in *Plasmodium falciparum*. *Molecular and Biochemical Parasitology,* **99**(1), pp. 11-19.

JOSLING, G.A., WILLIAMSON, K.C. and LLINÁS, M., 2018. Regulation of sexual commitment and gametocytogenesis in malaria parasites. *Annual Review of Microbiology,* **72**(1), pp. 501-519.

KAESTLI, M., COCKBURN, I.A., CORTÉS, A., BAEA, K., ROWE, J.A. and BECK, H., 2006. Virulence of malaria is associated with differential expression of *Plasmodium falciparum var* gene subgroups in a case-control study. *The Journal of Infectious Diseases,* **193**(11), pp. 1567-1574.

KAFSACK, B.F.C., ROVIRA-GRAELLS, N., CLARK, T.G., BANCELLS, C., CROWLEY, V.M., CAMPINO, S.G., WILLIAMS, A.E., DROUGHT, L.G., KWIATKOWSKI, D.P., BAKER, D.A., CORTÉS, A. and LLINÁS, M., 2014. A transcriptional switch underlies commitment to sexual development in malaria parasites. *Nature,* **507**(7491), pp. 248-252.

KALMBACH, Y., ROTTMANN, M., KOMBILA, M., KREMSNER, P.G., BECK, H. and KUN, J., 2010. Differential *var* gene expression in children with malaria and antidromic effects on host gene expression. *The Journal of Infectious Diseases,* **202**(2), pp. 313-317.

KANYAL, A., RAWAT, M., GURUNG, P., CHOUBEY, D., ANAMIKA, K. and KARMODIYA, K., 2018. Genome-wide survey and phylogenetic analysis of histone acetyltransferases and histone deacetylases of *Plasmodium falciparum*. *The FEBS Journal,* **285**(10), pp. 1767-1782.

KARMODIYA, K., PRADHAN, S.J., JOSHI, B., JANGID, R., REDDY, P.C. and GALANDE, S., 2015. A comprehensive epigenome map of *Plasmodium falciparum* reveals unique mechanisms of transcriptional regulation and identifies H3K36me2 as a global mark of gene suppression. *Epigenetics & Chromatin,* **8**(1), pp. 32.

KIRK, K., HORNER, H.A., ELFORD, B.C., ELLORY, J.C. and NEWBOLD, C.I., 1994. Transport of diverse substrates into malaria-infected erythrocytes via a pathway showing functional characteristics of a chloride channel. *Journal of Biological Chemistry,* **269**(5), pp. 3339-3347.

KOMAKI-YASUDA, K., OKUWAKI, M., KANO, S., NAGATA, K. and KAWAZU, S., 2008. 5′ sequence- and chromatin modification-dependent gene expression in *Plasmodium falciparum* erythrocytic stage. *Molecular and Biochemical Parasitology*, **162**(1), pp. 40-51

KRIEK, N., TILLEY, L., HORROCKS, P., PINCHES, R., ELFORD, B.C., FERGUSON, D.J.P., LINGELBACH, K. and NEWBOLD, C.I., 2003. Characterization of the pathway for transport of the cytoadherence-mediating protein, PfEMP1, to the host cell surface in malaria parasite-infected erythrocytes. *Molecular Microbiology*, **50**(4), pp. 1215-1227.

KRISHNA, S., WALLER, D.W. and KUILE, F.E.A., 1994. Lactic acidosis and hypoglycemia in children with severe malaria: pathophysiological and prognostic significance. *Transactions of the Royal Society of Tropical Medicine & Hygiene*, (88), pp. 67-73.

KÜLZER, S., CHARNAUD, S., DAGAN, T., RIEDEL, J., MANDAL, P., PESCE, E.R., BLATCH, G.L., CRABB, B.S., GILSON, P.R. and PRZYBORSKI, J.M., 2012. *Plasmodium falciparum*-encoded exported Hsp70/Hsp40 chaperone/co-chaperone complexes within the host erythrocyte. *Cellular Microbiology*, 14(11), pp. 1784-1795.

KÜLZER, S., RUG, M., BRINKMANN, K., CANNON, P., COWMAN, A., LINGELBACH, K., BLATCH, G.L., MAIER, A.G. and PRZYBORSKI, J.M., 2010. Parasite-encoded Hsp40 proteins define novel mobile structures in the cytosol of the *P. falciparum*-infected erythrocyte. *Cellular Microbiology*, **12**(10), pp. 1398-1420.

KWIATKOWSKI, D., 1989. Febrile temperatures can synchronize the growth of *Plasmodium falciparum* in vitro. *The Journal of Experimental Medicine*, **169**(1), pp. 357-361.

KYES, S., PINCHES, R. and NEWBOLD, C., 2000. A simple RNA analysis method shows *var* and *rif* multigene family expression patterns in *Plasmodium falciparum*. *Molecular and Biochemical Parasitology*, **105**(2), pp. 311-315.

KYES, S.A., KRAEMER, S.M. and SMITH, J.D., 2007. Antigenic variation in *Plasmodium falciparum*: gene organization and regulation of the *var* multigene family. *Eukaryote Cell,* **6**(9), pp. 1511.

KYRIACOU, H.M., STONE, G.N., CHALLIS, R.J., RAZA, A., LYKE, K.E., THERA, M.A., KONÉ, A., K., DOUMBO, O.K., PLOWE, C.V. and ROWE, J.A., 2006. Differential *var* gene transcription in *Plasmodium falciparum* isolates from patients with cerebral malaria compared to hyperparasitaemia. *Molecular and Biochemical Parasitology,* **150**(2), pp. 211-218.

LAMBERT, S.A., JOLMA, A., CAMPITELLI, L.F., DAS, P.K., YIN, Y., ALBU, M., CHEN, X., TAIPALE, J., HUGHES, T.R. and WEIRAUCH, M.T., 2018. The human transcription factors. *Cell,* **172**(4), pp. 650-665.

LAMBROS, C. and VANDERBERG, J.P., 1979. Synchronization of *Plasmodium falciparum* erythrocytic stages in culture. *The Journal of Parasitology,* **65**(3), pp. 418-420.

LAMOUR, S.D., STRASCHIL, U., SARIC, J. and DELVES, M.J., 2014. Changes in metabolic phenotypes of *Plasmodium falciparum* in vitro cultures during gametocyte development. *Malaria Journal,* **13**(1), pp. 468.

LAVSTSEN, T., SALANTI, A., JENSEN, A.T.R., ARNOT, D.E. and THEANDER, T.G., 2003. Sub-grouping of *Plasmodium falciparum* 3D7 *var* genes based on sequence analysis of coding and non-coding regions. *Malaria Journal,* **2**(1), pp. 27.

LAVSTSEN, T., TURNER, L., SAGUTI, F., MAGISTRADO, P., RASK, T.S., JESPERSEN, J.S., WANG, C.W., BERGER, S.S., BARAKA, V., MARQUARD, A.M., SEGUIN-ORLANDO, A., WILLERSLEV, E., GILBERT, M.T., LUSINGU, J. and THEANDER, T.G., 2012. *Plasmodium falciparum* erythrocyte membrane protein 1 domain cassettes 8 and 13 are

associated with severe malaria in children. *Proceedings of the National Academy of Sciences of the United States of America,* **109**(26), pp. E1791-E1800.

LE ROCH, K., G., JOHNSON, J.R., FLORENS, L., ZHOU, Y., SANTROSYAN, A., GRAINGER, M., YAN, S.F., WILLIAMSON, K.C., HOLDER, A.A., CARUCCI, D.J., YATES, JOHN R.,3RD and WINZELER, E.A., 2004. Global analysis of transcript and protein levels across the *Plasmodium falciparum* life cycle. *Genome Research,* 14(11), pp. 2308-2318.

LEOPOLD, S.J., GHOSE, A., ALLMAN, E.L., KINGSTON, H.W.F., HOSSAIN, A., DUTTA, A.K., PLEWES, K., CHOTIVANICH, K., DAY, N.P.J., TARNING, J., WINTERBERG, M., WHITE, N.J., LLINÁS, M. and DONDORP, A.M., 2018. Identifying the components of acidosis in patients with severe *Plasmodium falciparum* malaria using metabolomics. *The Journal of Infectious Diseases,* **219**(11), pp. 1766-1776.

LEROUX, M., LAKSHMANAN, V. and DAILY, J.P., 2009. *Plasmodium falciparum* biology: analysis of in vitro versus in vivo growth conditions. *Trends in Parasitology,* **25**(10), pp. 474-481.

LIVAK, K.J. and SCHMITTGEN, T.D., 2001. Analysis of relative gene expression data using real-time quantitative PCR and the 2(-Delta Delta C(T)) Method. *Methods,* **25**(4), pp. 402–408.

LOPEZ-RUBIO, J., GONTIJO, A.M., NUNES, M.C., ISSAR, N., HERNANDEZ RIVAS, R. and SCHERF, A., 2007. 5' flanking region of *var* genes nucleate histone modification patterns linked to phenotypic inheritance of virulence traits in malaria parasites. *Molecular Microbiology,* **66**(6), pp. 1296-1305.

LOPEZ-RUBIO, J., MANCIO-SILVA, L. and SCHERF, A., 2009. Genome-wide analysis of heterochromatin associates clonally variant gene regulation with perinuclear repressive centers in malaria parasites. *Cell Host & Microbe,* **5**(2), pp. 179-190.

LU, S. and LIN, S., 2010. Regulation of yeast sirtuins by NAD(+) metabolism and calorie restriction. *Biochimica et Biophysica Acta,* **1804**(8), pp. 1567-1575.

LU, X., BATUGEDARA, G., LEE, M., PRUDHOMME, J., BUNNIK, E.M. and LEÂ ROCH, K., 2017. Nascent RNA sequencing reveals mechanisms of gene regulation in the human malaria parasite *Plasmodium falciparum*. *Nucleic Acids Research,* **45**(13), pp. 7825-7840.

MACRAE, J.I., FAU, D.M., FAU, D.M., FAU, C.H., FAU, C.J., KENNY, S.F., BOTTOVA, I.F., TILLEY L FAU - MCCONVILLE, MALCOLM, J. and MCCONVILLE, M.J., 2013. Mitochondrial metabolism of sexual and asexual blood stages of the malaria parasite *Plasmodium falciparum*. *BMC Biology JID - 101190720,* **11**(67).

MANCIO-SILVA, L., SLAVIC, K., GRILO RUIVO, M.T., GROSSO, A.R., MODRZYNSKA, K.K., VERA, I.M., SALES-DIAS, J., GOMES, A.R., MACPHERSON, C.R., CROZET, P., ADAMO, M., BAENA-GONZALEZ, E., TEWARI, R., LLINÁS, M., BILLKER, O. and MOTA, M.M., 2017. Nutrient sensing modulates malaria parasite virulence. *Nature,* **547**, pp. 213.

MANNING, L., LAMAN, M., DAVIS, W.A. and DAVIS, T.M.E., 2014. Clinical features and outcome in children with severe *Plasmodium falciparum* malaria: a meta-analysis. *PloS One,* **9**(2), pp. e86737; e86737-e86737.

MANSKE, M., MIOTTO, O., CAMPINO, S., AUBURN, S., ALMAGRO-GARCIA, J., MASLEN, G., O'BRIEN, J., DJIMDE, A., DOUMBO, O., ZONGO, I., OUEDRAOGO, J.,

MICHON, P., MUELLER, I., SIBA, P., NZILA, A., BORRMANN, S., KIARA, S.M., MARSH, K., JIANG, H., SU, X., AMARATUNGA, C., FAIRHURST, R., SOCHEAT, D., NOSTEN, F., IMWONG, M., WHITE, N.J., SANDERS, M., ANASTASI, E., ALCOCK, D., DRURY, E., OYOLA, S., QUAIL, M.A., TURNER, D.J., RUANO-RUBIO, V., JYOTHI, D., AMENGA-ETEGO, L., HUBBART, C., JEFFREYS, A., ROWLANDS, K., SUTHERLAND, C., ROPER, C., MANGANO, V., MODIANO, D., TAN, J.C., FERDIG, M.T., AMAMBUA-NGWA, A., CONWAY, D.J., TAKALA-HARRISON, S., PLOWE, C.V., RAYNER, J.C., ROCKETT, K.A., CLARK, T.G., NEWBOLD, C.I., BERRIMAN, M., MACINNIS, B. and KWIATKOWSKI, D.P., 2012. Analysis of *Plasmodium falciparum* diversity in natural infections by deep sequencing. *Nature*, **487**(7407), pp. 375-379.

MARCHETTI, R.V., LEHANE, A.M., SHAFIK, S.H., WINTERBERG, M., MARTIN, R.E. and KIRK, K., 2015. A lactate and formate transporter in the intraerythrocytic malaria parasite, *Plasmodium falciparum*. *Nature Communications*, **6**, pp. 6721.

MARIGA, S.T., KOLKO, M., GJEDDE, A. and BERGERSEN, L.H., 2014. Lactate transport and receptor actions in cerebral malaria. *Frontiers in Neuroscience*, **8**, pp. 125; 125-125.

MAYER, C., SLATER, L., ERAT, M.C., KONRAT, R. and VAKONAKIS, I., 2012. Structural Analysis of the *Plasmodium falciparum* erythrocyte membrane protein 1 (PfEMP1) intracellular domain reveals a conserved interaction epitope. *Journal of Biological Chemistry*, **287**(10), pp. 7182-7189.

MCGREGOR, I.A., WILSON, M.E. and BILLEWICZ, W.Z., 1983. Malaria infection of the placenta in the Gambia, West Africa; its incidence and relationship to stillbirth, birthweight and placental weight. *Transactions of the Royal Society of Tropical Medicine and Hygiene*, **77**(2), pp. 232-244.

MÉNARD, R., 2013-last update, Malaria: methods and protocols [Homepage of Humana: Springer [distributor]], [Online].

MÉNARD, R., HEUSSLER, V., YUDA, M. and NUSSENZWEIG, V., 2008. *Plasmodium* pre-erythrocytic stages: what's new? *Trends in Parasitology,* **24**(12), pp. 564-569.

MERRICK, C.J. and DURAISINGH, M.T., 2007. *Plasmodium falciparum* Sir2: an unusual sirtuin with dual histone deacetylase and ADP-ribosyltransferase activity. *Eukaryotic Cell,* **6**(11), pp. 2081-2091.

MERRICK, C.J. and DURAISINGH, M.T., 2010. Epigenetics in *Plasmodium*: what do we really know? *Eukaryotic Cell,* **9**(8), pp. 1150-1158.

MERRICK, C.J., DZIKOWSKI, R., IMAMURA, H., CHUANG, J., DEITSCH, K. and DURAISINGH, M.T., 2010. The effect of *Plasmodium falciparum* Sir2a histone deacetylase on clonal and longitudinal variation in expression of the *var* family of virulence genes. *International Journal for Parasitology,* **40**(1), pp. 35-43.

MERRICK, C.J., HUTTENHOWER, C., BUCKEE, C., AMAMBUA-NGWA, A., GOMEZ-ESCOBAR, N., WALTHER, M., CONWAY, D.J. and DURAISINGH, M.T., 2012. Epigenetic dysregulation of virulence gene expression in severe *Plasmodium falciparum* malaria. *The Journal of Infectious Diseases,* **205**(10), pp. 1593-1600.

MERRICK, C.J., JIANG, R.H.Y., SKILLMAN, K.M., SAMARAKOON, U., MOORE, R.M., DZIKOWSKI, R., FERDIG, M.T. and DURAISINGH, M.T., 2015. Functional Analysis of Sirtuin Genes in Multiple *Plasmodium falciparum* Strains. *PLOS ONE,* **10**(3), pp. e0118865.

MIAO, J., FAN, Q., CUI, L., LI, J., LI, J. and CUI, L., 2006. The malaria parasite *Plasmodium falciparum* histones: Organization, expression, and acetylation. *Gene,* **369**, pp. 53-65.

MIAO, J., FAN, Q., CUI, L., LI, X., WANG, H., NING, G., REESE, J.C. and CUI, L., 2010. The MYST family histone acetyltransferase regulates gene expression and cell cycle in malaria parasite *Plasmodium falciparum*. *Molecular Microbiology,* **78**(4), pp. 883-902.

MILLER, L.H., ACKERMAN, H.C., SU, X. and WELLEMS, T.E., 2013. Malaria biology and disease pathogenesis: insights for new treatments. *Nature Medicine,* **19**(2), pp. 156-167.

MOCKENHAUPT, F.P., EHRHARDT, S., BURKHARDT, J., BOSOMTWE, S.Y., LARYEA, S., ANEMANA, S.D., OTCHWEMAH, R.N., CRAMER, J.P., DIETZ, E., GELLERT, S. and BIENZLE, U., 2004. Manifestation and outcome of severe malaria in children in northern Ghana. *The American Journal of Tropical Medicine and Hygiene,* **71**(2), pp. 167-172.

MOK, B.W., RIBACKE, U., RASTI, N., KIRONDE, F., CHEN, Q., NILSSON, P. and WAHLGREN, M., 2008. Default pathway of *var2csa* switching and translational repression in *Plasmodium falciparum*. *PloS One,* **3**(4), pp. e1982; e1982-e1982.

MORLAND, C., LAURITZEN, K.H., PUCHADES, M., HOLM-HANSEN, S., ANDERSSON, K., GJEDDE, A., ATTRAMADAL, H., STORM-MATHISEN, J. and BERGERSEN, L.H., 2015. The lactate receptor, G-protein-coupled receptor 81/hydroxycarboxylic acid receptor 1: Expression and action in brain. *Journal of Neuroscience Research,* **93**(7), pp. 1045-1055.

MOSSER, D.D., DUCHAINE, J. and MASSIE, B., 1993. The DNA-binding activity of the human heat shock transcription factor is regulated in vivo by hsp70. *Molecular and Cellular Biology,* **13**(9), pp. 5427-5438.

MUHLE, R.A., ADJALLEY, S., FALKARD, B., NKRUMAH, L.J., MUHLE, M.E. and FIDOCK, D.A., 2009. A *var* gene promoter implicated in severe malaria nucleates silencing

and is regulated by 3' untranslated region and intronic cis-elements. *International Journal for Parasitology,* **39**(13), pp. 1425-1439.

MURALIDHARAN, V., OKSMAN, A., PAL, P., LINDQUIST, S. and GOLDBERG, D.E., 2012. *Plasmodium falciparum* heat shock protein 110 stabilizes the asparagine repeat-rich parasite proteome during malarial fevers. *Nature Communications,* **3**, pp. 1310-1310.

MURPHY, M.E., 2013. The HSP70 family and cancer. *Carcinogenesis,* **34**(6), pp. 1181-1188.

NALBANDIAN, M. and TAKEDA, M., 2016. Lactate as a Signalling Molecule That Regulates Exercise-Induced Adaptations. *Biology,* **5**(4), pp. 38.

NEWTON, C.R.J.C. and KRISHNA, S., 1998. Severe Falciparum Malaria in Children: Current Understanding of Pathophysiology and Supportive Treatment. *Pharmacology & therapeutics,* **79**(1), pp. 1-53.

NGUYEN, V.T., MORANGE, M.F. and BENSAUDE, O., 1989. Protein denaturation during heat shock and related stress. *Escherichia coli* beta-galactosidase and *Photinus pyralis* luciferase inactivation in mouse cells. *The Journal of biological chemistry JID - 2985121R,* **264**(18), pp. 10487-10492.

NIELSEN, H.B., CLEMMESEN, J.O., SKAK, C., OTT, P. and SECHER, N.H., 2002. Attenuated hepatosplanchnic uptake of lactate during intense exercise in humans. *Journal of applied physiology,* **92**(4), pp. 1677-1683.

NKRUMAH, L.J., MUHLE, R.A., MOURA, P.A., GHOSH, P., HATFULL, G.F., JACOBS, WILLIAM R., JR and FIDOCK, D.A., 2006. Efficient site-specific integration in *Plasmodium falciparum* chromosomes mediated by mycobacteriophage Bxb1 integrase. *Nature Methods,* **3**(8), pp. 615-621.

OAKLEY, M.S., KUMAR, S., ANANTHARAMAN, V., ZHENG, H., MAHAJAN, B., HAYNES, J.D., MOCH, J.K., FAIRHURST, R., MCCUTCHAN, T.F. and ARAVIND, L., 2007. Molecular factors and biochemical pathways induced by febrile temperature in intraerythrocytic *Plasmodium falciparum* parasites. *Infection and Immunity*, **75**(4), pp. 2012-2025.

OCHOLA, L.B., SIDDONDO, B.R., OCHOLLA, H., NKYA, S., KIMANI, E.N., WILLIAMS, T.N., MAKALE, J.O., LILJANDER, A., URBAN, B.C., BULL, P.C., SZESTAK, T., MARSH, K. and CRAIG, A.G., 2011. Specific receptor usage in *Plasmodium falciparum* cytoadherence is associated with disease outcome. *PloS One*, **6**(3), pp. e14741.

O'DONNELL, R.A., PREISER, P.R., WILLIAMSON, D.H., MOORE, P.W., COWMAN, A.F. and CRABB, B.S., 2001. An alteration in concatameric structure is associated with efficient segregation of plasmids in transfected *Plasmodium falciparum* parasites. *Nucleic Acids Research*, **29**(3), pp. 716-724.

OLEINIKOV, A.V., AMOS, E., FRYE, I.T., ROSSNAGLE, E., MUTABINGWA, T.K., FRIED, M. and DUFFY, P.E., 2009. High throughput functional assays of the variant antigen PfEMP1 reveal a single domain in the 3D7 *Plasmodium falciparum* genome that binds ICAM1 with high affinity and is targeted by naturally acquired neutralizing antibodies. *PloS Pathogens*, **5**(4), pp. e1000386-e1000386.

OLSZEWSKI, K.L., MORRISEY, J.M., WILINSKI, D., BURNS, J.M., VAIDYA, A.B., RABINOWITZ, J.D. and LLINÁS, M., 2009. Host-parasite interactions revealed by *Plasmodium falciparum* metabolomics. *Cell Host & Microbe*, **5**(2), pp. 191-199.

OTHMAN, A.S., MARIN-MOGOLLON, C., SALMAN, A.M., FRANKE-FAYARD, B., JANSE, C.J. and KHAN, S.M., 2017. The use of transgenic parasites in malaria vaccine research. *Expert Review of Vaccines*, 16(7), pp. 685-697.

OTTO, T.D., WILINSKI, D., ASSEFA, S., KEANE, T.M., SARRY, L.R., BÖHME, U., LEMIEUX, J., BARRELL, B., PAIN, A., BERRIMAN, M., NEWBOLD, C. and LLINÁS, M., 2010. New insights into the blood-stage transcriptome of *Plasmodium falciparum* using RNA-Seq. *Molecular Microbiology*, **76**(1), pp. 12-24.

PAIN, A., FERGUSON, D.J., KAI, O., URBAN, B.C., LOWE, B., MARSH, K. and ROBERTS, D.J., 2001. Platelet-mediated clumping of *Plasmodium falciparum*-infected erythrocytes is a common adhesive phenotype and is associated with severe malaria. *Proceedings of the National Academy of Sciences of the United States of America*, **98**(4), pp. 1805-1810.

PAINTER, H.J., CHUNG, N.C., SEBASTIAN, A., ALBERT, I., STOREY, J.D. and LLINÁS, M., 2018. Genome-wide real-time in vivo transcriptional dynamics during *Plasmodium falciparum* blood-stage development. *Nature Communications*, **9**(1), pp. 2656.

PALLAVI, R., ACHARYA, P., CHANDRAN, S., DAILY, J.P. and TATU, U., 2010. Chaperone expression profiles correlate with distinct physiological states of *Plasmodium falciparum* in malaria patients. *Malaria Journal*, **9**, pp. 236-236.

PASTERNAK, N.D. and DZIKOWSKI, R., 2009. PfEMP1: An antigen that plays a key role in the pathogenicity and immune evasion of the malaria parasite *Plasmodium falciparum*. *The International Journal of Biochemistry & Cell Biology*, **41**(7), pp. 1463-1466.

PATTARADILOKRAT, S., LI, J., WU, J., QI, Y., EASTMAN, R.T., ZILVERSMIT, M., NAIR, S.C., HUAMAN, M.C., QUINONES, M., JIANG, H., LI, N., ZHU, J., ZHAO, K.,

KANEKO, O., LONG, C.A. and SU, X.-., 2014. *Plasmodium* genetic loci linked to host cytokine and chemokine responses. *Genes and Immunity*, **15**(3), pp. 145-152.

PAVITHRA, S.R., BANUMATHY, G., JOY, O., SINGH, V. and TATU, U., 2004. Recurrent fever promotes *Plasmodium falciparum* development in human erythrocytes. *Journal of Biological Chemistry*, **279**(45), pp. 46692-46699.

PÉREZ-TOLEDO, K., ROJAS-MEZA, A., MANCIO-SILVA, L., HERNÃ¡NDEZ-CUEVAS, N.A., DELGADILLO, D.M., VARGAS, M., MARTÃ-NEZ-CALVILLO, S., SCHERF, A. and HERNANDEZ-RIVAS, R., 2009. *Plasmodium falciparum* heterochromatin protein 1 binds to tri-methylated histone 3 lysine 9 and is linked to mutually exclusive expression of *var* genes. *Nucleic Acids Research*, **37**(8), pp. 2596-2606.

PESCE, E.R., ACHARYA, P.F., TATU U FAU - NICOLL, WILLIAM, S., FAU, N.W., SHONHAI A FAU - HOPPE, HEINRICH, C., FAU, H.H. and BLATCH, G.L., 2008. The *Plasmodium falciparum* heat shock protein 40, Pfj4, associates with heat shock protein 70 and shows similar heat induction and localisation patterns. *The International Journal of Biochemistry & Cell Biology JID - 9508482*, **40**(12), pp. 2914-2926.

PETERS, J.M., FOWLER, E.V., KRAUSE, D.R., CHENG, Q. and GATTON, M.L., 2007. Differential changes in *Plasmodium falciparum var* transcription during adaptation to culture. *The Journal of Infectious Diseases*, **195**(5), pp. 748-755.

PETTER, M., LEE, C.C., BYRNE, T.J., BOYSEN, K.E., VOLZ, J., RALPH, S.A., COWMAN, A.F., BROWN, G.V. and DUFFY, M.F., 2011. Expression of *P. falciparum var* genes involves exchange of the histone variant H2A.Z at the promoter. *PloS Pathogens*, **7**(2), pp. e1001292.

PFALLER, M.A., KROGSTAD, D.J., PARQUETTE, A.R. and NGUYEN-DINH, P., 1982. *Plasmodium falciparum*: Stage-specific lactate production in synchronized cultures. *Experimental Parasitology,* **54**(3), pp. 391-396.

PONNUDURAI, T., MEUWISSEN, J.H.E.T., LEEUWENBERG, A.D.E.M., VERHAVE, J.P. and LENSEN, A.H.W., 1982. The production of mature gametocytes of *Plasmodium falciparum* in continuous cultures of different isolates infective to mosquitoes. *Transactions of the Royal Society of Tropical Medicine and Hygiene,* 76(2), pp. 242-250.

PONTS, N., FU, L., HARRIS, E., ZHANG, J., CHUNG, D., CERVANTES, M., PRUDHOMME, J., ATANASOVA-PENICHON, V., ZEHRAOUI, E., BUNNIK, E., RODRIGUES, E., LONARDI, S., HICKS, G., WANG, Y. and LEÂ ROCH, K., 2013. Genome-wide mapping of DNA methylation in the human malaria parasite *Plasmodium falciparum*. *Cell Host & Microbe,* **14**(6), pp. 696-706.

PONTS, N., HARRIS, E.Y., PRUDHOMME, J., WICK, I., ECKHARDT-LUDKA, C., HICKS, G.R., HARDIMAN, G., LONARDI, S. and LE ROCH, K., G., 2010. Nucleosome landscape and control of transcription in the human malaria parasite. *Genome Research,* **20**(2), pp. 228-238.

QUINTANA, M.D.P., CH'NG, J., MOLL, K., ZANDIAN, A., NILSSON, P., IDRIS, Z.M., SAIWAEW, S., QUNDOS, U. and WAHLGREN, M., 2018. Antibodies in children with malaria to PfEMP1, RIFIN and SURFIN expressed at the *Plasmodium falciparum* parasitized red blood cell surface. *Scientific Reports,* **8**(1), pp. 3262-3262.

RABINDRAN, S.K., WISNIEWSKI, J., LI, L., LI, G.C. and WU, C., 1994. Interaction between heat shock factor and hsp70 is insufficient to suppress induction of DNA-binding activity in vivo. *Molecular and Cellular Biology,* **14**(10), pp. 6552-6560.

RADFAR, A., MÉNDEZ, D., MONERIZ, C., LINARES, M., MARÍN-GARCÍA, P., PUYET, A., DIEZ, A. and BAUTISTA, J.M., 2009. Synchronous culture of *Plasmodium falciparum* at high parasitemia levels. *Nature Protocols,* **4**, pp. 1899.

RANGANATHAN, P., SHANMUGAM, A., SWAFFORD, D., SURYAWANSHI, A., BHATTACHARJEE, P., HUSSEIN, M.S., KONI, P.A., PRASAD, P.D., KURAGO, Z.B., THANGARAJU, M., GANAPATHY, V. and MANICASSAMY, S., 2018. GPR81, a cell-surface receptor for lactate, regulates intestinal homeostasis and protects mice from experimental colitis. *The Journal of Immunology,* pp. ji1700604.

RASK, T.S., HANSEN, D.A., THEANDER, T.G., GORM PEDERSEN, A. and LAVSTSEN, T., 2010. *Plasmodium falciparum* erythrocyte membrane protein 1 diversity in seven genomes--divide and conquer. *PloS Computational Biology,* **6**(9), pp. e1000933.

RECKER, M., BUCKEE, C.O., SERAZIN, A., KYES, S., PINCHES, R., CHRISTODOULOU, Z., SPRINGER, A.L., GUPTA, S. and NEWBOLD, C.I., 2011. Antigenic variation in *Plasmodium falciparum* malaria involves a highly structured switching pattern. *PloS Pathogens,* **7**(3), pp. e1001306; e1001306-e1001306.

RELIGA, A.A. and WATERS, A.P., 2012. Sirtuins of parasitic protozoa: in search of function(s). *Molecular and Biochemical Parasitology*, 185(2), pp. 71-88.

ROBERGS, R.A., GHIASVAND, F. and PARKER, D., 2004. Biochemistry of exercise-induced metabolic acidosis. *American Journal of Physiology-Regulatory, Integrative and Comparative Physiology,* **287**(3), pp. R502-R516.

ROBINSON, B.A., WELCH, T.L. and SMITH, J.D., 2003. Widespread functional specialization of *Plasmodium falciparum* erythrocyte membrane protein 1 family members to

bind CD36 analysed across a parasite genome. *Molecular Microbiology,* **47**(5), pp. 1265-1278.

ROTTMANN, M., LAVSTSEN, T., MUGASA, J.P., KAESTLI, M., JENSEN, A.T., MULLER, D., THEANDER, T. and BECK, H.P., 2006. Differential expression of *var* gene groups is associated with morbidity caused by *Plasmodium falciparum* infection in Tanzanian children. *Infection and Immunity,* **74**(7), pp. 3904-3911.

ROVIRA-GRAELLS, N., GUPTA, A.P., PLANET, E., CROWLEY, V.M., MOK, S., RIBAS, D.P., PREISER, P.R., BOZDECH, Z. and CORTÉS, A., 2012. Transcriptional variation in the malaria parasite *Plasmodium falciparum*. *Genome Research,* **22**(5), pp. 925-938.

ROWE, J.A. and KYES, S.A., 2004. The role of *Plasmodium falciparum var* genes in malaria in pregnancy. *Molecular Microbiology,* **53**(4), pp. 1011-1019.

ROWE, J.A., CLAESSENS, A., CORRIGAN, R.A. and ARMAN, M., 2009. Adhesion of *Plasmodium falciparum*-infected erythrocytes to human cells: molecular mechanisms and therapeutic implications. *Expert Reviews in Molecular Medicine,* **11**, pp. e16; e16-e16.

ROWE, J.A., HANDEL, I.G., THERA, M.A., DEANS, A., LYKE, K.E., KONÉ, A., DIALLO, D.A., RAZA, A., KAI, O., MARSH, K., PLOWE, C.V., DOUMBO, O.K. and MOULDS, J.M., 2007. Blood group O protects against severe *Plasmodium falciparum* malaria through the mechanism of reduced rosetting. *Proceedings of the National Academy of Sciences of the United States of America,* **104**(44), pp. 17471-17476.

ROWE, J.A., MOULDS, J.M., NEWBOLD, C.I. and MILLER, L.H., 1997. *P. falciparum* rosetting mediated by a parasite-variant erythrocyte membrane protein and complement-receptor 1. *Nature,* **388**(6639), pp. 292-295.

RUBACH, M.P., MUKEMBA, J., FLORENCE, S., JOHN, B., CROOKSTON, B., LOPANSRI, B.K., YEO, T.W., PIERA, K.A., ALDER, S.C., WEINBERG, J.B., ANSTEY, N.M., GRANGER, D.L. and MWAIKAMBO, E.D., 2012. Plasma *Plasmodium falciparum* histidine-rich protein-2 concentrations are associated with malaria severity and mortality in Tanzanian children. *PloS one*, **7**(5), pp. e35985-e35985.

RUIZ, J.L., TENA, J., BANCELLS, C., CORTÉS, A., GÓMEZ-SKARMETA, J. AND GÓMEZ-DÍAZ, E., 2018. Characterization of the accessible genome in the human malaria parasite *Plasmodium falciparum*. *Nucleic Acids Research*, **46**(18), pp. 9414-9431.

RUSSELL, K., EMES, R. and HORROCKS, P., 2015. Triaging informative cis-regulatory elements for the combinatorial control of temporal gene expression during *Plasmodium falciparum* intraerythrocytic development. *Parasites & Vectors*, **8**, pp. 81; 81-81.

RÜTGERS, M., MURANAKA, L.S., SCHULZ-RAFFELT, M., THOMS, S., SCHURIG, J., WILLMUND, F. and SCHRODA, M., 2017. Not changes in membrane fluidity but proteotoxic stress triggers heat shock protein expression in *Chlamydomonas reinhardtii*. *Plant, Cell & Environment*, 40(12), pp. 2987-3001.

SALANTI, A., DAHLBÄCK, M., TURNER, L., NIELSEN, M.A., BARFOD, L., MAGISTRADO, P., JENSEN, A.T.R., LAVSTSEN, T., OFORI, M.F., MARSH, K., HVIID, L. and THEANDER, T.G., 2004. Evidence for the involvement of VAR2CSA in pregnancy-associated malaria. *The Journal of Experimental Medicine*, **200**(9), pp. 1197-1203.

SALANTI, A., STAALSOE, T., LAVSTSEN, T., JENSEN, A.T.R., SOWA, M.P.K., ARNOT, D.E., HVIID, L. and THEANDER, T.G., 2003. Selective upregulation of a single distinctly structured *var* gene in chondroitin sulphate A-adhering *Plasmodium falciparum* involved in pregnancy-associated malaria. *Molecular Microbiology*, **49**(1), pp. 179-191.

SALCEDO-AMAYA, A., VAN DRIEL, M.A., ALAKO, B.T., TRELLE, M.B., VAN, D.E., COHEN, A.M., JANSSEN-MEGENS, E., VAN, D.V., SELZER, R.R., INIGUEZ, A.L., GREEN, R.D., SAUERWEIN, R.W., JENSEN, O.N. and STUNNENBERG, H.G., 2009. Dynamic histone H3 epigenome marking during the intraerythrocytic cycle of *Plasmodium falciparum*. *Proceedings of the National Academy of Sciences of the United States of America*, **106**(24), pp. 9655.

SAMBROOK, J., 2001. *Molecular cloning: a laboratory manual Vol.1*. 3rd ed. edn. Cold Spring Harbor: Cold Spring Harbor: Cold Spring Harbor Laboratory Press.

SATYAL, S.H., CHEN, D., FOX, S.G., KRAMER, J.M. and MORIMOTO, R.I., 1998. Negative regulation of the heat shock transcriptional response by HSBP1. *Genes & Development*, **12**(13), pp. 1962-1974.

SCHERF, A., HERNANDEZ-RIVAS, R., BUFFET, P., BOTTIUS, E., BENATAR, C., POUVELLE, B., GYSIN, J. and LANZER, M., 1998. Antigenic variation in malaria: in situ switching, relaxed and mutually exclusive transcription of var genes during intra-erythrocytic development in *Plasmodium falciparum*. *The EMBO Journal*, **17**(18), pp. 5418-5426.

SCHNEIDER, C., SEPP-LORENZINO, L., NIMMESGERN, E., OUERFELLI, O., DANISHEFSKY, S., ROSEN, N. and HARTL, F.U., 1996. Pharmacologic shifting of a balance between protein refolding and degradation mediated by Hsp90. *Proceedings of the National Academy of Sciences of the United States of America*, **93**(25), pp. 14536-14541.

SETO, E. and YOSHIDA, M., 2014. Erasers of histone acetylation: the histone deacetylase enzymes. *Cold Spring Harbor Perspectives in Biology*, **6**(4), pp. a018713-a018713.

SHANKAR, A.H., 2000. Nutritional modulation of malaria morbidity and mortality. *The Journal of Infectious Diseases*, **182**, pp. S37-S53.

SHI, Y., MOSSER, D.D. and MORIMOTO, R.I., 1998. Molecular chaperones as HSF1-specific transcriptional repressors. *Genes & Development,* **12**(5), pp. 654-666.

SHOCK, J.L., FISCHER, K.F. and DERISI, J.L., 2007. Whole-genome analysis of mRNA decay in *Plasmodium falciparum* reveals a global lengthening of mRNA half-life during the intra-erythrocytic development cycle. *Genome Biology,* **8**(7), pp. R134.

SHONHAI, A., BOSHOFF, A. and BLATCH, G.L., 2007. The structural and functional diversity of Hsp70 proteins from *Plasmodium falciparum*. *Protein Science: a publication of the Protein Society,* **16**(9), pp. 1803-1818.

SILAMUT, K., PHU, N.H., WHITTY, C., TURNER, G.D., LOUWRIER, K., MAI, N.T., SIMPSON, J.A., HIEN, T.T. and WHITE, N.J., 1999. A quantitative analysis of the microvascular sequestration of malaria parasites in the human brain. *The American Journal of Pathology,* **155**(2), pp. 395-410.

SILVIE, O., MOTA, M.M., MATUSCHEWSKI, K. and PRUDÃªNCIO, M., 2008. Interactions of the malaria parasite and its mammalian host. *Current Opinion in Microbiology; Host-microbe interactions: fungi/parasites/viruses,* **11**(4), pp. 352-359.

SMILKSTEIN, M., SRIWILAIJAROEN, N., KELLY, J.X., WILAIRAT, P. and RISCOE, M., 2004. Simple and inexpensive fluorescence-based technique for high-throughput antimalarial drug screening. *Antimicrobial Agents and Chemotherapy,* **48**(5), pp. 1803-1806.

SMITH, T.G., LOURENCO, P.F., CARTER, R.F., WALLIKER D FAU - RANFORD-CARTWRIGHT, L.C. and RANFORD-CARTWRIGHT, L.C., 2000. Commitment to sexual differentiation in the human malaria parasite, *Plasmodium falciparum*. *Parasitology JID - 0401121,* **121**(Pt 2), pp. 127-133.

SRIBOONVORAKUL, N., GHOSE, A., HASSAN, M.M., HOSSAIN, M.A., FAIZ, M.A., Pukrittayakamee, S., CHOTIVANICH, K., SUKTHANA, Y., LEOPOLD, S.J., PLEWES, K., DAY, N.P.J., WHITE, N.J., TARNING, J. and DONDORP, A.M., 2018. Acidosis and acute kidney injury in severe malaria. *Malaria Journal*, **17**(1), pp. 128; 128-128.

SRIVASTAVA, A., PHILIP, N., HUGHES, K.R., GEORGIOU, K., MACRAE, J.I., BARRETT, M.P., CREEK, D.J., MCCONVILLE, M.J. and WATERS, A.P., 2016. Stage-specific changes in *Plasmodium* metabolism required for differentiation and adaptation to different host and vector environments. *PLoS pathogens*, **12**(12), pp. e1006094; e1006094-e1006094.

SRIVASTAVA, S., BHOWMICK, K., CHATTERJEE, S., BASHA, J., KUNDU, T.K. and DHAR, S.K., 2014. Histone H3K9 acetylation level modulates gene expression and may affect parasite growth in human malaria parasite *Plasmodium falciparum*. *The FEBS Journal*, **281**(23), pp. 5265-5278.

STEVENSON, M.M. and RILEY, E.M., 2004. Innate immunity to malaria. *Nature Reviews Immunology*, **4**, pp. 169.

STORM, J., JESPERSEN, J.S., SEYDEL, K.B., SZESTAK, T., MBEWE, M., CHISALA, N.V., PHULA, P., WANG, C.W., TAYLOR, T.E., MOXON, C.A., LAVSTSEN, T. and CRAIG, A.G., 2019. Cerebral malaria is associated with differential cytoadherence to brain endothelial cells. *EMBO Molecular Medicine*, **11**(2), pp. e9164.

SU, X., HEATWOLE, V.M., WERTHEIMER, S.P., GUINET, F., HERRFELDT, J.A., PETERSON, D.S., RAVETCH, J.A. and WELLEMS, T.E., 1995. The large diverse gene family *var* encodes proteins involved in cytoadherence and antigenic variation of *Plasmodium falciparum*-infected erythrocytes. *Cell*, **82**(1), pp. 89-100.

SYPNIEWSKA, P., DUDA, J.F., LOCATELLI, I., ALTHAUS, C.R., ALTHAUS, F. and GENTON, B., 2017. Clinical and laboratory predictors of death in African children with features of severe malaria: a systematic review and meta-analysis. *BMC Medicine,* **15**(1), pp. 147.

TANNY, J.C., KIRKPATRICK, D.S., GERBER, S.A., GYGI, S.P. and MOAZED, D., 2004. Budding yeast silencing complexes and regulation of Sir2 activity by protein-protein interactions. *Molecular and Cellular Biology,* **24**(16), pp. 6931.

THOMAS, P., SEDILLO, J., OBERSTALLER, J., LI, S., ZHANG, M., SINGH, N., WANG, C.C.Q., UDENZE, K., JIANG, R.H.Y. and ADAMS, J.H., 2016. Phenotypic screens identify parasite genetic factors associated with malarial fever response in *Plasmodium falciparum* piggyBac mutants. *mSphere,* **1**(5), pp. e00273-16.

THORNE, N., INGLESE, J. and AULD, D.S., 2010. Illuminating insights into Firefly Luciferase and other bioluminescent reporters used in chemical biology. *Chemistry & Biology,* 17 (6), pp. 647 – 657.

TIBÚRCIO, M., DIXON, M.W.A., LOOKER, O., YOUNIS, S.Y., TILLEY, L. and ALANO, P., 2015. Specific expression and export of the *Plasmodium falciparum* gametocyte EXported Protein-5 marks the gametocyte ring stage. *Malaria Journal,* **14**(1), pp. 334.

TONKIN, C.J., CARRET, C., DURAISINGH, M.T., VOSS, T.S., RALPH, S.A., HOMMEL, M., DUFFY, M.F., SILVA, L.M.D., SCHERF, A., IVENS, A., SPEED, T.P., BEESON, J.G. and COWMAN, A.F., 2009. Sir2 paralogues cooperate to regulate virulence genes and antigenic variation in *Plasmodium falciparum*. *PloS Biology,* **7**(4), pp. e84; e1000084-e84.

TONKIN-HILL, G., TRIANTY, L., NOVIYANTI, R., NGUYEN, H.H.T., SEBAYANG, B.F., LAMPAH, D.A., MARFURT, J., COBBOLD, S.A., RAMBHATLA, J.S.,

MCCONVILLE, M.J., ROGERSON, S.J., BROWN, G.V., DAY, K.P., PRICE, R.N., ANSTEY, N.M., PAPENFUSS, A.T. and DUFFY, M.F., 2018. The *Plasmodium falciparum* transcriptome in severe malaria reveals altered expression of genes involved in important processes including surface antigen-encoding *var* genes. *PloS Biology,* **16**(3), pp. e2004328-e2004328.

TRELLE, M.B., SALCEDO-AMAYA, A., COHEN, A.M., STUNNENBERG, H.G. and JENSEN, O.N., 2009. Global histone analysis by mass spectrometry reveals a high content of acetylated lysine residues in the malaria parasite *Plasmodium falciparum*. *Journal of Proteome Research,* **8**(7), pp. 3439-3450.

TUIKUE NDAM, N., MOUSSILIOU, A., LAVSTSEN, T., KAMALIDDIN, C., JENSEN, A.T.R., MAMA, A., TAHAR, R., WANG, C.W., JESPERSEN, J.S., ALAO, J.M., GAMAIN, B., THEANDER, T.G. and DELORON, P., 2017. Parasites causing cerebral falciparum malaria bind multiple endothelial receptors and express EPCR and ICAM-1-binding PfEMP1. *The Journal of Infectious Diseases,* **215**(12), pp. 1918-1925.

TUIKUE NDAM, N.G., SALANTI, A., BERTIN, G., DAHLBÄCK, M., FIEVET, N., TURNER, L., GAYE, A., THEANDER, T. and DELORON, P., 2005. High level of *var2csa* transcription by *Plasmodium falciparum* isolated from the placenta. The Journal of Infectious Diseases, 192(2), pp. 331-335.

TUJU, J., MACKINNON, M.J., ABDI, A.I., KARANJA, H., MUSYOKI, J.N., WARIMWE, G.M., GITAU, E.N., MARSH, K., BULL, P.C. and URBAN, B.C., 2019. Antigenic cartography of immune responses to *Plasmodium falciparum* erythrocyte membrane protein 1 (PfEMP1). *PloS Pathogens,* **15**(7), pp. e1007870.

TURNER, L., LAVSTSEN, T., BERGER, S.S., WANG, C.W., PETERSEN, J.E.V., AVRIL, M., BRAZIER, A.J., FREETH, J., JESPERSEN, J.S., NIELSEN, M.A., MAGISTRADO, P., LUSINGU, J., SMITH, J.D., HIGGINS, M.K. and THEANDER, T.G., 2013. Severe malaria is associated with parasite binding to endothelial protein C receptor. *Nature*, **498**(7455), pp. 502-505.

UDOMSANGPETCH, R., PIPITAPORN, B., SILAMUT, K., PINCHES, R., KYES, S., LOOAREESUWAN, S., NEWBOLD, C. and WHITE, N.J., 2002. Febrile temperatures induce cytoadherence of ring-stage *Plasmodium falciparum*-infected erythrocytes. *Proceedings of the National Academy of Sciences of the United States of America*, **99**(18), pp. 11825-11829.

UKAEGBU, U.E., KISHORE, S.P., KWIATKOWSKI, D.L., PANDARINATH, C., DAHAN-PASTERNAK, N., DZIKOWSKI, R. and DEITSCH, K.W., 2014. Recruitment of PfSET2 by RNA polymerase II to variant antigen encoding loci contributes to antigenic variation in *P. falciparum*. *PloS Pathogens*, **10**(1), pp. e1003854; e1003854-e1003854.

UKAEGBU, U.E., ZHANG, X., HEINBERG, A.R., WELE, M., CHEN, Q. and DEITSCH, K.W., 2015. A unique virulence gene occupies a principal position in immune evasion by the malaria parasite *Plasmodium falciparum*. *PloS Genetics*, **11**(5), pp. e1005234.

VANDER JAGT, D.L., HUNSAKER, L.A., CAMPOS, N.M. and BAACK, B.R., 1990. d-Lactate production in erythrocytes infected with *Plasmodium falciparum*. *Molecular and Biochemical Parasitology*, **42**(2), pp. 277-284.

VAUGHAN, A.M., ALY, A.S.I. and KAPPE, S.H.I., 2008. Malaria parasite pre-erythrocytic stage infection: gliding and hiding. *Cell Host & Microbe*, **4**(3), pp. 209-218.

VEMBAR, S.S., SCHERF, A. and SIEGEL, T.N., 2014. Noncoding RNAs as emerging regulators of *Plasmodium falciparum* virulence gene expression. *Current Opinion in Microbiology,* **20**(100), pp. 153-161.

VOLZ, J., BÁRTFAI, R., PETTER, M., LANGER, C., JOSLING, G., TSUBOI, T., SCHWACH, F., BAUM, J., RAYNER, J., STUNNENBERG, H., DUFFY, M. and COWMAN, A., 2012. PfSET10, a *Plasmodium falciparum* methyltransferase, maintains the active *var* gene in a poised state during parasite division. *Cell Host & Microbe,* **11**(1), pp. 7-18.

VOLZ, J., CARVALHO, T.G., RALPH, S.A., GILSON, P., THOMPSON, J., TONKIN, C.J., LANGER, C., CRABB, B.S. and COWMAN, A.F., 2010. Potential epigenetic regulatory proteins localise to distinct nuclear sub-compartments in *Plasmodium falciparum*. *International Journal for Parasitology,* **40**(1), pp. 109-121.

VOSS, T.S., MINI, T., JENOE, P. and BECK, H., 2002. *Plasmodium falciparum* possesses a cell cycle-regulated short type replication protein a large subunit encoded by an unusual transcript. *Journal of Biological Chemistry,* **277**(20), pp. 17493-17501.

WAGNER, W., KANIA, K.D., BLAUZ, A. and CISZEWSKI, W.M., 2017. The lactate receptor (HCAR1/GPR81) contributes to doxorubicin chemoresistance via ABCB1 transporter up-regulation in human cervical cancer HeLa cells. *Journal of Physiology and Pharmacology: An Official Journal of the Polish Physiological Society JID - 9114501,* **68**(4), pp. 555-564.

WALTHER, M., TONGREN, J.E., ANDREWS, L., KORBEL, D., KING, E., FLETCHER, H., ANDERSEN, R.F., BEJON, P., THOMPSON, F., DUNACHIE, S.J., EDELE, F., DE SOUZA, J.B., SINDEN, R.E., GILBERT, S.C., RILEY, E.M. and HILL, A.V.S., 2005.

Upregulation of TGF-beta, FOXP3, and CD4+CD25+ regulatory T cells correlates with more rapid parasite growth in human malaria infection. *Immunity,* **23**(3), pp. 287-296.

WARIMWE, G.M., KEANE, T.M., FEGAN, G., MUSYOKI, J.N., NEWTON, C.R.J.C., PAIN, A., BERRIMAN, M., MARSH, K. and BULL, P.C., 2009. *Plasmodium falciparum var* gene expression is modified by host immunity. *Proceedings of the National Academy of Sciences of the United States of America,* **106**(51), pp. 21801.

WARIMWE, G.M., RECKER, M., KIRAGU, E.W., BUCKEE, C.O., WAMBUA, J., MUSYOKI, J.N., MARSH, K. and BULL, P.C., 2013. *Plasmodium falciparum var* gene expression homogeneity as a marker of the host-parasite relationship under different levels of naturally acquired immunity to malaria. *PloS One,* **8**(7), pp. e70467.

WASSMER, S.C. and GRAU, G.E.R., 2017. Severe malaria: what's new on the pathogenesis front? *International Journal for Parasitology,* **47**(2-3), pp. 145-152.

WASSMER, S.C., TAYLOR, T., MACLENNAN, C.A., KANJALA, M., MUKAKA, M., MOLYNEUX, M.E. and GRAU, G.E., 2008. Platelet-induced clumping of *Plasmodium falciparum*-infected erythrocytes from Malawian patients with cerebral malaria-possible modulation in vivo by thrombocytopenia. *The Journal of Infectious Diseases,* **197**(1), pp. 72-78.

WILLEMS, E., LEYNS, L. and VANDESOMPELE, J., 2008. Standardization of real-time PCR gene expression data from independent biological replicates. *Analytical Biochemistry,* **379**(1), pp. 127-129.

WISER, M.F., 1999 updated 2019. Biochemistry of *Plasmodium*--Brief Overview. http://www.tulane.edu/~wiser/malaria/Summary.html#kk1.

WONG, E.H., HASENKAMP, S. and HORROCKS, P., 2011. Analysis of the molecular mechanisms governing the stage-specific expression of a prototypical housekeeping gene during intraerythrocytic development of *P. falciparum*. *Journal of Molecular Biology*, **408**(2), pp. 205-221.

WORLD HEALTH ORGANIZATION, 2008. *World Malaria Report 2008.* WHO.

WORLD HEALTH ORGANIZATION, 2014. *Severe malaria supplement.* WHO.

WORLD HEALTH ORGANIZATION, 2018. *World malaria report 2018.* WHO.

WU, B., RAMBOW, J., BOCK, S., HOLM-BERTELSEN, J., WIECHERT, M., SOARES, A.B., SPIELMANN, T. and BEITZ, E., 2015. Identity of a *Plasmodium* lactate/H+ symporter structurally unrelated to human transporters. *Nature Communications*, **6**, pp. 6284.

YANG, X. and SETO, E., 2008. The Rpd3/Hda1 family of lysine deacetylases: from bacteria and yeast to mice and men. *Nature Reviews. Molecular Cell Biology*, **9**(3), pp. 206-218.

YE, R., ZHANG, D., CHEN, B., ZHU, Y., ZHANG, Y., WANG, S. and PAN, W., 2015. Transcription of the *var* genes from a freshly-obtained field isolate of *Plasmodium falciparum* shows more variable switching patterns than long laboratory-adapted isolates. *Malaria Journal*, **14**, pp. 66; 66-66.

ZEREZ, C.R., ROTH, E.J., SCHULMAN, S. and TANAKA, K.R., 1990. Increased nicotinamide adenine dinucleotide content and synthesis in *Plasmodium falciparum*-infected human erythrocytes. *Blood*, **75**(8), pp. 1705.

ZHANG, Q., BHATTACHARYA, S., PI, J., CLEWELL, R.A., CARMICHAEL, P.L. and ANDERSEN, M.E., 2015. Adaptive posttranslational control in cellular stress response

pathways and its relationship to toxicity testing and safety assessment. *Toxicological Sciences: An Official Journal of the Society of Toxicology*, **147**(2), pp. 302-316.

ZHAO, K., CHAI, X., CLEMENTS, A. and MARMORSTEIN, R., 2003. Structure and autoregulation of the yeast Hst2 homolog of Sir2. Nature Structural & Molecular Biology, 10(10), pp. 864-871.

ZHU, A.Y., ZHOU, Y., KHAN, S., DEITSCH, K.W., HAO, Q. and LIN, H., 2012. *Plasmodium falciparum* Sir2A preferentially hydrolyzes medium and long chain fatty acyl lysine. *ACS Chemical Biology*, **7**(1), pp. 155-159.

ZININGA, T., ACHILONU, I., HOPPE, H., PRINSLOO, E., DIRR, H.W. and SHONHAI, A., 2015. Overexpression, purification and characterisation of the *Plasmodium falciparum* Hsp70-z (PfHsp70-z) Protein. *PloS One*, **10**(6), pp. e0129445; e0129445-e0129445.

ZOLG, J.W., MACLEOD, A.J., SCAIFE, J.G. and BEAUDOIN, R.L., 1984. The accumulation of lactic acid and its influence on the growth of *Plasmodium falciparum* in synchronized cultures. *In vitro*, **20**(3 Pt 1), pp. 205-215.

Appendices

Appendix I: Plasmid map of pLNSir2aGFP (pLNSG)

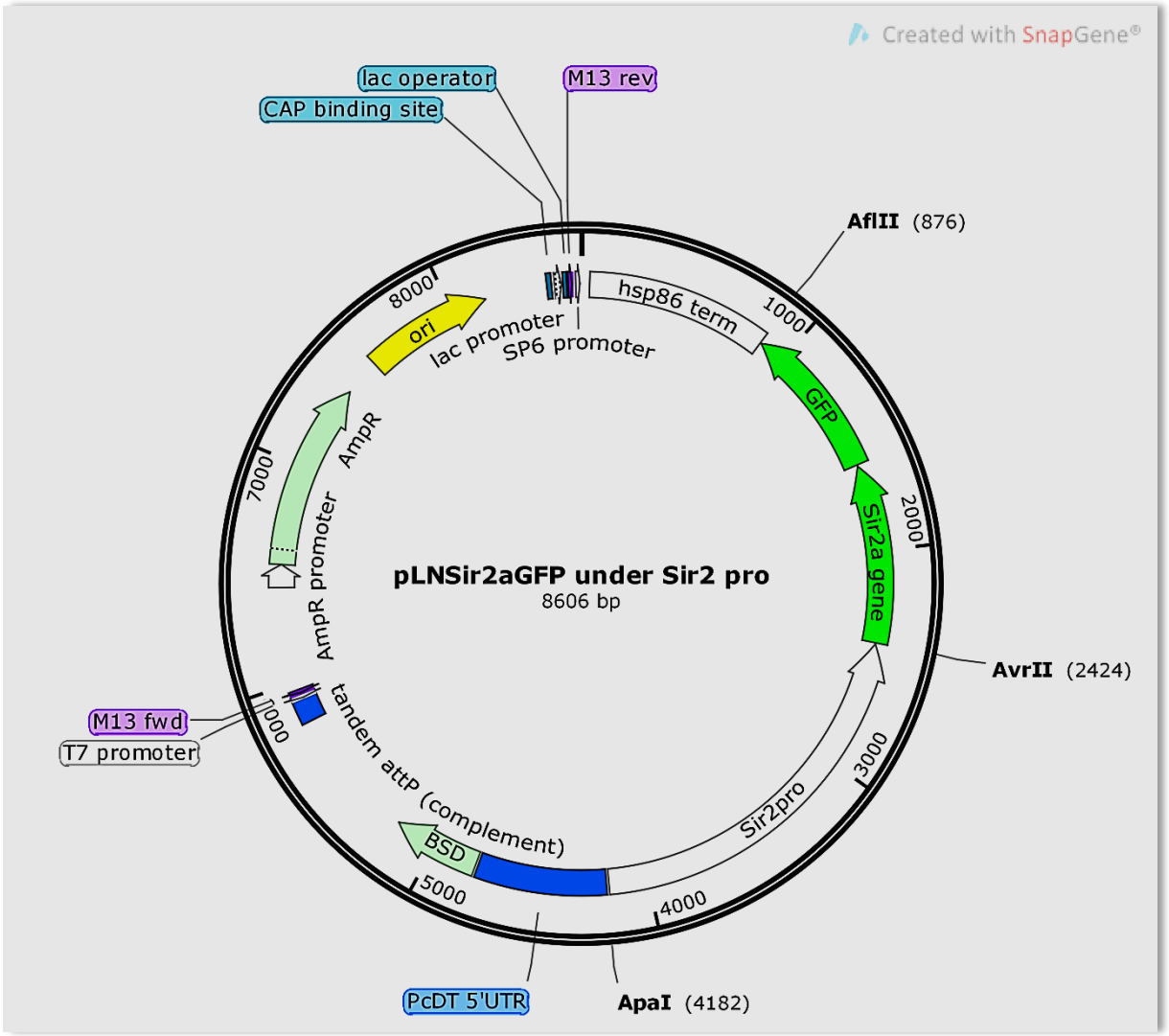

Appendix II: Formula for the buffer and media

SOC medium

1 L of SOC was prepared using the components in the Table below.

Components	**Quantity**
Tryptone	20 g
Yeast extract	5 g
NaCl	0.5 g
KCl	0.186 g
$MgCl_2$	0.952 g
ddH_20	Up to 1 L

The volume of ddH_20 was brought up to 900 ml and the pH adjusted to 7.4 with 10 M NaOH before finally making up the volume to 1 L with ddH_20. After sterilization of the media, 20 ml of sterile 1 M glucose was added immediately before use.

5X TBE buffer

1X TBE was prepared by diluting a 5X TBE, 5 fold with ddH_2O. The formula the 5X TBE is given in the Table below

Component	**Quantity**
Tris Base	54.00 g
Boric acid	27.50 g
EDTA	4.65 g
ddH_2O	Up to 1L

The pH should be adjusted to 8.3

LB medium

1 L of LB was prepared using the components in the Table below.

Components	**Quantity**
Tryptone	10 g
Yeast extract	5 g
NaCl	10 g
ddH_20	Up to 1 L

15 g of agar was added prior to sterilization to make LB agar.

Appendix III: Flipped plasmid map of pmPLP1 with *Fluc* primers designed using Snapgene software

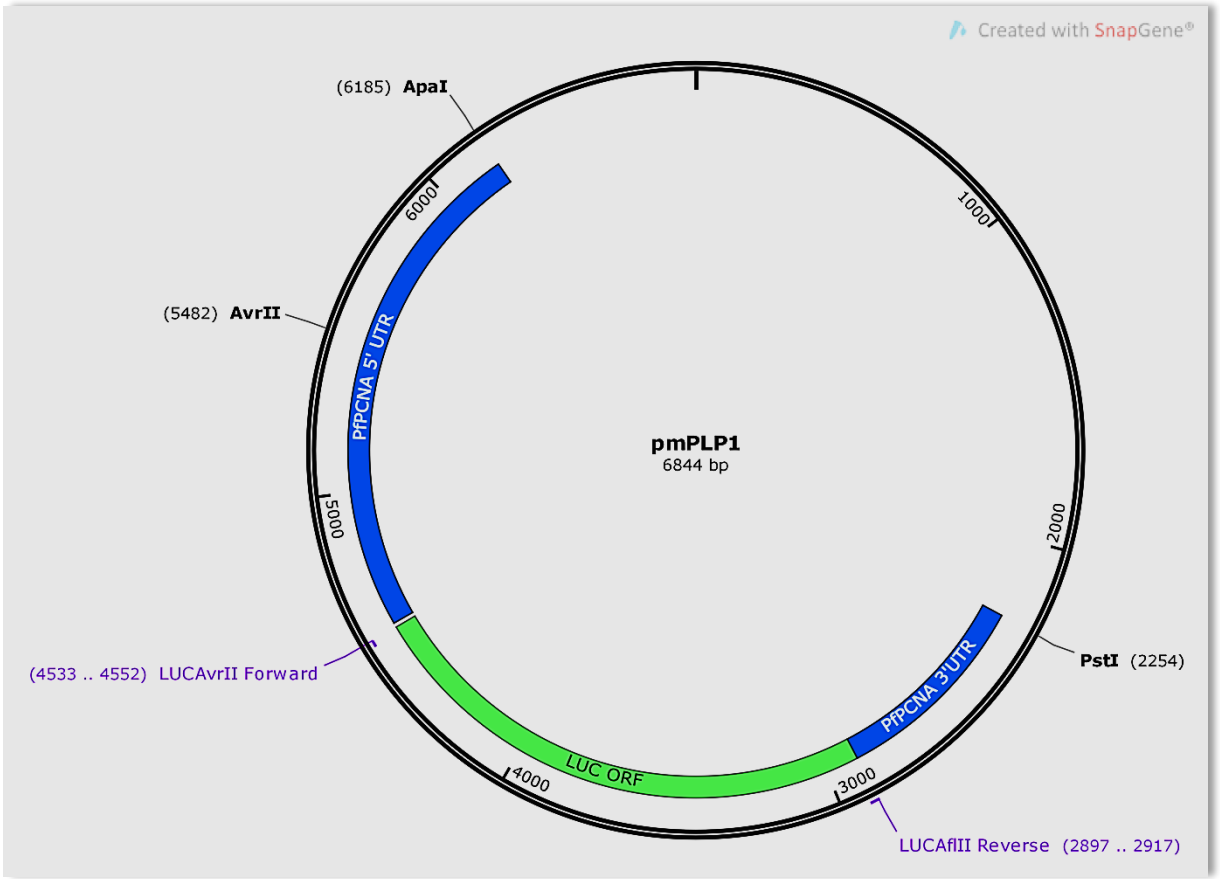

Appendix IV: *PfSir2A-luc* reporter construct

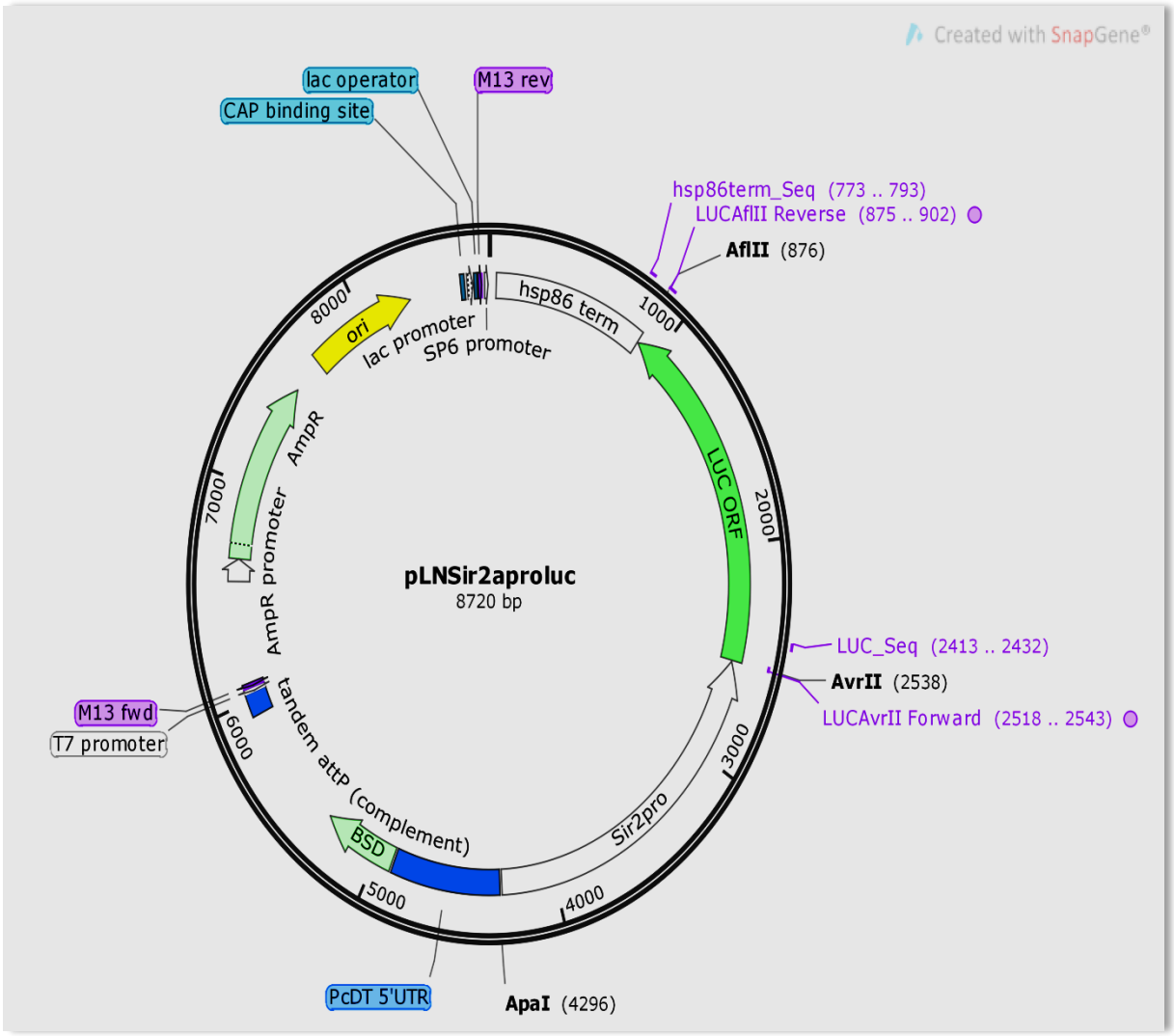

Appendix V: Fragment of PfSir2B promoter for cloning into pLNluc vector

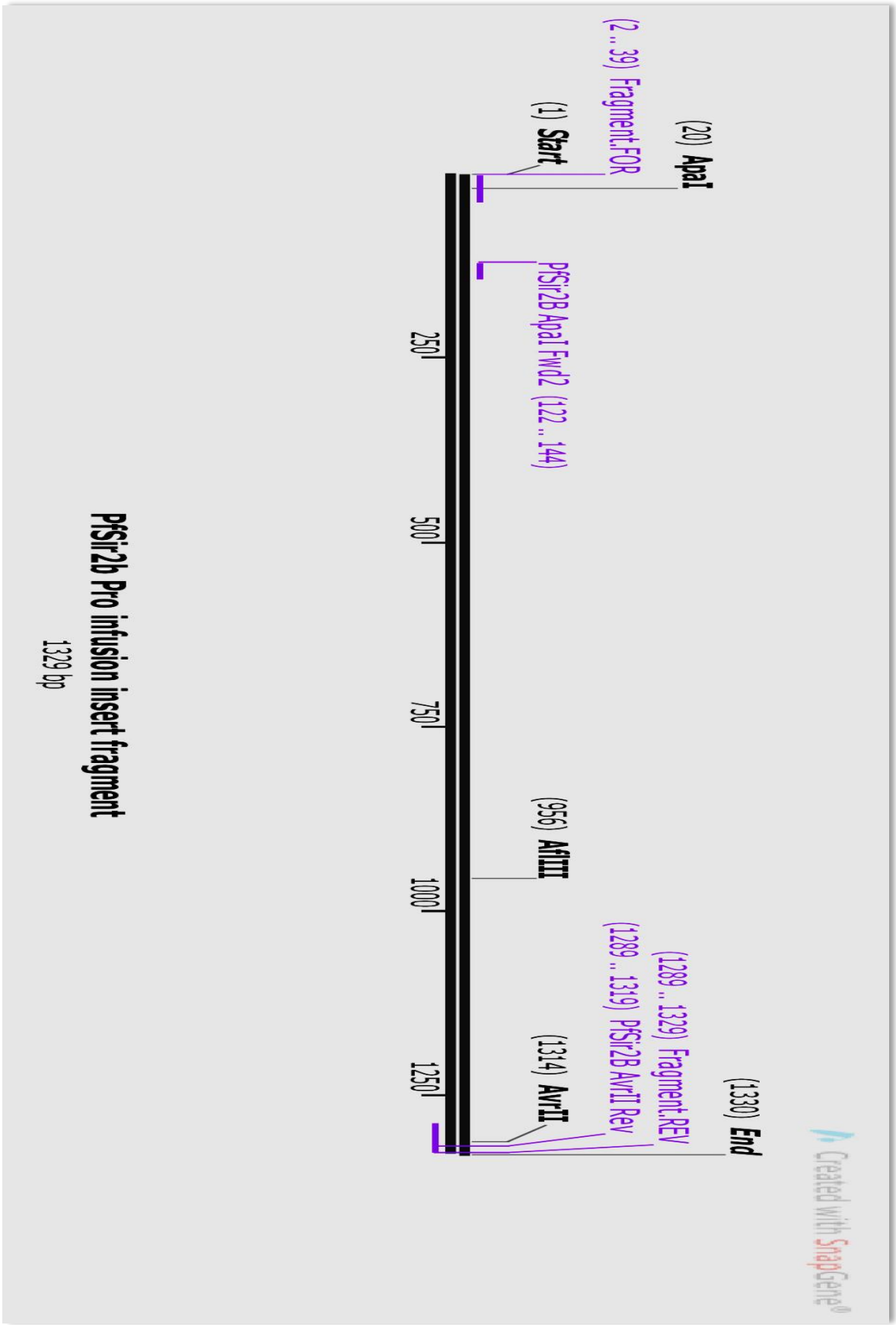

Appendix VI: RTPCR of trophozoite-staged *Pfpcna-luc* transfected lines after 2 h of stress

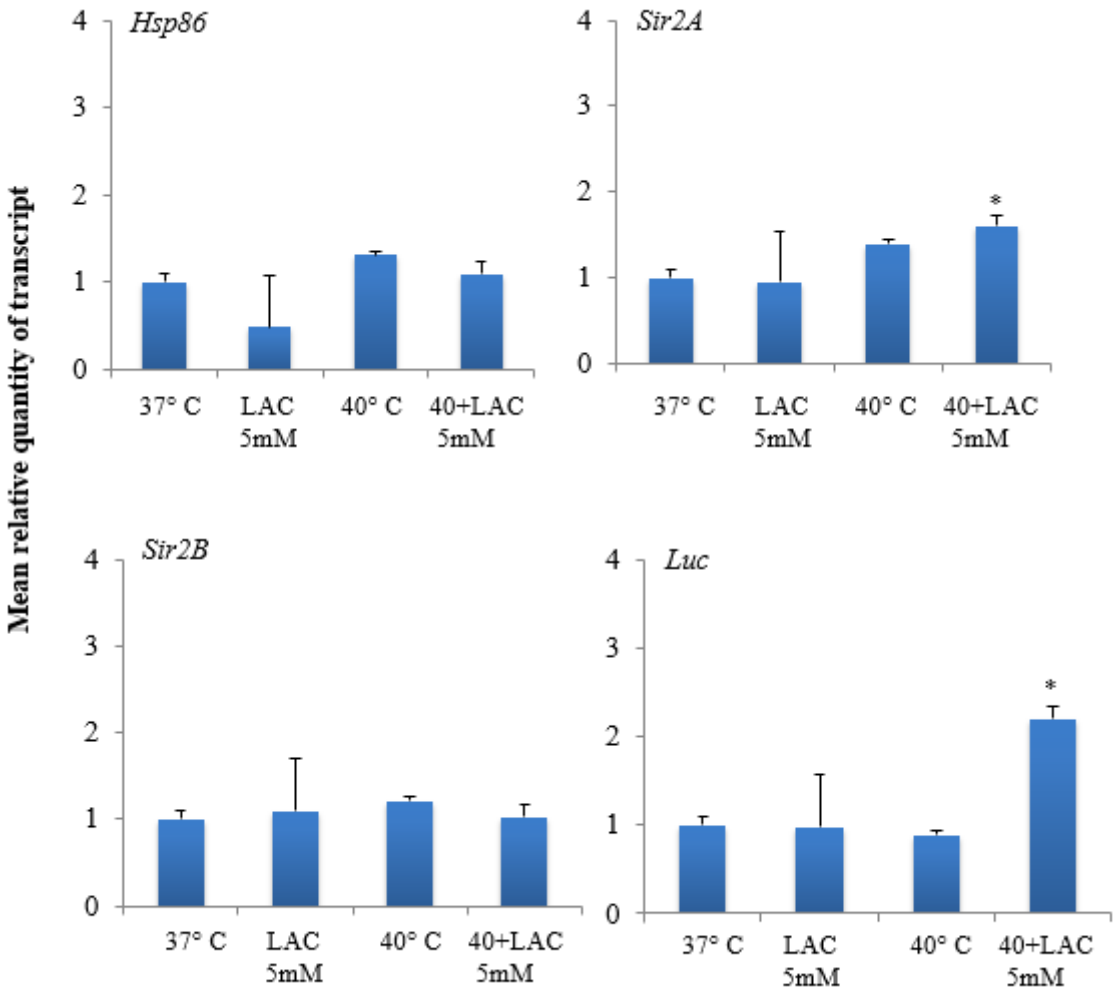

Transcriptional response of trophozoite-staged *Pfpcna-luc* line after stress. The quantity of transcripts relative to that of a control culture for *Hsp70*, *PfSir2A*, *PfSir2B* and *Luc*, after the exposure of the parasites to 5 mM lactate and/or 40°C in a single experiment done in technical triplicate, n = 3. Error bars are SEM. *p < 0.05 Kruskal-Wallis test of the relative copy number (RCN), derived from $2^{(-\Delta Cq)}$.

Appendix VII: RTPCR of schizont-staged 3D7 *PfSir2A-luc* reporter line after 2 h of stress

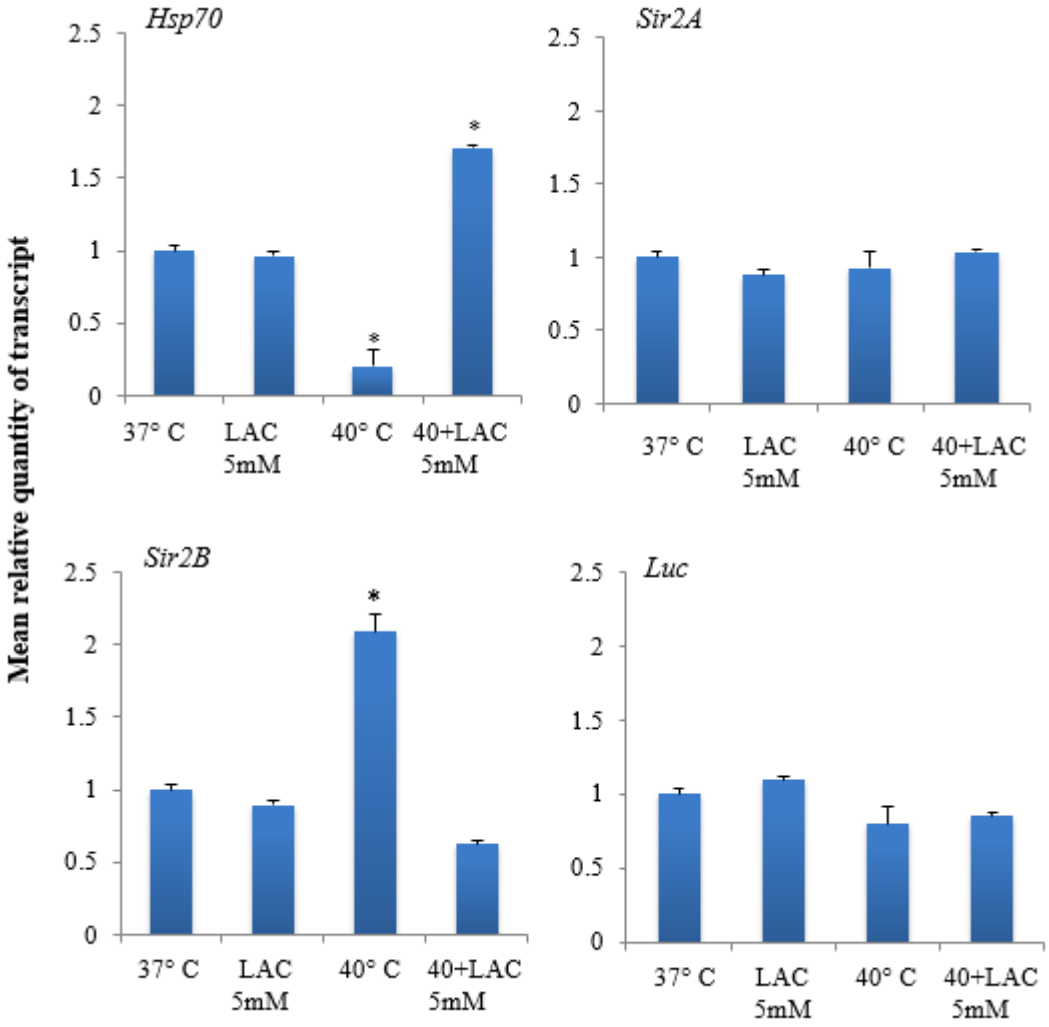

Transcriptional response of trophozoite-staged *PfSir2A-luc* line after stress. The quantity of transcripts relative to that of a control culture for *Hsp70*, *PfSir2A*, *PfSir2B* and *Luc*, after the exposure of the parasites to 5 mM lactate and/or 40°C in a single experiment done in technical triplicate, n = 3. Error bars are SEM. *p < 0.05 Kruskal-Wallis test of the relative copy number (RCN), derived from $2^{(-\Delta Cq)}$.

Appendices VIII: RCN of target genes under test, from biological duplicates, derived from $2^{(-\Delta Cq)}$. a) Trophozoite-staged 3518

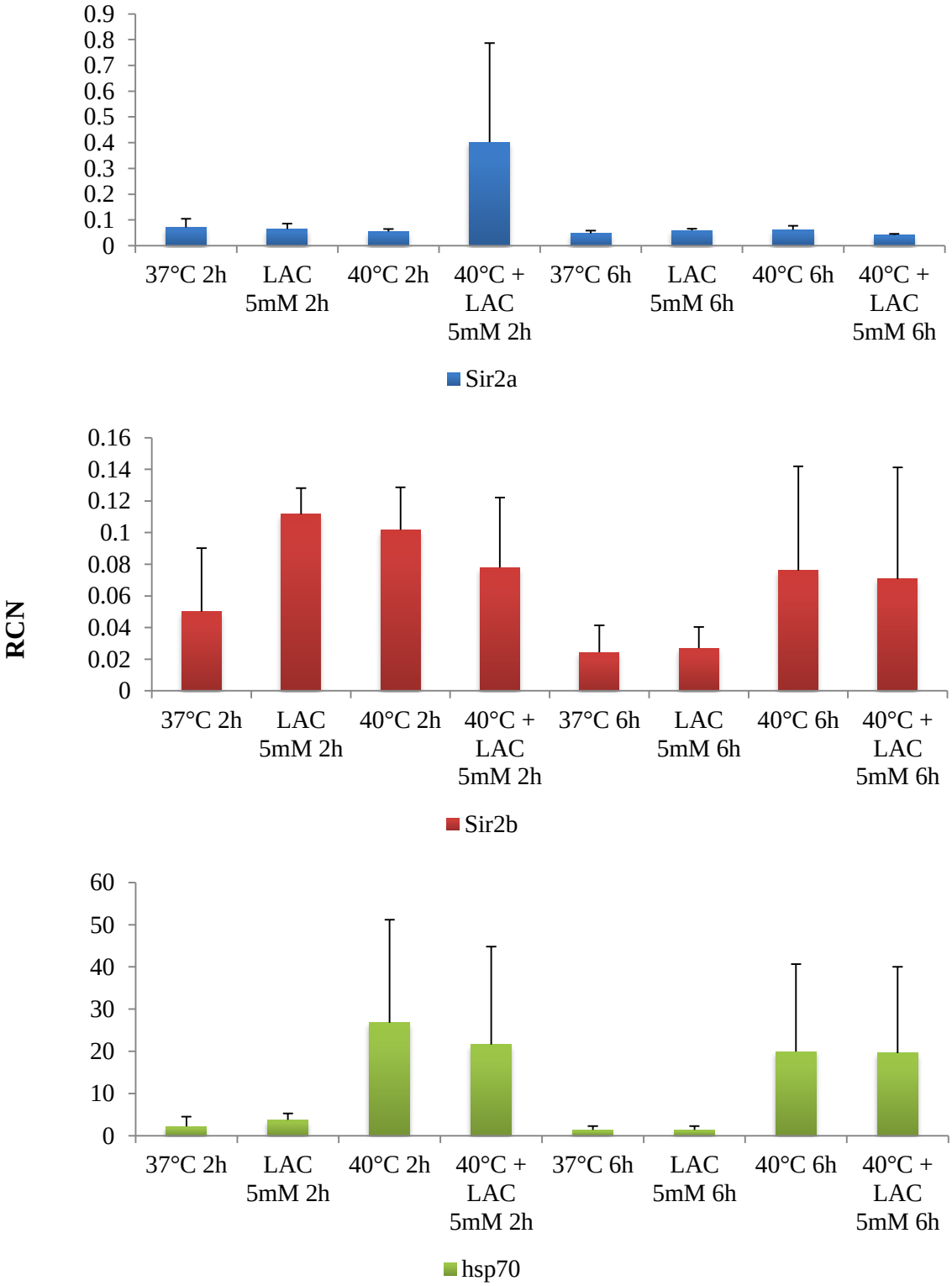

Mean Relative Copy Number (RCN) of expressed *PfSir2A*, *PfSir2B* & *Hsp70*. The relative copy number (RCN), derived from $2^{(-\Delta Cq)}$ of *PfSir2A* at 2 and 6 h (**blue bars**),

PfSir2B at 2 and 6 h (**red bars**) and *Hsp70* at 2 and 6 h (**green bars)**, after the exposure of Trophozoite-staged 3518 to no stress (37°C), 5 mM lactate and/or 40°C from independent biological duplicate experiments. The different coloured bars represent the gene being measured: *PfSir2A* (blue bars), *PfSir2B* (red bars) and *Hsp70* (green bars). Error bars are SEM. *$p < 0.05$ Kruskal-Wallis test.

b) Trophozoite-staged 9775

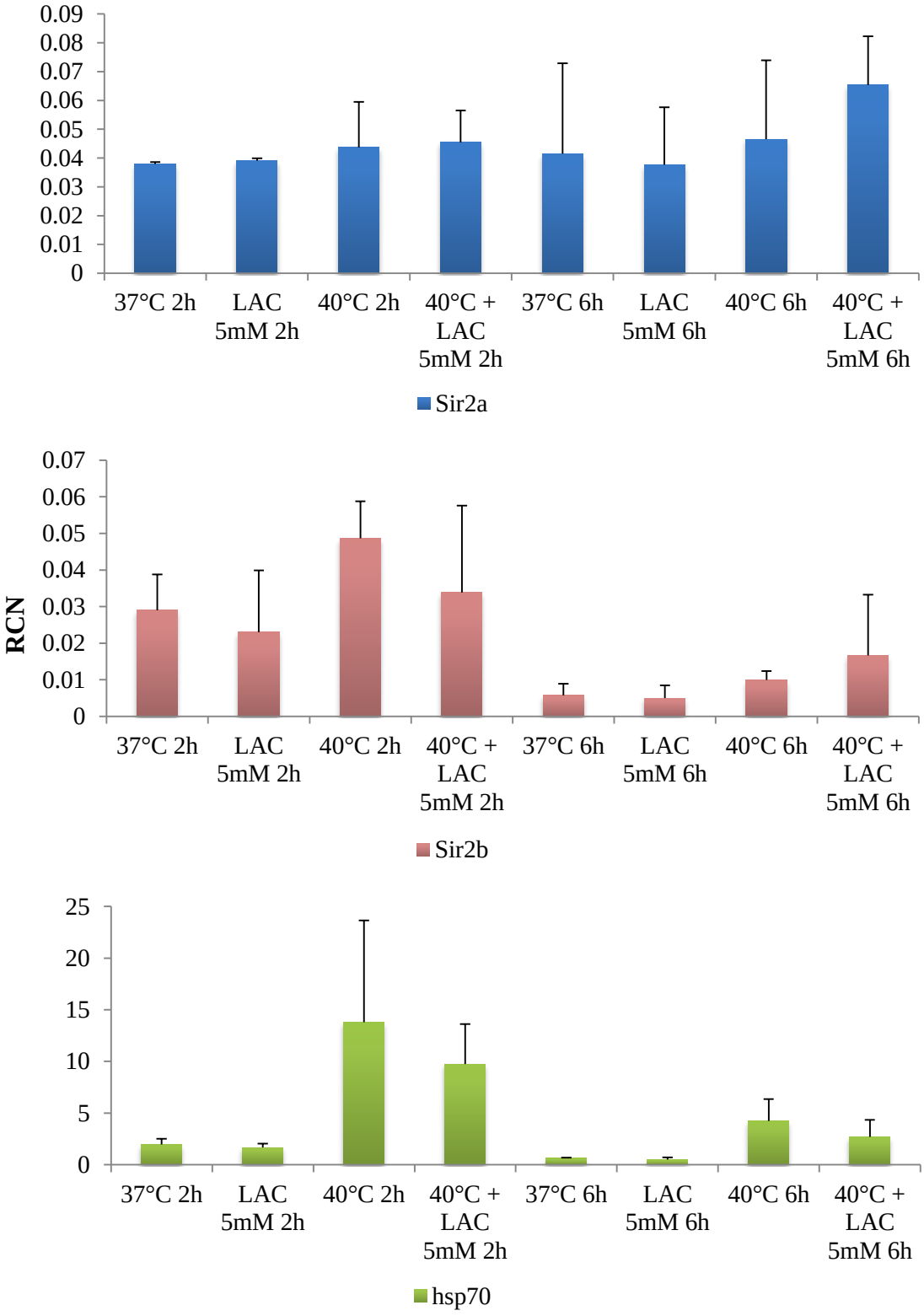

Mean Relative Copy Number (RCN) of expressed *PfSir2A*, *PfSir2B* & *Hsp70*. The relative copy number (RCN), derived from $2^{(-\Delta Cq)}$ of *PfSir2A* at 2 and 6 h (**blue bars**),

PfSir2B at 2 and 6 h (**red bars**) and *Hsp70* at 2 and 6 h (**green bars)**, after the exposure of Trophozoite-staged 9775 to no stress (37°C), 5 mM lactate and/or 40°C from independent biological duplicate experiments. The different coloured bars represent the gene being measured: *PfSir2A* (blue bars), *PfSir2B* (red bars) and *Hsp70* (green bars). Error bars are SEM. *$p < 0.05$ Kruskal-Wallis test.

c) Trophozoite-staged 10668

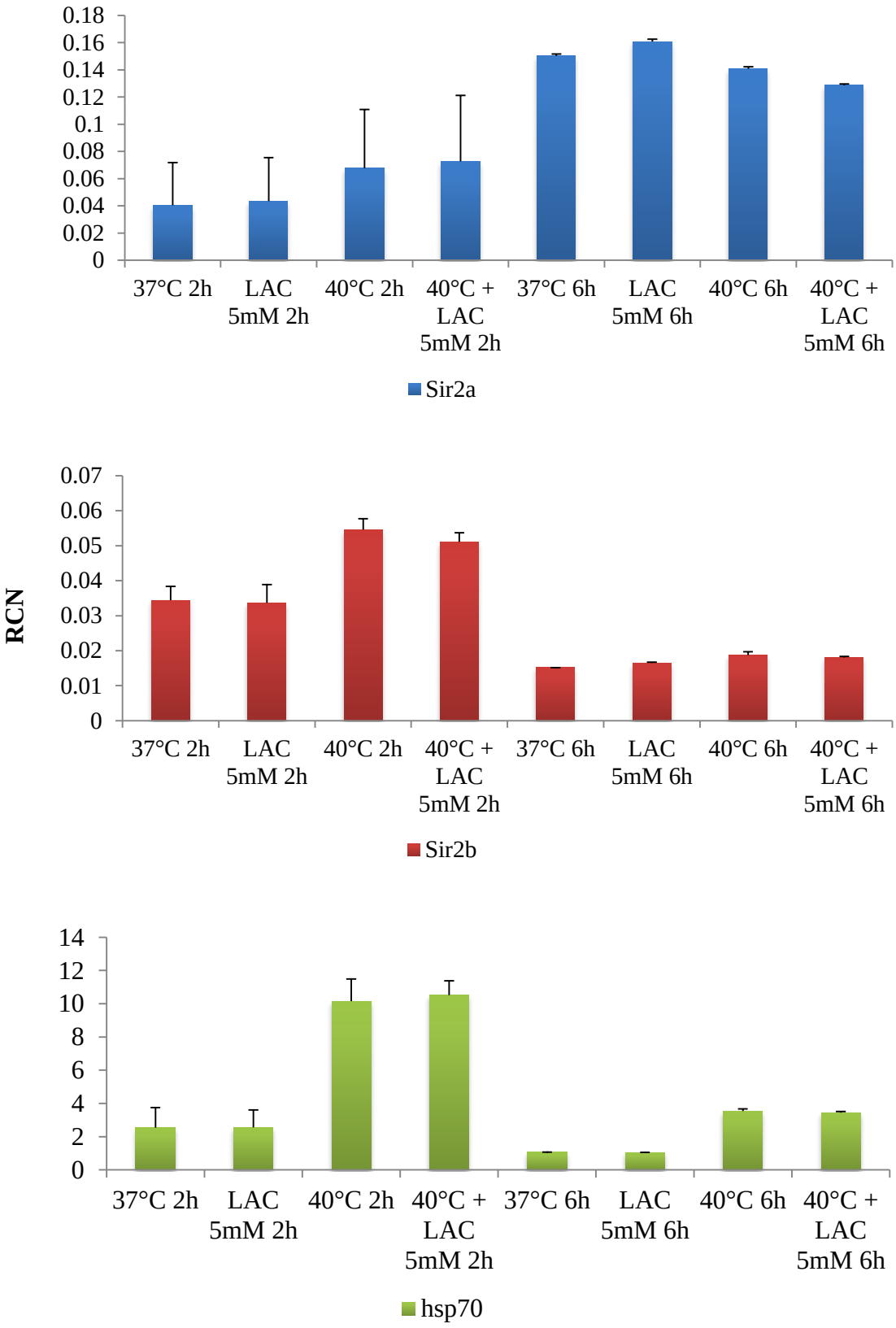

Mean Relative Copy Number (RCN) of expressed *PfSir2A*, *PfSir2B* & *Hsp70*. The

relative copy number (RCN), derived from $2^{(-\Delta Cq)}$ of *PfSir2A* at 2 and 6 h (**blue bars**), *PfSir2B* at 2 and 6 h (**red bars**) and *Hsp70* at 2 and 6 h (**green bars)**, after the exposure of Trophozoite-staged 10668 to no stress (37°C), 5 mM lactate and/or 40°C from independent biological duplicate experiments. The different coloured bars represent the gene being measured: *PfSir2A* (blue bars), *PfSir2B* (red bars) and *Hsp70* (green bars). Error bars are SEM. *$p < 0.05$ Kruskal-Wallis test.

Appendix IX: Unaltered western blot images

a)

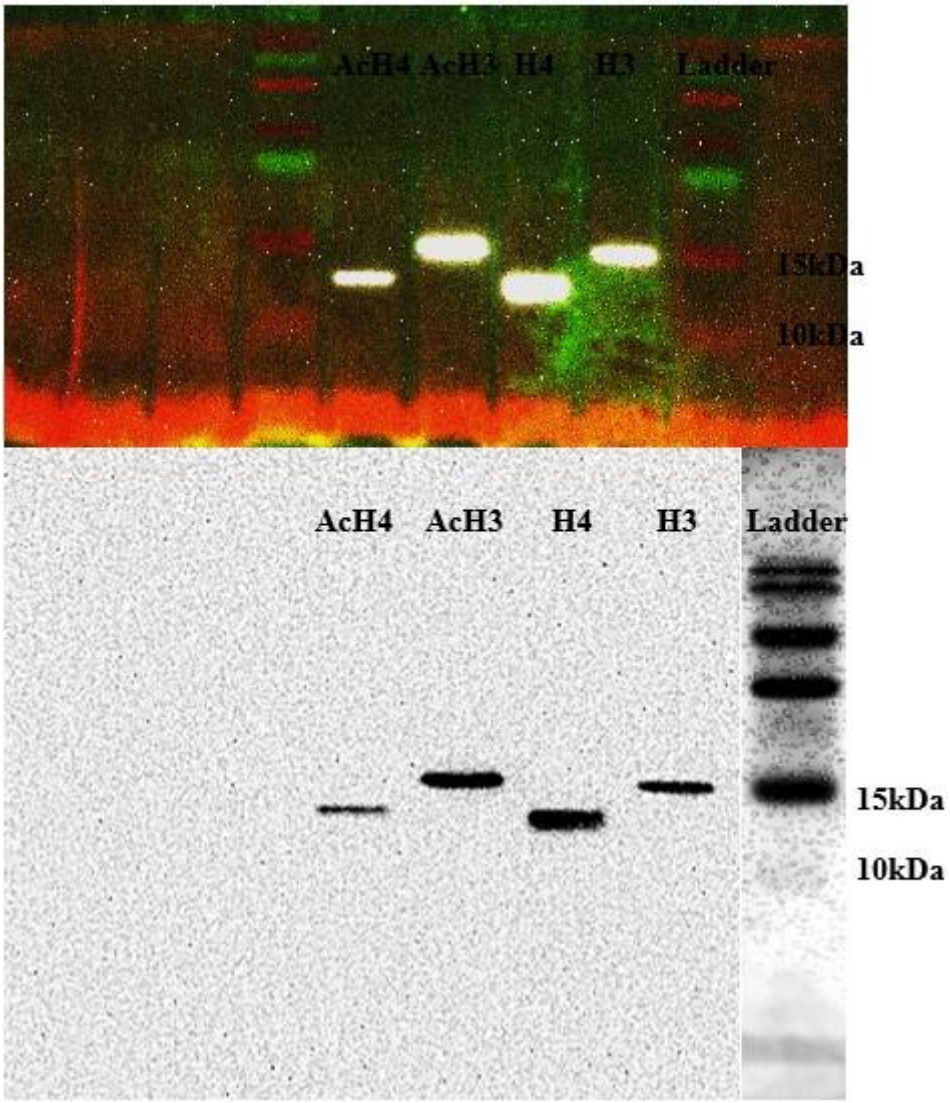

Unaltered image (top image) of detected unmodified and acetylated histone H3 and H4 extracted from *P. falciparum*.

b)

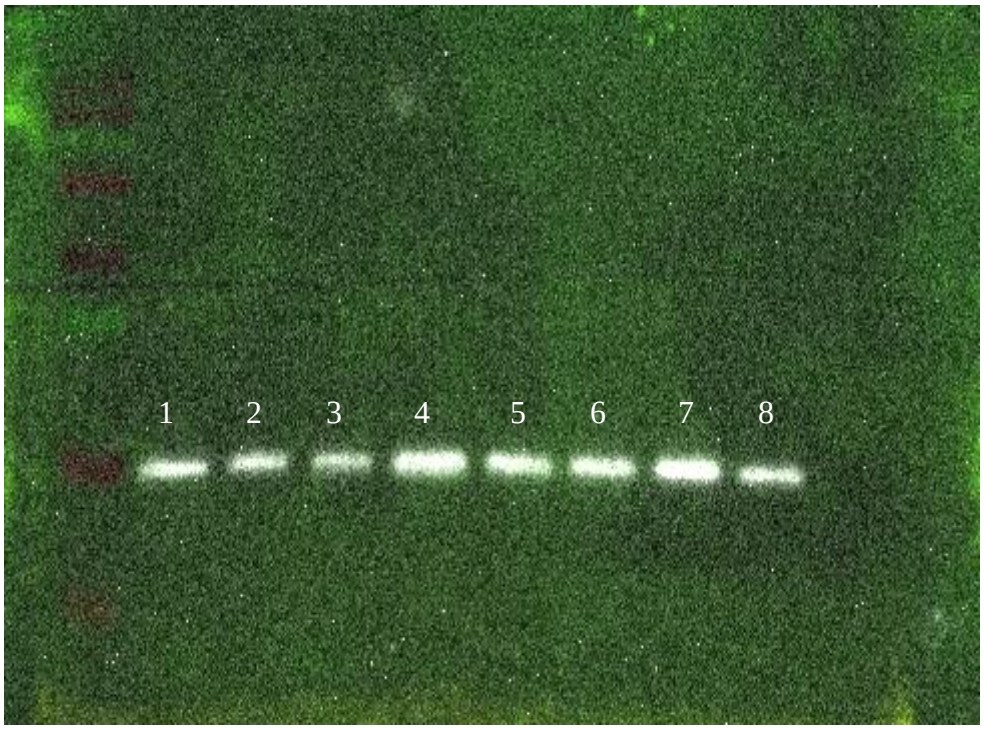

Unaltered panel A showing 60 minute reactions of histone and parasite nuclear extract from method 1 and 2 with controls 1, 2 and 3 included in the set of reactions. Lanes are:

1 = histone alone, control 1, 2 = method 2 nuclear extract test reaction, 3 = method 2 nuclear extract control 2 reaction, 4 = method 1 nuclear extract test reaction, 5 = method 1 nuclear extract control 2 reaction, 6 = method 3 test reaction, 7 = method 3 control 2 reaction, 8 = method 1 nuclear extract control 3 reaction.

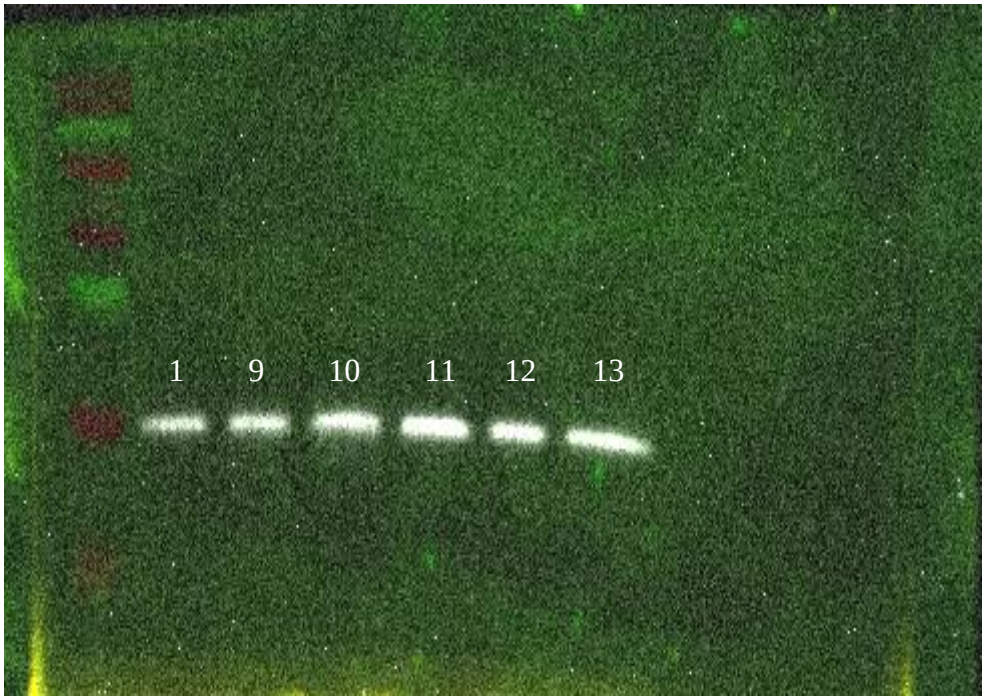

Unaltered panel B showing 60 minute reactions of histone and parasite nuclear plus cytoplasmic extract (combined extract) from method 1 and 2, with controls 1, 2 and 3 included in the set of reactions. Lanes are: 1 = histone alone, control 1, 9 = method 2 combined extract test reaction, 10 = method 2 combined extract control 2 reaction, 11 = method 1 combined extract test reaction, 12 = method 1 combined extract control 2 reaction, 13 = method 1 combined extract control 3 reaction.

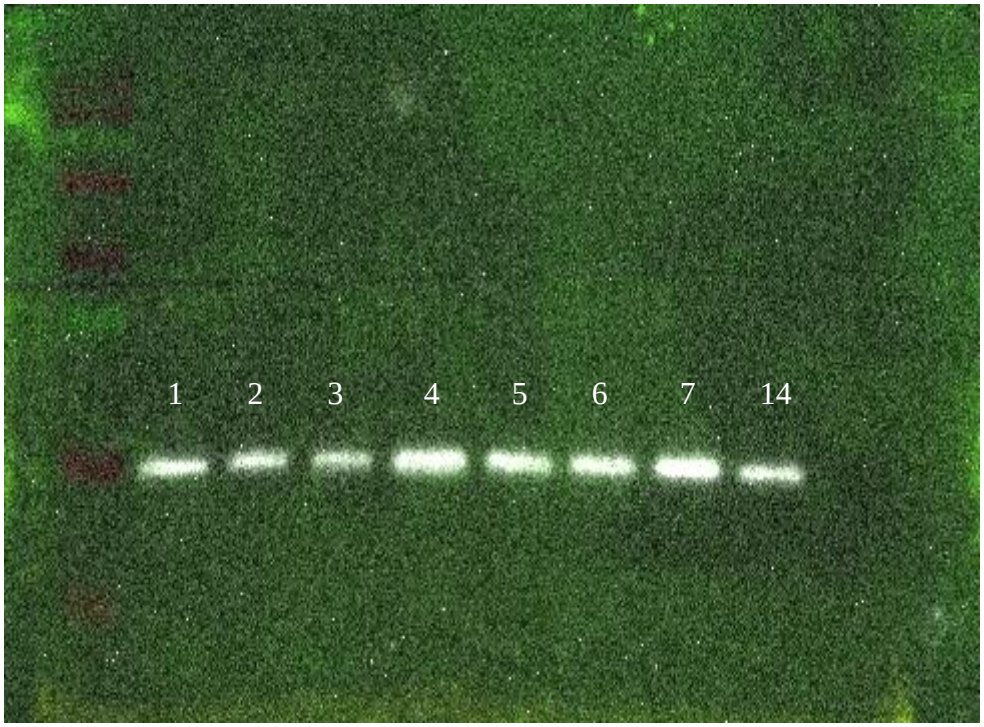

Unaltered panel C showing 120 minute reactions of histone and parasite extract from method 1 and 2 with controls 1 and 2, and a control 3 using extracts from method 3 included in the set of reactions. Lanes are: 1 = histone alone, control 1, 2 = method 2 nuclear extract test reaction, 3 = method 2 nuclear extract control 2 reaction, 4 = method 1 nuclear extract test reaction, 5 = method 1 nuclear extract control 2 reaction, 6 = method 3 test reaction, 7 = method 3 control 2 reaction 14 = method 3 control 3 reaction.

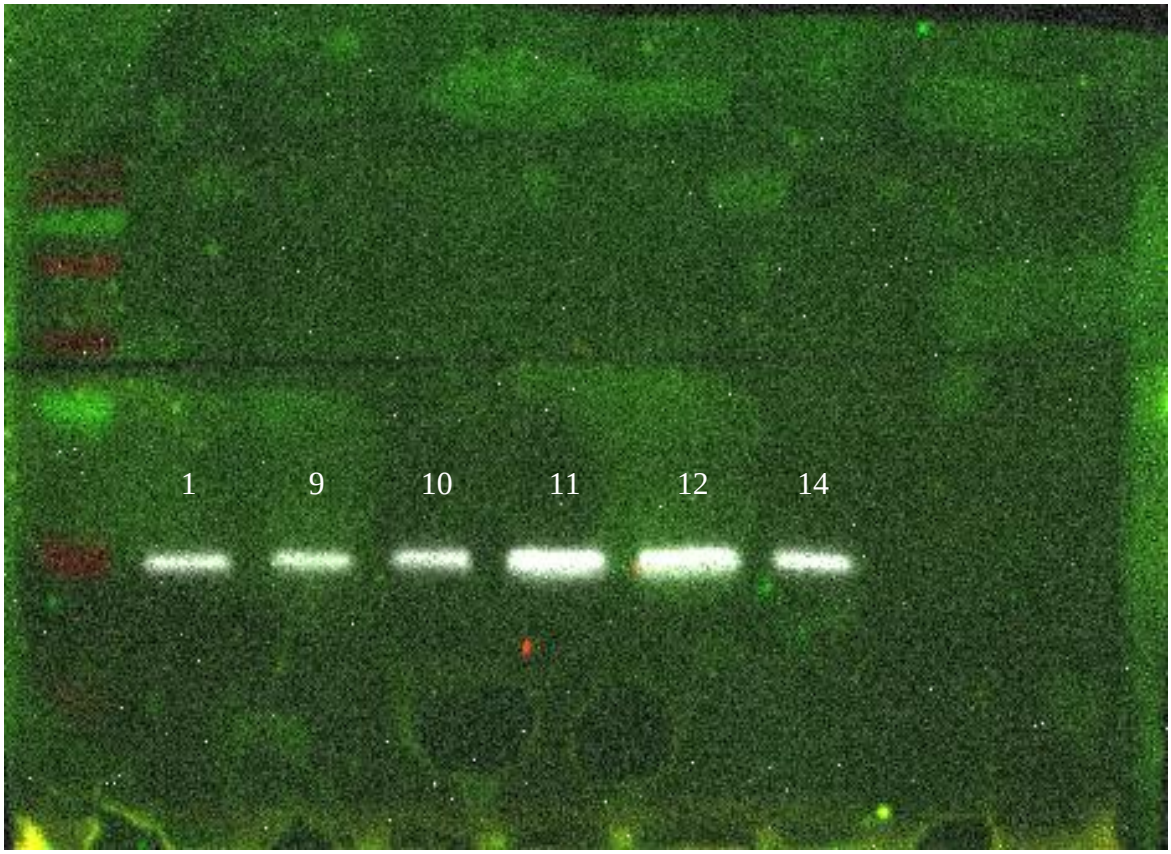

Unaltered panel D showing 120 minute reactions of histone and parasite nuclear plus cytoplasmic extract (combined extract) from method 1 and 2, with controls 1 and 2, and a control 3 using extracts from method 3. Lanes are: 1 = histone alone, control 1, 9 = method 2 combined extract test reaction, 10 = method 2 combined extract control 2 reaction, 11 = method 1 combined extract test reaction, 12 = method 1 combined extract control 2 reaction, 14 = method 3 control 3 reaction.

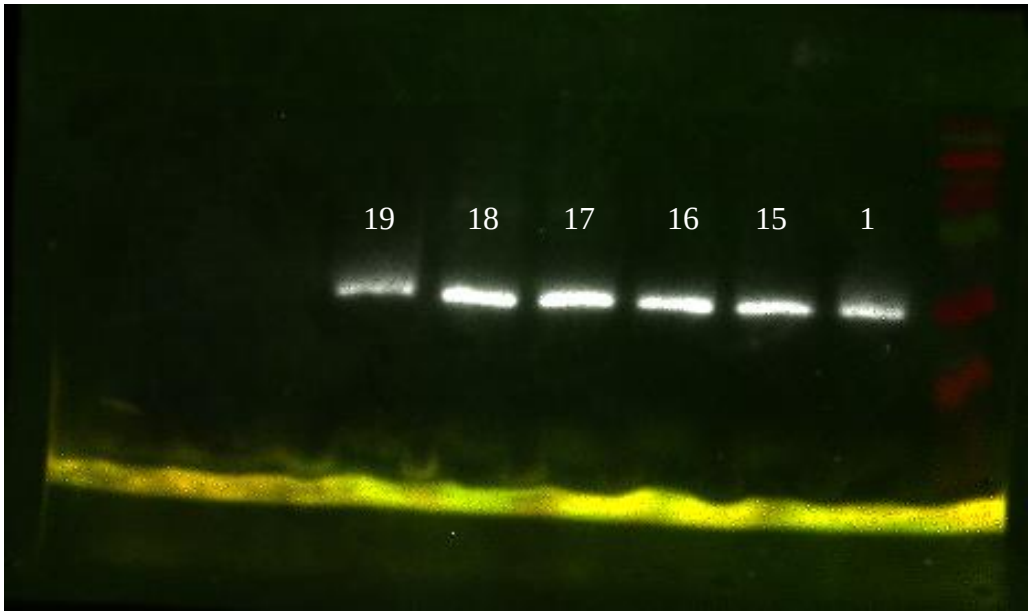

Unaltered panel E showing 180 minute reactions of histone and parasite extract from method 3 with or without NP-40, as well as controls 1 and 2. Lanes are: 1 = histone alone, control 1, 15 = method 3 with NP-40 test reaction, 16 = method 3 with NP-40 control 2 reaction, 17 = method 3 without NP-40 test reaction, 18 = method 3 without NP-40 control 2 reaction, 19 = histone from a 60 min parallel experiment with method 3 extract.

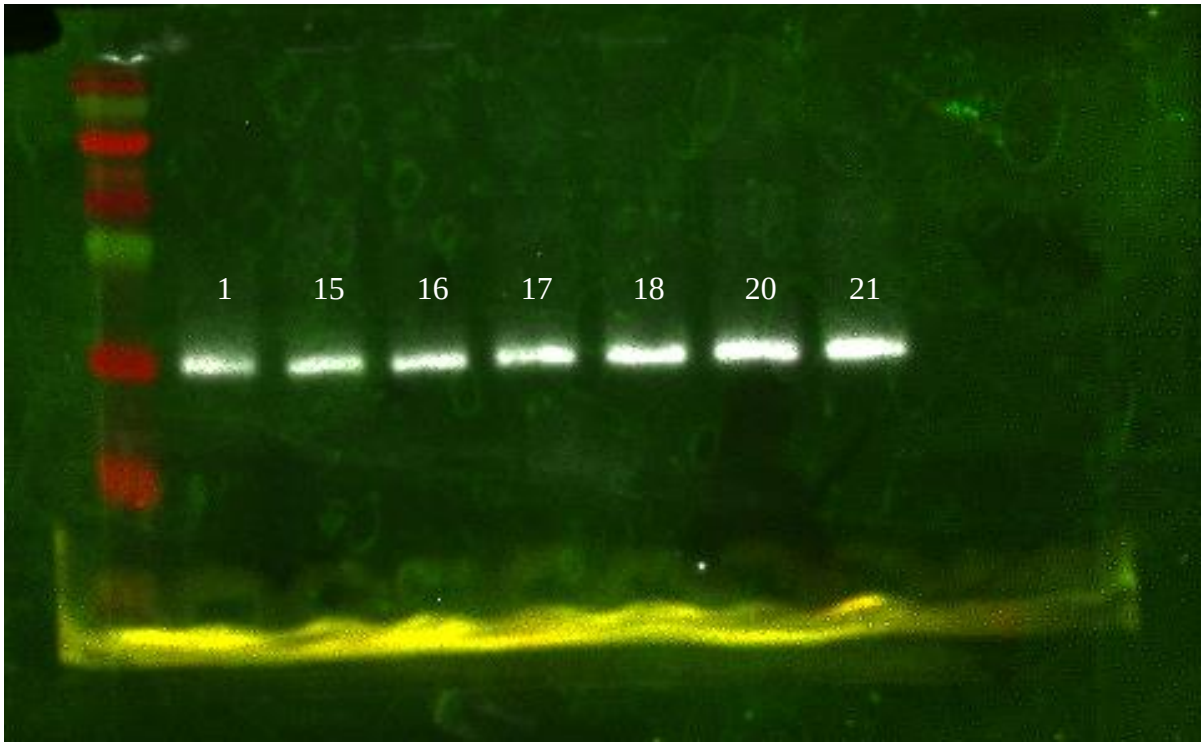

Unaltered panel F showing 6 h reactions of histone and parasite extract from method 3 with or without NP-40, as well as controls 1, 2 and 3. Lanes are: 1 = histone alone, control 1, 15 = method 3 with NP-40 test reaction, 16 = method 3 with NP-40 control 2 reaction, 17 = method 3 without NP-40 test reaction, 18 = method 3 without NP-40 control 2 reaction, 20 = method 3 with NP-40 control 3 reaction.

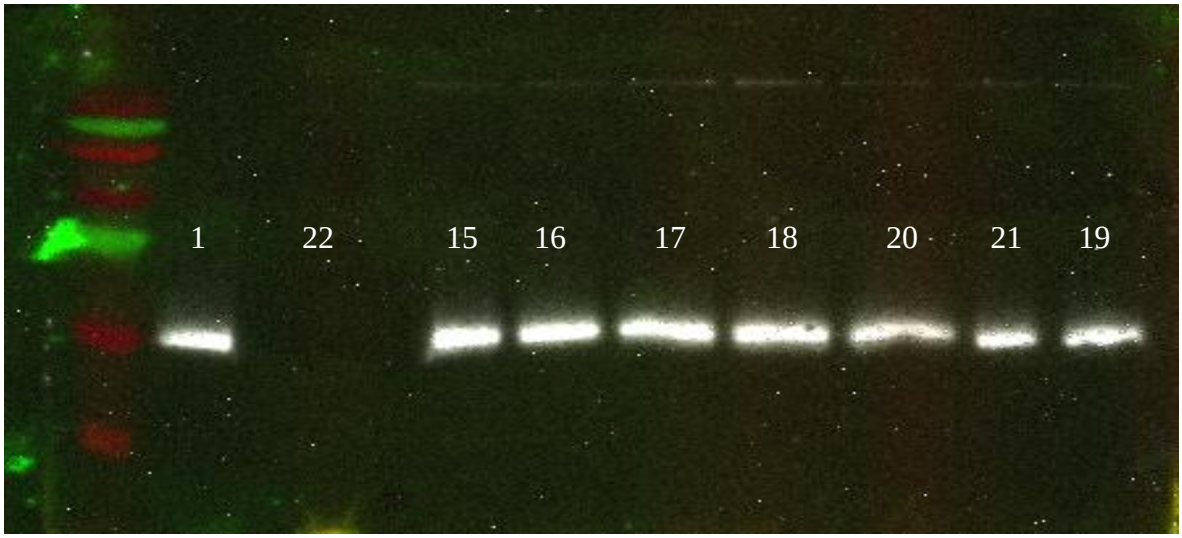

Unaltered panel G showing 6 h reactions (without sodium butyrate in the reaction mixture) of histone and parasite extract from method 3 with or without NP-40, as well as controls 1, 2 and 3. All reactions contain 100nM of NAD^+ except the control 2. Lanes are: 1 = histone alone, control 1, 15 = method 3 with NP-40 test reaction, 16 = method 3 with NP-40 control 2 reaction, 17 = method 3 without NP-40 test reaction, 18 = method 3 without NP-40 control 2 reaction, 19 = histone from a 60 min parallel experiment with method 3 extract, 20 = method 3 with NP-40 control 3 reaction, 21 = method 3 without NP-40 control 3 reaction and 22 = method 3 extract.

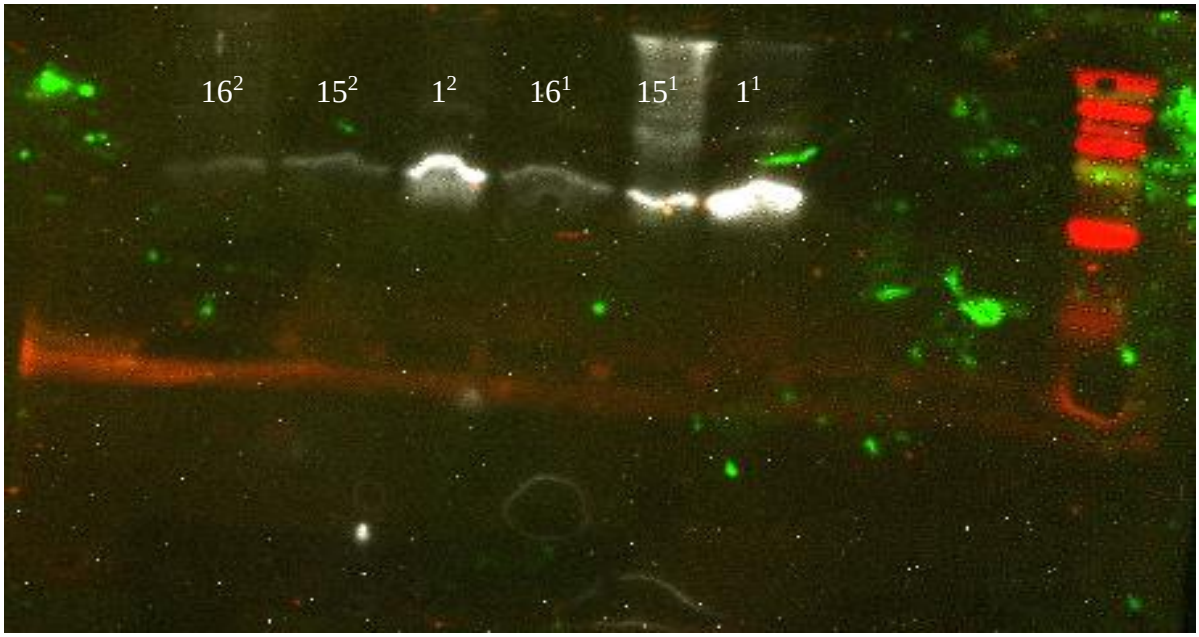

Unaltered panel H showing 24 and 48 h reactions of histone and parasite extract from method 3 with NP-40, as well as controls 1 and 2. Lanes are: 1 = histone alone, control 1, 15 = method 3 with NP-40 test reaction, 16 = method 3 with NP-40 control 2 reaction. ^{1}24 h reaction. ^{2}48 h reaction.

Appendix X: Up to a 120mM of sodium lactate does not change the pH of the physiological media used to grow *P. falciparum*